

BIRLA CENTRAL LIBRARY

PILANI (RAJASTHAN)

Call No. 532.5

R594F

Accession No. 33080

ENGINEERING SOCIETIES MONOGRAPHS

HARRISON W. CRAVER, *Consulting Editor*

FLUID MECHANICS
FOR
HYDRAULIC ENGINEERS

*The quality of the materials used in
the manufacture of this book is gov-
erned by continued postwar shortages.*

ENGINEERING SOCIETIES MONOGRAPHS

FOUR national engineering societies, the American Society of Civil Engineers, American Institute of Mining and Metallurgical Engineers, The American Society of Mechanical Engineers, and American Institute of Electrical Engineers, have made arrangements with the McGraw-Hill Book Company, Inc., for the production of selected books adjudged to possess usefulness for engineers or industry, but not likely to be published commercially because of too limited sale without special introduction. The societies assume no responsibility for any statements made in these books. Each book before publication has, however, been examined by one or more representatives of the societies competent to express an opinion on the merits of the manuscript.

ENGINEERING SOCIETIES MONOGRAPHS COMMITTEE

A. S. C. E.
LYNNE J. BEVAN
GEORGE W. BOOTH

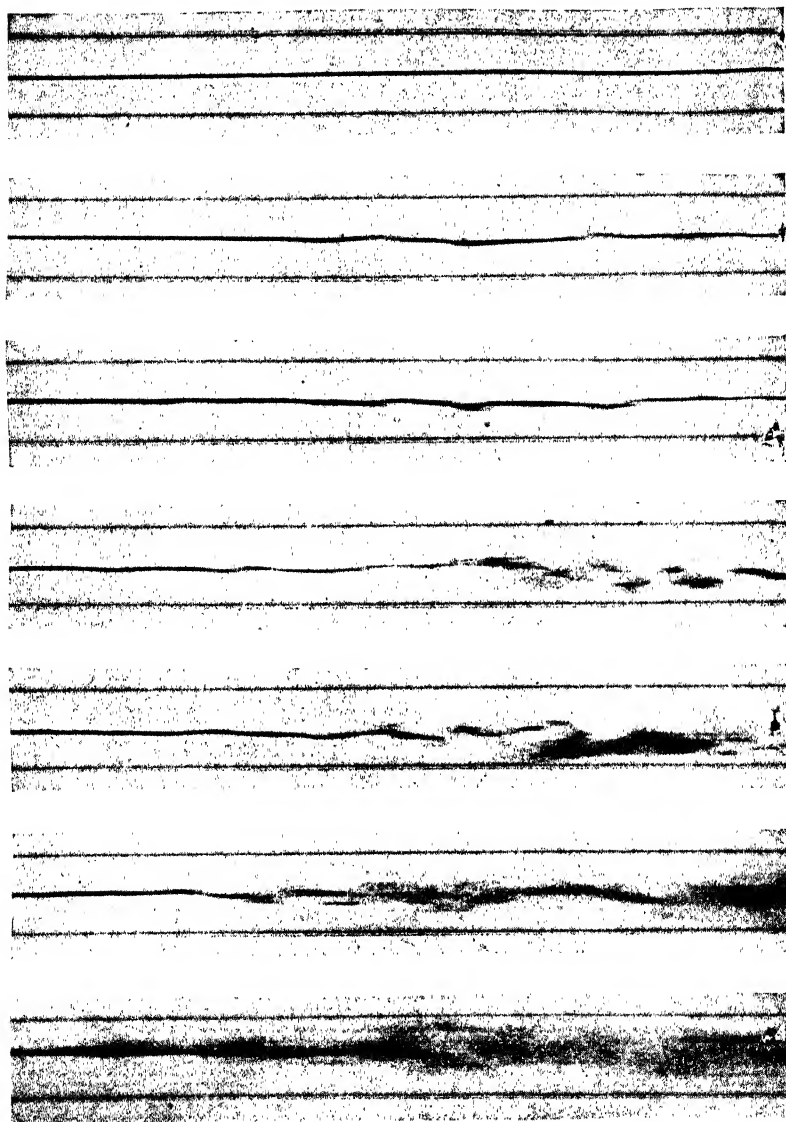
A. I. M. E.
REED W. HYDE
SAMUEL H. DOLBEAR

A. S. M. E.
C. B. PECK
G. B. KARELITZ

A. I. E. E.
F. MALCOLM FARMER
W. I. SLICHTER

HARRISON W. CRAVER,
CHAIRMAN

*Engineering Societies Library,
New York*



Columbia

Transition from laminar to turbulent flow with increasing values of the Reynolds number.

FLUID MECHANICS

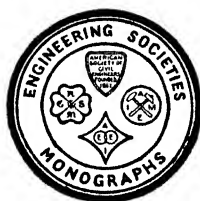
FOR

HYDRAULIC ENGINEERS

BY

HUNTER ROUSE, DR.-ING.

*Professor of Hydraulics, State University of Iowa;
Consulting Engineer, Iowa Institute of
Hydraulic Research; Iowa City, Iowa*



FIRST EDITION
FIFTH IMPRESSION

McGRAW-HILL BOOK COMPANY, INC.
NEW YORK AND LONDON
1938

Copyright, 1938, by the
UNITED ENGINEERING TRUSTEES, INC.
All rights reserved. This book, or parts thereof,
may not be reproduced in any form without per-
mission of the publishers.

Printed in the United States of America

COMPOSITION BY THE MAPLE PRESS COMPANY, YORK, PA.
PRINTED AND BOUND BY COMAC PRESS, INC., BROOKLYN, N. Y.

ENGINEERING SOCIETIES MONOGRAPHS

For many years those who have been interested in the publication of papers, articles, and books devoted to engineering topics have been impressed with the number of important technical manuscripts which have proved too extensive, on the one hand, for publication in the periodicals or proceedings of engineering societies or in other journals, and of too specialized a character, on the other hand, to justify ordinary commercial publication in book form.

No adequate funds or other means of publication have been provided in the engineering field for making these works available. In other branches of science, certain outlets for comparable treatises have been available, and besides, the presses of several universities have been able to take care of a considerable number of scholarly publications in the various branches of pure and applied science.

Experience has demonstrated the value of proper introduction and sponsorship for such books. To this end, four national engineering societies, the American Society of Civil Engineers, American Institute of Mining and Metallurgical Engineers, The American Society of Mechanical Engineers, and American Institute of Electrical Engineers, have made arrangements with the McGraw-Hill Book Company, Inc., for the production of a series of selected books adjudged to possess usefulness for engineers or industry but of limited possibilities of distribution without special introduction.

The series is to be known as "Engineering Societies Monographs." It will be produced under the editorial supervision of a Committee consisting of the Director of the Engineering Societies Library, Chairman, and two representatives appointed by each of the four societies named above.

Engineering Societies Library will share in any profits made from publishing the Monographs; but the main interest of the societies is service to their members and the public. With their aid the publisher is willing to adventure the production and dis-

tribution of selected books that would otherwise be commercially unpractical.

Engineering Societies Monographs will not be a series in the common use of that term. Physically the volumes will have similarity, but there will be no regular interval in publication, nor relation or continuity in subject matter. What books are printed and when will, by the nature of the enterprise, depend upon the manuscripts that are offered and the Committee's estimation of their usefulness. The aim is to make accessible to many users of engineering books information which otherwise would be long delayed in reaching more than a few in the wide domains of engineering.

ENGINEERING SOCIETIES MONOGRAPHS COMMITTEE
Harrison W. Craver, Chairman.

PREFACE

In the development of modern fluid mechanics, the past quarter century has witnessed a concerted effort to reconcile the theories of classical hydrodynamics with the findings of the practical engineer. Not only has much controversial matter of long standing already found satisfactory explanation, but many proponents of empirical methods have been won to the viewpoint that sound physical concepts must form the groundwork for further progress. In particular is this true of the field of aeronautics, for the simultaneous rise of aviation and applied aerodynamics is largely responsible for present trends in the study of fluid motion.

The hydraulic engineer, however, has as yet had few conclusive proofs that his methods might be bettered by subordinating empirical formulas to more rational methods of attack. Indeed, his justifiable pride in achievements of the past only strengthens a tendency to adhere to practices accepted in the days when engineers first learned to smile at the efforts of the theoreticians. Despite such natural conservatism in one of the oldest of engineering professions, many of the leading technical schools are gradually replacing elementary hydraulics courses with instruction in general fluid mechanics, while a number of excellent textbooks on the subject are now available in the English language. Nevertheless, existing texts beyond the elementary class are intended primarily for the student of aeronautics, and the hydraulic engineer will find in them little of direct application to his own field of endeavor.

It is with the hope of appealing specifically to this type of reader that the present volume has been prepared. The subject matter is definitely of an advanced nature, in that the author has presumed a reasonable familiarity on the part of the reader with the elementary principles of hydraulics as taught in American technical schools. On the other hand, every phase of the subject is developed from basic principles of mechanics, though a consistent effort is made to carry all such developments through

to their final application in a coherent and systematic fashion. At the same time, certain bugbears have been avoided which long have tended to arouse the antagonism of the practical engineer—in particular, the convenient creation of the so-called “perfect fluid”—for such assumptions commonly made by the theoretician have helped to preserve the rift between practice and theory for more than a century. The author seeks thereby to convince the hydraulic engineer that there is much to be gained by giving heed to rational methods of analysis and research.

The experience of the author in the experimental laboratory has led him to believe implicitly in the necessity both of experimental vindication of analytical studies and of correct physical groundwork for experimental research. It is to be hoped, therefore, that laboratory investigators will also find much of value in these pages. Yet if the engineering students of the present day, who will become the hydraulic engineers and investigators of the near future, are to be properly equipped for their profession, it is essential that the study of fluid mechanics form no small part of their training. With this in mind, the author has endeavored to make the volume suitable as a text in advanced hydraulics courses, to be supplemented by such practical applications as may be chosen by the instructor.

The need for such a book as this first became apparent to the author in 1930, during the course of research under Geheimrat Th. Rehbock at the Karlsruhe Technische Hochschule. At that time even the best hydraulic laboratories were still largely unaffected by the advances made in other research institutions for fluid mechanics, and securing the fundamentals of the science was a tedious process. In the years 1931–1933, however, the author was so fortunate as to be in close contact with Professor W. Spannhake, of Karlsruhe, then visiting professor at the Massachusetts Institute of Technology. While attending Professor Spannhake's lectures on applied hydrodynamics for the second successive year, the author prepared under his guidance a set of mimeographed notes for student use, which covered approximately the same ground as Part One of the present volume.

In the following years the author presented a similar course for advanced students in civil and mechanical engineering at

Columbia University. Lectures on the mechanics of fluids and the hydraulics of open channels by Professor B. A. Bakhmeteff, of the Columbia Department of Civil Engineering, further served to broaden the author's viewpoint, as did numerous discussions with Professor Bakhmeteff on the publications of various German, French, and English authorities, particularly in the field of fluid turbulence. It was during this period that much of the material presented in Part Two of this book was assimilated.

More recently the author has conducted classes in fluid mechanics and open-channel hydraulics for senior and graduate students at the California Institute of Technology, and has had the privilege of contact with Professor Th. von Kármán, to whose genius the engineering world is indebted for marked advances in nearly every phase of fluid mechanics. The experience of these last years not only led to considerable revision and unification of the earlier portions of the book, but permitted the addition of chapters on the transportation of sediment and the mechanics of wave motion—research subjects of primary concern in the hydraulic laboratories of the California Institute.

The various photographs appearing in this volume were taken by the author during his investigations at the Flussbau-laboratorium of the Karlsruhe Technische Hochschule, the River Hydraulics Laboratory of the Massachusetts Institute of Technology, and the Fluid Mechanics Laboratory of Columbia University, as indicated below each reproduction. Negatives of the photographs made at the Massachusetts Institute of Technology are the property of that institution and are reproduced with the permission of the Department of Civil Engineering of the M. I. T.

To Dr. Merit P. White the author expresses sincere appreciation for thorough critical examination of the original manuscript of this volume and for subsequent aid in the revision of the proofs. Valuable assistance by Miss Mary Arcularius and Mr. Hugh Stevens Bell in preparing manuscript and photographs for publication is also gratefully acknowledged.

HUNTER ROUSE.

PASADENA, CALIFORNIA,
June, 1938.

CONTENTS

	PAGE
ENGINEERING SOCIETIES MONOGRAPHS	vii
PREFACE	ix

CHAPTER I

DIMENSIONAL ANALYSIS

1. Empiricism versus Rational Analysis	1
2. Theory of Dimensions.	2
3. Properties of Fluid Matter.	5
4. Characteristics of Fluid Motion.	12
5. The Π -Theorem.	13
6. Typical Applications	18
7. Similitude	24
8. Classification of Flow Phenomena.	30

PART ONE

FUNDAMENTALS OF HYDROMECHANICS

CHAPTER II

ELEMENTARY PRINCIPLES OF FLOW

9. Velocity of a Fluid Particle as a Function of Time and Space	35
10. Relationship of the Velocity Fields for Steady and Unsteady Flow	37
11. Equations of Motion in Natural Coordinates.	42
12. Principles of Energy, Continuity, and Momentum.	47
13. Theory and Use of the Flow Net	54
14. Significance of the Force Potential	59

CHAPTER III

GENERALIZED EQUATIONS

15. Translation, Rotation, and Deformation of a Fluid Element	65
16. Circulation and Vorticity	72
17. Characteristics of the Vortex.	76

CHAPTER IV

IRROTATIONAL MOTION

18. The Velocity Potential.	83
19. Problems in Three-dimensional Flow	86
20. Two-dimensional Flow: the Stream Function.	93

CHAPTER V

CONFORMAL MAPPING

21. Theory of Complex Variables	96
22. Significance of Conformal Mapping	98
23. Elementary Transformations	102
24. Source-sink Combinations	105
25. Flow around a Cylinder	110
26. Successive Transformations	114
27. Kutta and Joukowsky Profiles	117
28. Methods of Application	120

CHAPTER VI

APPLICABILITY OF THE FUNDAMENTAL EQUATIONS

29. Résumé	125
30. Energy Criteria	126
31. Variation in Density	126
32. Cavitation	129
33. Separation	134

PART TWO

MECHANICS OF FLUID RESISTANCE

CHAPTER VII

FUNDAMENTAL EQUATIONS OF VISCOUS FLOW

34. Elementary Stresses within a Viscous Fluid	141
35. Viscous Stress in Terms of Rate of Deformation	143
36. Dissipation of Energy through Viscous Action	146
37. Equations of Navier-Stokes	148

CHAPTER VIII

PROBLEMS IN LAMINAR MOTION

38. Steady Flow between Parallel Boundaries	150
39. Elements of Lubrication	156
40. Uniform Flow in Circular Tubes	160
41. Percolation	163

CHAPTER IX

FLUID TURBULENCE

42. The Transition from Laminar to Turbulent Motion	169
43. Reynolds' Modification of the Navier-Stokes Equations	175
44. Stress Intensity in Terms of Momentum Transport	180
45. Kinetic Energy of Turbulence	182
46. Quantitative Analysis of the Turbulence Mechanism	185

CONTENTS

XV
PAGE

CHAPTER X

CHARACTERISTICS OF THE BOUNDARY LAYER

47. Boundary Influence in Non-uniform Motion	192
48. The Laminar Boundary Layer	195
49. The Turbulent Boundary Layer	200
50. Separation and the Turbulent Wake	205

CHAPTER XI

FLOW AROUND IMMERSED BODIES

51. Fundamental Concept of Drag	209
52. Resistance of Spherical Bodies	212
53. Drag Characteristics of the Cylinder	216
54. Lift and Drag of the Airfoil	223
55. Relative Drag of Miscellaneous Profiles	225
56. Wind Pressure	229

CHAPTER XII

FLOW IN CLOSED CONDUITS

57. General Aspects	232
58. Velocity Distribution in Uniform Flow	236
59. Universal Laws of Resistance	245
60. The Roughness Problem	251
61. Symmetrical Section Changes	255
62. Secondary Flow in Asymmetrical Conduits	266

CHAPTER XIII

FLOW IN OPEN CHANNELS

63. Survey of the General Problem	273
64. Velocity Distribution and Resistance in Uniform Motion	274
65. Energy and Discharge Diagrams	281
66. Equations of Gradually Varied Flow	288
67. Surface Profiles	290
68. Computation Procedure	294
69. The Hydraulic Jump	299
70. Rapidly Varied Flow	301
71. Weirs and Sluice Gates	307
72. Spillway Design	316
73. Critical-depth Meters	319

CHAPTER XIV

TRANSPORTATION OF SEDIMENT

74. Essential Aspects of the Problem	327
75. Bed-load Movement	331
76. Sediment Suspension	339
77. Sediment Characteristics	343

PART THREE

MECHANICS OF WAVE MOTION

CHAPTER XV

GENERAL CHARACTERISTICS OF WAVE PHENOMENA

78. Propagation of Disturbances in Fluid Media	353
79. Relative Velocities of Wave and Fluid	355
80. Wave Forms: Interference and Reflection	357
81. Properties of Elastic Waves	363
82. Properties of Gravity Waves	368
83. Properties of Capillary Waves	373

CHAPTER XVI

GRAVITY WAVES IN OPEN CHANNELS

84. Solitary Waves	377
85. Surges	382
86. The Hydraulic Jump as a Standing Surge	388
87. Wave Effects at Boundary Changes in the Vertical Plane . .	394
88. Wave Effects at Boundary Changes in the Horizontal Plane .	396

APPENDIX

PHYSICAL PROPERTIES OF COMMON FLUIDS	403
--	-----

INDEX	413
-----------------	-----

FLUID MECHANICS FOR HYDRAULIC ENGINEERS

CHAPTER I

DIMENSIONAL ANALYSIS

1. Empiricism versus Rational Analysis. Throughout the many centuries since the earliest hydraulician drew his first primitive conclusions with regard to the flow of water, engineers have relied almost entirely upon engineering judgment and empirical formulas in designing hydraulic structures and in predicting the behavior of the resulting flow. Such empirical formulas have been based on experimental measurement, although tempered, to a certain extent, with common sense and intuition; and for lack of a more rational means of approach, engineering judgment has been developed largely through the tedious process of trial and error. Inasmuch as experience is a very excellent disciplinarian, such methods have well served their purpose.

On the other hand, parallel with the rapid growth of empirical hydraulics during the past one hundred and fifty years, mathematicians and mathematical physicists have attempted completely rational solutions of the problems of fluid motion, without any recourse whatever to experimental measurement. These rational methods were made possible, however, only by such simplifying assumptions that the resulting solutions often bore little or no resemblance to the actual phenomena in question. Needless to say, the hydraulic world was quite justified in denying the practicability of methods leading to erroneous results. Nevertheless, there was considerable right in the point of view of the mathematicians, who were not content merely to formulate simple working rules from a limited range of experimental data.

Modern fluid mechanics recognizes the merits of each school. Based upon a healthy combination of physical analysis and

experimental verification, fluid mechanics eliminates both the improbability of recognizing fundamental principles by chance, as in empirical hydraulics, and the necessity of dealing with an ideal, non-existent fluid as in classical hydromechanics. Empirical hydraulics seeks to formulate simple working equations for design, dependability of numerical results being of more consequence than physical veracity of an equation; fluid mechanics, on the other hand, teaches that a sound physical basis for an equation is of primary importance, in that it may have far broader significance than might originally be apparent. Rigorous mathematical analysis usually encounters insurmountable obstacles, and simplifying assumptions without benefit of experimental background can often lead to completely fallacious conclusions; fluid mechanics avoids this difficulty by restricting its assumptions to those which experience and sound physical reasoning have shown to be without serious effect upon the essential features of the problem.

The tools of fluid mechanics are laboratory experience, dimensional analysis, and a process of reasoning that seeks to interpret phenomena of flow in the light of basic principles of mechanics. Where empiricism emphasizes the algebraic development of a formula from experimental data often with little physical justification, rational analysis attempts a complete solution for the correct function and the numerical constants involved. Fluid mechanics, on the other hand, uses the principles of dimensional analysis to incorporate those variables which experience has shown to be essential into a basic dimensionless expression systematically and significantly arranged; wherever possible, the functional relationship of the several members of this expression is then developed, at least approximately; finally, experimental investigation supplies the numerical constants and the essential check on the correctness of the analysis. Such methods lead not only to dependable practical results, but to a far more thorough understanding of the fundamental problem.

2. Theory of Dimensions.¹ Unfortunate indeed is the fact that the English language uses the same word, "dimension," to denote both the numerical magnitude of a measurement and its dimensional category; before proceeding farther, the significance

¹ To the reader is recommended P. W. Bridgman's admirable little volume, "Dimensional Analysis," Yale University Press, 1937.

of this distinction must be clearly understood. It is possible to ascribe an arbitrary dimensional unit to any measurable characteristic of matter or of its physical behavior; thus, one might well conceive of units of area, electrical permeability, or momentum. The magnitude of the momentum of a given body, for instance, would then be expressed as the numerical ratio of its momentum to that of the arbitrary momentum unit, this number referring specifically to the momentum dimension and to the size of the momentum unit.

Such promiscuous creation of dimensional units, fortunately, is neither convenient nor necessary. Since fluid motion is basically a problem of mechanics, and since for the present purposes thermal, electrical, optical, and chemical phenomena have no bearing on the problem, it is sufficient to restrict this study to four fundamental dimensions by means of which all quantities in mechanics may be described: length, time, mass, and force, to which categories the letters L , T , M , and F refer symbolically. To each dimensional category may be assigned some arbitrary unit, confusion too often resulting from the fact that nations cannot agree among themselves as to the choice of units. In the American system, which is adopted in this text, the length unit is the foot, the time unit the second, the mass unit the slug, and the force unit the pound. In the English system feet and seconds have the same significance, but the pound is the unit of mass and the poundal the unit of force. In the metric system the second is the only similar unit, for force is measured in dynes, length in centimeters, and mass in grams, although meters and kilograms are often used as more convenient units. Owing to the decimal nature of the system, this would not introduce serious difficulties—were it not for the fact that continental engineers are prone to ignore the dyne and measure force in grams or kilograms.

Whether the volume of a body is measured in terms of cubic inches or cubic miles makes no difference in the actual volume that it possesses, however much the numerical ratio of its volume to that of each unit may vary. Similarly, regardless of what dimensional system may be adopted, the volume dimension is dependent upon the third power of the fundamental length dimension, and hence is written L^3 . A quantity such as a force intensity is really a force per unit area and will thus depend in numerical magnitude upon the arbitrarily selected units of force and length,

this magnitude being found by dividing the numerical measure of the force by the numerical measure of the area. It is futile, however, to think of a fundamental dimension F being divided bodily by the second power of another fundamental dimension L —that is, the dimension of force intensity, in terms of the fundamental units, is merely symbolized in shorthand fashion— F/L^2 or FL^{-2} . Such a procedure is obviously far simpler than creating a new dimension and a new dimensional unit to describe each new characteristic.

This method of reasoning will readily explain points that sometimes tend toward confusion. It is often claimed that it is impossible to take the logarithm of a length; but when it is realized that the measured length, regardless of the unit upon which it is based, is simply a numerical ratio, then any mathematical operation upon it becomes fully justifiable. Such a ratio is not, however, dimensionally independent; only when a number does not refer to any dimension whatever, and hence is numerically independent of any change in dimensional units, does it become truly dimensionless.

Although length, time, mass, and force are all mechanical characteristics of fundamentally different nature, it is convenient to relate their dimensional units in definite fashion. Thus, it has been universally agreed that in any dimensional system the force unit is that force which will change the velocity of a unit mass one unit length per unit time in one unit of time. For instance, a force of one pound will accelerate one slug of matter one foot per second in one second. At the same time that this arbitrary correlation defines any one dimensional unit in terms of the other three independent units, it also makes any one dimensional category expressible through use of the other three categories. That is, F may now be replaced by a combination of L , T , and M , and so forth, so that

$$F = \frac{ML}{T^2}; \quad L = \frac{FT^2}{M}; \quad M = \frac{FT^2}{L}; \quad T = \sqrt{\frac{ML}{F}}$$

More generally,

$$\frac{ML}{FT^2} = 1$$

It is evident that in this manner any three of these fundamental dimensions may be used to describe completely the dimension of any mechanical characteristic, by eliminating the chosen dependent dimension through one of the above relationships. Power, for example, is measured in foot-pounds per second; its dimension may then be written correctly in any of the following ways:

$$\frac{LF}{T} = \frac{F^2 T}{M} = \sqrt{\frac{F^3 L}{M}} = \frac{L^2 M}{T^3}$$

Nevertheless, owing to the common usage of the length, time, and force scales in this country, and of the length, time, and mass scales in Europe, it is customary to adopt L , T , and either F or M as the three independent dimensions. On a later page in this chapter there will be found a table giving the dimensions of the common fluid properties and characteristics of motion, using both notations. To express the dimension in the American, English, metric, or any arbitrary system, one need only substitute the corresponding dimensional units, the dependent unit thereby being determined so long as that system is followed.

Conversion from one system to another follows the same basic procedure. For instance, if a force intensity expressed as 1000 dynes per square centimeter is desired in terms of pounds per square foot, the procedure will be as follows:

$$1 \text{ dyne} = 2.248 \times 10^{-6} \text{ lb.}; \quad 1 \text{ cm.} = 0.03281 \text{ ft.}$$

$$\frac{1000 \times 1 \text{ dyne}}{1 \text{ cm.}^2} = \frac{1000 \times 1 (2.248 \times 10^{-6} \text{ lb.})}{1 (0.03281 \text{ ft.})^2} = 2.088 \text{ lb./ft.}^2$$

If, on the other hand, the result must be in terms of slugs per foot-second²,

$$1 \text{ lb.} = 1 \text{ slug ft./sec.}^2$$

$$\frac{2.088 \times 1 \text{ lb.}}{1 \text{ ft.}^2} = \frac{2.088 \times 1 \text{ slug ft./sec.}^2}{1 \text{ ft.}^2} = 2.088 \text{ slugs/ft.-sec.}^2$$

3. Properties of Fluid Matter. All matter, whether solid, liquid, or gas, must occupy a certain portion of space, its geometrical form and the magnitude of its volumetric displacement being measurable in terms of an arbitrary length scale in each of three coordinate directions. By establishing some center for the coordinate system, the same length scale may be used to describe its position with relation to the coordinate center. Thus, geo-

metrical form and relative location in three-dimensional space are purely length characteristics.

The duration of existence of this body of matter as such cannot be measured in length terms, but requires a special scale of time. By selecting some arbitrary point on this scale, it becomes possible to relate the time at which the body is studied to a convenient reference datum. As a familiar example of such a practice, the reader need only recall that time scale for which the unit is the year, and on which the date of birth of Christ has been chosen as the arbitrary datum or zero point.

Mass is purely a quantitative measure of matter. Since neither the time nor the length scale is suitable for such measurement, it becomes necessary to establish an independent scale of mass, the unit of which is once more quite arbitrary. Because the mass of a given substance is quite unrelated to its volume, neither expansion nor contraction can affect its magnitude; while its geometrical form and location may be varied mechanically with time, material mass may be neither created nor destroyed. A characteristic inherent in mass is that of inertia, the tendency to remain at rest or in an existing state of motion unless acted upon by some external force.

A very convenient and significant combination of the mass and length scales is found in the characteristic known as mass density, or simply density. This characteristic is given the symbol ρ (the Greek letter rho), and is defined as the mass of a given substance per unit volume; it may be measured in terms of slugs per cubic foot, and will have the dimension M/L^3 . Evidently, expansion or contraction of the substance will result in a change in density.

To be distinguished carefully from density is the characteristic known as specific gravity, which represents merely a numerical ratio of two densities, that of water commonly being taken as a convenient reference; specific gravity is no more dimensionless than length or energy, in that it depends in magnitude upon what dimensional unit is selected—that is, upon the fluid density used as reference. In other words, it is not sufficient to say that the specific gravity of some liquid is 2.34—unless one tacitly concedes that what is meant is 2.34 “water-densities.”

Matter may be further described mechanically in terms of certain force characteristics—namely, mass attraction, molecular

friction, molecular attraction, and elasticity. While each of these is undoubtedly related to the basic molecular constitution of matter, in the study of fluid mechanics it is not only advisable, but entirely reasonable, to consider these several types of force action as quite distinct from one another—exactly as the molecular spacing is of no practical consequence in treating matter as homogeneous.

Mass attraction is that force which is exerted by two bodies of matter upon each other, and is proportional directly to the product of the masses and inversely to the square of the distance between them. In fluid mechanics mass attraction is significant only so far as that exerted by the earth upon a fluid is concerned, this attractive force being known as weight. So common and dangerous is the fallacy of confusing mass and weight that this distinction cannot be too strongly emphasized. Obviously, a change in volume of a given body of matter can cause no change in the magnitude of either mass or weight; on the other hand, although the mass of the body must remain constant, regardless of location, its weight will vary inversely with the square of its distance from the earth's center of mass. The force exerted by the earth upon a mass of one slug (at sea level in the United States) is approximately 32.17 pounds—corresponding to a force of 980.7 dynes upon a mass of one gram. Hence the American slug and the pound are, respectively, 32.17 times as large as the corresponding English units of mass and force, the pound and poundal; similarly, the gram as a force unit is 980.7 times as great as the dyne.

The property of specific weight (often called "weight density" to distinguish from the foregoing "mass density") is the weight of a given substance per unit volume, and is commonly given the symbol γ (gamma). It is measurable in terms of pounds per cubic foot, in the American system of units, and has the general dimension of F/L^3 . It is evident that the specific weight of any substance will vary with both expansion and contraction of the substance and with geographical location (refer to page 404 of the Appendix).

All matter may be subjected to a shearing force, the effect of such stress marking the primary distinction between the solid and the fluid states. A solid in a state of shear will deform elastically, the magnitude of deformation being in direct propor-

tion to the shearing force until the elastic limit is reached, beyond which plastic flow will generally occur until the point of final rupture. If a fluid is subjected to shear, it will also deform, but continuously so long as the shearing force is applied, the magnitude of the force now governing not the magnitude but the rate of deformation. Opposing such continuous fluid deformation is the molecular friction (viscous shear) within the substance, proportional to the rate of deformation and to the viscosity coefficient of the fluid. This is often called the absolute viscosity, with the customary symbol μ (mu)—dynamic viscosity, however, being a far more logical designation; from definition, it varies directly with the intensity of shear (F/L^2) and inversely with the rate of angular deformation ($1/T$), and hence has the dimension FT/L^2 . Since viscosity is that fluid property which resists angular deformation, and since fluid deformation under stress is continuous, the influence of viscosity is apparent only so long as there is relative motion within a fluid; in other words, viscous effects cannot exist in a fluid which is at rest. It is a pertinent fact that both liquids and gases under normal conditions display quite similar characteristics of viscous shear, regardless of the difference in molecular spacing.

While the magnitude of μ is independent of the state of motion, it is generally a function of temperature. This dependence differs considerably among the common fluids, but it is generally true that the viscosity of a gas increases with temperature, whereas that of a liquid decreases. Pressure has practically no effect upon viscosity except at very high values. Both air and water have relatively low viscosities, those of the various oils being much higher; glycerine is the most viscous of the better known fluids (roughly a thousand times as viscous as water), and its lack of color and ready miscibility with water render it of value in the laboratory as a means of producing solutions of any desired viscosity between the limits of pure water and pure glycerine.

Although viscous action is certainly a molecular phenomenon, it is basically as different from molecular attraction, which causes capillarity, as the latter is different from mass attraction. Although several theories attempt to explain capillary action, let it suffice for the present to say that all liquid molecules are presumed to exert an attractive force upon all others in their

immediate neighborhood, a force that would seem to be electrochemical in nature. At some point within a liquid medium, at an appreciable distance from a boundary, such molecular forces are necessarily in equilibrium. But at a boundary surface the forces are no longer the same on every side, so that a resultant force acts upon all surface molecules in a direction normal to the surface. In other words, superficial energy will exist at any such surface—and since its magnitude is proportional to the surface area, the surface therefore tends to contract until it has the minimum area possible. While the phenomenon might indicate an apparent tension in an imaginary surface skin, the common term “surface tension” is really a misnomer, for the lateral force at the surface is no greater than at any other point in the liquid. The magnitude of the actual “inward pull” exerted upon the surface molecules of a liquid depends not only upon the molecular attraction of the liquid molecules among themselves, but also upon the different degree of attraction between the liquid molecules and those of the boundary substance. Such a boundary might be formed by either a solid or an immiscible liquid or gas.

Assume, for instance, that a few drops of water were added to a container of nitrobenzene. Since nitrobenzene is more dense than water, and since the mutual attraction of the different molecules is less than that of the similar molecules, the water will remain on the surface in drop form. If, however, there had been added to a container of water a light oil whose internal molecular forces were less than the attraction between its molecules and those of water, the drops would have spread out on the water surface until the thickness of the oil film had reached a uniform minimum value. Similarly, drops of any liquid falling through a less dense liquid or gas will tend toward a spherical form, since a sphere has the minimum surface area per unit volume; the bubble analogy is obvious. In the case of such surface curvature, the difference between the pressure intensities on the two sides of the surface varies inversely with the radius of curvature.

If the boundary substance is a solid, the molecules of which attract the liquid molecules with a greater force than that which exists among the liquid molecules themselves, the liquid is commonly said to “wet” the solid wall; actually, the degree of wetting is variable, for it depends upon the relative value of the forces of adhesion and cohesion. Water wets glass readily, mercury to a

negligible degree. In the case of water in contact with both a solid and a gaseous boundary (for instance, water in a glass tube with a free surface exposed to air), the several forces will cause the free surface to assume a concave form, and thereby decrease the pressure just below the surface; the water must then rise in the tube to a height sufficient to balance this pressure drop. In the case of mercury, which does not wet a glass wall, the inward pull of the mercury molecules will result in a convex surface, an accompanying increase in internal pressure, and a corresponding drop in surface level. As proof of the conclusion that viscous effects are not dependent upon "adhesion" of fluid molecules to a solid wall, it must be noted that mercury displays the same property of viscous shear in boundary regions as any liquid which fully wets the boundary.

The magnitude of so-called surface tension is expressed by the factor σ (sigma), which has the dimension of force per unit length, F/L (since this is the dimensional equivalent of energy per unit area). It is not necessarily a constant for a given liquid, for it depends as well upon the other media with which the liquid is in contact.

The modulus of elasticity e of a fluid, identical with the bulk modulus of a solid, denotes the ratio between an increment of stress per unit area (pressure intensity p) and the resulting strain (relative change in volume V under this stress):

$$e = -\frac{dp}{dV/V}$$

The negative sign denotes a decrease in volume under a positive increment of pressure intensity. Since a small decrease in the original volume represents a proportional increase in the fluid density, the following relationships must hold:

$$e = \frac{dp}{d\rho/\rho} \quad \text{and} \quad \frac{dp}{e} = \frac{d\rho}{\rho}$$

The elastic modulus thus has the dimension of force per unit area, F/L^2 , and its reciprocal is a direct measure of fluid compressibility. Most liquids have a comparatively high elastic modulus, and hence are considered practically incompressible under ordinary conditions. The modulus varies with temperature, however, and also with pressure when the liquid is under

excessively high stress. The elastic modulus of a gas is relatively low, and, for adiabatic conditions (constant heat) may be found from the basic equation of thermodynamics

$$pV^k = \text{constant}$$

in which k is the adiabatic constant, equal to the ratio of the two specific heat coefficients of the gas in question ($k = c_p/c_v$).

TABLE I

Terms	Symbols	Dimensions in terms of	
		<i>L-T-M</i>	<i>L-T-F</i>
Geometrical:			
Length (any linear dimension).....	<i>L, l</i>	<i>L</i>	<i>L</i>
Area.....	<i>A</i>	<i>L</i> ²	<i>L</i> ²
Volume.....	<i>V</i>	<i>L</i> ³	<i>L</i> ³
Kinematic:			
Time.....	<i>T, t</i>	<i>T</i>	<i>T</i>
Velocity.....	<i>V, v</i>	<i>L/T</i>	<i>L/T</i>
Angular velocity.....	<i>ω</i>	<i>1/T</i>	<i>1/T</i>
Acceleration.....	<i>a, g</i>	<i>L/T</i> ²	<i>L/T</i> ²
Angular acceleration.....	<i>α</i>	<i>1/T</i> ²	<i>1/T</i> ²
Kinematic viscosity.....	<i>ν</i>	<i>L</i> ² / <i>T</i>	<i>L</i> ² / <i>T</i>
Rate of discharge.....	<i>Q</i>	<i>L</i> ³ / <i>T</i>	<i>L</i> ³ / <i>T</i>
Dynamic:			
Mass.....	<i>M</i>	<i>M</i>	<i>FT</i> ² / <i>L</i>
Force.....	<i>F</i>	<i>ML/T</i> ²	<i>F</i>
Density.....	<i>ρ</i>	<i>M/L</i> ³	<i>FT</i> ² / <i>L</i> ⁴
Specific weight.....	<i>γ</i>	<i>M/L</i> ² <i>T</i> ²	<i>F/L</i> ³
Dynamic viscosity.....	<i>μ</i>	<i>M/LT</i>	<i>FT/L</i> ²
Surface tension.....	<i>σ</i>	<i>M/T</i> ²	<i>F/L</i>
Elastic modulus.....	<i>e</i>	<i>M/LT</i> ²	<i>F/L</i> ²
Pressure intensity.....	<i>p</i>	<i>M/LT</i> ²	<i>F/L</i> ²
Momentum (and impulse).....	<i>M(I)</i>	<i>ML/T</i>	<i>FT</i>
Energy (and work).....	<i>E(W)</i>	<i>ML</i> ² / <i>T</i> ²	<i>LF</i>
Power.....	<i>P</i>	<i>ML</i> ² / <i>T</i> ³	<i>LF/T</i>

Expressed in logarithmic form this equation becomes

$$\ln p + k \ln V = \text{constant}'$$

Differentiating,

$$\frac{dp}{p} + k \frac{dV}{V} = 0 \quad \text{and} \quad \frac{dp}{p} = -k \frac{dV}{V}$$

whence

$$e = \frac{dp}{d\rho/\rho} = kp$$

Hence the elastic modulus of any gas under adiabatic conditions will depend only upon the absolute pressure intensity to which the gas is subjected and upon its adiabatic constant. Such is the case of an elastic wave. If the process is isothermal (constant temperature), on the other hand, the modulus will be exactly equal to the absolute pressure intensity:

$$e = p$$

4. Characteristics of Fluid Motion. Just as the properties of fluid matter have been defined in terms of four fundamental units, these same units may be used to describe any state of fluid motion. Corresponding to the geometrical form of a body of matter are the geometrical boundary conditions of flow—that is, the size and proportions of the fixed or moving solid boundaries of the fluid, all measurable in terms of the arbitrary length scale.

To describe the kinematics of fluid motion, it is evident that both time and length scales are necessary. Thus, the distance a fluid particle moves in a given direction per unit of time is a measure of its velocity, and its change of velocity per unit of time determines its acceleration. Similarly, the product of velocity and cross-sectional area of flow becomes a rate of discharge. Each of these dimensions is purely kinematic, in that it involves only the time and length scales; these are sufficient to describe the entire flow pattern, including the form of the paths followed by the individual fluid particles, without any knowledge of the forces causing such motion.

Once a dynamic statement of motion is required, recourse must be taken to the basic principle of mechanics—the Newtonian equation—which involves all four fundamental dimensions, any one of which is made dependent upon the other three. This principle states that the rate of change of momentum of a given mass is proportional to, and in the direction of, the acting force; or, more commonly, force is proportional to mass \times acceleration. Thus, per unit fluid volume,

$$f = \frac{d(\rho v)}{dt} = \rho a$$

Classical hydrodynamics dealt entirely with an idealized fluid assumed to be non-viscous, cohesionless, and inelastic, even the property of weight being a secondary characteristic, in that the fluid was generally presumed to extend to infinity (or to a fixed boundary) in every direction from the region under investigation; only in the study of surface waves did weight become an essential dynamic factor. In the general problem the only force which could produce an acceleration of the fluid mass was that due to a difference in pressure intensity from point to point within the fluid; thus, classical hydrodynamics was concerned essentially with the kinematic pattern of the flow (as evidenced by the velocity distribution) in its relation to the dynamic pattern (as evidenced by the distribution of pressure). Modern fluid mechanics, on the other hand, with due regard to the basic flow pattern expressed in the classical relationships, realizes that the other properties of fluid matter—weight, viscosity, surface tension, and elasticity—may sometimes modify this basic pattern to a very appreciable degree. Nevertheless, it must be remembered that classical hydrodynamics succeeded in developing a rational means of analysis only through elimination of all variables impossible to handle mathematically at one and the same time; if fluid mechanics hopes to replace these neglected characteristics, it is evident that a different means of analysis must be found before satisfactory results can be obtained.

5. The Π -Theorem. Before an attempt is made to develop a comprehensive statement of flow involving more than the basic characteristics treated in classical hydrodynamics, it is essential that the several variables be organized dimensionally in the smallest possible number of significant parametric groups. Such organization is facilitated by the fact that any mathematical equation of motion, in order to be physically correct, must be dimensionally homogeneous; that is, every term in an equation, when reduced to basic dimensions of length, time, and either force or mass, must contain identical powers of each of the respective dimensions. Thus, if one knows the variables to be included in any flow statement, one knows in addition that these variables must be so related in the statement that dimensional homogeneity will obtain.

The principal tool of dimensional analysis, by means of which one accomplishes the organization of the variables, is known

the Π (the Greek capital pi) theorem, first brought emphatically before the engineering world by Buckingham in 1915.¹ The essence of this theorem is as follows: If any variable, A_1 , depends upon the independent variables $A_2, A_3, \dots A_n$, and upon no others, the general functional relationship may be written in the form:

$$A_1 = f(A_2, A_3, \dots A_n)$$

Owing to the mathematical equilibrium between the dependent and the independent variables, these may be grouped in another functional relationship equal to zero:²

$$f'(A_1, A_2, A_3, \dots A_n) = 0$$

The Π -theorem then states that if all of these n variables may be described with m fundamental dimensional units, they may then be grouped into $n - m$ dimensionless Π -terms:

$$\varphi(\Pi_1, \Pi_2, \Pi_3, \dots \Pi_{n-m}) = 0$$

In each term there will be $m + 1$ variables, only one of which need be changed from term to term.

The variables of which each Π -term is composed must evidently appear in such exponential form that every term will be truly dimensionless. If the m repeating variables are given unknown exponents in each term, the fact that there are r fundamental dimensions with which each variable can be described at once provides a means by which these unknowns may be determined.

In general, the only variables that can influence fluid motion are of the following three categories: (1) the several linear dimensions fully defining the geometrical boundary conditions— a, b, c, d , etc.; (2) kinematic and dynamic characteristics of flow—a mean velocity V (or a rate of discharge Q or, less frequently, a time or an acceleration), and a pressure increment Δp or gradient dp/dx (or a resisting force, or an intensity of shear); and (3) the fluid properties of density, ρ , specific weight, γ , viscosity, μ , surface

¹ BUCKINGHAM, E., Model Experiments and the Forms of Empirical Equations, *Trans. A.S.M.E.*, vol. 37, 1915.

² Should this conversion at first puzzle the reader, he need only consider a simple example: $x = f(y) = y^2$; whence, $x - y^2 = f'(x, y) = 0$.

ension, σ , and elastic modulus, e . Assuming, for illustration, that each of these characteristics is involved in the motion to be investigated, then

$$f'(a, b, c, d, V, \Delta p, \rho, \gamma, \mu, \sigma, e) = 0$$

Since there are three fundamental dimensions in fluid mechanics (either L - T - M or L - T - F) and eleven variables, the final functional relationship must contain eight Π -terms, and three variables must be common to each. It is usually expedient to select for these three a representative length together with velocity and density, the remaining eight variables appearing separately in the eight groups; the latter are given, for convenience, the exponent -1 , the others, unknown exponents whose magnitudes are still to be determined:

$$\varphi(\Pi_1, \Pi_2, \Pi_3, \Pi_4, \Pi_5, \Pi_6, \Pi_7, \Pi_8) = 0$$

in which

$$\begin{aligned} \Pi_1 &= a^{x_1} V^{y_1} \rho^{z_1} b^{-1} & \Pi_2 &= a^{x_2} V^{y_2} \rho^{z_2} c^{-1} & \Pi_3 &= a^{x_3} V^{y_3} \rho^{z_3} d^{-1}; \\ \Pi_4 &= a^{x_4} V^{y_4} \rho^{z_4} \Delta p^{-1} & \Pi_5 &= a^{x_5} V^{y_5} \rho^{z_5} \gamma^{-1} & \Pi_6 &= a^{x_6} V^{y_6} \rho^{z_6} \mu^{-1}; \\ \Pi_7 &= a^{x_7} V^{y_7} \rho^{z_7} \sigma^{-1} & \Pi_8 &= a^{x_8} V^{y_8} \rho^{z_8} e^{-1} \end{aligned}$$

To yield dimensionless Π -terms, these unknown exponents must be such that if each variable is replaced by the corresponding combination of L , T , and M or F , the exponent of each independent dimension will finally reduce to zero. The solution thus becomes one of simultaneous linear equations:

$$\begin{aligned} \Pi_1: \quad (L)^{x_1} \left(\frac{L}{T}\right)^{y_1} \left(\frac{M}{L^3}\right)^{z_1} (L)^{-1} &= L^0 T^0 M^0 \\ L: \quad x_1 + y_1 - 3z_1 - 1 &= 0 \\ T: \quad -y_1 &= 0 \\ M: \quad z_1 &= 0 \\ x_1 = 1; \quad y_1 = 0; \quad z_1 = 0 \\ \Pi_1 &= \frac{a}{b} \end{aligned}$$

Evidently, if two variables of like dimension appear together in a group, the other variables disappear; hence Π_2 and Π_3 may be written by inspection:

$$\Pi_2 = \frac{a}{c}; \quad \Pi_3 = \frac{a}{d}.$$

The remaining Π -terms are determined as follows:

$$\begin{aligned} \Pi_4: \quad (L)^{x_4} \left(\frac{L}{T} \right)^{y_4} \left(\frac{M}{J^3} \right)^{z_4} \left(\frac{M}{LT^2} \right)^{-1} &= L^0 T^0 M^0 \\ L: \quad x_4 + y_4 - 3z_4 + 1 &= 0 \\ T: \quad \quad \quad - y_4 + 2 &= 0 \\ M: \quad \quad \quad \quad \quad z_4 - 1 &= 0 \\ x_4 = 0; \quad y_4 = 2; \quad z_4 = 1 & \\ \Pi_4 = \frac{V^2}{\Delta p / \rho} & \end{aligned}$$

$$\begin{aligned} \Pi_5: \quad (L)^{x_5} \left(\frac{L}{T} \right)^{y_5} \left(\frac{M}{L^3} \right)^{z_5} \left(\frac{M}{J^2 T^2} \right)^{-1} &= L^0 T^0 M^0 \\ L: \quad x_5 + y_5 - 3z_5 + 2 &= 0 \\ T: \quad \quad \quad - y_5 + 2 &= 0 \\ M: \quad \quad \quad \quad \quad z_5 - 1 &= 0 \\ x_5 = -1; \quad y_5 = 2; \quad z_5 = 1 & \\ \Pi_5 = \frac{V^2/a}{\gamma/\rho} & \end{aligned}$$

$$\begin{aligned} \Pi_6: \quad (L)^{x_6} \left(\frac{L}{T} \right)^{y_6} \left(\frac{M}{L^3} \right)^{z_6} \left(\frac{M}{LT} \right)^{-1} &= L^0 T^0 M^0 \\ L: \quad x_6 + y_6 - 3z_6 + 1 &= 0 \\ T: \quad \quad \quad - y_6 + 1 &= 0 \\ M: \quad \quad \quad \quad \quad z_6 - 1 &= 0 \\ x_6 = 1; \quad y_6 = 1; \quad z_6 = 1 & \\ \Pi_6 = \frac{Va}{\mu/\rho} & \end{aligned}$$

$$\begin{aligned} \Pi_7: \quad (L)^{x_7} \left(\frac{L}{T} \right)^{y_7} \left(\frac{M}{L^3} \right)^{z_7} \left(\frac{M}{T^2} \right)^{-1} &= L^0 T^0 M^0 \\ L: \quad x_7 + y_7 - 3z_7 &= 0 \\ T: \quad \quad \quad - y_7 + 2 &= 0 \\ M: \quad \quad \quad \quad \quad z_7 - 1 &= 0 \\ x_7 = 1; \quad y_7 = 2; \quad z_7 = 1 & \\ \Pi_7 = \frac{V^2 a}{\sigma/\rho} & \end{aligned}$$

$$\Pi_8: (L)^{x_8} \left(\frac{L}{T}\right)^{y_8} \left(\frac{M}{L^3}\right)^{z_8} \left(\frac{M}{LT^2}\right)^{-1} = L^0 T^0 M^0$$

$$\begin{aligned} L: & \quad x_8 + y_8 - 3z_8 + 1 = 0 \\ T: & \quad -y_8 + 2 = 0 \\ M: & \quad z_8 - 1 = 0 \\ x_8 = 0; & \quad y_8 = 2; \quad z_8 = 1 \\ \Pi_8 = & \quad \frac{V^2}{e/\rho} \end{aligned}$$

Introduction of these dimensionless groups of variables in the original expression results in the following significant relationship:

$$\varphi\left(\frac{a}{b}, \frac{a}{c}, \frac{a}{d}, \frac{V^2}{\Delta p/\rho}, \frac{V^2/a}{\gamma/\rho}, \frac{Va}{\mu/\rho}, \frac{V^2 a}{\sigma/\rho}, \frac{V^2}{e/\rho}\right) = 0$$

It is evident from the basic statement of the Π -theorem that this is not by any means the only possible grouping of the variables that will yield a dimensionally correct functional relationship, for aside from the several length characteristics, any three variables might have been selected to appear in each of the Π -terms. The fundamental significance of the choice that was made, however, is that this led to three basically different types of dimensionless parameters: (1) those defining the boundary conditions; (2) one characterizing the basic flow pattern of classical hydrodynamics; and finally (3) those four pertaining to the action of weight, viscosity, surface tension, and elasticity—the latter being known, respectively, as the Froude, Reynolds, Weber, and Cauchy numbers:

$$\mathbf{F} = \frac{V^2/a}{\gamma/\rho}; \quad \mathbf{R} = \frac{Va}{\mu/\rho}; \quad \mathbf{W} = \frac{V^2 a}{\sigma/\rho}; \quad \mathbf{C} = \frac{V^2}{e/\rho}$$

Although any of the foregoing Π -terms might be considered the dependent variable, the only logical choice is that containing the essential characteristics of the flow itself; thus

$$\frac{V^2}{\Delta p/\rho} = C\varphi'\left(\frac{a}{b}, \frac{a}{c}, \frac{a}{d}, \mathbf{F}, \mathbf{R}, \mathbf{W}, \mathbf{C}\right)$$

in which C is a constant numerical factor quite independent of the choice of dimensional units and of the variation of the Π -terms; φ' is also free from dimensional influence, provided that all variables in the relationship be expressed in units of the same

dimensional system. Of the several members of the dependent term, any one may now be chosen as the one whose variation is to be studied; for instance,

$$V = C' \varphi'' \left(\frac{a}{b}, \frac{a}{c}, \frac{a}{d}, \mathbf{F}, \mathbf{R}, \mathbf{W}, \mathbf{C} \right) \sqrt{\frac{\Delta p}{\rho}}$$

this velocity being readily convertible to a rate of discharge through multiplication of both sides of the equation by the corresponding flow area (the latter must be expressible in terms of the repeating length a).

Inspection of this general expression will show that it really incorporates a statement of flow conditions as found in classical hydrodynamics

$$V = C' \sqrt{\frac{\Delta p}{\rho}}$$

corrected to actual conditions by a variable factor φ'' , which depends upon the influence of the several force properties of the fluid. As yet no information is given as to the form of the function or the magnitude of the numerical constant C' ; nevertheless, the Π -theorem has well served its purpose in reducing the number of essential terms through systematic grouping, and has in addition yielded parameters quite independent of dimensional units. It now remains either to further analytical study or to experimental investigation to determine the characteristics of the function.

6. Typical Applications. Assume first that it is desired to develop an expression for discharge into the atmosphere from a circular orifice in a very large closed tank; if it is assumed, as in classical hydrodynamics, that the velocity of efflux is a function simply of fluid density and difference in pressure intensity within the tank and without,

$$V = \varphi'(\rho, \Delta p)$$

Since there are only three variables, there can be but one Π -term, and

$$\varphi_1(\Pi) = \varphi_1 \left(\frac{V^2}{\Delta p / \rho} \right) = 0$$

The fact that the function is zero indicates merely that the Π -term itself is equal to some numerical constant:

$$\frac{V^2}{\Delta p / \rho} = C$$

This relationship readers will recognize as the basic equation of orifice discharge, in which C is—for the assumed case of flow—equal to 2. By introducing the orifice area, $\frac{1}{4}\pi d^2$, and a numerical factor C_c representing the reduction in jet area at the contracted section,

$$Q = C_c \frac{\pi d^2}{4} \sqrt{\frac{2\Delta p}{\rho}}$$

Methods of classical hydrodynamics have shown that C_c for flow from a very large tank must have the value $\frac{\pi}{\pi + 2} = 0.611$.

Further analyses by von Mises have determined C_c as a function of the geometrical proportions of the tank for a wide range of shapes and sizes; as such, the various tank dimensions being simply lengths,

$$C_c = \frac{\pi}{\pi + 2} \varphi_2\left(\frac{d}{a}, \frac{d}{b}, \text{etc.}\right)$$

It is a well-known fact that the effect of weight on the rate of discharge is appreciable only if the velocity of efflux is very low; in such a case the downward deflection of the jet may cause a marked deformation of the otherwise symmetrical contraction even very close to the orifice itself. Under such circumstances, γ is an additional variable, and, for limiting boundary conditions,

$$C_c = \frac{\pi}{\pi + 2} \varphi_3(\mathbf{F})$$

Nevertheless, even though the flow boundaries do not vary in form and the velocity of efflux is high enough to yield a symmetrical jet near the orifice, experimental evidence will show that the factor C in the basic equation is actually a variable, $2C_c^2$. Realization that viscous influences may play an appreciable role then leads to the relationship, again for limiting boundary conditions,

$$Q = C_d \frac{\pi d^2}{4} \sqrt{\frac{2\Delta p}{\rho}}; \quad C_d = C_c C_v = \frac{\pi}{\pi + 2} \varphi_4(\mathbf{R})$$

As a matter of fact, a plot of experimental data for C_d against the Reynolds number not only substantiates this expression but yields a single curve along which fall all measured values for fluids as widely different as water, air, oil, and water-glycerine mixtures.

If one recalls that the action of capillary forces becomes the more appreciable as the curvature of a liquid surface increases, one might venture the opinion that in jets of small diameter the contraction would be altered, due not only to a sort of "elastic stocking" influence, but to the failure of the fluid to spring free directly at the orifice edge. Indeed, preliminary investigation of the discharge coefficient as a function of the Weber number points directly to the truth of this reasoning.

On combining these several influences in a single expression,

$$C_d = \frac{\pi}{\pi + 2} \varphi\left(\frac{d}{a}, \frac{d}{b}, \text{etc.}, \mathbf{F}, \mathbf{R}, \mathbf{W}\right)$$

whence it is clear that the actual function can be no simple one; not only does C_d vary individually with each parameter, but the variation of all together becomes hopelessly involved. Analytical treatment can succeed only by neglecting secondary effects, the results then being useful only under conditions in which such effects actually are relatively unimportant. Thus, weight is negligible at all except small Froude numbers; viscosity is of great importance only at small Reynolds numbers; and only if the Weber number is small need surface tension be considered.

In the foregoing example it was tacitly assumed that the outlines of the approaching flow were determined entirely by fixed boundaries—thus, there could exist no free surface inside the tank, the elevation of which above the orifice would determine the pressure intensity p ; the latter case would make one of the geometrical boundary conditions dependent upon pressure intensity (or vice versa), and the relationship would then contain two dependent variables, a condition contrary to the proper application of the II-theorem. Such a case is illustrated by gravity discharge over a weir. This problem would be handled exactly as the orifice problem, with the one exception that pressure intensity would necessarily have to be dropped from the

expression. A little reflection will show that in the case of a free surface, when the flow is caused by weight itself, the hydrostatic pressure, and any variation therefrom because of acceleration, will be due to weight as the motivating agent. Under such conditions the Froude number is selected as the dependent variable, the discharge coefficient for weirs, spillways, and sluice gates then depending primarily upon the geometrical parameters, and to a lesser degree upon the Reynolds and Weber numbers.

As a second illustration, take the case of flow through a circular pipe. If the motion is a laminar one, density will play no part, and the only variables are the pipe diameter, the mean velocity, the pressure gradient, and viscosity:

$$f\left(D, V, \frac{dp}{dx}, \mu\right) = 0$$

With only four variables, there can be but one Π -term, and this must have the form,

$$\Pi = \frac{D^2 dp/dx}{V\mu} = \text{constant}$$

There being so few variables, simple mathematical analysis can prove that the numerical constant must equal 32, as will be shown at a later point.

If the flow is turbulent, the eddies involve a continuous acceleration and deceleration of small fluid masses, the effect of which on the flow will depend upon the density of the fluid. Assuming, furthermore, that the roughness of the pipe walls can be described by a single linear parameter, k , the function will be:

$$f\left(D, V, \rho, \frac{dp}{dx}, \mu, k\right) = 0$$

Application of the Π -theorem will yield the following dimensionless groups:

$$\varphi\left(\frac{\rho V^2}{D dp/dx}, \frac{VD}{\mu/\rho}, \frac{D}{k}\right) = 0$$

whence

$$\frac{dp}{dx} = C\varphi'\left(\frac{VD}{\mu/\rho}, \frac{D}{k}\right)\frac{\rho V^2}{D}$$

Since the dependent Π -term is a function of two variables, the form of the function might best be shown by means of a three-dimensional plot; however, the most common procedure is to plot φ' as ordinate and \mathbf{R} as abscissa, with a separate curve for each value of the relative roughness D/k .

Flow in open channels is a much more difficult problem to handle because of the many new variables involved—shape of cross section, non-uniformity of depth, presence of sediment as bed and suspended load, and so forth. For the present it must suffice to say that, as in the case of weirs, the pressure gradient must be omitted, and in addition there must be introduced a further geometrical characteristic, channel slope. In the case of a very wide channel with uniform depth y and no bed load, the function would then be

$$\varphi\left(\frac{V^2 y}{\gamma/\rho}, S, \frac{Vy}{\mu/\rho}, \frac{y}{k}\right) = 0$$

It may be shown analytically that V will vary with \sqrt{S} , the above function then taking the form

$$V = C\varphi'\left(\mathbf{R}, \frac{y}{k}\right)\sqrt{\frac{\gamma}{\rho}yS}$$

As a final example, consider the resistance of a body moving fully immersed in a fluid. The resultant force F exerted by the fluid during relative motion will depend upon the geometrical form of the body, the roughness of its surface, the relative velocity, and the fluid density and viscosity. For a given geometrical form and roughness, a single length will suffice for the basic function:

$$F = f(D, V, \rho, \mu)$$

As there are five variables, there will be two Π -terms:

$$\varphi\left(\frac{F}{\rho V^2 D^2}, \frac{VD}{\mu/\rho}\right) = 0$$

whence

$$F = C_1\varphi_1(\mathbf{R})D^2\rho V^2$$

In the case of a gas, it is quite possible for the relative velocity to approach and even exceed the acoustic velocity; not only will

the fluid density then change appreciably, but the formation of elastic waves will augment the resistance, conditions which are often encountered in the case of projectiles and airplane propellers. In such instances the elastic modulus of the gas must be included in the basic statement. The function will then be

$$F = C_2 \varphi_2(\mathbf{R}, \mathbf{C}) D^2 \rho V^2$$

On the other hand, if the body moves in a liquid close to the free surface, gravity and capillary waves will be formed and will add to the resistance exactly as in the case of elastic waves; the specific weight and surface tension of the fluid then belong in the statement of flow:

$$F = C_3 \varphi_3(\mathbf{R}, \mathbf{F}, \mathbf{W}) D^2 \rho V^2$$

The form of this function is of basic importance in studying the resistance of ships, although the Weber number is significant only if the linear dimensions (a ship model, for instance) are very small.

In the light of parameters referring to wave motion, it will be interesting to note a pertinent similarity of the Froude, Weber, and Cauchy numbers; when written in the form

$$\mathbf{F} = \frac{V}{\sqrt{L\gamma/\rho}}; \quad \mathbf{W} = \frac{V}{\sqrt{\sigma/\rho L}}; \quad \mathbf{C} = \frac{V}{\sqrt{e/\rho}}$$

these parameters represent the ratio of the actual velocity of flow to that of a gravity, capillary, and elastic wave, respectively. The Reynolds number is related in so far as viscous action plays a predominant role, if not always in the formation, at least in the subsequent gradual demise of any type of fluid wave.

So long as the motion of a homogeneous fluid is studied in this manner, the method of treatment follows the foregoing general pattern. By no means infallible, dimensional analysis will not automatically correct for the investigator's failure to include all independent variables, nor for his overenthusiasm in including more than one dependent variable. On the other hand, too many independent variables will only serve to clutter up the equation, for experimental trial will finally show which of these are actually essential to the relationship. Needless to say, a certain understanding of fluid principles is essential to proper use of the

Π -theorem, coupled with a good share of common sense and ingenuity. Moreover, while the foregoing choice of repeating variables to be used in each of the Π -terms is by far the most logical, it sometimes happens that a more ingenious selection will disclose a functional relationship that has definite bearing upon further analytical study—such a case will be noted in a later section on flow in pipes.

That phase of hydraulic engineering having to do with river regulation is concerned to an ever-increasing degree with the movement of sediment. Once such foreign matter is carried by a fluid—whether as suspended or bed load—it is no longer possible to treat the flowing matter as homogeneous and having only those characteristics already outlined. It becomes essential to add a number of new variables to the functional relationship, variables fully describing the characteristics of the fluid mixture; these involve either the density or specific weight of the material in the fluid, together with parameters defining the particle size, grading, and possibly shape. To date such parameters have been chosen on purely empirical grounds, which has made the dimensional study of sediment transportation at best a haphazard process.

7. Similitude. Of recent years the popularity of hydraulic model studies has served to emphasize—if not exaggerate—the efficacy of small-scale experiments in designing and studying the probable behavior of hydraulic structures. Through use of models often a hundredfold reduced in size from natural scale, it is possible to experiment at low expense and without undue waste of time until the most favorable conditions of flow are realized, qualitative—and often quantitative—observations being significant when converted to the dimensions of the full-scale prototype.

Since a model has no prescribed scale relation, and since the investigator is not required to use the same fluid for the model as will flow in the prototype, it is evident that the model may be larger, smaller, or even the same size, and that the choice of both geometrical scale and fluid will be limited only by practical considerations. What, then, are the principles governing model construction and operation?

It should be evident to the reader that, for the type of flow to be realized in the prototype, there will exist a functional relation-

ship among the several variables pertinent to the case in question ---these variables including the geometrical boundary dimensions, the characteristics of flow, and the fluid properties, all of which may be grouped together in a number of dimensionless parameters or Π -terms. If true mechanical similarity is to exist between flow in the prototype and flow in its model, every dimensionless parameter referring to conditions in the model must have the same numerical magnitude as the corresponding parameter referring to the prototype. Since all geometrical Π -terms must then be the same in both cases, it is evident that model and prototype must be completely similar geometrically; the flow characteristics will then be similar if the fluid properties are such that the Froude, Reynolds, Weber, and Cauchy numbers (or whichever of these have bearing upon the phenomenon) are respectively equal in both cases. Once this condition is established, the characteristics of flow may be varied at will without destroying the similarity between prototype and model.

One is accustomed to think of the model scale simply as the ratio of corresponding geometrical dimensions of model and prototype. Nevertheless, dimensional considerations will show that a change in the length scale is impossible without due regard for the scales of time, mass, and force. Thus, a true model---illustrated, for instance, by some Lilliputian (or Brobdingnagian) water system---would have its own units of length, time, force, and mass, each of which would have its respective numerical ratio to the corresponding unit in our own system. Evidently, knowledge of the ratios of any three of these scales would automatically permit determination of the fourth. One may thus think of the foot or the second in the model world as some fraction or multiple of that in our own world; or, more conveniently, one may simply treat all model dimensions as some fraction of those of the prototype, each measured according to the same standard dimensional units. Thus, the model: prototype scales may refer to the ratios of dimensional units or of actual dimensional measurements; for instance, in a 1:25 pipe model, one may speak of the prototype pipe as being five prototype feet in diameter and the model pipe as being five model feet (each $\frac{1}{25}$ of a prototype foot) in diameter, or of the prototype pipe as having a diameter of five feet and the model a diameter of $\frac{1}{5}$ foot. The latter is by far the more common practice.

While it is fully correct to deal directly with the length, time, force, and mass scales (any three of which are arbitrary), this method will prove far more cumbersome than adopting a scale of length and a separate scale for each of the fluid properties. This is because the choice of any model fluid at once fixes every fluid property, thereby establishing once and for all the scales of mass and force.

Once the length scale and the prototype and model fluids are chosen, there is but one time scale that will permit full similarity of flow in the two systems. Although one might use such a scale by itself to measure the corresponding intervals required to discharge similar volumes in the two systems or to measure the time of transit of floats, it is far more pertinent to combine this time scale with the others to measure corresponding velocities, accelerations, pressures, and so forth; in fact, since the time scale is the dependent one, it may be replaced through a combination of the other three, the mass and force scales being inherent parts of the fluid-property scales, and the length scale remaining arbitrary.

In the Table II the reader will find a list of the more common flow characteristics—namely, velocity, acceleration, rate of

TABLE II

Flow characteristic	Dimension in terms of $L-M-F$	Scale			
		(1)	(2)	(3)	(4)
		F	R	W	C
Length.....	L	λ	λ	λ	λ
Time.....	$(LM/F)^{\frac{1}{2}}$	$\frac{\lambda^{\frac{1}{2}}}{(\gamma_s/\rho_s)^{\frac{1}{2}}}$	$\frac{\lambda^{\frac{1}{2}}}{\mu_s/\rho_s}$	$\frac{\lambda^{\frac{1}{2}}}{(\sigma_s/\rho_s)^{\frac{1}{2}}}$	$\frac{\lambda}{(e_s/\rho_s)^{\frac{1}{2}}}$
Velocity.....	$(LF/M)^{\frac{1}{2}}$	$\lambda^{\frac{1}{2}}(\gamma_s/\rho_s)^{\frac{1}{2}}$	$\frac{\mu_s/\rho_s}{\lambda}$	$\frac{(\sigma_s/\rho_s)^{\frac{1}{2}}}{\lambda^{\frac{1}{2}}}$	$(e_s/\rho_s)^{\frac{1}{2}}$
Acceleration.....	F/M	γ_s/ρ_s	$\frac{(\mu_s/\rho_s)^2}{\lambda^3}$	$\frac{\sigma_s/\rho_s}{\lambda^2}$	$\frac{e_s/\rho_s}{\lambda}$
Discharge.....	$(L^3F/M)^{\frac{1}{2}}$	$\lambda^{\frac{3}{2}}(\gamma_s/\rho_s)^{\frac{1}{2}}$	$\lambda \cdot \mu_s/\rho_s$	$\lambda^{\frac{3}{2}}(\sigma_s/\rho_s)^{\frac{1}{2}}$	$\lambda^{\frac{3}{2}}(e_s/\rho_s)^{\frac{1}{2}}$
Pressure intensity.....	F/L^2	$\lambda \gamma_s$	$\frac{\mu_s^2}{\lambda^2 \rho_s}$	$\frac{\sigma_s}{\lambda}$	e_s
Energy.....	LF	$\lambda^2 \gamma_s$	$\frac{\lambda \mu_s^2}{\rho_s}$	$\lambda^2 \sigma_s$	$\lambda^2 e_s$
Momentum.....	$(LMF)^{\frac{1}{2}}$	$\lambda^{\frac{1}{2}} \gamma_s^{\frac{1}{2}} \rho_s^{\frac{1}{2}}$	$\lambda^2 \mu_s$	$\lambda^{\frac{1}{2}} \sigma_s^{\frac{1}{2}} \rho_s^{\frac{1}{2}}$	$\lambda^{\frac{1}{2}} e_s^{\frac{1}{2}} \rho_s^{\frac{1}{2}}$

discharge, pressure intensity, energy, and momentum—each with its fundamental dimension taken from Table I. Designating by λ (lambda) the numerical value of the selected length scale (such as $\lambda = L_m/L_p = 1/25$), and by $\rho_s, \gamma_s, \mu_s, \sigma_s$, and c_s the numerical values of the corresponding fluid property scales, there is tabulated the combination of these scales according to which the flow characteristics must vary to insure complete similarity. Considerable insight will be gained by the reader through verification of these values.

It will be noted at once that each characteristic must vary in quite a different manner, depending upon which force property of the fluid governs the flow. Whenever the phenomenon is influenced by only one such property, the procedure is then quite straightforward. In particular is this true of weight; since most model studies are conducted under gravitational conditions similar to those under which the prototype will function, despite use of different fluids the ratio of specific weight to density will be identical in both systems—under such circumstances the ratio γ_s/ρ_s is unity, leaving such quantities as time, velocity, and discharge dependent only upon λ .

If two force properties play essential roles in the flow to be studied by model, the problem is not so simple. Assume, for instance, that a certain type of fluid motion involves the action of weight and viscosity; since any flow characteristic is then determined by both weight and viscosity criteria as shown in the corresponding columns, equating any two of these values will yield the following essential relationship:

$$\frac{\gamma_s}{\rho_s} = \frac{(\mu_s/\rho_s)^2}{\lambda^3} \quad \text{and} \quad \lambda^3 = \frac{(\mu_s/\rho_s)^2}{\gamma_s/\rho_s}$$

If the gravitational conditions for model and prototype are the same, the factor γ_s/ρ_s may be dropped from the relationship. whereupon

$$\frac{\mu_s}{\rho_s} = \lambda^{3/2}$$

That is, similarity is possible only if the fluids are so chosen that the ratio of the viscosity and density scales equals the $3/2$ power of the length scale.

Similar operations may be performed for any other pair of force properties, these steps being left for the reader's practice. Once three or more force properties are involved, however, such solution is mathematically impossible, as the reader will be convinced after a single trial. That is, when more than two force properties of a fluid appreciably influence some phenomenon of flow, it is impossible to obtain a true model on any but the same scale using any but the same fluid as in the prototype. Since hydraulic models are often operated with the same fluid—water—and under the same conditions as in the prototype, it is thus evident that only if a single force property is involved will it be possible to have model and prototype of different size.

The reader will long since have noted that the several force properties of matter often appear in their ratio to density. Each of these ratios will be found to have purely kinematic dimensional qualities, and although each depends upon two distinct fluid properties, it is often convenient to treat the ratios as significant characteristics. Thus, γ/ρ is commonly known as g , the acceleration of gravity. Similarly, μ/ρ is called the kinematic viscosity and given the symbol ν (nu). The ratio σ/ρ has neither name nor symbol, although it might properly be called the kinematic surface tension. The square root of the ratio e/ρ is generally designated by the symbol c , the acoustic velocity, or velocity of an elastic wave. The reader is cautioned to regard these ratios purely as derived quantities, lest confusion result in the more general application of dimensional analysis.

Since in the majority of hydraulic engineering problems the influence of fluid weight is greater than that of the other force properties, the flow characteristics in the operation of hydraulic models are usually determined through use of the Froude criterion alone. Water is used in the model as in the prototype, and since the factor g is generally the same for both model and prototype, these flow characteristics follow the simplified form of column 1 in Table II. Needless to say, such procedure permits simple control of the model behavior, and hydraulic model experiments under these conditions have come into world prominence in recent years.

Were the actual conditions governing model performance as straightforward as this, the investigator might well rest assured that tests on his model structure would yield quantitative results

accurately transferable to the prototype scale. The foregoing considerations, however, have shown that true similitude is generally impossible when one and the same fluid is used, for it seldom happens that only one force property is brought into play. Even if one could reproduce the geometrical characteristics to true model scale (such characteristics including surface roughness as well as structural form), too great a reduction in scale would most certainly make viscous and capillary action of appreciable importance. Yet so partial have many model laboratories become to the Froude number alone, that resulting discrepancies between model and prototype behavior are blamed upon imperfections—or “limitations”—of the theory of similitude.

Nevertheless, from the purely practical viewpoint, it is evident that however much one may strive after absolute similarity, its attainment is not always economically feasible. In such instances as turbine and pump studies, the investigation of pipes and pipe meters, or the testing of air and underwater craft, the fact that of the force properties usually viscosity alone can influence the flow at once enables the investigator so to choose his model fluid that the model velocities are of convenient magnitude. But the operation of hydraulic models in which a free surface is involved adds to the action of viscosity that of weight and surface tension—each to a different degree—so that accurate quantitative results are practically impossible.

Under such conditions, it is illogical to seek strict similitude—in particular since the cost of any fluid other than water for such studies will nearly always prove prohibitive. Instead, the investigator aims at qualitative indications of prototype performance, so governing the model slopes and discharges that the salient features of the flow are as similar as possible. Thus, if flow in the prototype is turbulent, that in the model must also be turbulent; if the prototype velocity is above the wave velocity, that of the model must also be above the wave velocity, and vice versa; if cavitation occurs in the prototype, the model behavior will be of value only if cavitation also takes place; if surface currents are of importance in the prototype, the influence of surface tension in the model must not be sufficient to distort the flow pattern.

Great reduction of scale in river models often leads to appreciable viscous and capillary influence in the very shallow regions

of flow, which obviously renders the model performance exceedingly open to doubt even so far as qualitative results are concerned. In such instances it is common practice to construct the model at a distorted scale, the vertical dimensions being reduced less than the horizontal in order to produce a relatively deeper channel. Thus, strict geometrical similarity, already sacrificed through necessary change in slope, then exists only as far as the plan of the model layout is concerned; only through extreme care may the investigator hope for dependable indications from such model behavior, for the free surface in regions of rapid acceleration will by no means follow his scheme of scale distortion.

The difficulties of true model similarity become all the more insurmountable in the case of river models with movable bed. Sediment cannot be reduced according to the geometrical scale without giving rise to suspension and flocculation as the scale becomes very small; hence, the model laboratories have been forced either to use sand mixtures such as occur in natural rivers, or to find other materials that better suit their purpose; for example, such substances as pulverized coal, punice, and amber have long since proved their worth in this respect. Since the totally different relative roughness in model and prototype now entails even further compensating change in surface slope and vertical scale, the investigator can hope to obtain qualitative similarity in only one general feature of the flow—the movement of the bed. In a straight flume the velocity-slope relationship is first found which will cause the chosen model sediment to move in characteristic bars for the given range of depth from low to high water. These factors, and in addition the high- and low-water time scale, are then adjusted in the actual model until it is possible to reproduce, qualitatively, known past stages of the bed development in the prototype, whereupon it is assumed that those modifications to be investigated will not disturb the degree of similarity. While the research world is slowly attacking the sediment problem from the analytical point of view (as a question of functional relationship rather than similitude), it will be evident to the reader that present methods of approach are at best empirical.

8. Classification of Flow Phenomena. Dimensional considerations have been seen to provide a logical means of subdividing the field of fluid mechanics, and hence might well serve as a guide

in presenting a systematic discussion of the various aspects of the science. Thus, from the geometrical standpoint, the different types of flow may be classed according to the boundary conditions; from the kinematic standpoint, according to the conditions of acceleration, *i.e.*, whether the flow is uniform or non-uniform, steady or unsteady; and from the dynamic point of view, according to the fluid property having the predominant influence upon the flow. Of these several criteria, one must be selected as a primary means of classification, the other two then serving as major and minor subdivisions.

Empirical hydraulics has perforce classified the various types of flow according to the boundary conditions, with the result that frequently no connection is apparent between definitely related phenomena. It is the purpose of fluid mechanics, on the contrary, to correlate existing knowledge—including that offered by empirical hydraulics—to the end of producing a soundly unified and coherent system of reasoning. For the purpose of the present volume, therefore, it has been deemed wisest to regard the dynamic aspects of flow as fundamental, fluid properties thereby playing predominant roles. It would then seem in order to treat, in turn, phenomena in which density, specific weight, viscosity, surface tension, and elasticity determine the essential pattern of motion. Yet, while rigorous adherence to such a plan might be the most systematic course, certain features of actual motion make advisable a slight departure from this procedure—in particular since in any problem of actual motion more than one fluid property is almost certain to be involved. Therefore, in order to permit a logical development of the final picture, the following method has been adopted.

While classical hydrodynamics stressed the interrelationship of density, pressure, and velocity—with little regard to the actual force properties of the fluid—the fundamental equations of hydrodynamics suffer no essential change if the action of fluid weight is considered from the outset. Part One, therefore, stresses the basic mechanics of motion, selecting from the classical treatment all that is immediately useful or will have bearing upon later developments; by giving due regard to fluid weight, such treatment is made applicable alike to confined flow and flow with a free surface. Part Two expands these basic principles by introducing the effect of viscosity, emphasizing first those cases

in which viscous action predominates, and finally those in which it is but one of the several influences determining the resultant flow pattern. Yet since capillary action and elasticity are definitely minor fluid properties, in so far as the interests of this book are concerned, such individual treatment of these is quite unwarranted. On the other hand, since the field of wave motion is not only of distinct importance to the engineer, but provides, as well, an excellent means of comparing the action of the several force properties, Part Three is devoted entirely to this purpose. Wave mechanics is first stressed in its general aspects, following which the individual effects of viscosity, elasticity, specific weight, and surface tension are discussed in such detail as is warranted by their relative importance. In every case, subdivision according to geometrical and kinematic aspects has been so devised as to coordinate—rather than isolate—specific problems of motion in the various fields.

PART ONE
FUNDAMENTALS OF HYDROMECHANICS

CHAPTER II

ELEMENTARY PRINCIPLES OF FLOW

9. Velocity of a Fluid Particle as a Function of Time and Space. Any fluid may be imagined to consist of innumerable small but finite particles, each having a volume so slight as to be negligible when compared with the total volume of the fluid, yet sufficiently large to be considered homogeneous in constitution. Since these fluid particles must be in constant contact with each other, true impact between particles is physically impossible; it follows that any relative motion within the fluid will generally involve both rotation and deformation of each individual particle.

Each particle at any instant of time will have its own particular velocity, which will generally vary as it travels from point to point; moreover, the velocity of successive particles passing a fixed point is likewise a variable in the most general case. The Lagrangian method of attack studies the behavior of a given fluid particle during its motion through space; opposed to this is the method of Euler, which observes the flow characteristics in the immediate vicinity of a given point as the particles pass by. While perhaps not so descriptive of the fate of the individual particle, equations of motion obtained by the Eulerian method lend themselves more readily to practical use.

Unlike scalar quantities, such as length or time, velocity and acceleration may vary in direction as well as in magnitude; they are, therefore, true vectors, with components in each of three coordinate directions. Variation with time of any vector quantity may result from a change either in direction or in magnitude—or in both—of the vector itself. However, knowledge of vector analysis is not essential to the study of fluid motion, for the variation of a vector may be fully described by the changes in magnitude of its three components.

What is known in hydromechanics as a stream line is an imaginary curve connecting a series of particles in a moving fluid in such manner that at a given instant the velocity vector of

every particle on that line is tangent to it (Fig. 1). In uniform flow the magnitude and direction of the velocity vector are constant over the entire length of any stream line at any instant; in other words, all stream lines remain parallel to one another, the distinction between uniformity and non-uniformity referring specifically to the geometry of the flow pattern. On the other hand, regardless of the relative form of the stream lines, if the flow is steady there may be no variation with time in either magnitude or direction of the velocity vector at any stationary point in the space through which the fluid moves.

It follows that a flow which is non-uniform and unsteady shows velocity variation both with distance and with time; that is, the velocity of fluid particles changes from point to

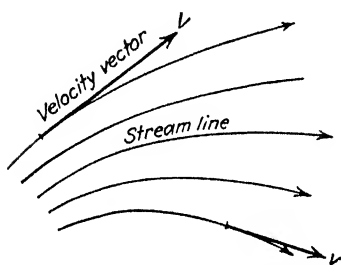


FIG. 1.—Stream lines.

point, and the velocity of the particles passing any given point changes from instant to instant. This is the most general case, and may be described mathematically by the expression

$$v = f(t, x, y, z)$$

which states simply that the velocity vector is a function of time

and of position with respect to the three coordinate axes. It is evident that in unsteady, non-uniform motion the entire flow pattern may be changing from instant to instant, in which case the stream lines must be regarded as instantaneous—that is, they represent the paths of particles for only a small increment of time. If the flow is either steady or uniform, the stream lines will represent the actual paths of the fluid particles; only in regions of uniform flow can these paths be parallel.

The same distinction that exists between a fluid particle and a point in the fluid medium may be used to define a stream filament as distinguished from a stream line: The reader must visualize a small filament or tube of fluid, bounded by stream lines and yet of inappreciable cross-sectional area, as shown schematically in Fig. 2. This stream filament might be considered, in either steady or uniform flow, as the passage through space of a fluid particle, and as such is the basis of the one-dimensional treatment

of certain flow problems. Indeed, elementary hydraulics is based largely upon this conception, a single filament being assumed to have the cross-sectional area of the entire flow.

In certain types of fluid motion the stream filaments are arranged in a very orderly fashion, and may be made visible experimentally by the introduction of colored fluid at some point in the flow. More generally, however, there occurs a complex interlacing of the actual stream lines; the various particles not only follow completely different and intricate courses but suffer continuous distortion and subdivision, so that no particle exists as an individual for more than a short interval of time. In such cases it is often practicable to represent by stream lines or filaments the temporal average of conditions throughout the movement. Such representation does not ignore the actual complexity of the motion, but serves only as a convenient aid in visualizing the underlying pattern of the flow.

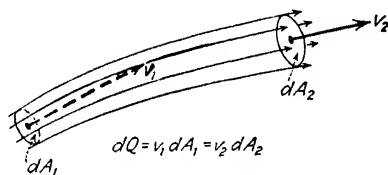


FIG. 2.---Stream filament.

The boundaries of fluid motion are the fixed or moving surfaces which define the borders of the fluid medium. These may either surround the flow, as is done by the walls of a pipe or turbine, or may be enclosed by the flow, as in the case of an airplane or the blade of a turbine runner. On the other hand, the free surface of a liquid in contact with a gas is not given its form by a solid boundary, but through the condition that the pressure intensity at every point on the free surface must be the same. In any case, the situation is fully described by what are known as boundary conditions. It should be clear that the borders of the flow are always stream lines, since by definition and physical fact, respectively, the flow cannot cross either a stream line or the boundary line of motion.

10. Relationship of the Velocity Fields for Steady and Unsteady Flow. In general hydromechanics it is customary to distinguish between absolute and relative motion. For the purpose of this text, however, it will be more feasible to disregard the absolute space of the theoretician, and simply place emphasis upon the relation of the flow picture either to the fluid itself, or to a fixed or moving boundary. In order to clarify this principle, consider

the two cases of a boat moving through still water, and water flowing around a bridge pier. The coordinate system may be represented by the quadrille-ruled ground glass of a camera which is suspended some distance above the water. If the camera is "related" (fixed) to the boat or to the bridge pier, the flow picture will be a steady one, and the stream lines will also

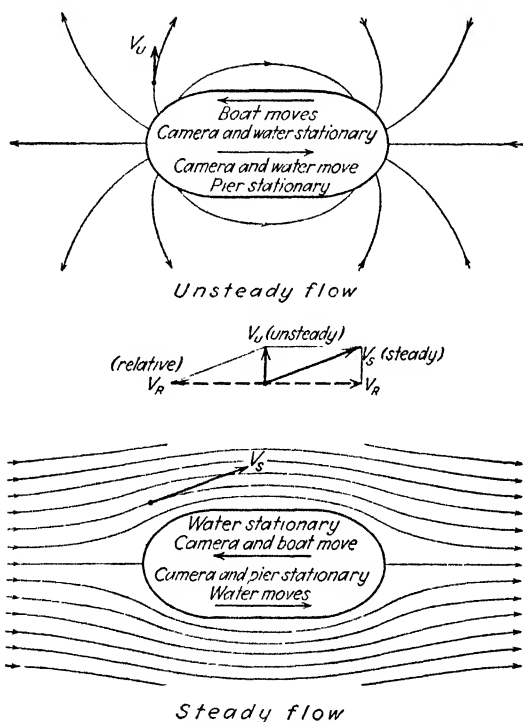


FIG. 3.—Patterns of relative motion between a fluid and a solid boundary.

be the apparent paths of the fluid particles (see Fig. 3). If, however, the camera is "related" to the water, the picture will change with time and will show the flow pattern caused by the pier or the boat at any instant. In the case of the bridge pier the water obviously moves through space, while in the other example it is the boat which moves; hence, in the first case the moving coordinate system gives a picture of unsteady motion, and in the second a picture of steady motion.

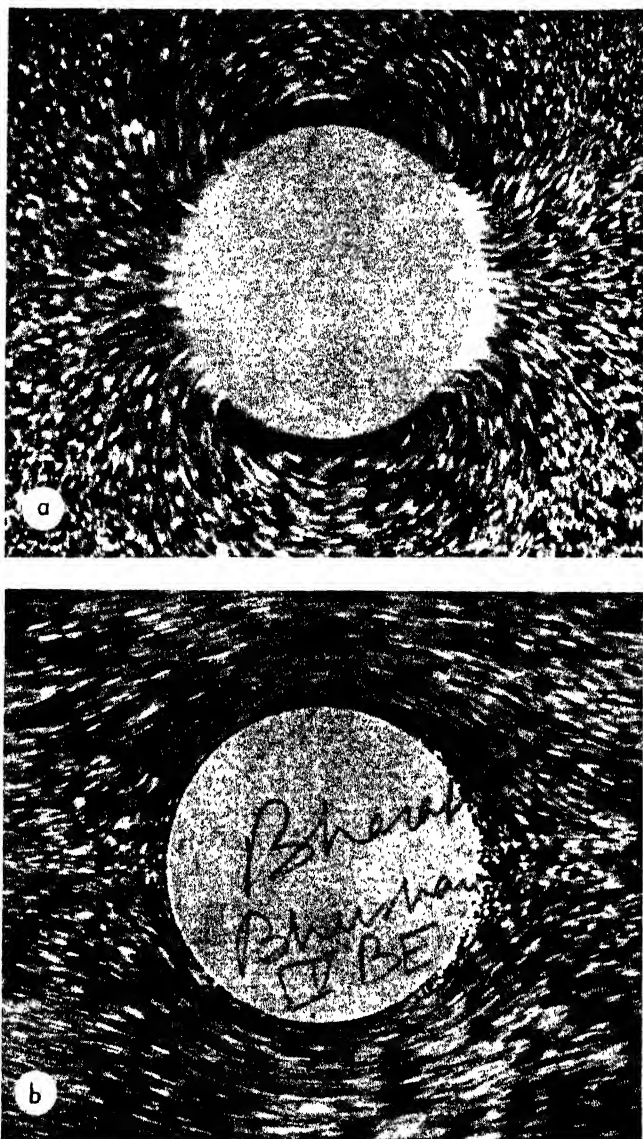
The relation between the two pictures is purely a vectorial one, as indicated in Fig. 3. Assume, for instance, that the camera

is stationary above the water, thereby yielding the unsteady pattern caused by the boat moving to the left. If the camera is now moved to the left with the boat, the resulting steady pattern will be the same as if the boat and all fluid particles in the unsteady pattern were moved to the right at the relative velocity V_R . Thus the steady vector V_S at any point is the vector sum of V_R and the unsteady vector V_U . Similarly, the steady pattern of flow around the bridge pier, observed when the camera is stationary, may be changed to an unsteady one by moving the camera to the right—*i.e.*, by giving the pier and all fluid particles an apparent velocity V_R to the left. V_U is then the vector sum of V_R and V_S . Interesting photographic studies of such relative motion caused by a body moving through a fluid may be made by sprinkling aluminum flakes or bits of finely divided paper on the fluid surface and then making short time exposures: first while the camera moves at the exact speed of the body (steady motion), and then with the camera held motionless (unsteady motion). Such photographs may be seen in Fig. 4.¹

A method of changing the picture of unsteady flow through a turbine or centrifugal pump, as would ordinarily be seen by an observer, to one of steady flow has been developed by Professor Thoma, of Munich. An apparatus known as a rotoscope, consisting of a small telescope and an objective prism, is mounted in line with the pump or turbine axis, the end of the casing having been replaced by a small section of plate glass. So long as the prism is at rest, the flow picture remains unsteady; but if the prism is made to rotate at the proper speed, through the telescope the blades will appear to be stationary. If dye is introduced at various points of the flow, a steady picture of the stream lines will result. Similar stroboscopic methods are in common use in studying the performance of high-speed machinery, involving the same principle of reducing unsteady motion to steady motion by relating the coordinate system to the moving parts.

It is customary to construct a stream-line diagram in such a fashion that the distance Δn between stream lines at every point

¹ For the purposes of simplicity, the stream lines in Figs. 3 and 5 have been drawn symmetrically at the front and rear of the body. That this is not an impossible case of flow is shown by the photographs, taken shortly after movement began. Further discussion of flow in the wake of a body must be reserved for a later chapter.



Columbia

FIG. 4.—Patterns of (a) unsteady and (b) steady flow around a cylinder as motion begins, the camera traveling with the fluid and with the cylinder, respectively. The stream lines are shown by the movement of highly illuminated aluminum particles during a short time exposure.

is inversely proportional to the length of the velocity vector at that point: $\Delta n = c/v$; this practice is possible on paper, of course, only in the case of two-dimensional or planar motion, such as that shown in Fig. 3. Because of such systematic selection of stream lines (in reality an infinite number of them exists), it is possible to simplify the construction of the pattern for steady flow from that of unsteady flow, and vice versa, with the following graphical method. For every system of flow there exists at each point of the pattern one and only one vector diagram representing the relation of the steady and unsteady velocity vectors to the velocity of translation; similarly, the magnitude of each vector represents a definite spacing of the stream lines. Since the relative velocity is constant, it may be represented by a series of equidistant lines parallel to the direction of motion,

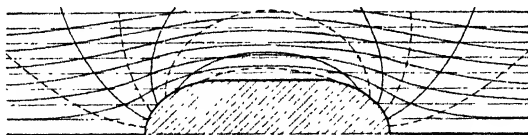


FIG. 5.—Graphical combination of velocity fields.

spaced according to the velocity and the proportionality constant. By connecting with smooth curves all points of intersection of these parallels with successive stream lines in either the steady or unsteady flow pattern, the corresponding pattern of flow lines will result, as shown in Fig. 5. This method of graphically combining (adding or subtracting) two vector fields is of especial value in the study of motion within the moving runner of a turbine, and will also be used in the following pages in the study of vector fields of force.

While the stream lines in steady flow represent the actual paths of fluid particles (with reference to the coordinate system), the paths traveled by particles in unsteady motion must, in general, be obtained by another graphical method. Since a given fluid particle in unsteady motion follows one stream line for only an infinitesimal increment of time, its velocity then being determined in direction and magnitude by the next stream line to cross its path, one must plot on a diagram of instantaneous stream lines the successive distances over which it will move in the direction of each stream line as the unsteady field of motion advances.

Thus, in Fig. 6, a particle at point 1 will move the distance a according to the direction and spacing of the stream line A at that point, the distance b according to conditions at point 2, and so on. The complete paths followed by the various particles in this particular system of motion will vary only with the original distance from the centerline of flow.

Stream lines and path lines must not be confused with so-called "streak" lines—the latter connecting all particles passing through a given point. Filaments of dye injected into a moving fluid therefore correspond to streak lines, and indicate path lines and stream lines as well only if the flow is steady.

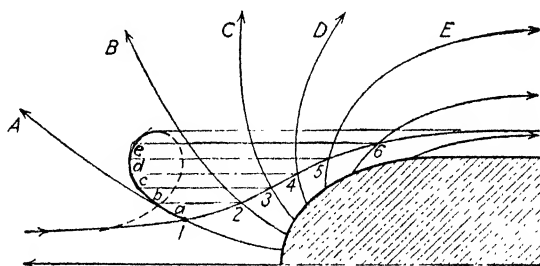


FIG. 6.—Construction of a path line.

11. Equations of Motion in Natural Coordinates. While the Cartesian coordinate system is by far the most general, it is at the same time very difficult to visualize states of motion described in this system, and just as difficult to adapt its equations of motion to various boundary conditions. Hence, it is customary to make extensive use of some specialized system, according to the case in question. In the study of flow through or around boundaries generally symmetrical about one axis, such as the surfaces of revolution in centrifugal pumps and turbines, the cylindrical coordinate system is particularly advantageous. The coordinates are again three in number, and consist of the radius r and the angle θ of the planar system of polar coordinates, and of the distance z measured along the axis of rotation. For very special cases the spherical (astronomical) system has its advantages, although its use is limited.

Because of its close relation to the stream-line picture, the natural coordinate system will be found particularly applicable to the methods of study in this book. This system is somewhat different from the others, in that it may be used to describe most

conveniently only that region of flow immediately surrounding the center of coordinates. The coordinate center is thus located at the point in the flow chosen for study (point o in Fig. 7), the s axis being tangent to the stream line at that point, the n axis normal to the stream line and containing its center of curvature, and the m axis normal to the other two. It is apparent that at the coordinate center the velocity vector lies along the s axis, there being no velocity components at that point in either of the other coordinate directions. At any other point q , however (refer to Fig. 7), according to the coordinate axes centered at o , the velocity vector will have components in all three directions.

Writing the velocity at any point of an unsteady, non-uniform flow as a function of time and of position with respect to the three natural coordinate axes

$$v = f(t, s, n, m)$$

it will be seen that the velocity of a fluid particle must then vary not only according to the change of conditions in that locality with time, since the flow is unsteady, but also according to the change of conditions in each of the coordinate directions, since the flow is non-uniform. Since the velocity is a true vector, it will generally have components in each of the three coordinate directions (v_s , v_n , and v_m), each of which is also a function of time and space:

$$\begin{aligned} v_s &= f_1(t, s, n, m) \\ v_n &= f_2(t, s, n, m) \\ v_m &= f_3(t, s, n, m) \end{aligned}$$

Since acceleration is a vector quantity defined as the temporal rate of change of the velocity vector,

$$a = \frac{dv}{dt}$$

its components in the three coordinate directions may be written as the temporal rates of change of the corresponding components of velocity:

$$a_s = \frac{dv_s}{dt}; \quad a_n = \frac{dv_n}{dt}; \quad a_m = \frac{dv_m}{dt}$$

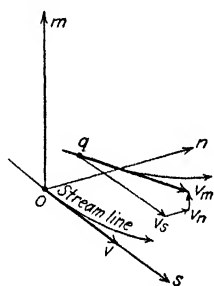


FIG. 7.—Characteristics of the natural coordinate system.

In moving an increment of distance in an increment of time, a particle will undergo acceleration for two distinct reasons: first, because of passage of time, without respect to its movement through space; second, because of its movement through space, without respect to passage of time. In other words, each component of total acceleration will consist of two parts: the first is written simply as the partial derivative of the velocity component with respect to time; the second is expressed as the partial derivative of the velocity component with respect to distance in the direction of motion, multiplied by the distance traveled per unit of time during the short time increment. Evidently the distance traveled per unit of time is equal either to the velocity component in the s direction or to the magnitude of the velocity vector itself, since the two differ by an exceedingly infinitesimal amount even after the particle has moved the short increment of distance. Hence, the three components of acceleration may be written in the following form:

$$a_s = \frac{dv_s}{dt} = \frac{\partial v_s}{\partial t} + \frac{\partial v_s}{\partial s} \frac{ds}{dt} = \frac{\partial v_s}{\partial t} + v \frac{\partial v_s}{\partial s} \quad (1s)$$

$$a_n = \frac{dv_n}{dt} = \frac{\partial v_n}{\partial t} + \frac{\partial v_n}{\partial s} \frac{ds}{dt} = \frac{\partial v_n}{\partial t} + v \frac{\partial v_n}{\partial s} \quad (1n)$$

$$a_m = \frac{dv_m}{dt} = \frac{\partial v_m}{\partial t} + \frac{\partial v_m}{\partial s} \frac{ds}{dt} = \frac{\partial v_m}{\partial t} + v \frac{\partial v_m}{\partial s} \quad (1m)$$

The partial derivatives express the local and the convective components of acceleration of the fluid particle, as distinguished from the total or substantial component of acceleration, and represent, respectively, variation with time, regardless of space, and with space, regardless of time. If the flow is steady, the local terms are zero; similarly, if the flow is uniform, the convective terms are zero. In a steady, uniform flow there is no acceleration whatsoever.

Owing to the nature of this coordinate system, these equations may be further simplified, for at the instant the fluid particle passes the origin o (Fig. 7) there can be no component of the velocity in either the n or the m direction, and the curvature of the stream filament will lie entirely in the sn plane over a short distance ds (i.e., the curvature of a line can be only two-dimensional at any point and hence over an infinitesimal distance on either side of that point). In Eq. (1s) the convective term may

now be written in the following form, which involves merely a change in mathematical wording:

$$v \frac{\partial v}{\partial s} = \frac{\partial (v^2/2)}{\partial s}$$

The convective term in Eq. (1n) may be replaced by the familiar term of mechanics representing the centripetal acceleration of any mass moving in a curved path. This may be proved by reference to Fig. 8, similarity of triangles resulting in the proportion

$$\frac{\partial v_n}{\partial s} = \frac{v}{r}$$

whence the convective term in the second equation becomes simply v^2/r . Since the plane of curvature of the filament is normal to the m axis over the distance ds , there can be no acceleration in the direction m as the particle travels this short distance. Hence, the convective term in Eq. (1m) may be omitted entirely. These three equations may now be written as follows for the immediate vicinity of the coordinate center:

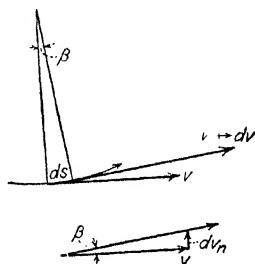


FIG. 8.—Centripetal acceleration.

$$\frac{dv_s}{dt} = \frac{\partial v_s}{\partial t} + \frac{\partial (v^2/2)}{\partial s} \quad (2s)$$

$$\frac{dv_n}{dt} = \frac{\partial v_n}{\partial t} + \frac{v^2}{r} \quad (2n)$$

$$\frac{dv_m}{dt} = \frac{\partial v_m}{\partial t} \quad (2m)$$

In order to study the individual action of any force property in producing such acceleration, it is necessary to eliminate, for the time being, the influence of all other force properties. This is accomplished in fundamental hydromechanics by arbitrarily setting the viscosity, surface tension, and compressibility of the fluid equal to zero, weight and pressure then being the forces under investigation. Thus, the forces exerted in an axial direction upon an elementary cylinder of fluid (see Fig. 9) will be the pressure at either end and the component of fluid weight acting parallel to the axis. While the pressure intensity at any point

within such a fluid is the same in every direction, it will in general vary from point to point, its rate of variation in any direction being called the pressure gradient. The difference in pressure intensity between the two ends of the fluid cylinder is thus given by the pressure gradient in the axial direction times the distance

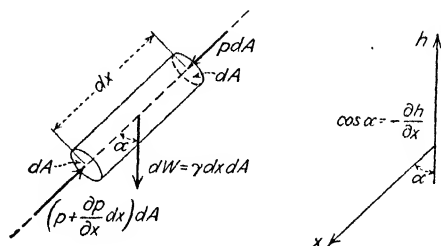


FIG. 9.—Elementary forces due to pressure gradient and weight.

between the two ends. The total force acting upon this fluid volume will then be:

$$dF_x = p dA - \left(p + \frac{\partial p}{\partial x} dx \right) dA + \gamma dx dA \cos \alpha$$

Introducing the rate of change of elevation h in the x direction ($\cos \alpha = -\partial h / \partial x$) this becomes:

$$dF_x = -\frac{\partial p}{\partial x} dx dA - \gamma \frac{\partial h}{\partial x} dx dA$$

This very important relationship may be expressed as follows: The force per unit volume, f , acting in any direction is equal to the rate of decrease of the sum $(p + \gamma h)$ in that direction:

$$\frac{dF_x}{dx dA} = f_x = -\frac{\partial}{\partial x}(p + \gamma h) \quad (3)$$

This force per unit volume divided by the density of the fluid will equal the force per unit mass, or, in accordance with the Newtonian equation, the rate of acceleration of the fluid in the given direction:

$$a_x = \frac{f_x}{\rho} \quad (4)$$

$$a_x = \frac{dv_x}{dt} = -\frac{1}{\rho} \frac{\partial}{\partial x}(p + \gamma h) \quad (5)$$

From Eq. (5) it will be seen that if any component of the substantial acceleration is zero, there can be no variation in the sum $(p + \gamma h)$ in that direction. In other words, the distribution of pressure intensity must be hydrostatic (*i.e.*, $p = \text{constant} - \gamma h$) in any direction in which no acceleration takes place.

Equation (5) may now be combined with the expressions for acceleration already developed:

$$\frac{\partial v_s}{\partial t} + \frac{\partial(v^2/2)}{\partial s} = -\frac{1}{\rho} \frac{\partial}{\partial s}(p + \gamma h) \quad (6s)$$

$$\frac{\partial v_n}{\partial t} + \frac{v^2}{r} = -\frac{1}{\rho} \frac{\partial}{\partial n}(p + \gamma h) \quad (6n)$$

$$\frac{\partial v_m}{\partial t} = -\frac{1}{\rho} \frac{\partial}{\partial m}(p + \gamma h) \quad (6m)$$

These are special forms of the most basic relationships in hydro-mechanics, first published in 1755 by the founder of the science, the Swiss mathematician Leonhard Euler, and generally known as the Euler equations of acceleration.

12. Principles of Energy, Continuity, and Momentum. Equation (6s) may be written directly in the following pertinent form:

$$\rho \frac{\partial v_s}{\partial t} + \frac{\partial}{\partial s} \left(\frac{\rho v^2}{2} + p + \gamma h \right) = 0$$

The three terms within parentheses may be set equal to the quantity E_s . If the flow is assumed steady, the local acceleration will then be equal to zero, and integration of this differential expression over s will yield a general statement of conditions of steady flow along any stream line:

$$\int^s dE_s = \rho \frac{v^2}{2} + p + \gamma h = f(t) \quad (7)$$

Although the flow was expressly made a steady one, Eq. (7) states that the quantity E_s may still be a function of time. The reader will recall, however, that from definition the word "steady" specifies only that the velocity must remain constant with time at all points in the flow, and thereby places no restriction upon temporal variation of the pressure intensity. Equation (7) simply means that variation in the hydrostatic load on the system, as included in the sum $(p + \gamma h)$, will exactly equal the change in E_s with time and will extend uniformly over the entire length

of the stream line; as such, it can have no effect whatever upon the velocity at any point.

If E_v is not a function of time, along any stream line

$$E_v = \rho \frac{v^2}{2} + p + \gamma h = \text{constant} \quad (8)$$

Each term of this equation has the dimension of energy per unit volume, the equation embodying a complete statement of the energy principle, or the essential balance between kinetic energy and potential energy over every part of a stream line in steady flow. The equation of energy is more commonly known as the Bernoulli theorem, named for Daniel Bernoulli (like Euler a Swiss mathematician), who discussed the various forms of flow energy in a treatise on hydraulics (1738) nearly two decades before Euler laid the foundations of hydromechanics. The equation appears above in its most general form—one particularly well adapted to flow that is entirely confined by solid boundaries. Judging from previous remarks and from the interrelation of the three terms in this equation, it is evident that the pressure intensity will vary along the stream line with change in velocity, with change in elevation, and (when E_v is a function of time) with change in the hydrostatic load on the enclosed system. Under such conditions it is appropriate to distinguish that portion of the pressure intensity resulting from dynamic effects from that resulting from hydrostatic conditions. Designating these by the subscripts d and s , respectively, Eq. (8) may be written in the form

$$E_v = \rho \frac{v^2}{2} + p_d + p_s + \gamma h \quad (9)$$

in which the sum $(p_s + \gamma h)$ is either a constant or some function of time; in either case,

$$\rho \frac{v^2}{2} + p_d = \text{constant} \quad (10)$$

If Eq. (8) is divided by the fluid density ρ , there will result an alternate expression in which each term has the dimension of energy per unit mass of fluid:

$$E_m = \frac{v^2}{2} + \frac{p}{\rho} + gh \quad (11)$$

This general form is particularly significant when dealing with the flow of gases. A form more familiar to engineers, since it is appropriate in cases of flow with a free surface, is derived from Eq. (8) by dividing all terms by the specific weight of the fluid:

$$E_w = \frac{v^2}{2g} + \frac{p}{\gamma} + h \quad (12)$$

Each term now has the dimension of energy per unit weight of fluid; since this is equivalent to length, the several terms are characterized as heads, and are called, respectively, the total head, the velocity head, the pressure head, and the geodetic head or elevation. Since the pressure head and elevation represent potential energy, as distinguished from the kinetic energy embodied in the velocity head, the sum $\left(\frac{p}{\gamma} + h\right)$ is properly known as the potential head. It follows from Eq. (8) that the sum of velocity and potential heads will not vary with distance along any stream line in steady flow. Evidently, no restriction is placed upon variation from one stream line to another.

At every point along a fluid surface exposed to the atmosphere, the pressure intensity must be that of the atmosphere itself. Hence, while the hydrostatic load in a closed system may be varied at will without changing the flow pattern, there is no possible way of changing the pressure intensity in flow with a free surface (except through atmospheric variation) without altering the entire pattern of motion. Under such circumstances differentiation between hydrostatic and dynamic influence upon the pressure intensity would be quite pointless, for the two can no longer be considered independent of each other.

Equation (12) finds a very valuable application in the graphical representation of the total head and its component parts. For a given stream filament in steady flow, the magnitude of its elevation at every point is plotted as a vertical distance above some assumed geodetic datum. The magnitude of the pressure head is then added vertically to the elevation of the stream line, the locus of these latter points being called the pressure line. From each point on the pressure line the corresponding velocity head is then laid off, resulting in a line of total head—the energy line—lying the distance E_w above the geodetic datum. Thus, in a single diagram is contained the entire story of energy trans-

formation undergone by a fluid particle as it moves from point to point along its path, the method being quite as applicable to confined as to open flow.

If all neighboring filaments happen to possess the same total head, it is only reasonable to allow the same energy line to apply to the entire group. But since this in no way prevents pressure intensity and velocity from varying from one stream line to another, there will evidently be cases in which a different pressure line would have to be drawn for each individual filament; such is always the case if the stream filaments display appreciable curva-

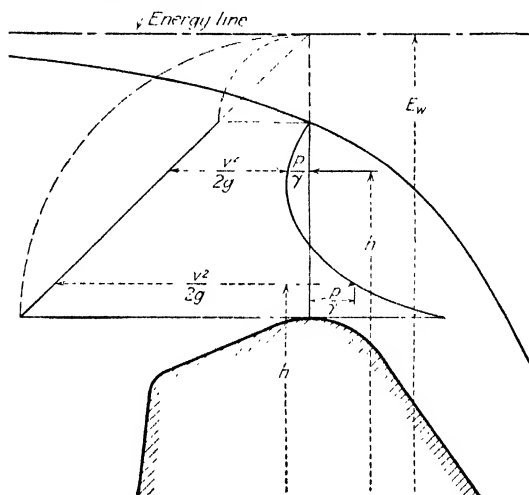


FIG. 10.—Non-hydrostatic pressure distribution in curvilinear motion.

ture. For illustration, in Fig. 10 is shown a longitudinal section through the crest of a spillway. Each filament passing the vertical line erected at the topmost point of the crest will be under a different pressure intensity, the pressure head at each elevation being plotted horizontally from the section line. Since the distance between the filament and the energy line is equal to the sum of pressure and velocity heads, it is obvious that the pressure line for every filament would lie a different distance below the energy line. As a matter of fact, only in parallel flow will a single pressure line suffice for all filaments at once: if the upper surface is exposed to the atmosphere, the pressure line will then coincide with the free surface; if the flow is confined, the pressure line may lie either above or below the centerline of flow, depend-

ing upon whether the mean pressure head is positive or negative (*i.e.*, greater or less than atmospheric).

In the most general case, however, one may not assume that all stream filaments possess the same energy of flow, for the total head often varies from one filament to the next. (It will be recalled that the Bernoulli theorem makes no mention of the relative energy of neighboring filaments.) Under such conditions, if one is still to use a common energy line for the entire flow, it is essential that the total head which this indicates be a true measure of the mean flow energy. In other words, since head represents energy per unit weight of fluid passing a given section, the total head for each increment of cross-sectional area must be weighted according to the rate of weight discharge through that elementary area.

Designating by $\Delta Q = v \Delta A$ the rate of discharge through the increment of cross-sectional area, the product of this quantity and the specific weight of the fluid will yield the desired weight passing the increment of area per unit time, and thus give the factor by which the total head of each filament must be multiplied before integrating over the entire cross section of flow. This integral, when divided by the mean rate of weight discharge, γVA (based on the mean velocity V), will equal the weighted mean total head:

$$(E_w)_m = \frac{1}{\gamma VA} \int^A \left(\frac{v^2}{2g} + \frac{p}{\gamma} + h \right) \gamma v dA \quad (13)$$

If the flow is parallel, on the other hand, the sum of pressure head and elevation—that is, the potential head—must be a constant over any cross section, so that only the velocity head will then vary from one filament to the next. Under such circumstances, a weighted mean velocity head must be added to the common potential head to determine the weighted mean total head. The procedure is similar to the foregoing one:

$$\left(\frac{v^2}{2g} \right)_m = \frac{1}{VA} \int^A \frac{v^2}{2g} v dA = K_e \frac{V^2}{2g} \quad (14)$$

The kinetic-energy correction factor K_e will then be:

$$K_e = \frac{1}{V^3 A} \int^A v^3 dA \quad (15)$$

It may vary in magnitude from unity, for uniform total head, through an average practical value of about 1.1, to a general maximum of 2 when the velocity distribution (over a circular section) is paraboloidal. Needless to say, if the velocity distribution is modified by a change in flow section, the magnitude of this correction factor cannot remain constant.

In addition to the principle of energy, which is really the law of conservation of energy applied to the stream filament, the law of conservation of matter plays an essential role in hydro-mechanics. Since from definition there can be no passage of fluid through the walls of a stream filament (and since there may be no change in fluid density from one point to the next), unless the cross-sectional area changes with time, the rate of discharge must be the same at all cross sections of the filament at any instant:

$$v dA = \text{constant}$$

If one integrate this increment of discharge through the individual filament over the entire cross section of flow, the same conditions of continuity must hold through the flow at any one instant of time:

$$Q = \int^A v dA = \text{constant} \quad (16)$$

This equation applies to both steady and unsteady flow so long as the outermost stream lines do not change in form.

The Euler equations of acceleration, from which the energy equation was derived, embody the application of Newton's momentum principle to a particle at a given point in a moving fluid. With little modification, this principle may be applied conveniently to an entire region of flow, by integrating over the total volume of that region the elementary forces producing mass acceleration. The basic vector relationship between the force per unit volume and the rate of change of momentum

$$f = \frac{d(\rho v)}{dt} = \rho \frac{dv}{dt} = \rho a$$

may best be integrated over a given volume V by reducing the vector terms to their components in the three Cartesian coordi-

nate directions; thus, the integral expression for any direction x will be:

$$F_x = \Sigma (f_x) = \rho \int^V a_x dV$$

The term on the left includes the x component of all forces acting upon every particle in the volume at a given instant. But since every force upon a particle within the volume requires the existence of an equal and opposite force upon the neighboring particles, all such internal forces will counterbalance each other, so that one need consider only those forces exerted externally. In its most general application, this quantity must include every type of force action; for the present, only pressure and weight are to be considered.

In the case of steady motion, the term on the right of the equation may be made more explicit by considering the fluid volume to be composed of innumerable fluid filaments of permanent form, the surface of this volume then consisting of the walls of the outermost filaments and the sum of all the cross-sectional areas dA at either end of every one. The component of acceleration, a_x , may now be expressed in terms of a differential length, ds , along any filament:

$$a_x = \frac{dv_x}{dt} = \frac{\partial v_x}{\partial s} \frac{ds}{dt} = v \frac{\partial v_x}{\partial s}$$

Since the differential volume dV is equal to the product $ds dA$, and since the term $v dA$ is equal to an increment of discharge dQ (from the equation of continuity), the term on the right of the original equation finally becomes:

$$\rho \int^s \int^A v \frac{\partial v_x}{\partial s} ds dA = \rho \int^s \frac{\partial v_x}{\partial s} ds \int^A v dA = \rho \int^{Q_2} (v_{x_2} - v_{x_1}) dQ$$

in which v_{x_1} and v_{x_2} denote the components of the velocity at entrance to and at exit from the given space.¹

The equation of momentum applied to an appreciable section of the flow will then have, for any coordinate direction, this general form:

¹ This development, as well as many another feature of elementary hydro-mechanics, is clearly and simply presented in MISES, R. von, "Technische Hydromechanik," B. G. Teubner, Leipzig, 1914.

$$F_x = \Sigma (f_x) = \rho \int^Q v_{x_2} dQ - \rho \int^Q v_{x_1} dQ \quad (17)$$

When reduced to the simple form used in hydraulics, the two integral terms are replaced by the product of the rate of discharge and the average velocity components at entrance and exit. In this form the equation is commonly applied to cases of jets deflected by curved surfaces, to pipe bends, nozzles, and similar elementary hydraulic devices. Just as in the case of the total head, however, if the velocity is not uniformly distributed over the section, it is not correct simply to use the mean value V of the velocity in the momentum equation. From Eq. (17) it is evident that to the product $\rho V^2 A$ at each section there must be applied a correction factor of the form:

$$K_m = \frac{1}{V^2 A} \int^A v^2 dA \quad (18)$$

This factor must not be confused with K_e , used in the energy equation, for the velocity appears to the second power in the former and to the third power in the latter.

In the general case of curvilinear flow, in which average values of neither velocity nor pressure intensity may be used, Eq. (17) must be followed strictly, actual curves of velocity and pressure distribution forming the basis for integration, and the actual volume of the fluid being used to determine the component of the fluid weight in the given direction. Yet such methods will require experimental measurement of velocity and pressure distribution at one section or the other, for the general principles of momentum, energy, and continuity have as yet provided no means of determining these characteristics by rational analysis.

13. Theory and Use of the Flow Net. If the total energy is constant not only along any stream filament but also from one filament to another, Eq. (6n) may be simplified, owing to the fact that the sum of kinetic and potential energy cannot vary in the n direction. Since the flow must necessarily be steady, the term $\partial v_n / \partial t$ can be dropped at once. Then subtracting the quantity $\frac{\partial(v^2/2)}{\partial n}$ from both sides of the equation,

$$\frac{v^2}{r} - \frac{\partial(v^2/2)}{\partial n} = -\frac{1}{\rho} \frac{\partial}{\partial n} \left(\frac{\rho v^2}{2} + p + \gamma h \right)$$

and since the flow is one of uniform energy distribution, the right side of this equation must equal zero; hence,

$$\frac{v^2}{r} = v \frac{\partial v}{\partial n} \quad \text{or} \quad \frac{\partial v}{\partial n} = \frac{v}{r} \quad (19)$$

This equation may be integrated to give

$$\ln v = \int \frac{dn}{r} + C \quad \text{or} \quad v = C' e^{\int \frac{dn}{r}} \quad (20)$$

In combination with the principle of continuity and the Bernoulli theorem, Eq. (19) affords a means of determining the pressure and velocity distribution in steady two-dimensional flow in which the total head is reasonably uniform at all points. While this method is necessarily graphical (with the exception of certain cases to be discussed later), it is nevertheless based upon physically exact principles, and is limited only by the degree of graphical accuracy which may be attained. Consider, for instance, the fixed boundaries shown in Fig. 11a. A flow net is first sketched in by eye, consisting of an arbitrary number of stream lines, and of such a number of orthogonal lines as to divide the flow area into as nearly perfect squares as possible, all stream lines and orthogonal lines meeting at right angles. It is evident that a network of diagonals through all points of intersection should also yield squares, and thus permit a convenient test for angular error. Obviously the squares in the vicinity of the bend will be distorted, but they should become more nearly perfect as the number of lines is increased. Mathematically speaking, they can become true squares only as they become infinitesimal in size. However, by adjusting the position of stream lines and orthogonal lines, with plentiful use of pencil and eraser, a very systematic progression of the stream lines will finally result.

There is only one arrangement of the chosen number of stream lines that will fulfill the mathematical statement of the equations of Euler; consequently, their positions may now be checked for correctness by means of Eq. (19). For any orthogonal line a plot is made of the relationship between distance along the orthogonal in the direction n and the radii of curvature of the stream filaments at the points of intersection with the orthogonal. These values must be determined graphically. From the principle of continuity as applied to the flow between each pair of stream lines

(i.e., the velocity must vary inversely with the spacing), the velocity vector at each point of intersection is next determined and plotted against n on the same diagram. If the stream lines are correctly spaced, it is evident from Eq. (19) that the slope of the velocity curve at any point must equal the ratio between the velocity and the radius of curvature, which can be checked

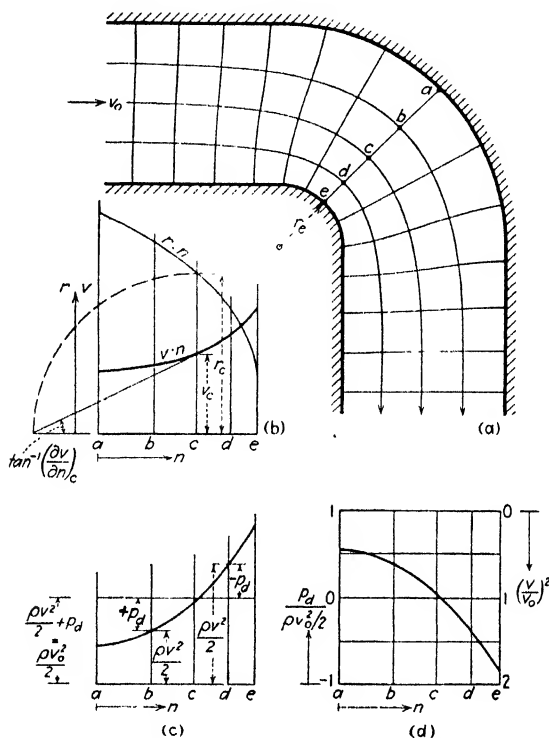


FIG. 11.—Application of the flow net.

graphically on the plot (see Fig. 11b). If these values do not agree as they should, the stream lines must be redrawn.

Usually a single check at several typical points will serve to make the diagram as accurate as is required. Once the correct velocity curve is obtained, the pressure distribution may be found through use of the energy equation (see Fig. 11c). Since the flow is enclosed, the change in pressure intensity with change in elevation (or with variation in hydrostatic load upon the system) can have no effect whatever upon the velocity distribu-

tion or upon the distribution of dynamic pressure. Indeed, if the pressure distribution were computed in terms of head, the variation in p_a/γ with n would be exactly equal to the variation in reading of manometric columns connected to piezometers at the several points in question.

Little thought will be required to convince the reader that the same flow net may apply equally well to rates of discharge other than that selected for investigation, for the pattern of stream lines depends not upon the velocity represented by the chosen spacing, but purely upon the geometrical form of the boundaries. Since a change in velocity will change the scale but not the form of the distribution curves in Fig. 11c, it would be most expedient to devise a single diagram containing the ratio of velocity, density, and dynamic pressure intensity for the given section, regardless of the rate of discharge (Fig. 11d). If this ratio is put in the form

$\frac{p_a}{\rho v_0^2/2}$, it will not only be dimensionless but will be identical with the flow parameter derived by means of the II-theorem in the preceding chapter. In other words, at any given point in the flow pattern, this parameter must remain constant regardless of change in rate of discharge or hydrostatic load—a fact of fundamental importance.

If the flow has one or more free surfaces, the problem becomes considerably more difficult, although no less subject to solution. If the profile of the free surface is known from experimental measurement, the procedure is the same as though this curve were one of the given boundaries; but if such experimental information is not available, since the stream lines at the border between liquid and atmosphere are not governed in position by a fixed boundary, they too must be sketched in by eye. The identical construction of the flow net then follows. However, in checking the position of the stream lines, not only must Eq. (19) be satisfied, but the pressure distribution curve must pass through zero (atmospheric) at every point lying on a free surface. If this does not check, not only the profile of the free surface, but the form of all other stream lines as well, must be modified.

As has already been mentioned, use of the energy equation written in terms of head is best suited to such conditions of flow. The scale used in plotting velocity and pressure head is then determined directly by the linear scale of the flow profile, and

consequently the several distribution curves have immediate quantitative significance. For illustration, in Fig. 12 is shown the flow net for discharge under a sluice gate, the solution yielding curves of pressure head over the gate and along the lower boundary of the flow.

The gradual rise in the upper surface approaching the sluice gate illustrates a characteristic of flow in the neighborhood of a so-called point of stagnation. Wherever a stream line changes abruptly in direction, the spacing of the stream lines at that point is either infinity or zero, depending upon whether the change

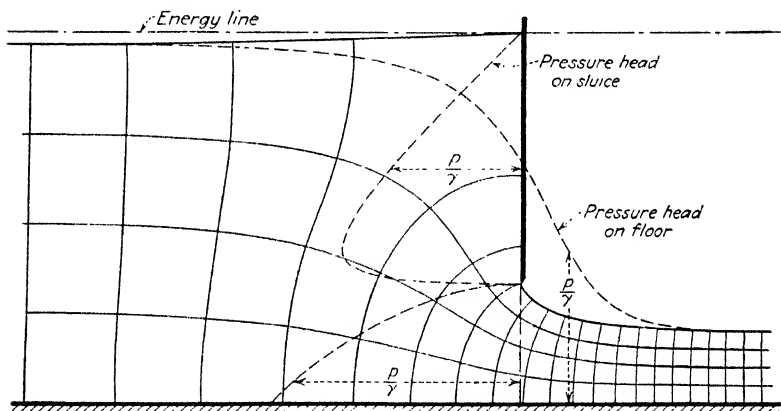
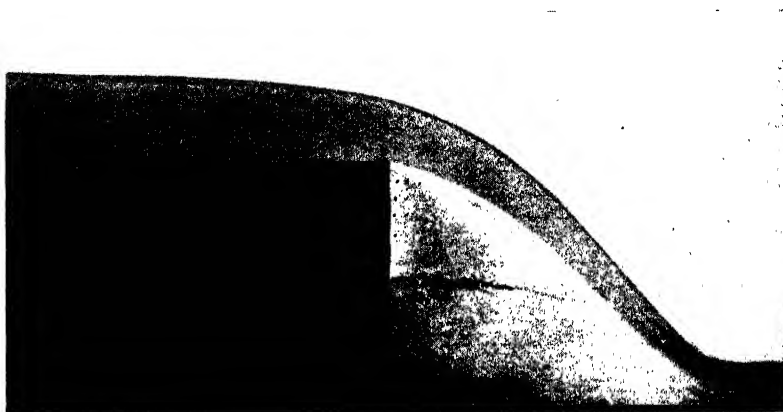


FIG. 12.—Pressure distribution for sluice-gate discharge as determined from the flow net.

in direction is toward or away from the other stream lines. Since, from continuity, the product of the spacing and the velocity must remain constant for a given rate of discharge, a zero spacing denotes an infinitely high velocity, and vice versa. Although a velocity equal to infinity (corresponding, in enclosed flow, to a dynamic pressure intensity of negative infinity) is physically impossible, a velocity of zero is obviously quite conceivable. If there are no free surfaces involved, this simply means that the intensity of dynamic pressure must increase to the magnitude of the constant in Eq. (10), and then be known as the stagnation pressure intensity. Indeed, it is upon this condition of stagnation that operation of the Pitot tube depends, for the nose of the tube pointing upstream merely produces a small region of stagnation at which the pressure intensity is measured; the ratio of stagnation pressure to the density and the square of the velocity

of the surrounding flow must remain constant, regardless of change in magnitude of the velocity itself. However, if the stagnation point lies at a free surface, as in the case of the sluice gate, the pressure intensity must evidently remain atmospheric; since the total head along this upper stream filament must be the same at all points, it is clear that the decrease in velocity head must be accompanied by an increase in elevation of the filament, its highest position coinciding with the energy line itself at the point of stagnation.



Karlsruhe

FIG. 13.—Flow profile at a ventilated overfall.

14. Significance of the Force Potential. According to the Euler equations, two distinct components of the accelerative force per unit volume act upon fluid particles in two-dimensional flow: one (f_s) in the direction of motion, and the other (f_n) in the direction of the center of curvature of the stream filament; these force components are normal to the orthogonal lines and the stream lines, respectively, of the flow net, and are equal to the negative gradients of the sum ($p + \gamma h$) in the corresponding directions, in accordance with Eq. (3). On the other hand, the resultant force f per unit volume at any point might also be considered to have components in two other directions: one (f_p) normal to a line of constant pressure intensity, and the other (f_w) normal to a line of constant elevation. Figures 14 and 15, based upon flow conditions at the free overfall,¹ clearly indicate

¹ ROUSE, H., "Verteilung der hydraulischen Energie bei einem lotrechten Absturz," Oldenbourg, Munich, 1933.

this essential distinction, the two force parallelograms for the same point in the flow yielding the same vector f .

A force potential may be defined in hydromechanics as a quantity whose derivative in any direction equals the component of force per unit volume acting in that direction. From this

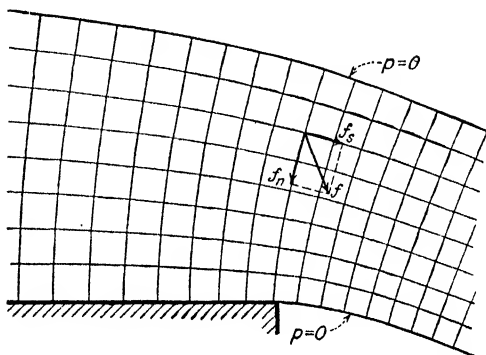


FIG. 14.—Velocity field at overfall crest.

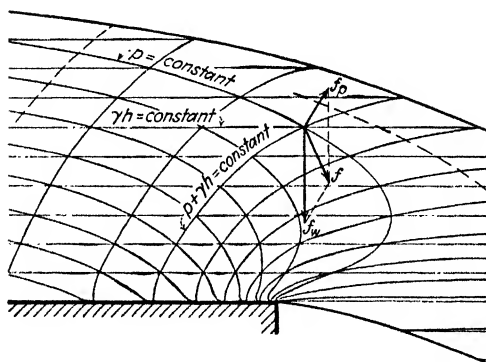


FIG. 15.—Force field at overfall crest.

definition it is evident that the force potential for flow under the action of weight and pressure must be the quantity $-(p + \gamma h)$, as will be seen from reference to Eq. (3). But since this expression may also be written in the form

$$f_x = \frac{\partial(-p)}{\partial x} + \frac{\partial(-\gamma h)}{\partial x}$$

it is clear that the quantities $-p$ and $-\gamma h$ also have the nature of force potentials; these may be called the pressure potential

and the weight potential, respectively, since

$$(f_p)_x = -\frac{\partial p}{\partial x} \quad \text{and} \quad (f_w)_x = -\frac{\partial(\gamma h)}{\partial x}$$

The lines of constant pressure intensity shown in Fig. 15 thus represent lines of constant pressure potential, while the lines of constant elevation are lines of constant weight potential; in either case successive lines represent constant increments of potential. Hence, while the lines of weight potential are necessarily equidistant parallels, variation in pressure intensity from point to point in the flow results in a gradual change in form and spacing of the pressure-potential lines. Because of the constant increment in potential from line to line, at a given point the force component in any direction for either pressure or weight is inversely proportional to the spacing of the lines in that direction; evidently, it attains its maximum value when normal to the potential line passing through the given point.

Since either system of lines represents a vector field of force, the two systems may be combined vectorially to yield a resultant system corresponding to the vector field of the resultant force f . Moreover, inasmuch as a line of total force potential must represent a constant value of the sum $(p + \gamma h)$, such vectorial combination may be accomplished graphically simply by connecting with smooth curves (the heavy lines in Fig. 15) successive points of intersection of the two component systems. Since the total force per unit volume at any point must be normal to the resultant potential line passing through this point, it is evident that the convective acceleration produced by this field of force must also be normal to the potential lines at all points of the flow. In other words, while the flow net shows at a glance the direction and relative magnitude of the velocity vector, the pattern of the potential field indicates the direction and relative magnitude of the vector of force or acceleration.

It should be evident from the foregoing discussion that the actual magnitude of either the pressure or the weight potential is of no consequence, for the corresponding force component is determined entirely by the rate of change of the potential in the given direction. The components f_p and f_w may vary greatly with respect to one another in different regions of a given flow, although if the flow is uniform their vector sum must always be

zero. They will approach this condition as a limit, for instance, a very great distance upstream from the crest of the free overfall, where the lines of constant pressure and of constant elevation practically coincide; f_w will then be directed downward and f_p , upward, the resultant lines of constant force potential then being vertical and extremely far apart. Within the falling nappe, on the other hand, as the pressure intensity approaches the atmospheric, the pressure gradient will approach zero, so that the lines of constant force potential will become more nearly coincident with lines of constant elevation.

So long as a given state of steady unconfined flow is the immediate result of gravitational action, at any point in the flow

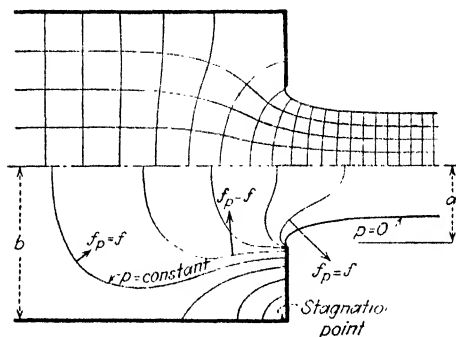


FIG. 16.—Velocity and force patterns for a two-dimensional orifice.

the ratio of f_p to f_w (*i.e.*, the direction of f) is fixed once and for all by the existing boundary conditions. Variation in the fluid properties of density and specific weight will most certainly change the magnitudes of these components and of the velocity of flow as well, but the flow net and the lines of force potential cannot possibly change in form. Similar circumstances are encountered in the case of completely confined flow, with the exception that either velocity or the fluid properties may be varied independently, and thereby produce a change in magnitude—but not direction—of the acceleration at any point; since weight can produce no acceleration in confined flow, $f_w = 0$ and $f = f_p$.

Distinctly different is the case of flow that is confined over only a part of its course, a condition illustrated by efflux of a liquid from a closed conduit into the atmosphere. In Fig. 16, for instance, is shown the flow net for discharge from a two-

dimensional orifice (*i.e.*, from a very wide rectangular opening). So long as the velocity of efflux is very high, the magnitude of f_w is quite negligible in comparison with the high values of f_p in the neighborhood of the orifice, so that only as f_p approaches zero some distance from the orifice does the action of weight in deflecting the jet become appreciable. However, f_p may be varied at will simply by changing the pressure intensity within the conduit (thus producing a change in the total energy of flow), gradual lowering of which will make f_p and f_w more and more nearly of the same order. Under such conditions the deflection of the jet will become more and more appreciable in the neighborhood of the opening, the jet thereby losing its original symmetry.

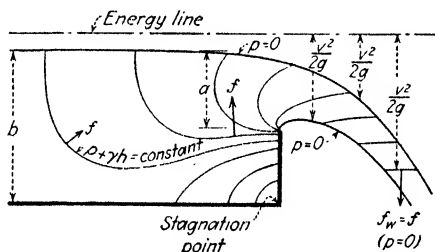


FIG. 17. Force pattern for a sharp-crested weir.

The evident limit of such variation is reached when the flow occurs entirely as a result of gravitational attraction, under which condition the flow energy is a minimum for the given boundaries. Such a case is illustrated by the suppressed weir of Fig. 17, the proportions of which have been made to correspond to the lower half of the orifice of Fig. 16. Significant is the fact that the lines of constant force potential are identical some distance upstream in both cases, despite the fact that weight is of no moment whatever in the one; only in the unconfined portion of the flow do these lines differ appreciably in form, and even then one can readily visualize a systematic progression from one to the other with variation in the relative magnitudes of the two force components. The reader will realize that horizontal acceleration within the nappe becomes negligible only as the potential lines approach the horizontal; only then will the nappe assume the parabolic trajectory of free fall.

It has been shown that the relative magnitudes of f_p and f_w in cases of efflux may be varied over a great range through

variation in the energy of flow. Though the fact is not generally appreciated, similar circumstances may be realized in weir flow as well. In the former instance, energy variation was accomplished by a change in pressure intensity within the conduit; with flow upstream from the weir freely exposed to the atmosphere, however, arbitrary change in pressure intensity is impossible. Yet the energy of flow may still be increased through increase in velocity head—accomplished, for instance, through discharge from a sluice gate or down a steep incline. Under such circumstances, it is evident from the momentum principle that the distribution of pressure intensity, and hence of pressure potential, could be altered almost at will with respect to a constant pattern of weight potential. Obviously, this would entail considerable variation in the form of the free surface, along which the pressure intensity must always remain atmospheric.

CHAPTER III

GENERALIZED EQUATIONS

15. Translation, Rotation, and Deformation of a Fluid Element.

For a more detailed study of the behavior of the individual particle than is possible in natural coordinates, one must turn to a more general coordinate system, the Cartesian. While the method of Lagrange, in which the particle is followed along its course, yields equations of definite significance, continued adherence to the procedure originated by Euler of observing conditions at fixed points in space will prove of greater value in the present discussion; the behavior of particles will then be studied as they pass the points in question.¹

During the very small increment of time dt the total variation of any velocity component v_x of a fluid particle must be equal to its rate of change with time $\partial v_x / \partial t$ multiplied by the time increment, plus its rate of change with movement in each of the coordinate directions, $\partial v_x / \partial x$, $\partial v_x / \partial y$, and $\partial v_x / \partial z$, multiplied by the increment of distance traveled in the corresponding direction in the same increment of time:

$$dv_x = \frac{\partial v_x}{\partial t} dt + \frac{\partial v_x}{\partial x} dx + \frac{\partial v_x}{\partial y} dy + \frac{\partial v_x}{\partial z} dz$$

As before, the partial derivatives represent variation with time, regardless of space, and with each direction in space, regardless of time and of the other two coordinate directions.

Since the distance a particle travels in any direction during an increment of time is equal to its component of velocity in this direction multiplied by the time increment, the following relationships exist:

$$dx = v_x dt; \quad dy = v_y dt; \quad dz = v_z dt$$

¹ LAMB, H., "Hydrodynamics," 6th ed., pp. 2-6, 31-35, Cambridge University Press, 1932.

From these three equations it is evident that the increments of distance traveled in the three directions in the same increment of time must be proportional to the velocity components in the respective directions; this proportionality is, in effect, the differential equation of the instantaneous stream line to which the velocity vector of the particle is tangent:

$$\frac{dx}{v_x} = \frac{dy}{v_y} = \frac{dz}{v_z} = \frac{ds}{v} \quad (21)$$

If the foregoing equivalents of dx , dy , and dz are substituted in the original expression, there will result:

$$dv_x = \frac{\partial v_x}{\partial t} dt + v_x \frac{\partial v_x}{\partial x} dt + v_y \frac{\partial v_x}{\partial y} dt + v_z \frac{\partial v_x}{\partial z} dt$$

Similar operations, of course, may be performed for each of the remaining coordinate directions. It is then obvious from inspection that division of each equation by the time increment will yield the total or substantial acceleration of the particle in each coordinate direction. From Eq. (5) these components of acceleration may then be equated to the component of force per unit mass acting upon the particle in the corresponding direction; thus are derived the three fundamental equations of Euler:

$$\frac{\partial v_x}{\partial t} + v_x \frac{\partial v_x}{\partial x} + v_y \frac{\partial v_x}{\partial y} + v_z \frac{\partial v_x}{\partial z} = -\frac{1}{\rho} \frac{\partial}{\partial x}(p + \gamma h) \quad (22x)$$

$$\frac{\partial v_y}{\partial t} + v_x \frac{\partial v_y}{\partial x} + v_y \frac{\partial v_y}{\partial y} + v_z \frac{\partial v_y}{\partial z} = -\frac{1}{\rho} \frac{\partial}{\partial y}(p + \gamma h) \quad (22y)$$

$$\frac{\partial v_z}{\partial t} + v_x \frac{\partial v_z}{\partial x} + v_y \frac{\partial v_z}{\partial y} + v_z \frac{\partial v_z}{\partial z} = -\frac{1}{\rho} \frac{\partial}{\partial z}(p + \gamma h) \quad (22z)$$

Consider now a fluid element of cubical form (shown in Fig. 18) having small but finite sides δx , δy , and δz , each parallel to the respective axis. At the point (x, y, z) —the corner of the cube nearest the origin—the velocity vector has the three components v_x , v_y , and v_z . Since the given state of flow varies with distance in each of the coordinate directions, at any instant the velocity components at every other corner of the cube will differ from these three by amounts depending upon the length of the sides and upon the gradient of each velocity component in each of the three coordinate directions.

In order to avoid the confusion of considering variations in all three directions at once, it will suffice to follow the changes in

any one face of the cube, later extending the relationships thereby developed to the other faces. Taking, for instance, the face nearest the plane of the x and y axes, the velocity components in the directions x and y at the four corners of this face will be as indicated in Fig. 19. Neglecting for the moment the local varia-

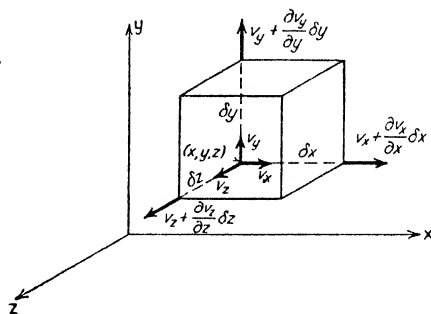


FIG. 18.—Variation in velocity along the boundaries of a fluid element.

tion (the change with time at a fixed point in space), it will be seen from the illustration that during a small time increment dt the actual motions of the several corners of the face must be different. Hence, not only will the face be moved bodily through space, but it must at the same time suffer a change in its original form.

In order to bring clarity into such a complex picture, let the motion be reduced to the four essential types of movement which the face may undergo: Superposed upon the translation of the square in the x and y directions, there will be in the most general case a change in the length of each pair of parallel sides (linear deformation), a change in each of the four corner angles (angular deformation), and a turning movement in one direction or the other (rotation). Each of these essential types of displacement is shown schematically in Fig. 20.

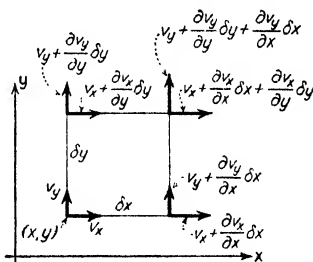


FIG. 19.—Velocity components in the xy plane.

During the time increment dt the magnitude of the translation in the two directions will be represented by the quantities

$$v_x dt \quad \text{and} \quad v_y dt$$

The magnitude of the linear deformation will be given by the difference between the distances moved by each pair of opposite sides:

$$\frac{\partial v_x}{\partial x} \delta x dt \quad \text{and} \quad \frac{\partial v_y}{\partial y} \delta y dt$$

Angular deformation, considering only the change in the right angle at the point (x, y, z) , will depend upon the difference between the angular movements $d\alpha$ and $d\beta$ of the two sides δx and δy . Since over a very short time these angular increments

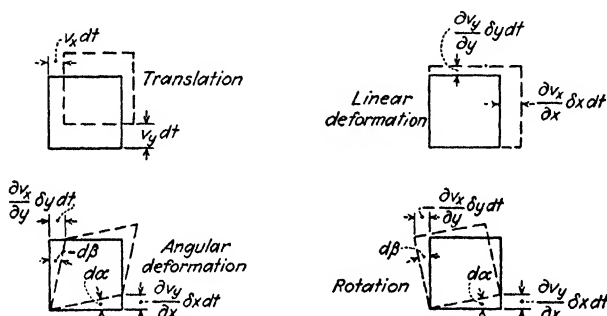


FIG. 20.—Schematic representation of translation, deformation, and rotation in the xy plane.

will be small, they may be considered numerically equal to their respective tangents; selecting the counterclockwise direction as positive:

$$d\alpha = \frac{\partial v_y}{\partial x} \delta x dt; \quad d\beta = -\frac{\partial v_x}{\partial y} \delta y dt$$

$$d\alpha - d\beta = \left(\frac{\partial v_y}{\partial x} + \frac{\partial v_x}{\partial y} \right) dt$$

Rotation, on the other hand, will occur if the angular increments are unequal or of like sign; the total angle through which the face is rotated will be equal to their average value:

$$\frac{d\alpha + d\beta}{2} = \frac{1}{2} \left(\frac{\partial v_y}{\partial x} - \frac{\partial v_x}{\partial y} \right) dt$$

It will be apparent that translation and rotation are allied types of displacement, since each denotes a bodily movement of

the face without changing its original form. Similarly, linear and angular deformation bear a definite relationship to each other, since the former generally involves a change in the angles formed by the diagonals, whereas the latter involves a change in the diagonal lengths. Thus, linear deformation would become angular deformation according to axes turned through 45° , and vice versa.

Owing to the finite dimensions of the original cube, the values just given for each type of displacement are not exact, variables of order higher than the first having been omitted. But if the sides of the cube are now assumed to become infinitesimal, all corners then approaching the point (x, y, z) as a limit, each type of movement may be expressed exactly as a rate of change with time. At the given point the rate of translation in the three coordinate directions will be simply the three velocity components

$$v_x, \quad v_y, \quad v_z \quad \text{and} \quad v = \sqrt{v_x^2 + v_y^2 + v_z^2}$$

The rate of linear deformation in each of the coordinate directions will be

$$\frac{\partial v_x}{\partial x} dx, \quad \frac{\partial v_y}{\partial y} dy, \quad \frac{\partial v_z}{\partial z} dz$$

each denoting the velocity at which the respective opposite faces are drawing apart. Since the density (and hence the volume) of a fluid particle must remain constant during such deformation, it is obvious that an elongation of the particle in two directions must be compensated by a contraction in the third, and vice versa. Thus, the rates of linear deformation in the three coordinate directions (*i.e.*, the changes per unit time of the distances between opposite faces) multiplied by the areas of the respective faces must have a sum of zero:

$$\frac{\partial v_x}{\partial x} dx(dy dz) + \frac{\partial v_y}{\partial y} dy(dz dx) + \frac{\partial v_z}{\partial z} dz(dx dy) = 0$$

Dividing each term by the elementary volume yields the most general form of the equation of continuity, which states that the "divergence" of the velocity vector must equal zero in a flow in which the density is not a variable quantity; in other words, the velocity cannot increase or decrease in all three directions at once.

$$\operatorname{div} v = \frac{\partial v_x}{\partial x} + \frac{\partial v_y}{\partial y} + \frac{\partial v_z}{\partial z} = 0 \quad (23)$$

The rate of angular deformation at a given point (a quantity which varies with direction but which is not a true vector) is designated in each of the coordinate directions by the symbols ξ (xi), η (eta), and ζ (zeta). These symbols then represent the rate of angular deformation in planes normal to each of the three axes; for purposes which will be clear directly, they are arbitrarily made equal to one-half the actual rate of angular deformation:

$$\xi = \frac{1}{2} \left(\frac{\partial v_z}{\partial y} + \frac{\partial v_y}{\partial z} \right); \eta = \frac{1}{2} \left(\frac{\partial v_x}{\partial z} + \frac{\partial v_z}{\partial x} \right); \zeta = \frac{1}{2} \left(\frac{\partial v_y}{\partial x} + \frac{\partial v_x}{\partial y} \right) \quad (24)$$

On the other hand, the rate of rotation—angular velocity—is a true vector quantity and is given the customary symbol ω (omega); its components will then denote the rotation per unit of time in planes normal to the three axes, the sense of rotation determining the direction of the vector:

$$\omega_x = \frac{1}{2} \left(\frac{\partial v_z}{\partial y} - \frac{\partial v_y}{\partial z} \right); \omega_y = \frac{1}{2} \left(\frac{\partial v_x}{\partial z} - \frac{\partial v_z}{\partial x} \right); \omega_z = \frac{1}{2} \left(\frac{\partial v_y}{\partial x} - \frac{\partial v_x}{\partial y} \right) \quad (25)$$

The vector 2ω is known in hydromechanics as the curl of the velocity vector:

$$\omega = \sqrt{\omega_x^2 + \omega_y^2 + \omega_z^2} = \frac{1}{2} \operatorname{curl} v \quad (26)$$

Since the convective acceleration at any point in space must depend not only upon the magnitude and direction of the velocity vector at the given point but also upon the divergence of the velocity vector and upon angular deformation and rotation, it should be possible to incorporate these quantities in the three equations of Euler. Thus the convective terms of Eq. (22x) may be rewritten as follows, through simultaneous addition and subtraction of the proper quantities:

$$\begin{aligned} v_x \frac{\partial v_x}{\partial x} + v_y \frac{\partial v_x}{\partial y} + v_z \frac{\partial v_x}{\partial z} + \frac{1}{2} v_y \frac{\partial v_y}{\partial x} - \frac{1}{2} v_y \frac{\partial v_y}{\partial x} + \frac{1}{2} v_z \frac{\partial v_z}{\partial x} - \frac{1}{2} v_z \frac{\partial v_z}{\partial x} \\ = v_x \frac{\partial v_x}{\partial x} + \frac{1}{2} v_y \left(\frac{\partial v_y}{\partial x} + \frac{\partial v_x}{\partial y} \right) - \frac{1}{2} v_y \left(\frac{\partial v_y}{\partial x} - \frac{\partial v_x}{\partial y} \right) \\ + \frac{1}{2} v_z \left(\frac{\partial v_z}{\partial x} + \frac{\partial v_x}{\partial z} \right) + \frac{1}{2} v_z \left(\frac{\partial v_z}{\partial x} - \frac{\partial v_x}{\partial z} \right) \end{aligned}$$

On performing a similar operation upon each of the three components of convective acceleration and substituting the corresponding symbols from Eqs. (24) and (25), there will result:

$$\frac{\partial v_x}{\partial t} + v_x \frac{\partial v_x}{\partial x} + v_y \zeta + v_z \eta - v_y \omega_z + v_z \omega_y = -\frac{1}{\rho} \frac{\partial}{\partial x}(p + \gamma h) \quad (27x)$$

$$\frac{\partial v_y}{\partial t} + v_y \frac{\partial v_y}{\partial y} + v_z \xi + v_x \zeta - v_z \omega_x + v_x \omega_z = -\frac{1}{\rho} \frac{\partial}{\partial y}(p + \gamma h) \quad (27y)$$

$$\frac{\partial v_z}{\partial t} + v_z \frac{\partial v_z}{\partial z} + v_x \eta + v_y \xi - v_x \omega_y + v_y \omega_x = -\frac{1}{\rho} \frac{\partial}{\partial z}(p + \gamma h) \quad (27z)$$

Owing to the general character of the Cartesian system, it is seldom necessary to develop more than one of the three equations for any condition of flow, for the remaining two may always be found from the first through the method of cyclic permutation. Thus Eqs. (27y) and (27z) may be derived from Eq. (27x) by substituting y for x , z for y , and x for z in every instance in which these symbols occur. This method applies fully as well to such expressions as the components of ω as to the general equations of Euler, and will assist the reader in comprehending the otherwise complex nature of this system.

So long as the vector of rotation ω has a finite value, the flow is characterized as rotational, the significance of which may be shown by the following operation: If each component of this vector is reduced to zero, the flow will become irrotational, whereupon,

$$\frac{\partial v_z}{\partial y} = \frac{\partial v_y}{\partial z}; \quad \frac{\partial v_x}{\partial z} = \frac{\partial v_z}{\partial x}; \quad \frac{\partial v_y}{\partial x} = \frac{\partial v_x}{\partial y} \quad (28)$$

Adding and subtracting equivalent terms in Eq. (27x), now written for irrotational motion,

$$\begin{aligned} \frac{\partial v_x}{\partial t} + v_x \frac{\partial v_x}{\partial x} + \frac{1}{2} v_y \frac{\partial v_y}{\partial x} + \frac{1}{2} v_y \frac{\partial v_x}{\partial y} + \frac{1}{2} v_z \frac{\partial v_x}{\partial z} + \frac{1}{2} v_z \frac{\partial v_x}{\partial x} \\ + \frac{1}{2} v_y \frac{\partial v_y}{\partial x} - \frac{1}{2} v_y \frac{\partial v_x}{\partial y} - \frac{1}{2} v_z \frac{\partial v_x}{\partial z} + \frac{1}{2} v_z \frac{\partial v_x}{\partial x} \\ = -\frac{1}{\rho} \frac{\partial}{\partial x}(p + \gamma h) \end{aligned}$$

whence

$$\frac{\partial v_x}{\partial t} + v_x \frac{\partial v_x}{\partial x} + v_y \frac{\partial v_y}{\partial x} + v_z \frac{\partial v_z}{\partial x} = -\frac{1}{\rho} \frac{\partial}{\partial x}(p + \gamma h)$$

This result may also be written in the form

$$\frac{\partial v_x}{\partial t} + \frac{\partial(v_x^2/2)}{\partial x} + \frac{\partial(v_y^2/2)}{\partial y} + \frac{\partial(v_z^2/2)}{\partial z} = -\frac{1}{\rho} \frac{\partial}{\partial x}(p + \gamma h)$$

in which the convective portion of the left side of the equation is simply the derivative of the square of the resultant velocity, since

$$\frac{v_x^2 + v_y^2 + v_z^2}{2} = \frac{v^2}{2}$$

Similar results will be obtained for the two other coordinate directions through the same operation, from which it is at once obvious that throughout the entire flow

$$\frac{\partial v_x}{\partial t} + \frac{\partial E_m}{\partial x} = \frac{\partial v_y}{\partial t} + \frac{\partial E_m}{\partial y} = \frac{\partial v_z}{\partial t} + \frac{\partial E_m}{\partial z} = 0 \quad (29)$$

The significance of the above result cannot be overemphasized; expressed in words, this important fact is as follows: Except for arbitrary change in the hydrostatic load, in irrotational motion the energy of a particle can vary in magnitude from point to point in the flow only if conditions are changing with time. In other words, steady irrotational flow is always one of constant energy. It will be recalled that in developing Eq. (19) the energy was assumed constant from one stream line to the next, so that

$$\frac{\partial v}{\partial n} - \frac{v}{r} = 0 \quad \text{or} \quad \frac{\partial v_s}{\partial n} - \frac{\partial v_n}{\partial s} = 0$$

Referred to the natural coordinate system, this quantity is merely the one component (ω_m) of the rotation vector which can be present in two-dimensional motion, and which must be zero if the motion is to be one of constant energy.

Perhaps even more important is the converse of this conclusion: In unsteady, rotational motion the energy of flow can never be constant, for it will vary at a given point with time, and at a given instant with distance in any direction.

16. Circulation and Vorticity. To visualize clearly the phenomenon of rotation, it is necessary to introduce a new expression, circulation, which is customarily given the symbol Γ (the Greek capital letter gamma). Circulation is defined as the line integral of the tangential velocity component around any closed curve

(see Fig. 21):

$$\Gamma = \oint v_L dL \quad (30)$$

It must be understood that such a curve in itself is independent of the velocity field and may be given any desired shape, size, and position. Moreover, as shown in Fig. 22, the circulation around any such three-dimensional curve will be equal to the sum of all the circulations around any system of figures into which the surface bordered by the curve is subdivided. This is true because the line integral along the neighboring sides of each pair of subdivisions will be of opposite sign, so that the algebraic

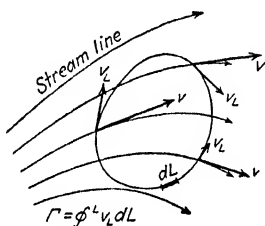


FIG. 21.—Line integral.

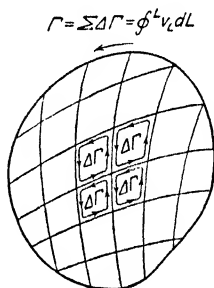


FIG. 22.—Circulation.

sum of all will simply result in the circulation around the outer curve.

If any such surface becomes exceedingly small, the circulation around its enclosing curve will indicate actual rotation about an axis normal to the small increment of area. Thus, the limit of the circulation per unit of area, as the area approaches zero, is equal to twice the component of the rotation vector ω normal to the surface:

$$\lim_{A \rightarrow 0} \frac{\Gamma_A}{A} = 2\omega_{\perp A} \quad (31)$$

The significance of this relationship will be apparent after considering the circulation around the rectangle in the xy plane shown in Fig. 19. If the elementary rectangle is sufficiently small, the line integral of tangential velocity along each side will equal the average velocity between the two corners times the length of the side. Writing the circulation in the counter-

clockwise direction,

$$\delta\Gamma_{xy} = \left(v_x + \frac{1}{2} \frac{\partial v_x}{\partial x} \delta x \right) \delta x + \left(v_y + \frac{\partial v_y}{\partial x} \delta x + \frac{1}{2} \frac{\partial v_y}{\partial y} \delta y \right) \delta y \\ - \left(v_x + \frac{\partial v_x}{\partial y} \delta y + \frac{1}{2} \frac{\partial v_x}{\partial x} \delta x \right) \delta x - \left(v_y + \frac{1}{2} \frac{\partial v_y}{\partial y} \delta y \right) \delta y.$$

As the area of the surface approaches the limit zero, the resulting expression for circulation per unit area will be:

$$\lim_{\delta x \delta y \rightarrow 0} \frac{\delta\Gamma_{xy}}{\delta x \delta y} = 2\omega_z = \frac{\partial v_y}{\partial x} - \frac{\partial v_x}{\partial y}$$

The remaining components of the rotation vector may be derived in a similar manner:

$$\lim_{\delta y \delta z \rightarrow 0} \frac{\delta\Gamma_{yz}}{\delta y \delta z} = 2\omega_x = \frac{\partial v_z}{\partial y} - \frac{\partial v_y}{\partial z} \\ \lim_{\delta z \delta x \rightarrow 0} \frac{\delta\Gamma_{zx}}{\delta z \delta x} = 2\omega_y = \frac{\partial v_x}{\partial z} - \frac{\partial v_z}{\partial x}$$

Since ω is a vector quantity and similar in many respects to the velocity vector v , its distribution in space may be represented in a similar way; that is, a system of vortex lines may be constructed in space, having the same relation to the rotation or vorticity at any point as a stream line has to velocity. Thus a vortex line shows through tangency to the vorticity vector the sense of rotation and the direction of its axis at every point for a given instant, it being assumed that the vector indicates the direction of rotation of a right-hand screw—i.e., clockwise when looking in the positive direction. If the quantities dx , dy , and dz represent the projections of dw , a differential length of vortex line, on the three axes, Eq. (21) for the stream line will have its counterpart in the differential equation of the vortex line:

$$\frac{dx}{\omega_x} = \frac{dy}{\omega_y} = \frac{dz}{\omega_z} = \frac{dw}{\omega} \quad (32)$$

Just as a small group of stream lines may form a stream filament of varying cross-sectional area ΔA , the rate of discharge past all such sections being the same at a given instant, so may a group of vortex lines form a vortex filament of varying cross-sectional area ΔA (Fig. 23), the circulation around the perimeter

of all cross sections being the same at any instant:

$$v \Delta A = \Delta Q = \text{constant} \quad \text{and} \quad 2\omega \Delta A = \Delta \Gamma = \text{constant}$$

Inasmuch as the law of continuity applied to a stream filament thus has its counterpart in the law of constant strength of a

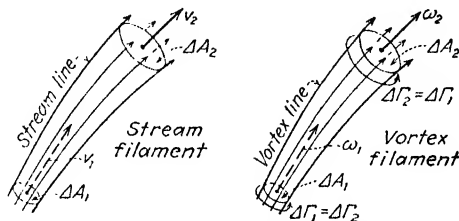


FIG. 23.—Parallel characteristics of stream and vortex filaments.



M.I.T.

FIG. 24.—Vortex filament at the base of a weir (compare with Fig. 141).

vortex filament, it might be assumed that the mathematical expression for the divergence of the velocity vector could be written in a similar fashion for the vector of rotation:

$$\text{div } v = \frac{\partial v_x}{\partial x} + \frac{\partial v_y}{\partial y} + \frac{\partial v_z}{\partial z} = 0; \quad \text{div } \omega = \frac{\partial \omega_x}{\partial x} + \frac{\partial \omega_y}{\partial y} + \frac{\partial \omega_z}{\partial z} = 0$$

That this is true may be proved by substituting in the above expression the components of ω in terms of the space derivatives of the velocity.

17. Characteristics of the Vortex. While stream lines generally exist throughout all portions of a fluid in motion, a single vortex line may exist in an otherwise irrotational flow, so that only those infinitesimal fluid particles lying directly upon that line will undergo rotational motion. Such a case may be illustrated by the movement of fluid in concentric layers around a vertical axis in such a way that all particles not lying upon that

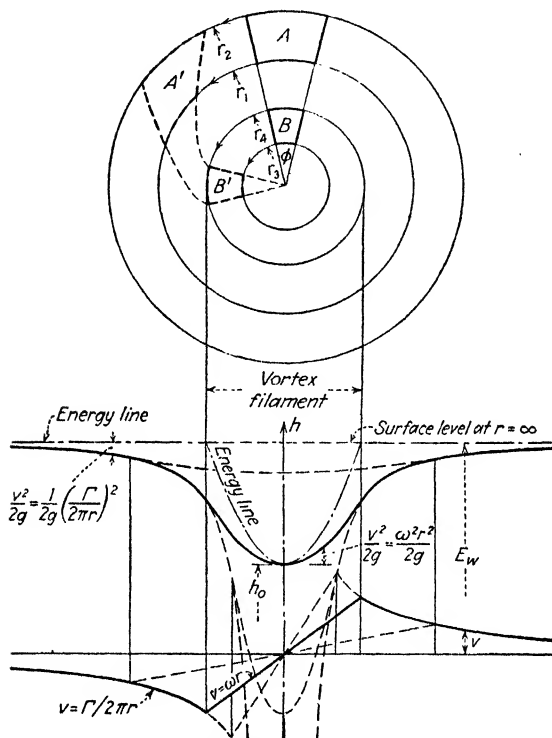


FIG. 25.—Characteristics of the combined vortex.

axis have the same total energy of flow—i.e., the flow is steady and irrotational. If these conditions are fulfilled, the circulation around any horizontal curve (not including the center) must be equal to zero.

Referring to Fig. 25, the circulation around the area A bounded by any two radial lines and any two circular arcs having the radii r_1 and r_2 may be written as follows:

$$\Gamma = v_2 \phi r_2 - v_1 \phi r_1$$

If this quantity is equal to zero, the flow is irrotational and the velocity distribution must be such that

$$v_1 r_1 = v_2 r_2 \quad \text{and} \quad v = \frac{C}{r}$$

This is in agreement with Eq. (19) for irrotational flow:

$$\frac{\partial v}{\partial n} = \frac{v}{r}, \quad dn = -dr; \quad \ln v = -\ln r; \quad vr = C$$

Since the total head is constant, the pressure head along any horizontal plane will be

$$\frac{p}{\gamma} = E_w - h - \frac{v^2}{2g} = E_w - h - \frac{C^2}{2gr^2}$$

If the fluid is a liquid with a free surface at constant (atmospheric) pressure, the elevation of this surface above any geodetic datum may be written

$$h = E_w - \frac{C^2}{2gr^2}$$

in which E_w represents the surface elevation an infinite distance from the axis. The profile of such concentric motion is shown in Fig. 25, the phenomenon being known as the free or potential vortex.

Around any circular stream line, however, the circulation will have a finite magnitude

$$\Gamma = 2\pi rv$$

which will be a constant irrespective of the radius of the circle. The term $\Gamma/2\pi$ is then the constant (*i.e.*, the product of the velocity and the radius of curvature) in the above equations. But since the circulation around any such circle, no matter how small, is a finite constant, then the ratio Γ/A becomes infinitely great as the area of the circle approaches zero. Hence, the rotation vector ω is infinite along the axis (the axis being a vortex line) but equal to zero at every other point in the flow.

Obviously, this is an impossible condition, for it requires either that the surface at the center drop an infinite distance below any geodetic datum chosen, or, if the fluid is completely enclosed, that the pressure intensity at the center be negative

infinity. However, the space in the neighborhood of the single vortex line may contain fluid which does not follow the potential relationship of the general flow, but behaves as a vortex filament, all particles of which have a constant rate of rotation.

The velocity characteristics of such a filament are similar to those of the tank of liquid rotating with constant angular velocity ω as studied in hydraulics. Since the fluid particles have no motion relative to one another, the velocity must vary directly with the radius:

$$v = \omega r$$

The circulation around any stream line will then vary with the square of the radius

$$\Gamma = 2\pi r v = 2\pi \omega r^2$$

as will the circular area πr^2 bounded by the stream line. Hence, the rotation vector at the center must be

$$\omega = \frac{\Gamma}{2A} = \frac{2\pi \omega r^2}{2\pi r^2} = \omega$$

But the circulation around any area B (Fig. 25) bounded by two radial lines and two circular arcs and not including the central axis, divided by the area of this surface, yields the identical rotation vector for any fluid particle in the vortex filament:

$$\omega = \frac{\Gamma}{2A} = \frac{v_4 \phi r_4 - v_3 \phi r_3}{\phi (r_4^2 - r_3^2)} = \omega$$

It is obvious that the energy of flow cannot be a constant, because of this rotational motion. Denoting by h_0 the surface level at the axis, the elevation of the free surface at any radius may be found from Eq. (6n):

$$\begin{aligned} \frac{v^2}{r} &= -\frac{1}{\rho} \frac{\partial}{\partial n} (p + \gamma h) = g \frac{\partial h}{\partial r} \\ \frac{v^2}{gr} &= \frac{\omega^2 r}{g} = \frac{\partial h}{\partial r}; \quad \int \frac{\omega^2 r}{g} dr = \int dh \\ h &= C + \frac{\omega^2 r^2}{2g} = h_0 + \frac{v^2}{2g} \end{aligned}$$

A combination of the two types of motion is known as the Rankine combined vortex, with profile and velocity distribution as shown in Fig. 25.

Observation with time of the two elementary areas A and B in the light of the foregoing study of the four essential types of displacement should serve to clarify the general conclusions reached at that time. Since a velocity vector exists at every point of the motion with the sole exception of the central axis, all particles are being translated through space at a rate varying with the distance from the central axis. While a mathematical treatment of deformation and rotation in this case requires use of the cylindrical coordinate system, inspection of Fig. 25 will suffice to show that in addition to translation surface A will undergo both linear and angular deformation, but not rotation, whereas surface B will be rotated but not deformed.

Such an isolated vortex filament in an otherwise irrotational state of fluid motion must always be surrounded by a velocity field, as shown in Fig. 25, which extends outward to the boundaries of the flow, the velocity in this field being inversely proportional to the distance from the axis of the vortex filament. The existence of two or more neighboring filaments thus results in a relative movement of each filament in accord with the velocity fields of the others. Two vortices of equal strength and opposite directions of rotation will propel each other in a direction normal to the plane of their axes, as shown in Fig. 26, the velocity of translation depending upon the strength and spacing of the filaments (refer to the curve of velocity distribution as a function of distance from the filament in Fig. 25); on the other hand, if the vortices are of unequal strength, they will move with different velocities around concentric circles of unequal radii. If the filaments are of equal strength and have the same direction of rotation, both will move around the same circle; if of unequal strength, they will travel about concentric circles of unequal radii, on opposite sides of the common center. If a single filament exists near a plane boundary parallel to the axis of the filament, it will move parallel to the boundary as though impelled by an imaginary vortex (its "mirror image") on the other side of the wall. The vortex ring (exemplified by the common smoke ring) moves through space under the influence of its own velocity field; the direction of translation is normal to the plane of the

ring. It should be obvious that the presence of many vortices of different strengths in a moving fluid will give rise to a very complex velocity field throughout the fluid.

The reader may readily convince himself of the existence of such movements by generating small vortices with a paddle in a basin of water, the upper ends of the filaments being visible as small depressions in the water surface. The potential vortex is

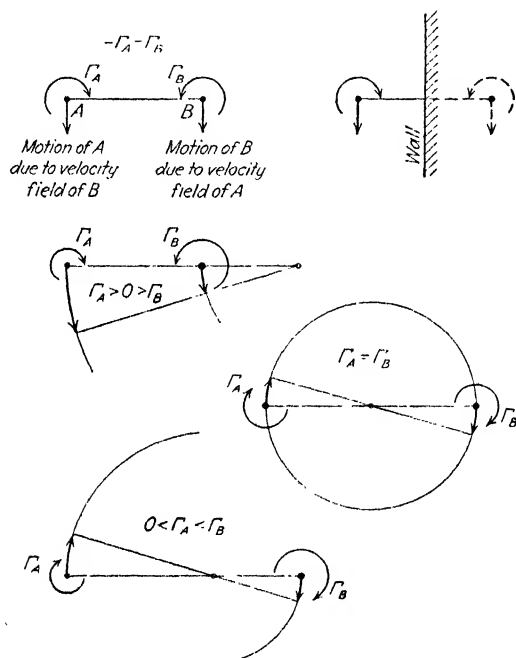


FIG. 26.—Interaction of neighboring vortices.

illustrated by the movement developing in a tank of water shortly after a drain has been opened in the bottom of the tank, a hollow space forming in the surface and extending downward to the drain, and displaying a profile very similar to the outer curve shown in Fig. 25. If the drain is then partially closed, the profile will become that of the Rankine combined vortex. Cyclonic twisters and water spouts are also examples of vortex motion, in which the filament itself is made visible by dust and by water, respectively.

A principle of classical hydrodynamics, known as Thomson's law, states that irrotational motion can never become rotational

so long as only gravitational and pressure forces act upon the fluid particles; similarly, under these conditions rotational motion must always remain rotational. Moreover, since the strength of a vortex filament must remain constant throughout

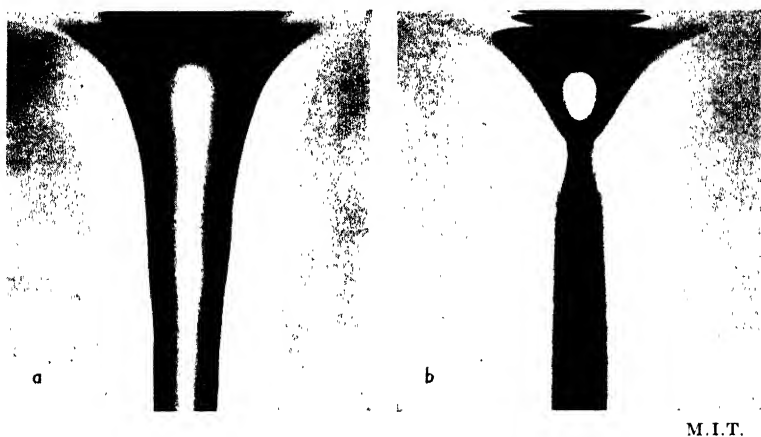


FIG. 27.—Profiles of (a) the potential and (b) the combined vortex, occurring above an orifice in the bottom of a tank. The central portion of the combined vortex has been colored by dye.



FIG. 28.—Velocity distribution of the combined vortex as indicated by the paths of aluminum particles during a short time exposure.

its length, it is impossible for a filament to end abruptly within a fluid medium; it must either be a closed curve, as in the case of a smoke ring, or terminate at a free surface or a solid boundary. While these principles have long since been vindicated by rigid

mathematical proof, the fact remains that rotational movement may be started in any fluid at will, the motion then gradually becoming irrotational as the fluid again comes to rest.

These circumstances lead at once to the following conclusion: Since neither weight nor the normal force of fluid pressure upon a particle can produce rotation, any change in rotational energy must be the result of tangential stress, which can be caused only through viscous shear. Indeed, the very basis of modern progress in fluid mechanics lies in the appreciation of the role played by viscosity; the fact has been verified repeatedly in experimental investigations that viscous action is essential to the generation of rotational motion, and that only by conversion into heat through viscous shear can rotational energy be diminished.

It has been shown in the foregoing pages that rotational motion may often be studied quite satisfactorily at any instant in the light of the non-viscous flow equations, regardless of whether the rotation is continuously distributed throughout the fluid, or discontinuously, as in the case of isolated vortex filaments. On the other hand, the rotational characteristics of many types of flow are of so secondary a nature that the assumption of irrotational motion is often fully justified. A more intensive study of rotation will, therefore, be left until a later chapter on viscous flow.

CHAPTER IV

IRROTATIONAL MOTION

18. The Velocity Potential. Returning now to the case of irrotational movement, since at every point in the field of motion all three components of the vorticity vector ω must equal zero, the following equalities will obtain:

$$\frac{\partial v_z}{\partial y} = \frac{\partial v_y}{\partial z}; \quad \frac{\partial v_x}{\partial z} = \frac{\partial v_z}{\partial x}; \quad \frac{\partial v_y}{\partial x} = \frac{\partial v_x}{\partial y} \quad (33)$$

Under these conditions there will exist a velocity potential ϕ (phi) throughout the flow, the space derivatives of which at any point will equal the velocity components in the corresponding directions:

$$v_x = \frac{\partial \phi}{\partial x}; \quad v_y = \frac{\partial \phi}{\partial y}; \quad v_z = \frac{\partial \phi}{\partial z} \quad (34)$$

This relationship may be verified by substituting in Eqs. (33) the velocity components as expressed in Eqs. (34):

$$\frac{\partial^2 \phi}{\partial z \partial y} = \frac{\partial^2 \phi}{\partial y \partial z}; \quad \frac{\partial^2 \phi}{\partial x \partial z} = \frac{\partial^2 \phi}{\partial z \partial x}; \quad \frac{\partial^2 \phi}{\partial y \partial x} = \frac{\partial^2 \phi}{\partial x \partial y}$$

Since differentiation with respect to two variables is independent of the order of differentiation, the above values will be seen to be identities, and Eqs. (34) are thereby substantiated.

The significance of such a velocity potential may be seen through comparison with the force potential, a mathematical relationship already used in the development and application of the three equations of Euler. It was shown that the derivative of the quantity $-(p + \gamma h)$ in any direction must equal the component of the accelerative force per unit volume in that direction; $-(p + \gamma h)$ is obviously a scalar quantity, its magnitude varying generally with time and three-dimensional space. Thus at any instant imaginary surfaces of constant force potential may be considered to exist throughout the moving fluid, the resultant vector f of accelerative force per unit volume at every

point being normal to one of these surfaces. ϕ is likewise a scalar quantity and a function of time and space, and at any instant surfaces of constant velocity potential may also be imagined to exist throughout the fluid, the velocity vector at every point being normal to such a surface. A surface of constant velocity potential is thus normal at all points to the direction of motion, whereas a surface of constant force potential is normal at all points to the direction of acceleration.

Inasmuch as every velocity vector is tangent to a stream line at a given instant, a surface of constant velocity potential must cut all instantaneous stream lines at right angles. Therefore,

$$v = \frac{\partial \phi}{\partial s} \quad (35)$$

and it is apparent that the magnitude of ϕ must increase in the direction of flow according to this relationship. It should also be apparent to the reader that the normal trajectories of the two-dimensional flow net are merely intersections of surfaces of constant velocity potential with the plane of motion. The systematic spacing of these n trajectories resulted in constant increments of ϕ from one line to the next, so that the relative velocity at any point could be seen from the spacing of these potential lines, according to Eq. (35) written in approximate form:

$$v = \frac{\Delta \phi}{\Delta s} = \frac{C}{\Delta s}$$

It has already been shown that flow with constant specific energy must be both irrotational and steady. Even if irrotational motion is unsteady, there is still a direct relationship between the energy of flow and the rate of change of the velocity potential with time, $\partial \phi / \partial t$, which may be developed as follows: Any one of the three equations of Euler written for unsteady irrotational motion (see page 71),

$$\frac{\partial v_x}{\partial t} + v_x \frac{\partial v_x}{\partial x} + v_y \frac{\partial v_y}{\partial x} + v_z \frac{\partial v_z}{\partial x} = -\frac{1}{\rho} \frac{\partial}{\partial x} (p + \gamma h)$$

may now be written in the form,

$$\frac{\partial^2 \phi}{\partial x \partial t} + \frac{\partial (v^2/2)}{\partial x} = -\frac{1}{\rho} \frac{\partial}{\partial x} (p_a + p_s + \gamma h)$$

Integrating with respect to x , this will then become:

$$\rho \frac{\partial \phi}{\partial t} + \rho \frac{v^2}{2} + p_d = F(t) - (p_s + \gamma h) \quad (36)$$

The term $F(t)$ represents merely an arbitrary function of time allowing for possible variation of the hydrostatic pressure load on a closed system; it has already been shown that this will have no effect whatsoever upon the pattern of flow (so long as the absolute pressure does not reach zero at any point). Equation (36) may thus be rewritten in the form¹

$$\rho \frac{\partial \phi}{\partial t} + \rho \frac{v^2}{2} + p_d = \text{constant} \quad (37)$$

showing that in unsteady irrotational flow the dynamic characteristics are directly dependent upon the temporal variation of the velocity potential.

As yet no restriction has been placed on the variation of ϕ , for it remains to be stated that the motion described by the velocity potential must also fulfill the conditions of continuity. The equation of continuity may be written in terms of ϕ , through substitution of its space derivatives [Eqs. (34)] in Eq. (23):

$$\frac{\partial^2 \phi}{\partial x^2} + \frac{\partial^2 \phi}{\partial y^2} + \frac{\partial^2 \phi}{\partial z^2} = 0 \quad (38)$$

This general relationship, known as the equation of Laplace, must be satisfied by any velocity potential.

If, for a given set of boundary conditions, ϕ could be expressed mathematically as a continuous function of time and space which would satisfy Eq. (38), the state of flow would then be completely defined by this one expression; it would at once be possible to determine from it any desired characteristic of flow at any point, through substitution in Eqs. (34) and (37), and thus entirely eliminate further use of the three equations of Euler and the one of continuity—obviously a great simplification.

However, unless a given state of unsteady motion can be reduced to a steady one through introduction of a moving coordinate system, except in certain special cases it will be found exceedingly difficult to express the variation of ϕ with both time and space. Hence, the question of unsteady motion must be

¹ Compare with LAMB, "Hydrodynamics," pp. 19-22.

left for the time being, the discussion of potential flow henceforth dealing entirely with movement that is independent of time. Under these circumstances, the local acceleration will be zero at every point, and Eq. (36) will then become the equation of Bernoulli.

19. Problems in Three-dimensional Flow. It might now be assumed that ϕ could be written at once as a function of coordinate space for any given boundary conditions. Unfortunately, this is by no means the case. While a velocity potential unquestionably exists for every possible type of irrotational motion, the mathematical ingenuity of the scientist is not yet of such calibre as to enable him to derive at will expressions for more than the simplest cases of such motion. As a matter of fact, classical hydrodynamics advanced largely through the reverse procedure of finding boundary conditions to which known functions of the velocity potential would apply. These known functions for three-dimensional motion are comparatively few in number and deal generally with flow around such bodies of revolution as airships and undersea craft. Since each has its counterpart in the more highly developed study of two-dimensional potential flow, which will be discussed directly, only brief mention of several typical examples will be necessary at this point.

Just as rotation may exist along a single vortex line in otherwise irrotational fluid motion—a singular line, mathematically speaking—it is also permissible to introduce what is known in hydrodynamics as a point source or a point sink—a singular point in the fluid medium at which fluid matter is either created or destroyed at a given constant rate. The equation of continuity for a fluid of constant density will then hold exactly at every point in the flow, with the one exception of the point source or sink, at which point the divergence of the velocity vector will change abruptly from zero to negative or positive infinity. Similar conditions were found to hold in the case of the vortex line, the rotation vector being infinitely great on the line itself, and zero throughout the remainder of the flow.

Since the equation of continuity still applies to all regions of flow other than the one singular point, the rate of discharge Q through all imaginary spheres surrounding the singular point must be the same as the rate at which fluid is presumed to be created or destroyed at that point. Denoting by R the radius

of any sphere concentric with the source or sink, since the flow is radial in all directions, the velocity $v = v_r$ at a given radius may be found from the expression

$$v_r = \pm \frac{Q}{4\pi R^2}$$

the plus sign applying to the source and the minus to the sink (Fig. 29). Since this velocity vector is equal to the gradient of the velocity potential in the radial direction, ϕ must then have the following form:

$$\phi = \int v_r dR = \mp \frac{Q}{4\pi R}$$

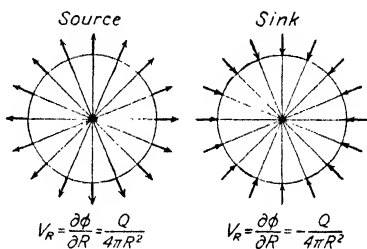


FIG. 29.—Source and sink.

Motion of this sort may be more clearly visualized if compared with flow toward a small orifice in the side of an extremely large tank. With the exception of the immediate neighborhood of the orifice itself, where the motion is curvilinear, the velocity will be radial and will vary inversely with the square of the radius. The orifice symbolizes the point sink, the flow picture in this case being just one-half of the symmetrical pattern of stream lines approaching a true sink from all directions (see Fig. 30).

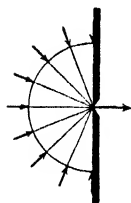


FIG. 30.
Flow toward
a small orifice.

If a source and a sink of equal magnitude are located a distance m apart in a fluid otherwise at rest, all of the fluid leaving the source will return sooner or later to the sink, following stream lines shown schematically in Fig. 31. Placing the cylindrical coordinate origin midway between the source (Q_1) and the sink ($-Q_2$), the velocity potential of the combined flow will be simply the sum of the velocity potential of the source ϕ_1 and that of the sink ϕ_2 ; since the radius R of the spherical system now becomes $\sqrt{r^2 + z^2}$ (refer to Fig. 31),

$$\phi = \phi_1 + \phi_2 = - \frac{Q}{4\pi\sqrt{r^2 + \left(z + \frac{m}{2}\right)^2}} + \frac{Q}{4\pi\sqrt{r^2 + \left(z - \frac{m}{2}\right)^2}}$$

The velocity at any point of the flow will then be the vector sum of the components in the r and z directions, each of which may be found by taking the proper space derivative of ϕ . If the source is greater or smaller than the sink, there will be a positive or negative surplus of fluid ($Q_1 - Q_2$), which must either go out to, or come in from, infinity, as the case may be.

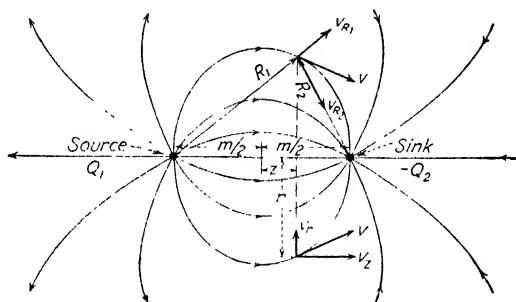


FIG. 31.—Flow between a source and sink of equal strength.

When a source and a sink of equal magnitude are made to approach each other in such manner that the product of rate of discharge and distance Qm is held constant, as m approaches the limit zero the flow pattern will become that of a doublet, shown in Fig. 32. The velocity potential of the doublet (the mathematical development is omitted)¹ will then be

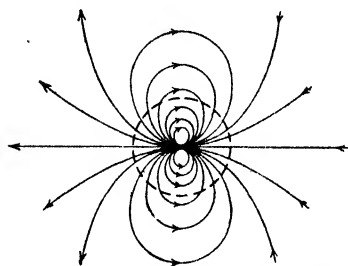


FIG. 32.—Three-dimensional doublet.

in which C is an arbitrary constant. The velocity at any point may be found in the usual manner.

If there be added to any of these source-sink combinations a linear flow in a direction parallel to the line connecting the singular points, it is evident that the interaction of the two

$$\phi = \frac{Cz}{(r^2 + z^2)^{3/2}}$$

¹ For this derivation, as well as for a more extensive treatment of examples of potential motion, the reader is referred to PRANDTL-TIETJENS' "Fundamentals of Hydro- and Aeromechanics," Engineering Societies Monograph, McGraw-Hill Book Company, Inc., 1934, and to vol. I of W. F. DURAND'S "Aerodynamic Theory," Julius Springer, Berlin, 1934.

systems must produce an entirely new flow pattern. An imaginary surface of revolution may now be considered to separate the flow of the source-sink group from the outer flow, the surface having such a shape that the velocity determined from the combined potential will be tangential to it at all points through which it passes. Since this surface must then be composed of those stream lines forming the boundary between the two systems of flow, the inner flow could be replaced by a solid body of exactly the same surface form without disturbing the flow around it.

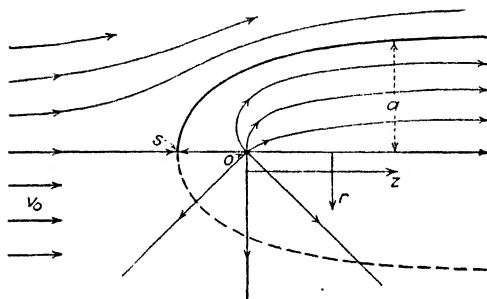


FIG. 33.—Combination of parallel flow and a source—the half body.

As a simple example, consider the combination of a single source with parallel flow. The velocity potential of the linear motion (in the positive z direction) must be:

$$\phi_1 = v_0 z$$

The velocity potential of the source has already been developed. The velocity potential of the resulting flow will be simply the sum of these two:

$$\phi = \phi_1 + \phi_2 = v_0 z - \frac{Q}{4\pi\sqrt{r^2 + z^2}}$$

In Fig. 33 is shown the pattern of stream lines corresponding to this velocity potential. It is obvious that the space occupied by the fluid emerging from the source could be replaced by a solid body of the same form without changing the flow around it in any way, relationships then being at hand for finding the pressure and velocity distribution at any point in the surrounding fluid. Such a profile is known as a half body or a semi-infinite body, since it extends to infinity in the positive z direction.

The velocity component parallel to the z axis may be found by taking the derivative of ϕ in this direction:

$$v_z = \frac{\partial \phi}{\partial z} = v_0 + \frac{Qz}{4\pi(r^2 + z^2)^{3/2}}$$

It may be seen by inspection that the velocity will become parallel and equal to the original magnitude of the oncoming flow only an infinite distance along the z axis in either direction. The position of the nose of the body, which is a point of stagnation, may be determined by placing r and v_z equal to zero in the above expression, with the result:

$$z_s = -\sqrt{\frac{Q}{4\pi v_0}}$$

The imaginary flow through any normal section of the half body to the right of the coordinate origin (refer to Fig. 33) must be equal to the discharge from the source,

$$\int_0^a v_z 2\pi r dr = Q$$

whereas between the origin and the nose of the body this must equal zero; *i.e.*, all fluid leaving the source in the negative z direction must eventually return and pass to the right. By substituting the value for v_z in this integral expression, an equation may be derived for the radius a of the profile at any given value of z , by which means the exact form of the body may be determined.

Had the velocity potential for a parallel flow been added in similar fashion to that for a source and a sink of equal magnitude, equations would have resulted for flow around a symmetrical body of approximately ellipsoidal form, since under these conditions the discharge from the source would have been entirely absorbed by the near-by sink; the relative dimensions of such a body depend upon the assumed velocity of the oncoming flow and the magnitude and spacing of the source and sink.

The combination of a parallel flow with a doublet results in the pattern of flow around a sphere (Fig. 34); the velocity potential of such a flow will be, in terms of the arbitrary doublet constant C ,

$$\phi = v_0 z + \frac{Cz}{(r^2 + z^2)^{3/2}}$$

the derivative of which in the z direction yields the axial component of velocity at any point:

$$v_z = v_0 + \frac{C}{(r^2 + z^2)^{3/2}} - \frac{3Cz^2}{(r^2 + z^2)^{5/2}}$$

The magnitude of the doublet constant C may now be determined by writing the conditions at the stagnation point ($r = 0, v_z = 0$) in terms of the radius a of the sphere:

$$0 = v_0 + \frac{C}{a^3} - \frac{3C}{a^3}; \quad C = \frac{v_0 a^3}{2}$$

Introducing this value in the above relationships, the velocity potential and the two velocity components for flow around a sphere of radius a will then be:

$$\begin{aligned} \phi &= v_0 z + \frac{a^3 v_0 z}{2(r^2 + z^2)^{3/2}} \\ v_z &= v_0 + \frac{a^3 v_0}{2(r^2 + z^2)^{3/2}} - \frac{3}{2} \frac{a^3 v_0 z^2}{(r^2 + z^2)^{5/2}} \\ v_r &= -\frac{3}{2} \frac{a^3 v_0 z r}{(r^2 + z^2)^{5/2}} \end{aligned}$$

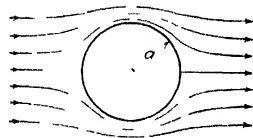


FIG. 34 Pattern of steady flow around a sphere.

The velocity $v = \sqrt{v_r^2 + v_z^2}$ at any point on the surface of the sphere may now be found through substitution of the term $a = \sqrt{r^2 + z^2}$ in the above expressions. This tangential velocity will vary from zero at the point of stagnation to a maximum value of $1.5v_0$ around the circumference of the sphere in a plane normal to the longitudinal axis.

The intensity of dynamic pressure at any point on the surface of the sphere—and similarly at any point throughout the flow—may be determined from the following general relationship for all such types of flow,

$$\rho \frac{v^2}{2} + p_d = \text{constant} = \rho \frac{v_0^2}{2}; \quad p_d = \rho \frac{v_0^2}{2} - \frac{\rho v^2}{2}$$

since p_d has a magnitude of zero an infinite distance from the sphere, where $v = v_0$. Thus p_d will have a maximum positive value of $\rho v_0^2/2$ at the points of stagnation, and a minimum value of $-5/4 \rho v_0^2/2$ in the region of highest velocity.

In each of these cases, the pattern of steady flow around an immersed body has been obtained by superposing parallel motion

upon some existing state of movement. Assume now that the body and the surrounding flow are given a rate of motion equal and opposite to the velocity of the parallel flow (the coordinate system thereby remaining stationary); the stream-line pattern of the original flow will evidently be restored to its earlier form—through subtraction of the quantity that had just been added—with the exception that these stream lines now represent the instantaneous pattern for unsteady flow caused by movement of the immersed boundary, as indicated for the sphere and half body in Figs. 32 and 33.

Since the velocity of the parallel flow and the discharge and location of the sources and sinks are entirely optional in any of these problems, it should also be possible to combine as many sources and sinks of different magnitudes as one might desire,

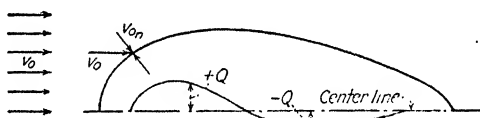


FIG. 35.—Development of the velocity potential for a boundary of complex form.

in order to produce velocity functions for bodies of revolution covering a wide range of profiles. Indeed, this method has been used satisfactorily to develop the velocity potential for flow around an airship—in both forward and lateral motion—by combining with a parallel flow a series of sources and sinks systematically distributed along the axis of the body (see Fig. 35). For the given airship profile and the given velocity of the oncoming flow, the sources and sinks are so grouped that at every point on the profile the normal velocity component caused by the parallel flow is exactly equal and opposite to that caused at the same point by all the sources and sinks together. That is, the resulting normal velocity component must be zero over the entire surface. Obviously, the total discharge from the sources must equal the total discharge into the sinks. When these conditions are satisfied, the resulting velocity potential may be determined through summation.

By carefully grouping sources and sinks in this manner, and by addition of ring vortices in planes normal to the axis, it is possible to determine the velocity and pressure distribution around a body of revolution of almost any desired form, although

the computations will become quite involved. If carried to an extreme, this method might be expected to yield results for bodies of any irregular shape, through groups of sources, sinks, and ring vortices at other points than the axis; the complicated form of the resulting velocity potential, however, would hardly warrant such a procedure.

20. Two-dimensional Flow: the Stream Function. If the conditions of steady, irrotational flow are such that the motion is entirely two-dimensional—that is, if the stream-line pattern is identical in a series of parallel planes (xy), there being no movement whatever in a direction (z) normal to these planes—the relationships just developed for three-dimensional potential flow become greatly simplified. The principle of continuity [Eq. (23)], which must hold for any type of flow at constant density, reduces to

$$\operatorname{div} v = \frac{\partial v_x}{\partial x} + \frac{\partial v_y}{\partial y} = 0 \quad (39)$$

whereas the fact that in two-dimensional motion only one component (ω_z) of the vorticity vector could possibly exist, leads to the following simplification of Eqs. (33) for irrotational motion:

$$\frac{\partial v_y}{\partial x} = \frac{\partial v_x}{\partial y} \quad (40)$$

The Bernoulli theorem, of course, requires no modification, while Eqs. (34) will become,

$$v_x = \frac{\partial \phi}{\partial x}; \quad v_y = \frac{\partial \phi}{\partial y} \quad (41)$$

Substitution of these components in the equation of continuity results in the equation of Laplace for two-dimensional flow, a relationship that must be satisfied by any true velocity potential:

$$\frac{\partial^2 \phi}{\partial x^2} + \frac{\partial^2 \phi}{\partial y^2} = 0 \quad (42)$$

Moreover, because of the condition expressed by Eq. (39), there will also exist a stream function ψ (psi), the derivatives of which in the two coordinate directions yield the velocity components in directions normal to the respective axes:

$$v_x = \frac{\partial \psi}{\partial y}; \quad v_y = -\frac{\partial \psi}{\partial x} \quad (43)$$

Since the velocity vector at any point is tangent to the stream line passing through that point, it is evident that the components of v must be proportional to the respective components of an increment of distance ds along the stream line. Thus, the differential equation of the stream line must be as follows:

$$\frac{dx}{v_x} = \frac{dy}{v_y} \quad \text{or} \quad v_x dy - v_y dx = 0 \quad (44)$$

Introducing the components of the velocity vector expressed as derivatives of ψ into this expression,

$$\frac{\partial \psi}{\partial y} dy + \frac{\partial \psi}{\partial x} dx = d\psi = 0 \quad (45)$$

from which it will be seen that the stream line is that line along which the stream function is constant. Substitution of Eq. (43) in Eq. (40),

$$\frac{\partial^2 \psi}{\partial x^2} + \frac{\partial^2 \psi}{\partial y^2} = 0 \quad (46)$$

shows that the stream function must also satisfy the equation of Laplace.

Fig. 36.—Stream and potential lines.

Since each component of the velocity vector is now expressible in terms of either ϕ or ψ , the following identities must exist:

$$\frac{\partial \phi}{\partial x} = \frac{\partial \psi}{\partial y}; \quad \frac{\partial \phi}{\partial y} = -\frac{\partial \psi}{\partial x} \quad (47)$$

That is, lines of constant velocity potential and lines of constant stream function must always intersect each other at right angles. It should now be clear to the reader that the stream lines and normal trajectories of the two-dimensional flow net are really lines of constant ψ and constant ϕ , respectively, so placed that the spacing between every pair of stream lines and every pair of potential lines represents a constant increment of ψ and of ϕ . As will be clear from Fig. 36, according to the natural coordinate notation,

$$\frac{\partial \phi}{\partial s} = v = \frac{\partial \psi}{\partial n} \quad (48)$$

and

$$\frac{\partial \phi}{\partial n} = 0 = \frac{\partial \psi}{\partial s} \quad (49)$$

Hence, since the product $v \, dn$ represents the increment of rate of discharge dq per unit distance normal to the plane of motion (*i.e.*, volume per unit time per unit length equals area per unit time), it will be evident that the quantity of fluid passing per second between any two stream lines Δq must be both dimensionally and numerically equal to the change in magnitude of the stream function $\Delta \psi$ from one stream line to the next:

$$\Delta q = \int^{\Delta n} v \, dn = \Delta \psi \quad (50)$$

This is, of course, merely another way of expressing the law of continuity for two-dimensional irrotational motion.

Just as in the case of three-dimensional potential motion, the velocity potential for certain types of two-dimensional flow may be formulated analytically through combination of sources, sinks, circulation, and parallel motion. Since the flow must be entirely planar in such problems, the stream-line patterns may often be found conveniently through graphical combination of the elementary flow patterns, in the manner indicated early in Chap. II. In many cases, however, the boundary conditions make an exact mathematical derivation of the velocity potential either impossible or at best extremely difficult—despite the fact that a velocity potential must exist for every case of steady, irrotational motion. In such instances, the construction of the flow net by graphical means, without heed to the velocity potential as a mathematical function, is the most practical means of solution. This procedure will, of course, yield the same results for velocity distribution as would differentiation of ϕ , were the latter function known, for the construction of the flow net is based upon identical physical relationships. In addition to the foregoing methods of solution, there exists a very significant type of mathematical operation involving the use of complex variables, whereby the number of available expressions for the velocity potential is tremendously increased. Owing to the nature of this method, it will be discussed separately in the following chapter.

CHAPTER V

CONFORMAL MAPPING

21. Theory of Complex Variables. A complex number is one composed of real and imaginary terms. Any imaginary term, such as $\sqrt{-a}$, may be reduced to the product of a real quantity, \sqrt{a} , and the unreal or imaginary root $\sqrt{-1}$, the latter commonly being given the symbol i ; an imaginary quantity, hence, always contains the factor i . Thus a complex number z may be written as the sum of a real term x and an imaginary term iy ,

$$z = x + iy \quad (51)$$

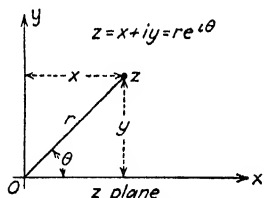


FIG. 37. —Graphical representation of a complex number.

Such a number may be plotted, however, by presuming an imaginary axis along which is measured the real part y of the imaginary term, and a real axis at right angles to it along which is measured the real term x of the complex quantity. Thus in the z plane, according to the above relationship, the point z lies a distance x along the horizontal or real axis, and the distance y along the vertical or imaginary axis, the magnitude of the complex number z then being given by the sum $x + iy$, as shown in Fig. 37.

Polar notation may also be used to express the value of a complex variable. Denoting by r the distance of any point z from the coordinate origin, and by θ the angle between this radius vector and the real axis x , the following relationships will be seen to hold:

$$r = \sqrt{x^2 + y^2}, \quad \text{or} \quad x = r \cos \theta, \quad y = r \sin \theta$$

Hence

$$z = r (\cos \theta + i \sin \theta) \quad (52)$$

The radius r is known as the modulus of z , and the angle θ as the amplitude or argument of z . Refer to Fig. 37.

If the quantity $e^{i\theta}$ is expanded in a series,

$$e^{i\theta} = 1 + \frac{i\theta}{1} - \frac{\theta^2}{1 \cdot 2} - \frac{i\theta^3}{1 \cdot 2 \cdot 3} + \frac{\theta^4}{1 \cdot 2 \cdot 3 \cdot 4} + \frac{i\theta^5}{1 \cdot 2 \cdot 3 \cdot 4 \cdot 5}$$

and the real and imaginary terms separated,

$$\left(1 - \frac{\theta^2}{1 \cdot 2} + \frac{\theta^4}{1 \cdot 2 \cdot 3 \cdot 4} - \cdots\right) = \cos \theta$$

$$i \left(\frac{\theta}{1} - \frac{\theta^3}{1 \cdot 2 \cdot 3} + \frac{\theta^5}{1 \cdot 2 \cdot 3 \cdot 4 \cdot 5} - \cdots\right) = i \sin \theta$$

it is at once evident that Eq. (52) may be written in the more convenient form:

$$z = r e^{i\theta} \quad (53)$$

Inasmuch as a complex number may be represented vectorially by the direction and magnitude of r , it will be clear that the sum or difference of two complex numbers may be obtained by the vector sum or

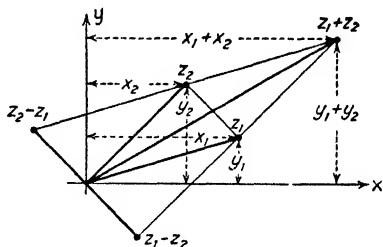


FIG. 38.—Addition and subtraction.

difference of their respective moduli (see Fig. 38). From Eq. (52) it is obvious that the same result may be obtained by adding or subtracting the real and imaginary parts of the two complex quantities, as shown in the illustration; that is,

$$z_3 = z_1 + z_2 = x_1 + i y_1 + x_2 + i y_2$$

$$= (x_1 + x_2) + i (y_1 + y_2)$$

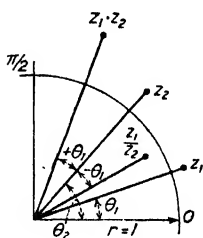


FIG. 39.—Multiplication and division.

since

$$z_3 = z_1 \cdot z_2 = r_1 e^{i\theta_1} \cdot r_2 e^{i\theta_2} = r_1 r_2 e^{i(\theta_1 + \theta_2)}$$

The operation is shown in Fig. 39. In the same manner, the power of a complex number is found through raising the modulus

to the power and multiplying the argument by the exponent, as illustrated in Fig. 40, since

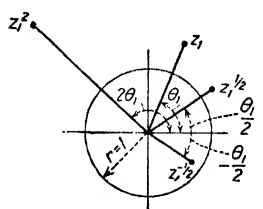


FIG. 40.—Powers of complex numbers.

$$z_2 = z_1^n = (r_1 e^{i\theta_1})^n = r_1^n e^{in\theta}$$

Evidently, the relative change as a result of the operation depends in part upon the proximity of the original complex quantity to the unit circle, for which $r = 1$.

The logarithm of a complex number may be obtained by a combination of rectangular and polar coordinates. From Eqs. (53) and (51),

$$z_2 = \ln z_1 = \ln r_1 e^{i\theta_1} = \ln r_1 + i\theta_1 = x_2 + iy_2$$

Therefore,

$$x_2 = \ln r_1; \quad y_2 = \theta_1$$

As shown in Fig. 41 the effect of this operation upon z will depend upon the magnitude of the modulus with respect to the

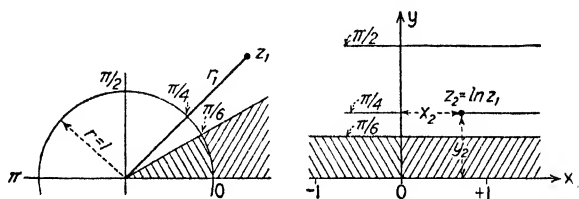


FIG. 41.—Logarithmic operations.

unit circle, and upon its direction with respect to the coordinate axes. That is, if r_1 in the polar notation is greater than unity, x_2 in the rectangular notation will be positive; if r_1 is less than unity, x_2 will be negative; y_2 will always be equal to θ_1 plotted vertically in radians. Thus, the shaded areas in the rectangular plane correspond to the logarithms of the similarly shaded areas in the polar plane.

22. Significance of Conformal Representation. Performing such operations upon a given complex variable is the essence of the mathematical process known as conformal mapping. If one complex variable can be expressed as a function of another com-

plex variable, and if either one of these can also be expressed as a known function of coordinate space, then the expression of the other as a function of coordinate space may be readily derived.

Assume, now, that one complex variable w is plotted in the w plane, of which the ψ axis is imaginary and the ϕ axis is real, and that w is a function of another complex variable z , which is plotted in the z plane. Then

$$w = \phi + i\psi = f(z) = f(x + iy) \quad (54)$$

Assume further that in the w plane are drawn two families of equidistant lines, parallel, respectively, to the real and imaginary axes, as shown in Fig. 42. These will denote lines of constant ψ and constant ϕ , the increments $\Delta\psi$ and $\Delta\phi$ being equal throughout

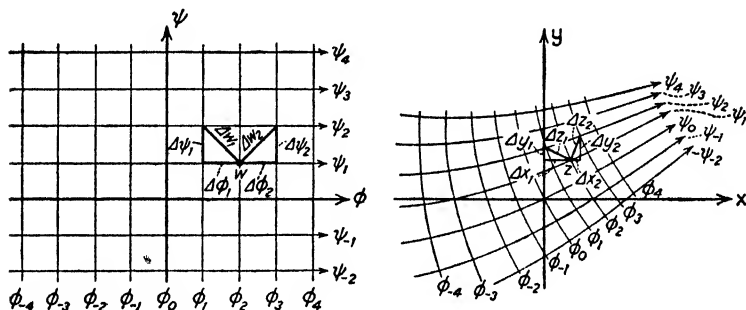


FIG. 42.—Conformal transformation.

the system. If z now be assumed to vary in such manner that the real part (ϕ) of w changes, the imaginary part ($i\psi$) remaining constant, there will be traced in the z plane a line conforming to this line of constant ψ in the w plane. If this procedure is followed for both families of parallel lines in the w plane, there will result a conformal map of this network in the z plane, the shape and position of the transformed image depending upon the functional relationship between w and z as expressed generally in Eq. (54), and shown schematically in Fig. 42.

Certain pertinent characteristics of this operation must be noted. First of all, it is evident that both ϕ and ψ are real functions of x and y , and vice versa:

$$\phi = \phi(x, y), \quad \psi = \psi(x, y); \quad \text{or} \quad x = x(\phi, \psi), \quad y = y(\phi, \psi)$$

That is, for a given functional relationship of the two complex variables, the real quantities x , y , ϕ , and ψ will also be interrelated in a manner independent of the imaginary factor i . Thus, a knowledge of the function will provide a means of reproducing in a real xy plane the transformed $\phi\psi$ network; if the characteristics of the original network are known, then the characteristics of the transformed network will also be known.

Since for every point w_1 in the w plane there is a corresponding point z_1 in the z plane according to the relationship of Eq. (54), it follows that for every change dw in the one complex variable there must be a corresponding change dz in the other. These increments, furthermore, must be equal to the sum of the variations of their real and imaginary parts, respectively; hence, the ratio of the two corresponding increments will be equal to:

$$\frac{dw}{dz} = \frac{d\phi + i d\psi}{dx + i dy}$$

But the partial derivatives of z with respect to x and to y , [see Eq. (51)]

$$\frac{\partial z}{\partial x} = 1; \quad \frac{\partial z}{\partial y} = i$$

when substituted in the expressions for the partial derivatives of w with respect to x and to y will yield the following pertinent relationships for the variation of w with respect to z :

$$\frac{\partial w}{\partial x} = \frac{dw}{dz} \frac{\partial z}{\partial x} = \frac{dw}{dz}; \quad \frac{\partial w}{\partial y} = \frac{dw}{dz} \frac{\partial z}{\partial y} = i \frac{dw}{dz}$$

Therefore,

$$\frac{dw}{dz} = \frac{\partial w}{\partial x} = \frac{\partial \phi}{\partial x} + i \frac{\partial \psi}{\partial x}$$

and

$$\frac{dw}{dz} = \frac{1}{i} \frac{\partial w}{\partial y} = \frac{1}{i} \left(\frac{\partial \phi}{\partial y} + i \frac{\partial \psi}{\partial y} \right)$$

Hence,

$$\frac{dw}{dz} = \frac{\partial \phi}{\partial x} + i \frac{\partial \psi}{\partial x} = \frac{1}{i} \frac{\partial \phi}{\partial y} + \frac{\partial \psi}{\partial y} \quad (55)$$

Since the real and imaginary parts of any complex relationship are quite distinct, it is evident that the real terms in the above equation must equal each other and that the imaginary terms must also be equal:

$$\frac{\partial \phi}{\partial x} = \frac{\partial \psi}{\partial y}; \quad \frac{\partial \phi}{\partial y} = -\frac{\partial \psi}{\partial x}$$

These two equalities, known as the Cauchy-Riemann equations, are identical with Eqs. (47); since Eq. (54) may be shown to satisfy the equation of Laplace, ϕ and ψ represent the velocity potential and the stream function for two-dimensional irrotational flow; hence,

$$\frac{\partial \phi}{\partial x} = v_x = \frac{\partial \psi}{\partial y}; \quad \frac{\partial \phi}{\partial y} = v_y = -\frac{\partial \psi}{\partial x} \quad (56)$$

Introducing these velocity components into Eq. (55),

$$\frac{dw}{dz} = v_x - i v_y \quad (57)$$

from which it is evident that the velocity may also be considered a complex variable of the form $v = v_x - i v_y$, which is then a function of $z = x + i y$. From this expression may be obtained the magnitude and direction of the velocity vector, although v itself is not a true vector, for it has both real and imaginary parts. Since the two complex variables v and w are functions of a third complex variable z , it follows that a functional relationship must also exist between w and v :

$$w = f(v) = f(v_x - i v_y) \quad (58)$$

It is this general expression which permits solution of certain problems of flow from solid boundaries into the atmosphere, as in the case of jets and weir nappes.

From Eq. (55) it will be obvious that the variation of w with respect to z is independent of the direction of the increment dz —i.e., independent of the ratio dy/dx . In Fig. 42, for instance, as the diagonals Δz_1 and Δz_2 approach zero, the limits of $\Delta w_1/\Delta z_1$ and $\Delta w_2/\Delta z_2$ will be identical, despite the differences between Δx_1 and Δx_2 , and Δy_1 and Δy_2 . Since the derivative dw/dz depends upon the position, but not the direction, of dz , it thus can represent only the magnitude of rotation and linear distortion involved in the transformation, for from Eqs. (56) it is apparent

that the transformed flow net has the identical angular characteristics of the original—that is, all lines of the net still meet at right angles, while every “mesh” of the net is still a perfect square when reduced to the infinitesimal. Thus, the operation of conformal transformation will change the linear characteristics of a network of lines without affecting in any way whatever the angular intersections.

A familiar application of this operation is illustrated by the Mercator projection used in mapping. In this projection the parallels of latitude and the great circles of longitude on the terrestrial globe are reproduced in a two-dimensional plane as two rectilinear families of parallel lines. At the equator the linear distortion is zero, but the poles are changed from points to lines of the same length as the equator. Since no angular distortion results from this operation, such “infinitesimal” areas as the maps of towns and cities will remain practically unchanged in shape, despite the obvious distortion of large continental areas at high latitudes. Moreover, if the same method is used to show the polar region, the two-dimensional projection will be a series of radial lines representing the longitudinal meridians, and a series of concentric circles of constant latitude, of which one is the equator. Obviously, conditions at the pole remain unchanged, whereas the regions farthest from the pole undergo the greatest distortion. Again, however, angular characteristics are unaffected, and infinitesimal areas that were originally square will remain so. If now the first projection be called the w plane and the second the z plane, it is apparent that a single functional relationship must exist between the two, since every point in the one has its counterpart in the transformed or conformal map, and vice versa.

23. Elementary Transformations. As a preliminary exercise in the methods of conformal mapping, consider the function

$$w = \phi + i\psi = f(z) = f(x + iy) = (a + ib)z$$

At once one may write

$$\phi + i\psi = (a + ib)(x + iy) = ax + ibx + iay - by$$

from which it is apparent that through equating the real and imaginary parts there will result:

$$\phi = ax - by; \quad \psi = bx + ay$$

The velocity components may be found directly through differentiation of the velocity potential or the stream function, or through the operation:

$$\frac{dw}{dz} = v_x - i v_y = a + i b$$

Again equating the real and imaginary parts,

$$v_x = a; \quad v_y = -b$$

The lines of constant ϕ and constant ψ in the z plane may be found by setting the expressions just found for ϕ and ψ equal to successive numerical constants, the increments always being

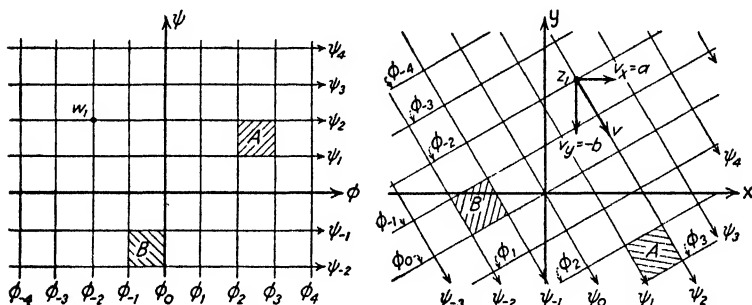


FIG. 43.—Conformal representation of the function $w = (a + i b)z$.

the same. If a and b are both positive, the original and the transformed flow nets will be as shown in Fig. 43, the slope and spacing of the conformal lines depending upon the magnitude of a and of b . If these constants are equal, the slope will be 45° ; if a is positive, the horizontal component of flow will be to the right—if negative, to the left; if b is positive, flow will have a downward component—if negative, an upward component; if a is zero, the flow will be vertical; similarly, if b is zero, the flow will be horizontal. Obviously, if b is zero and a is unity, the pictures in the two planes will be identical. Similarly, if a is zero and b is unity, although the scale will be the same, the stream lines will be changed to potential lines, and the potential lines to stream lines. It is thus evident that multiplication of any function by i will rotate the pattern of motion through 90° , while multiplication by $i^2 = -1$ will completely reverse the direction of flow.

A general function of the type

$$w = az^\alpha$$

may through the relationship $z = re^{i\theta}$ be written in the form

$$w = a r^{\frac{\pi}{\alpha}} e^{\frac{i\pi\theta}{\alpha}} = ar^{\frac{\pi}{\alpha}} \left(\cos \frac{\pi\theta}{\alpha} + i \sin \frac{\pi\theta}{\alpha} \right)$$

from which it is apparent that the velocity potential and the stream function will be as follows:

$$\phi = a r^{\frac{\pi}{\alpha}} \cos \frac{\pi\theta}{\alpha}; \quad \psi = a r^{\frac{\pi}{\alpha}} \sin \frac{\pi\theta}{\alpha}$$

The flow net resulting from this transformation will evidently

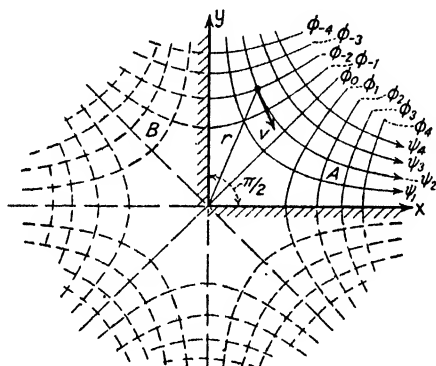


FIG. 44.—Potential flow at a 90° boundary angle.

depend in form upon the magnitude of the angle α . If this angle is 90°,

$$w = a r^2 e^{2i\theta}$$

and

$$\phi = a r^2 \cos 2\theta = a (x^2 - y^2); \quad \psi = a r^2 \sin 2\theta = 2axy$$

The velocity components may now be found through differentiation of the velocity potential, giving

$$v_x = \frac{\partial \phi}{\partial x} = 2ax; \quad v_y = \frac{\partial \phi}{\partial y} = -2ay$$

and

$$v = \sqrt{v_x^2 + v_y^2} = 2a\sqrt{x^2 + y^2} = 2ar$$

A plot of the lines of constant stream function, with constant increments between lines, will result in a series of hyperbolas in the four quadrants of the polar coordinate plane. Selecting the axes x and y as solid boundaries of flow, the stream and potential lines in the first quadrant (see Fig. 44) will then form the flow net for potential motion at a 90° angle in the boundary, there being a point of zero velocity at the corner.

Since the angle α evidently represents the angle between the two straight boundary walls, this function may be used to determine the flow characteristics at a corner of any desired angle. Use of the angle $\alpha = \pi$ must then yield parallel flow along a straight wall, as may be seen from the form of the original function.

24. Source-sink Combinations. The function

$$w = a \ln z$$

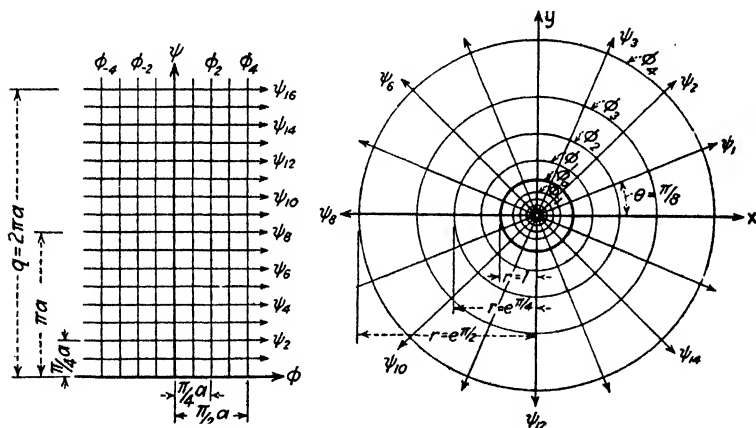


FIG. 45.—Transformation from parallel flow to flow from a source.

may be treated as follows:

$$\begin{aligned}\phi + i\psi &= a \ln re^{i\theta} = a \ln r + ai\theta \\ \phi &= a \ln r; \quad \psi = a\theta \\ v_r &= \frac{\partial \phi}{\partial r} = \frac{a}{r}; \quad v_t = \frac{\partial \phi}{r \partial \theta} = 0\end{aligned}$$

Since flow that is entirely radial, the tangential component of the velocity being zero at all points, must be flow from a two-dimensional source (if a is positive) or into a sink (if a is negative)

then the constant a may be expressed in terms of the two-dimensional rate of discharge q :

$$q = 2\pi r v_r = 2\pi a; \quad a = \frac{q}{2\pi}$$

The transformation is shown in Fig. 45.

The similar function

$$w = a i \ln z$$

may be treated in a corresponding manner:

$$\phi + i\psi = a i \ln r e^{i\theta} = a i \ln r - a\theta$$

$$\phi = -a\theta; \quad \psi = a \ln r$$

$$v_r = \frac{\partial \phi}{\partial r} = 0; \quad v_t = \frac{\partial \phi}{r \partial \theta} = -\frac{a}{r}$$

Since in this case the velocity is entirely tangential, the transformed image represents flow in concentric circles with constant

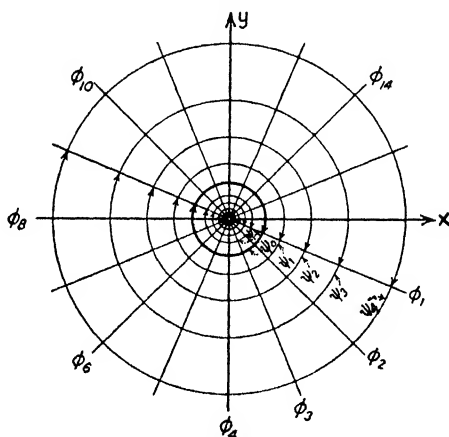


FIG. 46.—Potential flow with constant circulation.

circulation; the constant a will then be (assuming Γ positive in the clockwise direction):

$$-\Gamma = 2\pi r v_t = -2\pi a; \quad a = \frac{\Gamma}{2\pi}$$

The flow pattern in the z plane may be seen from Fig. 46.

If a composite function be written in the form

$$w = \frac{q + i \Gamma}{2\pi} \ln z$$

the operation will result in a family of logarithmic spirals, as illustrated in Fig. 47, the direction and curvature of the spirals depending upon the sign and magnitude of q and Γ . It is evident that this flow pattern may also be obtained graphically according to the method already discussed of adding velocity fields. As will be seen from the foregoing development, the velocity potential and the stream function of the family of logarithmic spirals are merely the sums of those for radial and concentric motion.

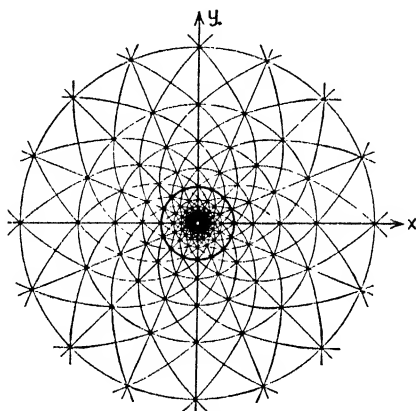


FIG. 47.—Combination of potential vortex with source or sink.

A source and sink of equal magnitude and spaced a distance $2m$ apart will result from the function of transformation

$$w = \frac{q}{2\pi} \ln \frac{z + m}{z - m}$$

Referring to the flow net shown in Fig. 48 (which may also be constructed graphically through combination of the stream and potential lines of the source and sink), it will be seen that

$$w = \phi + i\psi = \frac{q}{2\pi} \ln \frac{r_1 e^{i\theta_1}}{r_2 e^{i\theta_2}} = \frac{q}{2\pi} \left[\ln \frac{r_1}{r_2} + i(\theta_1 - \theta_2) \right]$$

from which the velocity potential and the stream function may be found by inspection:

$$\phi = \frac{q}{2\pi} \ln \frac{r_1}{r_2}; \quad \psi = \frac{q}{2\pi} (\theta_1 - \theta_2)$$

Thus, potential lines and stream lines will all be circles, the loci of $r_1/r_2 = \text{constant}$ and $(\theta_1 - \theta_2) = \text{constant}$, respectively.

Through use of Eq. (57) it may be shown that the magnitude of the velocity vector at any point will be

$$v = \frac{m q}{\pi r_1 r_2}$$

although the development of this relationship is too involved to be presented in this text. This velocity may also be found by

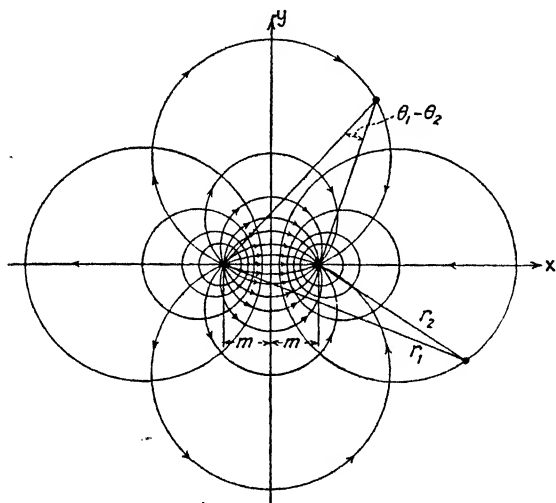


FIG. 48.—Source and sink of equal strength.

adding vectorially the velocities of flow from the source and toward the sink at any point.

As in the foregoing example, the picture of flow from a source to a sink may be transformed into the pattern of circulation around two vortex lines simply by multiplying the original function of z by the factor i . In this way the potential lines in Fig. 48 will become stream lines, and vice versa, and the flow net will represent the unsteady flow pattern of the two vortex filaments in the upper left-hand corner of Fig. 26. The pattern of steady flow may be developed by adding graphically a parallel flow equal and opposite to the velocity of translation of the two filaments; that is, $v_0 = \Gamma/4\pi m$. Obviously, the outline of either filament must be formed by one of the circular stream lines, it being of no

consequence whether or not the two filaments are of the same diameter so long as the circulations around their circumferences are of the same magnitude and opposite sign.

Any portion of any potential flow may be replaced by a solid boundary whose outline coincides with a stream line without changing the characteristics of flow in any way. Thus, the foregoing pattern of circulatory motion may be used to find the approximate velocity and pressure distribution for flow under a movable cylindrical weir profile by fitting one stream line of the flow net to the cross section of the cylinder, as shown in Fig. 49.¹ This method is not exact,

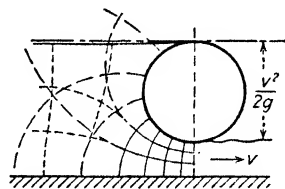


FIG. 49.—Flow under a cylindrical gate.

because the lines of flow upstream from the weir deviate from those of the potential function, although the latter may be used to good advantage as the first approximation in the graphical construction of the net. Moreover, the point at which the flow separates from the cylinder moves upstream with increasing head; that this will affect the velocity of flow will be apparent from the fact that only through knowing the elevation of this point of atmospheric pressure can one establish the velocity corresponding to the given spacing of stream lines.

25. Flow around a Cylinder. If the distance m in the source-sink combination approach zero, the product $m\gamma$ thereby remaining constant, the flow pattern will approach that of the two-dimensional doublet, or dipole, shown in Fig. 50. The corresponding complex function will then have the form

$$w = \frac{a}{z}$$

The velocity potential and the stream function are found as follows:

$$\begin{aligned}\phi + i\psi &= \frac{a}{x + iy} = \frac{a(x - iy)}{(x + iy)(x - iy)} = \frac{ax}{x^2 + y^2} - \frac{aiy}{x^2 + y^2} \\ \phi &= \frac{ax}{x^2 + y^2} = \frac{a \cos \theta}{r}; \quad \psi = -\frac{ay}{x^2 + y^2} = -\frac{a \sin \theta}{r}\end{aligned}$$

¹ For extensive application of conformal mapping to the design of hydraulic structures, see KULKA, H., "Der Eisenwasserbau," vol. I, Wilhelm Ernst & Son, Berlin, 1928.

Both ϕ and ψ are thus constant along circles passing through the coordinate origin; in Fig. 50 ψ and ϕ are increased successively by constant increments, the radii of the stream and potential lines

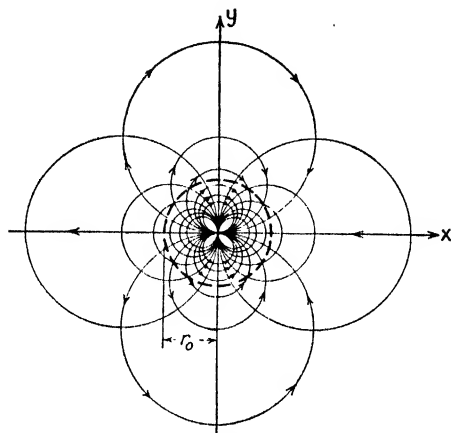


FIG. 50.—Two-dimensional doublet.

varying inversely with these quantities. The velocity components will be found to be

$$v_x = \frac{\partial \phi}{\partial x} = \frac{a(y^2 - x^2)}{(x^2 + y^2)^2}; \quad v_y = \frac{\partial \phi}{\partial y} = \frac{-2axy}{(x^2 + y^2)^2}$$

from which the magnitude of the velocity vector at any point will equal

$$v = \sqrt{v_x^2 + v_y^2} = \sqrt{\frac{a^2(y^2 - x^2)^2 + 4a^2x^2y^2}{(x^2 + y^2)^4}} = \frac{a}{x^2 + y^2} = \frac{a}{r^2}$$

Comparable to the three-dimensional doublet, from this flow net may be determined the unsteady stream-line picture resulting from the motion through a fluid of an infinitely long circular cylinder, simply by constructing upon the flow net a circle concentric with the coordinate origin to represent the cross section of the cylinder. Designating by v_0 the velocity of translation of the cylinder, the magnitude of a may be found by setting equal to v_0 the velocity of the fluid immediately in front (or in back) of the body (refer to Fig. 50), at the distance r_0 from the origin:

$$v = \frac{a}{r_0^2} = v_0 \quad \text{and} \quad a = v_0 r_0^2$$

Obviously the usual methods cannot be used to find the pressure distribution around the body, for unsteady motion denotes variable energy of flow. The steady picture, however, may be obtained directly through adding (either graphically or analytically) to the above potential and stream functions those of a parallel flow with the velocity v_0 —that is, the body is brought to rest through superposing vectorially upon the entire flow picture a velocity v_0 equal and opposite to that of the cylinder:

$$\phi = v_0 x + \frac{v_0 r_0^2 x}{x^2 + y^2}; \quad \psi = v_0 y - \frac{v_0 r_0^2 y}{x^2 + y^2}$$

This is satisfied by the complex function

$$w = v_0 \left(z + \frac{r_0^2}{z} \right)$$

since

$$w = \phi + i\psi = v_0 (x + iy) + \frac{v_0 r_0^2 (x - iy)}{x^2 + y^2}$$

The velocity components may be found either by differentiating the above relationships or by adding algebraically to v_x for unsteady motion the quantity v_0 ; v_y , of course, must remain unchanged by this operation. Furthermore, since $r^2 = x^2 + y^2$, $x = r \cos \theta$, and $y = r \sin \theta$, the velocity at all points around the circumference of the cylinder may be found from the relationship:

$$v = v_t = 2v_0 \sin \theta, \quad \text{when} \quad r = r_0$$

The pressure distribution around the cylinder may now be found from the expression already developed,

$$p_d = \frac{\rho}{2} (v_0^2 - v^2)$$

from which it will be seen that there is a maximum pressure intensity of $\rho \frac{v_0^2}{2}$ at both points of stagnation, and a minimum intensity of $-3\rho \frac{v_0^2}{2}$ at either intersection of the circle with the y axis. The stream-line pattern for flow around a cylinder is shown in Fig. 51; this flow net may be found by combining graphically a parallel flow with a doublet, the spacing of the parallel stream lines for a given doublet depending only upon the

diameter of the cylinder; such spacing may then represent any desired magnitude of the parameter $\rho \frac{v_0^2}{2}$.

If one now superpose upon the flow picture just found the pattern of stream lines for a constant positive circulation Γ around the cylinder, graphical addition of the two systems will yield a flow net resembling that shown in Fig. 52. As can be seen

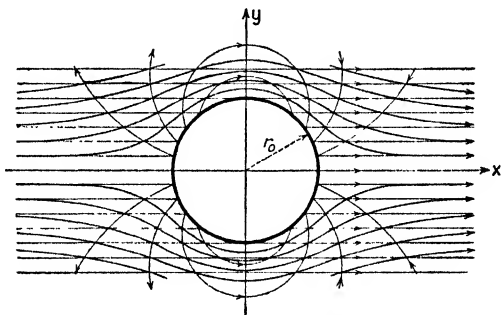


FIG. 51.—Potential flow around a cylinder—graphical combination of parallel flow with a doublet.

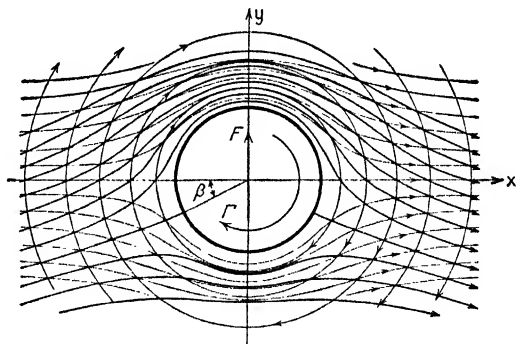


FIG. 52.—Displacement of stream lines around a cylinder through addition of circulation.

from the illustration, the points of stagnation will be displaced downward, while the velocities will be augmented on the upper side and reduced accordingly on the lower. The degree of displacement of the stagnation points will depend upon the ratio of the tangential velocity due to circulation, $v_c = \Gamma/2\pi r_0$, to the velocity of the oncoming flow v_0 ; the larger this ratio, the greater the displacement.

The form of this complex function will then be:

$$w = v_0 \left(z + \frac{r_0^2}{z} \right) + \frac{i \Gamma}{2\pi} \ln z$$

from which,

$$\phi = v_0 x \left(1 + \frac{r_0^2}{x^2 + y^2} \right) - \frac{\Gamma}{2\pi} \theta$$

and

$$\psi = v_0 y \left(1 - \frac{r_0^2}{x^2 + y^2} \right) + \frac{\Gamma}{2\pi} \ln r$$

The tangential velocity around the circumference of the cylinder, which is of particular importance, may be found simply by combining with v_t , the tangential velocity without circulation, the velocity v_c due to the circulatory motion:

$$v = v_t + v_c = 2v_0 \sin \theta + \frac{\Gamma}{2\pi r_0}$$

The two are obviously added on the upper side and subtracted on the lower. It is evident that at the points of stagnation, where the resultant velocity must be zero, the two velocities will be equal and opposite; the ratio of v_c and v_0 , therefore, determines the angle of displacement, $\beta = \theta - 180^\circ$:

$$v = 0 = v_t + v_c = 2v_0 \sin \theta + v_c; \quad \sin \beta = \frac{1}{2} \frac{v_c}{v_0}$$

Thus β will be 30° when the two velocities are equal, 90° when their ratio is equal to 2; as the ratio becomes greater than 2, the point of stagnation will move away from the cylinder, which will then be entirely surrounded by fluid moving in the same angular direction.

Inasmuch as the velocities are higher on the one side of the cylinder and lower on the other, there must be a resultant pressure acting in the positive y direction. The component of force in this direction due to the pressure intensity over an increment of circular arc when integrated entirely around the circle should give the magnitude of this force per unit length:

$$\begin{aligned} \frac{F}{L} &= \int_0^{2\pi} p_a r_0 \sin \theta d\theta = \frac{\rho}{2} \int_0^{2\pi} (v_0^2 - v^2) r_0 \sin \theta d\theta \\ &= \frac{\rho}{2} \int_0^{2\pi} \left[v_0^2 - \left(2v_0 \sin \theta + \frac{\Gamma}{2\pi r_0} \right)^2 \right] r_0 \sin \theta d\theta \end{aligned}$$

It must again be noted that the two terms are to be added while θ varies through 180° , and subtracted for the remaining 180° of the cycle.

Integration will result in the very pertinent relationship

$$\frac{F}{L} = \rho v_0 \Gamma \quad (59)$$

which states that the force per unit length of cylinder is a direct product of fluid density, velocity of flow, and circulation. The identical expression applies to circulation around bodies of many other shapes. This so-called "Magnus effect" explains in a general manner the principle of the rotor (applied at various times to the propulsion of ships, airplanes, windmills, and so forth), and the reason for the deviation of a spinning ball from its natural trajectory.

26. Successive Transformations. The foregoing conformal transformations involved relationships between only two complex variables, w and z , the flow picture in the z plane being considered in each case a conformal map of the parallel flow in the original w plane. It must be realized, however, that the parallel flow pattern is also a conformal map of the flow net in the z plane in every case, and may be obtained from the latter through the identical functional relationship; that is, if w is a known function of z [$w = f_w(z)$], it is obvious that z must then also be a known function of w [$z = f_z(w)$]. Moreover, beginning with the original flow picture, any number of transformations may be performed in succession, each operation resulting in a new conformal map of the preceding flow net, all such maps then being related through the series of successive functional operations.

In performing more than one conformal transformation it is most expedient to introduce an additional plane for the complex variable ζ (zeta) = $\xi + i\eta$, in which the ξ (xi) axis is real and the η (eta) axis is imaginary. If now z is any known function of ζ , and w in turn is some known function of z , then w is also a function of ζ , which may be written as follows:

$$w = f_w(z); \quad z = f_z(\zeta); \quad w = f_w[f_z(\zeta)] = f'_w(\zeta)$$

Substituting the real and imaginary parts of the several complex variables, this becomes:

$$\phi + i\psi = f_w(x + iy) = f'_w(\xi + i\eta)$$

Hence, the real variables ϕ and ψ must be functions of the real variables ξ and η , so that the ζ plane will again represent a transformed flow net of ϕ and ψ lines.

Since further transformation of the picture of flow around a cylinder offers a wide variety of useful flow nets, it is customary to accept the transformation from the w plane to the z plane as performed once and for all, and to proceed at once from the flow picture as shown in Fig. 53*a*. This procedure is based upon the methods of conformal mapping already discussed at length, and will simply be outlined in the following pages.

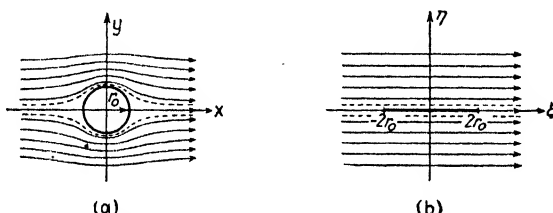


FIG. 53.—Transformation from flow around a cylinder to flow along a thin plate.

If the functional relationship between the z and ζ planes is such that

$$\zeta = v_0 \left(z + \frac{r_0^2}{z} \right) \quad \text{or} \quad z = \frac{\zeta \pm \sqrt{\zeta^2 - 4 v_0^2 r_0^2}}{2 v_0}$$

it is evident that the conformal map of the flow around the cylinder will become simply a case of parallel flow identical with that in the original w plane. The operation will, however, flatten the circular cross section of the cylinder into an ellipse having a major axis equal to twice the diameter of the circle and a minor (or vertical) axis with a length of zero; that is, the body immersed in the parallel flow is bounded by two straight lines, both of which are superposed upon the real axis of the ζ plane. This flow net is simply that of movement along an infinitely thin plate parallel to the flow (refer to Fig. 53*b*).

If, on the other hand, the function given above is multiplied by the imaginary factor i ,

$$\zeta = i v_0 \left(z + \frac{r_0^2}{z} \right)$$

the conformal map of flow around a cylinder will be that of flow

around an infinitely thin plate that is normal to the oncoming fluid, as shown in Fig. 54a. If these two operations are combined in the form

$$\zeta = (a + i b) v_0 \left(z + \frac{r_0^2}{z} \right) = a v_0 \left(z + \frac{r_0^2}{z} \right) + i b v_0 \left(z + \frac{r_0^2}{z} \right)$$

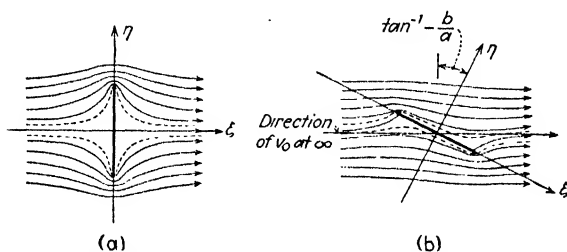


FIG. 54.—Change in flow pattern resulting from rotation of plate.

variation of the constants a and b will change the slope of the plate (see Fig. 54b) and at the same time change the scale of the general picture. This operation will be clear after reference to the elementary principle of rotating the coordinate axes, as illustrated in Fig. 43.

It will be apparent from inspection of Fig. 54b that the unsymmetrical location of the two stagnation points will result in a

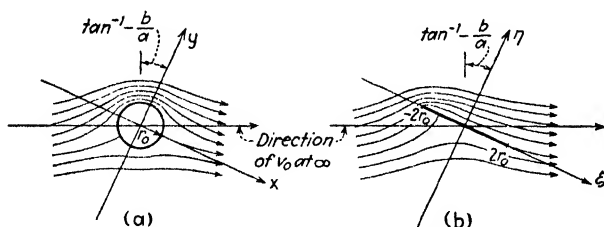


FIG. 55.—Introduction of circulation to eliminate infinite velocity at trailing edge.

force couple tending to rotate the plate about its center of gravity (the coordinate origin), although in such potential motion there can exist no resultant force that would cause a displacement of the center of gravity itself. In order to produce such a force in one direction or another, it is necessary to introduce a constant circulation about the original cylinder, as shown in Fig. 55a. If the above-given functional relationship between ζ and z still exists, the picture of flow in the ζ plane will now represent a combination of parallel flow and circulation around a flat plate

inclined at any angle, the force acting upon the plate in a direction normal to the oncoming flow again being given by Eq. 59.

Since the edges of an infinitely thin plate have a zero radius of curvature, it is evident that in general the velocity at such points must be infinitely great. One such region, however, may be obviated in the following manner. Since the position of the two points of stagnation of the circumference of the cylinder may be controlled through varying v_0 and Γ , and since the angle of inclination of the plate to the oncoming flow may also be controlled through variation of the constants a and b , it is possible either to change Γ or to rotate the coordinate axes in Fig. 55a through such an angle that one point of stagnation will coincide with the intersection of the real axis and the circular cross section of the cylinder. Under these conditions in the transformed picture one stagnation point must lie at one end of the thin plate—that is, the stream line at this point will be a smooth continuation of the line of the plate itself, as shown in Fig. 55b.

27. Kutta and Joukowski Profiles. If the coordinate axes in the picture of flow around a cylinder are transposed bodily in the negative y direction, application of the foregoing transformation will result in the following interesting picture: In Fig. 56 the original section is shown as a heavy circle, the real axis having been displaced downward a distance f . The lighter circle has its center at the new coordinate origin, both circles crossing the real axis at the same two points. It is evident that the operation which transforms the lighter circle into a double line lying upon the real axis in the ζ plane will affect the heavy circle in the same way only at the two points common to both. Every other point on the heavy circle will be shifted upward through the transformation by an amount varying with the distance from the imaginary axis; that is, since points a and b are transformed to $a'b'$ at the real axis, the fact that c and d lie above a and b , respectively, signifies that $c'd'$ must also lie above $a'b'$. The two points on the y axis will finally lie the distance $2f$ above the origin, and the conformal map of the heavy circle will be a double circular arc passing through these three points, as drawn in Fig. 56. Obviously, all stream and potential lines of flow around the heavy circle will undergo a corresponding transformation, so that the final flow net will represent potential motion around a plate bent in the form of a circular arc, called the Kutta profile.

The addition of circulation to the picture will then produce a force upon the curved plate at right angles to the oncoming flow, and by rotating the coordinate axes, in addition to transposing them, the point of stagnation may be moved to the rear edge of the plate as the plate is inclined to the flow.

Had the coordinate axes been shifted to the right, instead of downward, the conformal map of the original circle would have been given the form of a streamlined body symmetrical about

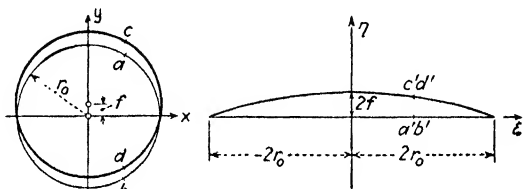


FIG. 56.—The Kutta transformation.

the real axis. That this is true will be seen from Fig. 57; since the heavy circle lies outside of the one concentric with the new coordinate origin at all points but one, then the transformed image of the heavy circle must lie outside of the image of the other (in this case the image is a straight line) at all points except the one common to them both. If the axes are first displaced and then rotated through a given angle, the transformed image will be that of a symmetrical streamlined body of infinite length

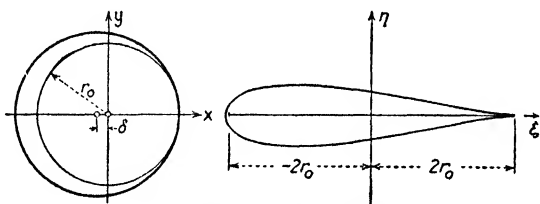


FIG. 57.—Streamlined foil.

(*i.e.*, infinite in a direction normal to the plane of motion) inclined at the given angle to the direction of oncoming flow. Circulation may then be introduced and the rear point of stagnation brought to the trailing edge of the body in the manner already described. It is evident that through this general transformation both regions of infinite velocity have been eliminated.

A combination of these two types of displacement of the coordinate axes—downward and to the right simultaneously—

will result, obviously, in a form of profile that is a combination of the circular arc of the first example with the symmetrical streamlined section of the second example. As shown in Fig. 58, the image of the original section (both image and original are shown in heavy lines) must have in general the same position relative to the other two images as the heavy circle has to the other two original circles—that is, where the heavy circle lies between the other two, its image must also lie between the arc and the straight line; where the heavy circle lies outside the others, its image must also lie outside. Careful study of the illustration will serve to clarify this point.

It will be evident to the reader that this form of section, called the Joukowsky profile after the scientist who developed the trans-

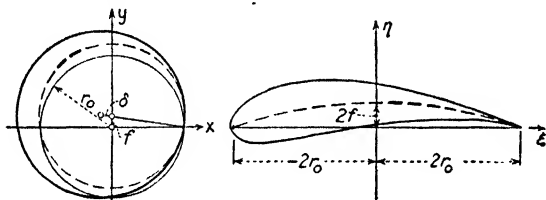


FIG. 58.—The Joukowsky profile.

formation, bears a striking resemblance to the airfoil cross section used for airplane wings and propeller and turbine blades of various sorts. Since the Joukowsky profile may be given almost any thickness and shape through varying f and δ (refer to Fig. 58), and since the velocity and pressure distribution in the surrounding fluid may be found analytically by means of the proper functional relationships, the method has been of great aid in the study of actual airfoil sections. The foil may not only be inclined at any desired angle to the oncoming flow, but through the introduction of circulation the flow net may be made to pass the trailing edge without a singular point of infinitely high velocity; and since the leading edge is rounded, the singular point of the Kutta profile is entirely obviated. Under these conditions the magnitude of the lift, or force normal to the oncoming flow, may be computed from Eq. (59).

• Although the problem of velocity distribution around such a profile does not warrant further discussion in this text, a simple graphical method of determining the form of the profile itself may be of interest to the reader. From the origin of the ζ plane

the distance $\eta = f$ is laid off along the imaginary axis. Through this point and the point $\xi = r_0$ on the real axis is drawn a straight line, along which, on either side of the imaginary axis, is measured the distance δ , as shown in Fig. 59. Using these two points as centers, two circles are described, both of which pass through the intersection of the straight line with the real axis. Two lines are now drawn from the origin, making equal positive and negative angles with the real axis; from the intersection of one line with the larger circle and from that of the other line with the small circle two more lines are drawn to form a parallelogram. Since the corner of this parallelogram opposite the coordinate origin determines one point on the profile, the operation may be per-

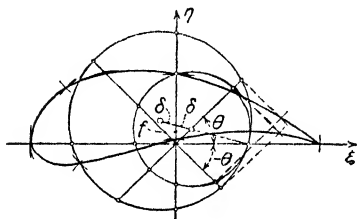


FIG. 59.—Graphical construction of a Joukowski foil.

formed simply by swinging two circular arcs having radii equal respectively to the two sides already drawn. This operation is then repeated for as many points as are necessary to complete the profile. Obviously, if the distance δ is equal to zero, the foil will have the form of a circular arc—the Kutta profile—the degree of

curvature depending upon the relative magnitude of f and r_0 ; similarly, if f is zero, there will result a symmetrical streamlined section, its relative thickness depending upon the ratio between δ and r_0 .

28. Methods of Application. In a few specific instances the several elementary transformations already discussed may be applied directly to problems of fluid motion. That such cases are not more numerous is due in part to the restrictions noted in the following chapter, but also to the fact that these elementary transformations are definitely limited in scope. Nevertheless, it is sometimes possible to combine a number of basic functions—namely, those for parallel flow, circulation, and sources and sinks—in such a way as to approximate the desired conditions of motion to a satisfactory degree. This method has been used, for instance, by Spannhake¹ in the study of flow around the impeller

¹ SPANNHAKE, W., "Neue Darstellung der Potentialströmung durch Kreisräder für beliebige Schaufelform," Vorträge aus dem Gebiete der Aerodynamik und verwandter Gebiete (Aachen, 1929), Springer, Berlin, 1930.

blades of a centrifugal pump. In general, however, it must be said that a procedure such as this requires considerable persistence and mathematical ingenuity, and becomes the more difficult as the boundary conditions increase in complexity.

Mention has already been made of the fact that a flow net may be fitted graphically to any two-dimensional boundary profile, however involved the form may be. Justification for this procedure is embodied in the Cauchy integral theorem,¹ which states, in effect, that any pattern of potential motion is determined uniquely by the boundary geometry. The Cauchy integral formula, moreover, provides a means of obtaining this pattern of motion for any two-dimensional boundary conditions whatever, by relating the complex function for any point in the flow to that of a point moving around the boundary profile.² Although the calculation must proceed by means of graphical integration, the resulting solution is far more accurate than that obtained by graphical adjustment of the flow net.

This process is very laborious, however, and certain mechanical substitutes for the mathematical analysis will yield the same results with far less trouble. Principal among these is the electrical analogy, which warrants a brief explanation at this point. It has long been known that the potential patterns used herein to describe fluid motion apply fully as well to magnetic and electrical fields. Indeed, the lines of constant velocity potential for a given flow pattern would coincide with lines of constant electrical potential were a current to be passed through a plane conductor having the same boundary outlines. This fact at once suggests the use of the analogy between the two cases as a method of obtaining electrically the flow pattern for any desired boundary conditions. The conducting medium is given the required form, a known potential is applied between the two extremities, and the drop in potential is measured at suitable points over the profile; by selecting equal potential increments, successive lines of constant potential can readily be traced. In some instances a metallic conductor is desirable, although use of an electrolyte is often advantageous. In the latter instance, since the boundaries are formed by flexible strips immersed in the bath and curved to the required shape, the potential may be applied

¹ DURAND, W. F., *Mathematical Aids, "Aerodynamic Theory,"* vol. 1, p. 10, Springer, Berlin, 1934.

² *Ibid.*, p. 11.

between either pair of opposite boundaries by proper choice of conducting and non-conducting material. If the outermost stream lines are formed by metallic strips, and the end potential lines by strips of an insulating material, the drop in electrical potential will then indicate the change in ψ from one stream line to the next. That is, the method will permit the location of both stream and potential lines, since in any conformal net the terms ϕ and ψ may be interchanged without affecting the mathematical nature of the pattern. Further information on apparatus and experimental technique may be found elsewhere.¹

As yet no attempt has been made in this chapter to treat cases of motion which are not determined by fixed boundaries. Since the outermost stream lines invariably coincided with the boundary profiles, no restriction had to be made as to the boundary pressure distribution, the latter following from the existing distribution of velocity. A free surface, on the other hand, not only denotes a discontinuity of the fluid medium, but also represents a stream line along which the pressure intensity must be constant. Needless to say, the Cauchy theorem applies as well to such cases of motion, although if the action of fluid weight can still be neglected, other methods will prove more useful. For instance, it has been found helpful in conformal mapping to introduce an intermediate transformation to the v plane [refer to Eqs. (57) and (58)], in which the pattern—known as a hodograph²—indicates by the magnitudes of r and θ the magnitude and direction of the velocity vector at every point of the flow profile in the z plane. By similar means Helmholtz and Kirchhoff first investigated the problem of jet contraction,³ while von Mises⁴ determined the contraction and discharge coefficients for a wide variety of orifice forms.

¹ HOHENEMSER, K., Experimentelle Lösung ebener Potentialströmung, *Forschung auf dem Gebiete des Ingenieurwesens*, vol. 2, no. 10, p. 370, 1931. For an extensive bibliography see HAGUE, B., *The Electrician*, vol. 102, pp. 185, 315, 1929.

² PRANDTL-TIETJENS, "Fundamentals of Hydro- and Aerodynamics," p. 178. See also BETZ, A., and PETERSOHN, E., Anwendung der Theorie der freien Strahlen, *Ingenieur-Archiv*, vol. 2, 1931.

³ LAMB, "Hydrodynamics," p. 94.

⁴ MISES, R. von, Berechnung von Ausfluss- und Ueberfallzahlen, *Zeitschrift VDI*, p. 47, 1917. See also SCHACH, W., Umlenkung eines freien Flüssigkeitsstrahles an einer ebenen Platte, *Ingenieur-Archiv*, vol. 4, 1934; vol. 6, 1935.

Once fluid weight plays an essential role, the hodograph method is not always sufficient, although the Cauchy integral formula may still be counted upon to yield satisfactory results. The approach is now indirect, however, for application of the formula requires prior knowledge of the boundary form, whereas the form of a free surface is the principal variable to be determined. Nevertheless, the formula will yield a flow net for any assumed boundaries, and it is, therefore, only necessary to make a reasonable assumption and then check the resulting solution for constancy of pressure along the assumed free surface. This may be accomplished in the following manner: Since along the free surface

$$v = \sqrt{2g} (E_w - \bar{h}) = \frac{\partial \phi}{\partial s}$$

the magnitude of ϕ at any point on this stream line may be found by integrating v along s from some arbitrary point of reference s_0 :

$$\phi = \int_{s_0}^s \sqrt{2g} (E_w - \bar{h}) ds \quad (60)$$

Comparison of this distribution of ϕ with that obtained by application of the Cauchy formula will show at once the manner in which the assumed profile must be adjusted for the next approximate solution. Evidently, successive trials will lead closer and closer to the exact profile form, three or four approximations generally being sufficient. Unfortunately, space does not permit more detailed discussion of this method, in particular since it has not yet received the attention which it merits. A complete description may be found in a paper by Lauck,¹ who determined therewith the profile of flow over a weir of infinite height.

Since application of the electrical analogy makes recourse to the Cauchy theorem unnecessary in dealing with problems of confined flow, it should also be useful in cases of flow with a free surface—although the possibility of such application apparently

¹ LAUCK, A., Ueberfall über ein Wehr, *Z. angew. Math. Mech.*, vol. 5, p. 1, 1925.

has escaped the notice of the research world. The process of successive approximation would then proceed in the manner just outlined, the electrical method replacing the Cauchy formula in obtaining the distribution of ϕ to check against that determined by means of Eq. (60). Unfortunately, the hydraulician who is still so optimistic as to seek a simple mathematical method of expressing the form of surface profiles will doubtless continue to seek in vain; no other means of analysis is known for curvilinear flow under gravitational action.

CHAPTER VI

APPLICABILITY OF THE FUNDAMENTAL EQUATIONS

29. Résumé. Classical hydrodynamics, in the course of its two centuries of development, centered its attention upon the interplay of velocity and dynamic pressure for a given fluid density and given boundary geometry. Although the resulting equations of motion pertain to the case of confined flow, introduction of a single force property—specific weight—readily permits extension of these equations to the case of flow with a free surface. The foregoing chapters have placed considerable emphasis upon the more essential concepts of classical hydrodynamics, since these basic equations are the foundation of modern fluid mechanics. Thus, in Chapter II the elementary principles of momentum, energy, and continuity were discussed in their relationship to the general pattern of motion. Chapter III inquired more thoroughly into the behavior of the fluid particle, stressing the kinematic—rather than the dynamic—aspects of flow. Then, under the assumption of steady, irrotational motion (a restriction that is in itself purely kinematic), certain methods were outlined in Chapters IV and V, permitting the determination of the flow pattern for given boundary conditions—namely, the concept of potential flow, conformal mapping, and the Cauchy integral theorem; the flow net may be looked upon as the graphical representation of the latter principles.

In addition to providing a preliminary structure for the refinements of fluid mechanics, in many instances these basic concepts are directly applicable to engineering problems without further modification. Moreover, the elementary principle of energy provides a qualitative check upon their limit of applicability. This limit depends, obviously, upon the extent to which the original premises of classical hydrodynamics are actually fulfilled in the given problem. Thus, if the principle of potential motion is accepted as the most useful immediate tool provided by the science, it is evident that any flow studied by this means must be

essentially one of constant energy, constant density, and complete conformity with the boundary geometry.

30. Energy Criteria. Whenever flow proceeds from a state of rest, the fluid energy will at first be uniformly distributed; it is then only reasonable to presume that the flow net will satisfactorily describe the pattern of motion. For instance, the discharge under a sluice gate leading from a large reservoir will differ only imperceptibly from potential motion. As will be seen in Part Two of this book, however, the energy of flow will change with distance in the direction of motion, varying not only along each stream line but from one stream line to the next. At low velocities the rate of change of energy in the longitudinal direction will be small, but the energy will then vary appreciably over a normal section. At high velocities, on the other hand, the energy will be fairly uniform across the flow, while the rate of change in the direction of motion will be relatively large. It so happens that the latter type of motion is most often encountered in engineering practice.

In problems of rapid variation in velocity, indeed, the distribution of dynamic pressure is of paramount importance, interest in energy variation then being completely secondary. If the boundary transition is short, the longitudinal energy change will often be of negligible magnitude, and if, in addition, the velocity is sufficiently high, the energy will also be approximately uniform over the cross section of flow. One might therefore conclude that use of the flow net would then be justifiable—at least so far as energy criteria are concerned—regardless of whether the fluid accelerates or decelerates as a result of the boundary form. Nevertheless, the remaining two restrictions—constant density and conformity with the boundary—often limit the extent to which rapid variation may occur if the flow net is to provide satisfactory results.

31. Variation in Density. An extreme case of rapid transition is shown in the case of a thin flat plate in a plane normal to the direction of motion (Fig. 54a). Although the fluid comes to rest at the point of stagnation, with an accompanying increase in the dynamic pressure, at the edges of the plate the acceleration is infinitely great—a condition requiring a velocity of positive infinity and a pressure intensity of negative infinity. Such conditions are mathematically possible in potential flow, but

since they are physically quite out of the question, it is evident that the flow net cannot possibly describe the actual state of motion past such a boundary.

Since a change in velocity must always be accompanied by a change in dynamic pressure, it is evident that either acceleration or deceleration must tend to change the density of the moving fluid. The reader will realize that in the case of a gas, which is readily compressible, the flow net will have quantitative significance only if the relative change in density is limited to a very small magnitude. Otherwise, the actual flow pattern will differ from that of potential motion in the distribution of both pressure and velocity. Of distinct value, therefore, would be an approximate relationship for the permissible variation in velocity or pressure whereby change in density will not seriously affect such computations.

The differential equation of energy for steady flow applies just as well to a gas as to a liquid, provided the density is no longer treated as a constant; thus,

$$\rho v dv + dp + d(\gamma h) = 0$$

Since the increment $d(\gamma h)$ is ordinarily insignificant in gaseous motion, it may be omitted without appreciable error. Dividing by ρ , and integrating along a stream line between points 1 and 2,

$$\frac{v_2^2 - v_1^2}{2} + \int_{p_1}^{p_2} \frac{dp}{\rho} = 0$$

Although the first term is identical with that for liquid motion, the second differs in that the integration cannot be performed until the two variables are related to one another. This relationship is found in the thermodynamic principle

$$(\text{absolute pressure}) \times (\text{specific volume})^k = \text{constant}$$

Since specific volume is defined as volume per unit weight, it is seen to be the reciprocal of specific weight, whence

$$\frac{p}{\gamma^k} = \text{constant} = \frac{p_1}{\gamma_1^k}$$

and therefore

$$\frac{p}{\rho^k} = \frac{p_1}{\rho_1^k}$$

or, solving for ρ ,

$$\rho = \rho_1 \left(\frac{p}{p_1} \right)^{\frac{1}{k}}$$

The second term of the energy equation may now be rewritten in the form,

$$\int_{p_1}^{p_2} \frac{dp}{\rho} = \frac{p_1^{\frac{1}{k}}}{\rho_1} \int_{p_1}^{p_2} p^{-\frac{1}{k}} dp = \frac{p_1}{\rho_1} \frac{k}{k-1} \left[\left(\frac{p_2}{p_1} \right)^{\frac{k-1}{k}} - 1 \right]$$

introduction of which in the energy equation then yields,

$$\frac{v_2^2 - v_1^2}{2} + \frac{p_1}{\rho_1} \frac{k}{k-1} \left[\left(\frac{p_2}{p_1} \right)^{\frac{k-1}{k}} - 1 \right] = 0$$

This expression represents the counterpart of the Bernoulli equation for a gas under adiabatic conditions.

Solving for p_2 ,

$$p_2 = p_1 \left[1 + \frac{\rho_1}{p_1} \frac{v_1^2 - v_2^2}{2} \frac{k-1}{k} \right]^{\frac{k}{k-1}}$$

Subtracting p_1 from both sides of the equation, and expanding the right side in a series,

$$p_2 - p_1 = p_1 \left[1 + \frac{\rho_1}{p_1} \frac{v_1^2 - v_2^2}{2} + \frac{1}{2k} \left(\frac{\rho_1}{p_1} \frac{v_1^2 - v_2^2}{2} \right)^2 + \cdots - 1 \right]$$

Finally, writing the pressure and velocity differences in simplified form,

$$\Delta p = \rho_1 \frac{\Delta(v^2)}{2} \left[1 + \frac{\rho_1 \Delta(v^2)}{4kp_1} + \cdots \right]$$

Immediately apparent is the fact that the first term of the series corresponds to conditions of flow at constant density. It then follows that for relatively small changes in velocity the per cent error in pressure change caused by assuming the density constant will be indicated approximately by the magnitude of the quantity

$$\frac{\rho \Delta(v^2)}{4kp} \times 100$$

For instance, in the case of air under normal atmospheric conditions, a change in velocity from 50 to 250 feet per second will result in an error in pressure change of only 1.2 per cent if computed on the basis of constant density. As a matter of fact, the influence of variable density upon the dynamic pattern must be taken into account only under relatively high velocity changes—such as are encountered, for instance, in the free efflux of gas from a high-pressure container, or in the motion of airplane propellers and projectiles.

32. Cavitation. A liquid, unlike a gas, may be considered truly incompressible so far as those types of flow usually encountered in hydraulic engineering are concerned. Nevertheless, while compressive stresses will thus have no further bearing upon the applicability of the flow net in cases of liquid motion, it must be recalled that liquids may not ordinarily be expected to withstand tension to any appreciable degree. In the laboratory, to be sure, it has been shown that water has a tensile strength of at least 34 atmospheres; but it is essential that the water so stressed be extremely clean and free from dissolved air. Under average conditions a liquid will seldom fail to boil once the pressure of vaporization is reached—close to absolute zero at normal temperature.

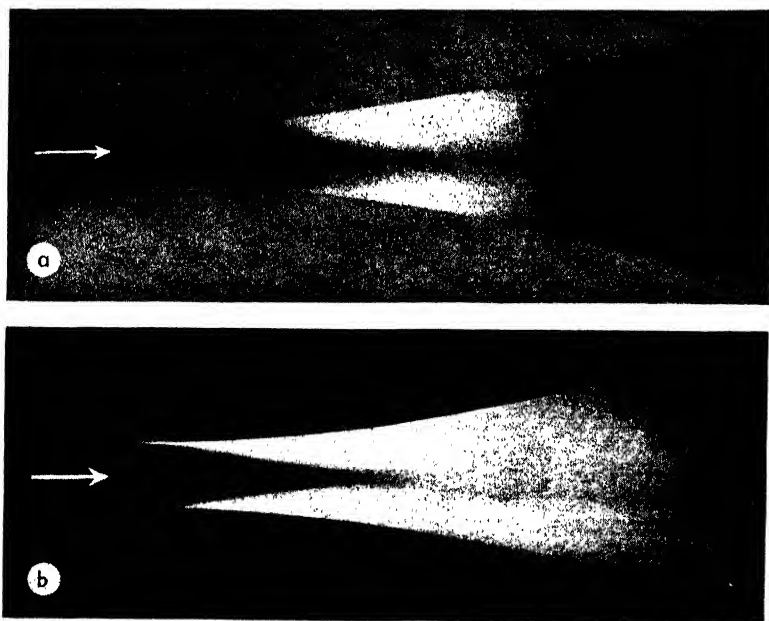
It is evident that for given boundary conditions either the velocity of flow or the hydrostatic load on a closed system may so be varied that a pressure intensity of absolute zero will be approached at some point on the boundary; that is,

$$p_{abs} = E_v - \rho \frac{v^2}{2} - \gamma h \rightarrow 0$$

In the case of the two-dimensional bend of Fig. 11a, the point of minimum pressure intensity will occur along the inner wall near the midpoint of the bend. If now the pressure intensity at this point is reduced to the vapor pressure of the liquid, either by increasing the discharge or by reducing the pressure load, it is evident that the liquid passing this point will just begin to vaporize. If the discharge is further increased, the region of vaporization will grow in size, a cavity forming immediately beyond the midpoint of the bend and appearing to ease the curvature of the innermost filaments. Continued increase

in discharge will cause further growth of this vapor pocket, until finally the flow as a whole becomes unstable.

A simple laboratory demonstration of this phenomenon—cavitation—was devised long ago by Osborne Reynolds,¹ and may easily be repeated by the reader. A small glass tube is heated over a flame and drawn out in the form of a Venturi meter



Columbia

FIG. 60.—Cavitation in a two-dimensional Venturi throat; (a) front illumination, (b) rear illumination, under identical conditions of flow.

with a fairly great contraction. If this is connected with a water faucet by means of rubber tubing, at even relatively low rates of flow a white cloud of vapor may be observed just beyond the throat. As the discharge is increased, the zone of cavitation will lengthen, the intensity of the formation and subsequent collapse of the vapor bubbles making itself apparent through a distinct hissing sound and perceptible vibration of the tube. Photographs of a two-dimensional contraction of this nature may be seen in Fig. 60, front illumination emphasizing the region

¹ REYNOLDS, OSBORNE, "Papers on Mechanical and Physical Subjects," vol. 2, p. 578, 1901.

of actual cavitation and illumination from the rear showing the appreciable quantity of air which is brought out of solution by the extreme reduction of pressure and not redissolved. It is quite evident from the photographs that the effect does not extend entirely across the flow section, but is limited to the region of maximum curvature—and hence maximum velocity and minimum pressure—at the boundary.

The occurrence of cavitation in hydraulic machinery is obviously a disadvantage, if only because of the resulting loss in efficiency. There is, however, a far more serious aspect of the problem, the importance of which has led to extensive research on cavitation in this country and abroad. High-speed motion pictures of this process indicate that conditions in the cavitation zone are far from steady—in fact, the vapor cloud seen with the naked eye is merely an average impression, for the successive stages of vaporization, movement downstream, and condensation repeat themselves so many times a second (the number of cycles varying directly with the velocity) that the eye is quite incapable of following. The formation of the vapor pockets is in itself of little consequence—but the abrupt collapse of these cavities as they are carried into regions of higher pressure is accompanied by sudden compressive stresses of exceedingly high magnitude. If the point of collapse is close to a solid boundary, the boundary surface is then subjected to countless intermittent shocks, and will sooner or later fail through fatigue. It was formerly thought that the corrosion—pitting—of metal parts of hydraulic machinery was due to a chemical action intensified by the low pressure. But laboratory tests indicate that such chemically inert (though brittle) substances as glass will fail quite readily, the zone of failure even lying somewhat below the exposed surface. Moreover, in every case the pitting has not been found to occur at the point where the pressure drops, but where the pressure abruptly rises, this marking the region of collapse of the vapor pockets.

Measurements of the pressure distribution along a Venturi throat during cavitation provide an excellent picture of the mean dynamic pattern.¹ In Fig. 61a may be seen a typical series of pressure distribution curves, taken under conditions of constant

¹ ACKERET, J., Kavitation, "Handbuch der Experimentalphysik," vol. IV-1, Akademische Verlagsgesellschaft, Leipzig, 1931.

discharge and constant pressure intensity at the entrance, such that the vapor pressure of the liquid would prevail at the point of maximum velocity at the throat. The intensity of cavitation was then governed by varying the downstream pressure, the end of the visible vapor pocket corresponding invariably with the point at which the pressure abruptly began to rise—for example, at point *C* as shown in the illustration.

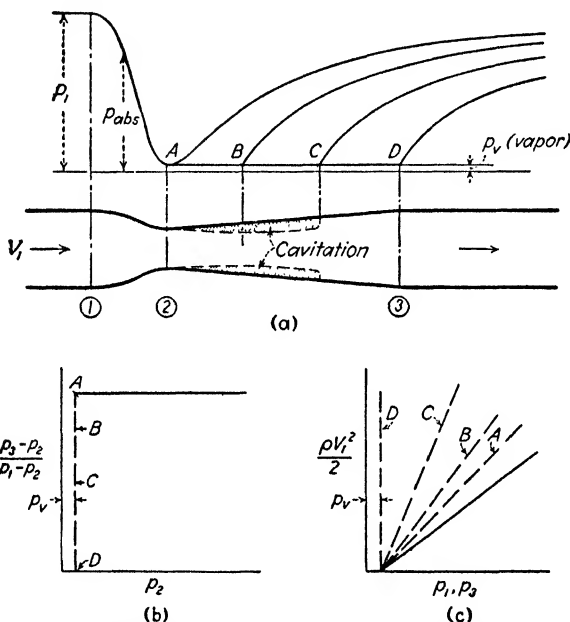


FIG. 61.—Characteristics of cavitation at a Venturi throat.

Since the magnitude of the downstream pressure intensity is seen to determine the intensity of the cavitation phenomenon for the given conditions of flow, one can only conclude that the extent to which the kinetic energy is restored to potential energy beyond the throat will decrease with increasing intensity of cavitation. The plot of relative pressure recovery at section 3 (Fig. 61b) indicates this fact; it will be found, moreover, that if section 3 is moved downstream, points *B*, *C*, and *D* will lie higher on this plot, but will never reach the elevation of point *A*.¹ It is apparent that the vertical scale then represents the efficiency

¹ Compare MOODY, L. F., and SORENSON, A. E., Progress in Cavitation Research at Princeton University, *Trans. A.S.M.E.*, vol. 57, 1935.

of the meter, cavitation effectively lowering the efficiency of any hydraulic device.

While the foregoing measurements applied to specific pressure and velocity conditions in the approach, they may be generalized in the following manner: Writing the mean energy equation between sections 1 and 2 (ignoring, for convenience, the secondary effects of curvature),

$$\rho \frac{V_1^2}{2} + p_1 = \rho \frac{V_2^2}{2} + p_2$$

whence

$$p_1 - p_2 = \rho \frac{V_2^2 - V_1^2}{2} = \rho \frac{V_1^2}{2} \left(\frac{V_2^2}{V_1^2} - 1 \right)$$

The ratio V_2/V_1 is determined by the meter dimensions, and the quantity $\left(\frac{V_2^2}{V_1^2} - 1 \right)$ may therefore be considered constant for the given meter. Once cavitation begins, p_2 will become equal to p_v , the magnitude of which is also independent of flow conditions. It then follows that p_1 should be a linear function of $\rho V_1^2/2$ for all stages of cavitation; that is,

$$p_1 = C \rho \frac{V_1^2}{2} + p_v$$

as shown by the full line in Fig. 61c; for any point in the region to the right of the line, cavitation will not occur. Furthermore, for a given magnitude of $\rho V_1^2/2$ (and hence of p_1), the degree of cavitation is governed by the pressure intensity at some downstream section. It is then apparent that a given state of cavitation—corresponding, for instance, to the pressure distribution *A*, *B*, *C*, or *D*—will be indicated by a linear relationship between p_3 and $\rho V_1^2/2$:

$$p_3 = C' \rho \frac{V_1^2}{2} + p_v$$

The factor C' will vary in magnitude with the stage to which it corresponds, as indicated by the broken lines in Fig. 61c. Moreover, it will remain essentially constant for a given stage of cavitation only if the air content of the water is negligible,

for experiments have shown that the characteristics of cavitation will vary with the amount of air in solution.¹

Cavitation occurs most frequently in two related types of hydraulic machinery—turbine runners and ship propellers—both of which operate under conditions of relatively low pressure. Since as yet no material has been found which resists pitting to a satisfactory degree, the elimination of cavitation remains the only means of solving this costly problem. Three possible courses should be apparent to the reader: reducing the mean velocity of flow, increasing the hydrostatic load, or modifying the curvature at the danger point of the boundary. Since high average velocities and low hydrostatic loads are often essential in the operation of hydraulic machinery at peak efficiency, it is evident that boundary design is of considerable importance. The flow net will be found of considerable assistance in such design, although it is no longer directly applicable once cavitation begins.

33. Separation. In stating that boundary conditions uniquely determine the form of the corresponding flow net, the Cauchy integral theorem presumes that the outermost stream lines of the resulting flow conform exactly with the boundary profile over their entire length. In other words, neither may cavities exist between the boundary and the fluid medium, nor may a stream line abruptly leave the boundary and wander into the central portion of the flow.

Considering once again the equation of energy along a given stream line,

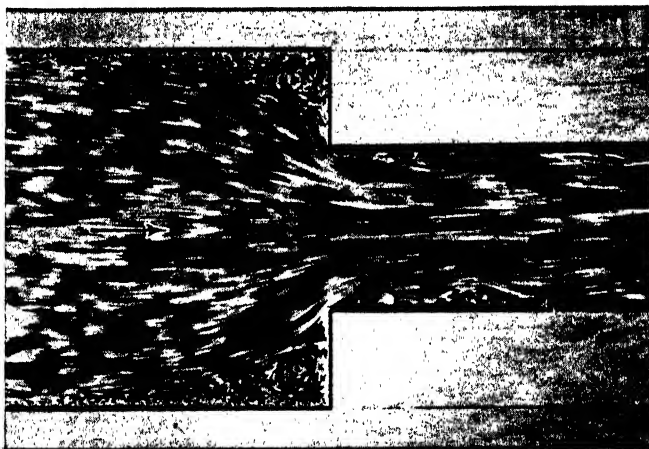
$$E_v = \rho \frac{v^2}{2} + p + \gamma h = \text{constant}$$

it is evident that for constant values of h a rise in pressure is limited by a zero magnitude of the velocity, just as a rise in velocity is limited by an absolute zero magnitude of the pressure intensity. If the energy is uniformly distributed, the maximum dynamic pressure will then occur at a point of stagnation. But if the energy is different for any two neighboring stream lines, continued increase in pressure in the direction of flow would call for a point of stagnation on one line while the other still displays a finite velocity. Should the stream line of lowest energy lie at a solid boundary, this outermost stream line can no longer

¹HUNSAKER, J. C., Cavitation Research, *Mech. Eng.*, vol. 57, no. 4, pp. 211-216, 1935.

continue along the boundary once the point of zero velocity is reached, for at a stagnation point the stream line must abruptly change direction.

If the energy equation for any stream line is differentiated (assuming, for convenience, that h is constant), it will be apparent that for a given pressure increment the corresponding change in



Columbia

FIG. 62.—Abrupt contraction in a conduit, showing separation in regions of local deceleration.

velocity will be inversely proportional to the magnitude of the velocity vector:

$$dv = -\frac{dp}{\rho v}$$

Should the pressure gradient along two neighboring stream lines be essentially the same, the ratio of the corresponding velocity increments will be indicated by the inverse ratio of the velocities:

$$\frac{dv_1}{dv_2} \approx \frac{v_2}{v_1}$$

Evidently, when the pressure decreases (acceleration), the velocity distribution will grow more uniform (Fig. 63a). On the other hand, an increase in pressure (deceleration) will cause the velocities to become more and more unequal, until one eventually reaches the limiting magnitude of zero.

Such circumstances are physically possible only if the point of zero boundary velocity is a true point of stagnation—that is, the

stream line must then abruptly change direction, the flow thereby separating from the boundary, as indicated in Fig. 63*b*. There thus results a discontinuity in the flow—but not in the fluid, as in the case of cavitation, for the region of discontinuity is generally filled with fluid moving along the boundary in the upstream direction. Since the line of separation nevertheless

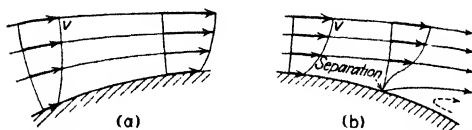


FIG. 63.—Effect of (a) acceleration and (b) deceleration upon velocity distribution.

marks a border of the flow that was not considered in the original boundary conditions, it is obvious that the phenomenon of separation cannot be studied further in the light of potential motion.

While the energy equation permits at least qualitative information as to discontinuity, more thorough discussion of this problem must be left to a later chapter. It must be noted, however, that either local or general deceleration of flow with non-

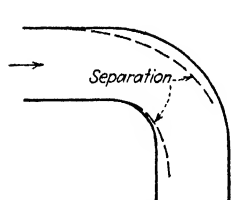


FIG. 64.—Separation at a two-dimensional bend.

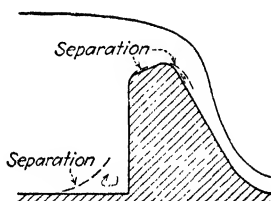


FIG. 65.—Separation at a spillway.

uniform energy distribution will almost invariably result in zones of discontinuity. Two such regions are indicated in Fig. 64, conforming with the two-dimensional bend already studied by means of the flow net. Only if the velocity of approach is practically constant from one side to the other, or if the curvature is very gradual, will separation fail to occur. Figure 65, on the other hand, shows a case of generally accelerated motion, the two regions of discontinuity at points of local deceleration near

the crest of the spillway being due entirely to poor design. It should be apparent to the reader, therefore, that the flow net attains its greatest significance in the case of rapidly accelerated motion—and, conversely, that a flow profile attains its maximum efficiency when it conforms most closely to conditions of potential motion.

PART TWO
MECHANICS OF FLUID RESISTANCE

CHAPTER VII

FUNDAMENTAL EQUATIONS OF VISCOUS FLOW

34. Elementary Stresses within a Viscous Fluid. If, in addition to the influence of weight, one considers the effect upon fluid motion of the next most important force property—viscosity—one must return first of all to the basic expressions for the equilibrium of a fluid element. Aside from gravitational attraction, the element is now subjected to two distinct types of stress: compression, and shear; in accordance with the Newtonian principle of momentum, the resultant of these several forces must equal the mass times the acceleration of the fluid element. Since the expressions for the components of acceleration are independent of the character of the acting forces, it remains only to incorporate in the basic force equation the effect of viscous action.

Consider now a small fluid element in the form of a cube whose center lies at the coordinate origin and whose sides are parallel to the coordinate axes (Fig. 66). Gravitational attraction necessarily retains its original nature, the force vector for fluid weight being directed vertically downward and passing through the center of the cube. But the resultant force upon each face of the cube no longer acts normally, for it is composed of a direct stress—pressure intensity—and a tangential stress—viscous shear; and owing to the nature of the viscous action, both of these must be considered to vary generally with distance and direction. Thus, at the center of the cube the pressure intensity will have different magnitudes parallel to each of the coordinate axes: p_x , p_y , and p_z ; the pressure intensity at the midpoint of each face of the cube will then differ from the corresponding component at the origin by the product of the pressure gradient at right angles to the face and the distance of the face from the center, as shown in Fig. 66. Similarly, since there will be shear in two directions on each of the three planes passing through the origin, at the center of the cube the intensity of shear (τ) must be expressed by six different quantities: τ_{xy} , τ_{yx} , τ_{yz} , τ_{zy} , τ_{zx} , τ_{xz} (τ_{xy} , for example, representing the shear intensity in the plane

normal to the x axis and acting in the y direction); the intensity of shear in either of two directions along any face of the cube will then differ from that at the origin by the product of the gradient at right angles to the face and the distance of the face from the origin, as shown in Fig. 66. If the fluid element is so small that the force intensities at the center of any face may be treated as average values for the entire face without appreciable error, the total direct or tangential stress upon a face in any direction will

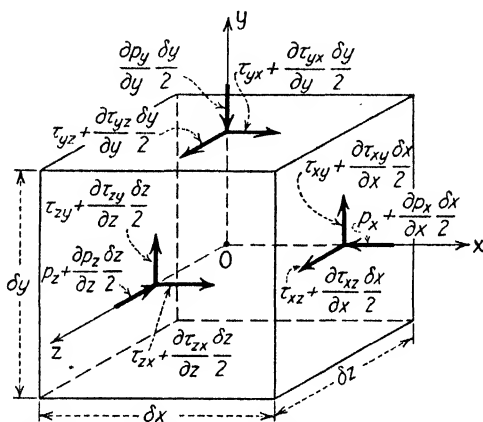


FIG. 66.—Components of normal and tangential stress acting upon a fluid element.

be equal to the product of its area and the corresponding stress intensity.

The weight components of the fluid element can be written directly as the product of the specific weight of the fluid, the volume of the element, and the negative rate of change of elevation in each coordinate direction:

$$x \text{ direction: } -\gamma \delta x \delta y \delta z \frac{\partial h}{\partial x}$$

$$y \text{ direction: } -\gamma \delta x \delta y \delta z \frac{\partial h}{\partial y}$$

$$z \text{ direction: } -\gamma \delta x \delta y \delta z \frac{\partial h}{\partial z}$$

The components of the resultant force due to pressure gradient may also be written at once, as the differences between the normal forces exerted upon each pair of opposite faces; thus,

$$x \text{ direction: } -\frac{\partial p_x}{\partial x} \delta x (\delta y \delta z)$$

$$y \text{ direction: } -\frac{\partial p_y}{\partial y} \delta y (\delta z \delta x)$$

$$z \text{ direction: } -\frac{\partial p_z}{\partial z} \delta z (\delta x \delta y)$$

In similar fashion one may formulate the components of shear to which the fluid element is subjected, with the exception that force components parallel to any one of the coordinate axes will now involve two different pairs of opposite faces of the cube; the components of tangential stress will then be:

$$x \text{ direction: } \frac{\partial \tau_{yx}}{\partial y} \delta y (\delta x \delta z) + \frac{\partial \tau_{zx}}{\partial z} \delta z (\delta x \delta y)$$

$$y \text{ direction: } \frac{\partial \tau_{xy}}{\partial x} \delta x (\delta y \delta z) + \frac{\partial \tau_{zy}}{\partial z} \delta z (\delta y \delta x)$$

$$z \text{ direction: } \frac{\partial \tau_{xz}}{\partial x} \delta x (\delta z \delta y) + \frac{\partial \tau_{yz}}{\partial y} \delta y (\delta z \delta x)$$

There are now at hand relationships for the components of gravitational attraction, normal stress, and tangential stress upon a fluid mass of elementary volume. These relationships are only approximate, owing to the finite dimensions of the fluid element, but as the dimensions become smaller, the expressions will become more nearly exact. Division of each term by the fluid volume, as the latter approaches the infinitesimal, will then yield the components of force per unit volume acting at a point in space;

$$(f_w)_x = -\gamma \frac{\partial h}{\partial x}; \quad (f_w)_y = -\gamma \frac{\partial h}{\partial y}; \quad (f_w)_z = -\gamma \frac{\partial h}{\partial z} \quad (61)$$

$$(f_p)_x = -\frac{\partial p_x}{\partial x}; \quad (f_p)_y = -\frac{\partial p_y}{\partial y}; \quad (f_p)_z = -\frac{\partial p_z}{\partial z} \quad (62)$$

$$(f_s)_x = \frac{\partial \tau_{yx}}{\partial y} + \frac{\partial \tau_{zx}}{\partial z}; \quad (f_s)_y = \frac{\partial \tau_{xy}}{\partial x} + \frac{\partial \tau_{zy}}{\partial z}; \quad (f_s)_z = \frac{\partial \tau_{xz}}{\partial x} + \frac{\partial \tau_{yz}}{\partial y} \quad (63)$$

35. Viscous Stress in Terms of Rate of Deformation. Fortunately, the foregoing relationships for viscous stress may be simplified considerably, for it can be shown that at a given point the intensity of shear in a plane normal to any axis x and acting

in a direction parallel to any other axis y (τ_{xy}) must be identical with the intensity of shear at that point in a plane normal to the y axis and acting in the x direction (τ_{yx}). This may be seen (through reference to Fig. 66) by taking moments about the z axis of all forces in the directions x and y , and then placing these equal to the product of the mass, the square of the radius of gyration, and the angular acceleration of the cube about the z axis. All components of fluid weight and normal force will lie along lines passing through the center of the cube, and hence will have no moments; the remaining terms will have the form

$$\begin{aligned} & \left(\tau_{xy} + \frac{\partial \tau_{xy}}{\partial x} \frac{\delta x}{2} + \tau_{xy} - \frac{\partial \tau_{xy}}{\partial x} \frac{\delta x}{2} \right) (\delta y \delta z) \frac{\delta x}{2} \\ & - \left(\tau_{yx} + \frac{\partial \tau_{yx}}{\partial y} \frac{\delta y}{2} + \tau_{yx} - \frac{\partial \tau_{yx}}{\partial y} \frac{\delta y}{2} \right) (\delta z \delta x) \frac{\delta y}{2} \\ & = \rho \delta x \delta y \delta z r^2 \alpha \end{aligned}$$

from which

$$\tau_{xy} - \tau_{yx} = \rho r^2 \alpha$$

If the dimensions of the cube are now made to approach the limit zero, the square of the radius of gyration will become an infinitesimal of the second order, in which case the right side of the equation may be neglected. Extending the operation to the remaining coordinate directions will then prove the existence of the following identities:

$$\tau_{xy} = \tau_{yx}, \quad \tau_{yz} = \tau_{zy}, \quad \tau_{zx} = \tau_{xz} \quad (64)$$

Readers will recall that the dynamic viscosity of a fluid was defined quite generally as the ratio of intensity of shear to rate of angular deformation. This definition may now be made more explicit by expressing the intensities of shear in the three directions in terms of the dynamic viscosity and the rates of angular deformation in the corresponding directions:

$$\tau_{xy} = \tau_{yx} = \mu \left(\frac{\partial v_y}{\partial x} + \frac{\partial v_x}{\partial y} \right) \quad (65x)$$

$$\tau_{yz} = \tau_{zy} = \mu \left(\frac{\partial v_z}{\partial y} + \frac{\partial v_y}{\partial z} \right) \quad (65y)$$

$$\tau_{zx} = \tau_{xz} = \mu \left(\frac{\partial v_x}{\partial z} + \frac{\partial v_z}{\partial x} \right) \quad (65z)$$

Substitution of these quantities in Eqs. (63) will give

$$(f_s)_x = \mu \left(\frac{\partial^2 v_y}{\partial x \partial y} + \frac{\partial^2 v_x}{\partial y^2} \right) + \mu \left(\frac{\partial^2 v_x}{\partial z^2} + \frac{\partial^2 v_z}{\partial x \partial z} \right) \quad (66x)$$

$$(f_s)_y = \mu \left(\frac{\partial^2 v_x}{\partial y \partial z} + \frac{\partial^2 v_y}{\partial z^2} \right) + \mu \left(\frac{\partial^2 v_y}{\partial x^2} + \frac{\partial^2 v_x}{\partial y \partial x} \right) \quad (66y)$$

$$(f_s)_z = \mu \left(\frac{\partial^2 v_x}{\partial z \partial x} + \frac{\partial^2 v_z}{\partial x^2} \right) + \mu \left(\frac{\partial^2 v_z}{\partial y^2} + \frac{\partial^2 v_y}{\partial z \partial y} \right) \quad (66z)$$

With reference to the close relationship between linear and angular deformation mentioned in Chapter III, the reason for the variation in pressure intensity in the three coordinate directions should now be evident. Just as the difference in tangential stress in any two directions is proportional to the difference in rate of angular deformation in those directions, the difference in pressure intensity in two directions must vary with the difference in rate of linear deformation. Designating by the symbol p the mean pressure intensity at the center of the fluid element, the difference between this mean value and the actual intensity of normal stress may be written as follows for each of the coordinate directions:¹

$$p - p_x = 2\mu \frac{\partial v_x}{\partial x} - \frac{2}{3}\mu \left(\frac{\partial v_x}{\partial x} + \frac{\partial v_y}{\partial y} + \frac{\partial v_z}{\partial z} \right) \quad (67x)$$

$$p - p_y = 2\mu \frac{\partial v_y}{\partial y} - \frac{2}{3}\mu \left(\frac{\partial v_x}{\partial x} + \frac{\partial v_y}{\partial y} + \frac{\partial v_z}{\partial z} \right) \quad (67y)$$

$$p - p_z = 2\mu \frac{\partial v_z}{\partial z} - \frac{2}{3}\mu \left(\frac{\partial v_x}{\partial x} + \frac{\partial v_y}{\partial y} + \frac{\partial v_z}{\partial z} \right) \quad (67z)$$

These expressions are in their most general form, for it is obvious that the divergence of the velocity vector (the terms within parentheses) must be equal to zero under conditions of constant density. In either case the relationships will be found to satisfy the requirement that

$$p = \frac{p_x + p_y + p_z}{3}$$

Retaining, for the present, the divergence terms, substitution of Eqs. (67) in Eqs. (62) will yield

¹ LAMB, "Hydrodynamics," pp. 571-574.

$$(f_p)_x = -\frac{\partial p}{\partial x} + 2\mu \frac{\partial^2 v_x}{\partial x^2} - \frac{2}{3}\mu \frac{\partial}{\partial x} \left(\frac{\partial v_x}{\partial x} + \frac{\partial v_y}{\partial y} + \frac{\partial v_z}{\partial z} \right) \quad (68x)$$

$$(f_p)_y = -\frac{\partial p}{\partial y} + 2\mu \frac{\partial^2 v_y}{\partial y^2} - \frac{2}{3}\mu \frac{\partial}{\partial y} \left(\frac{\partial v_x}{\partial x} + \frac{\partial v_y}{\partial y} + \frac{\partial v_z}{\partial z} \right) \quad (68y)$$

$$(f_p)_z = -\frac{\partial p}{\partial z} + 2\mu \frac{\partial^2 v_z}{\partial z^2} - \frac{2}{3}\mu \frac{\partial}{\partial z} \left(\frac{\partial v_x}{\partial x} + \frac{\partial v_y}{\partial y} + \frac{\partial v_z}{\partial z} \right) \quad (68z)$$

Addition of the components of force due to pressure, weight, and shear in each of the coordinate directions will result in the following essential equations for the force components per unit volume of fluid at any point in a viscous fluid:

$$f_x = -\frac{\partial}{\partial x}(p + \gamma h) + 2\mu \frac{\partial^2 v_x}{\partial x^2} - \frac{2}{3}\mu \left(\frac{\partial^2 v_x}{\partial x^2} + \frac{\partial^2 v_y}{\partial x \partial y} + \frac{\partial^2 v_z}{\partial x \partial z} \right) + \mu \left(\frac{\partial^2 v_y}{\partial x \partial y} + \frac{\partial^2 v_x}{\partial y^2} \right) + \mu \left(\frac{\partial^2 v_x}{\partial z^2} + \frac{\partial^2 v_z}{\partial x \partial z} \right) \quad (69x)$$

$$f_y = -\frac{\partial}{\partial y}(p + \gamma h) + 2\mu \frac{\partial^2 v_y}{\partial y^2} - \frac{2}{3}\mu \left(\frac{\partial^2 v_x}{\partial y \partial x} + \frac{\partial^2 v_y}{\partial y^2} + \frac{\partial^2 v_z}{\partial y \partial z} \right) + \mu \left(\frac{\partial^2 v_z}{\partial y \partial z} + \frac{\partial^2 v_y}{\partial z^2} \right) + \mu \frac{\partial^2 v_y}{\partial x^2} + \frac{\partial^2 v_x}{\partial y \partial x} \quad (69y)$$

$$f_z = -\frac{\partial}{\partial z}(p + \gamma h) + 2\mu \frac{\partial^2 v_z}{\partial z^2} - \frac{2}{3}\mu \left(\frac{\partial^2 v_x}{\partial z \partial x} + \frac{\partial^2 v_y}{\partial z \partial y} + \frac{\partial^2 v_z}{\partial z^2} \right) + \mu \left(\frac{\partial^2 v_x}{\partial z \partial x} + \frac{\partial^2 v_z}{\partial x^2} + \mu \left(\frac{\partial^2 v_x}{\partial y^2} + \frac{\partial^2 v_y}{\partial z \partial y} \right) \right) \quad (69z)$$

From these equations it is quite evident that in viscous flow the existence of a force potential is generally impossible, for there is no quantity whose derivation in a single direction can yield the component of force in that direction.

36. Dissipation of Energy through Viscous Action. Inasmuch as the continuous deformation of a moving fluid is opposed by viscous stresses that vary directly with the rate of deformation, such movement can take place only if energy of flow is expended in doing work; in other words, such a process will involve a continuous transformation of mechanical energy into heat. Further insight into this process may be gained through the following development.

The temporal rate at which work is done by a given force is equal to the product of the force and the velocity at the point of application. Thus, the work done by any component of weight, per unit time and per unit volume of fluid, is simply the unit weight component multiplied by the corresponding velocity

component at the given point. On the other hand, the work done by a direct or tangential stress, per unit time and per unit volume of fluid, is equal to the gradient of the product of the stress intensity and the corresponding component of velocity. The reader may verify this fact by expressing the work done on each face of the fluid element in Fig. 66 as the dimensions of the element approach the infinitesimal. It then follows that the total rate per unit volume at which work is done at any point in a viscous fluid may be written:

$$\begin{aligned}
 & -\gamma \left(\frac{\partial h}{\partial x} v_x + \frac{\partial h}{\partial y} v_y + \frac{\partial h}{\partial z} v_z \right) + \frac{\partial}{\partial x} (-p_x v_x + \tau_{xy} v_y + \tau_{xz} v_z) \\
 & + \frac{\partial}{\partial y} (-p_y v_y + \tau_{yx} v_x + \tau_{yz} v_z) + \frac{\partial}{\partial z} (-p_z v_z + \tau_{zx} v_x + \tau_{zy} v_y)
 \end{aligned}$$

With the exception of the work done by weight, each of these terms is the space derivative of the product of two quantities; after the rules of differential calculus, each term is equal to (1) the derivative of a stress intensity times a velocity plus (2) the derivative of a velocity times a stress intensity. The sum of all terms of type (1), including the work done by weight, expresses the rate at which the unit forces change the kinetic energy of the flow:

$$\begin{aligned}
 & \left[-\frac{\partial}{\partial x} (p_x + \gamma h) + \frac{\partial \tau_{yx}}{\partial y} + \frac{\partial \tau_{zx}}{\partial z} \right] v_x \\
 & + \left[-\frac{\partial}{\partial y} (p_y + \gamma h) + \frac{\partial \tau_{xy}}{\partial x} + \frac{\partial \tau_{zy}}{\partial z} \right] v_y \\
 & + \left[-\frac{\partial}{\partial z} (p_z + \gamma h) + \frac{\partial \tau_{xz}}{\partial x} + \frac{\partial \tau_{yz}}{\partial y} \right] v_z
 \end{aligned}$$

The remaining terms will then be:

$$\begin{aligned}
 & -p_x \frac{\partial v_x}{\partial x} - p_y \frac{\partial v_y}{\partial y} - p_z \frac{\partial v_z}{\partial z} \\
 & + \tau_{xy} \left(\frac{\partial v_y}{\partial x} + \frac{\partial v_x}{\partial y} \right) + \tau_{yz} \left(\frac{\partial v_z}{\partial y} + \frac{\partial v_y}{\partial z} \right) + \tau_{zx} \left(\frac{\partial v_x}{\partial z} + \frac{\partial v_z}{\partial x} \right)
 \end{aligned}$$

Substitution from Eqs. (65) and (67) will yield:

$$\begin{aligned}
 & -p \left(\frac{\partial v_x}{\partial x} + \frac{\partial v_y}{\partial y} + \frac{\partial v_z}{\partial z} \right) - \frac{2}{3} \mu \left(\frac{\partial v_x}{\partial x} + \frac{\partial v_y}{\partial y} + \frac{\partial v_z}{\partial z} \right)^2 \\
 & + 2\mu \left[\left(\frac{\partial v_x}{\partial x} \right)^2 + \left(\frac{\partial v_y}{\partial y} \right)^2 + \left(\frac{\partial v_z}{\partial z} \right)^2 \right] \\
 & + \mu \left[\left(\frac{\partial v_y}{\partial x} + \frac{\partial v_x}{\partial y} \right)^2 + \left(\frac{\partial v_z}{\partial y} + \frac{\partial v_y}{\partial z} \right)^2 + \left(\frac{\partial v_x}{\partial z} + \frac{\partial v_z}{\partial x} \right)^2 \right]
 \end{aligned}$$

Since the divergence of the velocity vector must be zero, regardless of the nature of the acting forces, it is evident that variation of the hydrostatic load can have no effect whatever upon the rate of dissipation of energy. Moreover, owing to the continuity (homogeneity) of the fluid medium, energy loss through so-called "impact" is impossible. Therefore, as shown by the remaining terms of the foregoing expression, only through linear and angular deformation can energy of flow be converted into heat. It follows that the energy of a given flow may remain constant so long as deformation does not take place at any point (refer to the case of the forced vortex in Chapter III), a condition which is possible only if the entire fluid mass is displaced bodily (whether through translation or rotation), or if the fluid is completely at rest.¹

37. Equations of Navier-Stokes. Rearrangement of terms in Eqs. (69) and division by the fluid density yields expressions for the force components per unit mass in the following form:

$$\begin{aligned} \frac{f_x}{\rho} = & -\frac{1}{\rho} \frac{\partial}{\partial x}(p + \gamma h) + \frac{1}{3} \frac{\mu}{\rho} \frac{\partial}{\partial x} \left(\frac{\partial v_x}{\partial x} + \frac{\partial v_y}{\partial y} + \frac{\partial v_z}{\partial z} \right) \\ & + \frac{\mu}{\rho} \left(\frac{\partial^2 v_x}{\partial x^2} + \frac{\partial^2 v_x}{\partial y^2} + \frac{\partial^2 v_x}{\partial z^2} \right) \quad (70x) \end{aligned}$$

$$\begin{aligned} \frac{f_y}{\rho} = & -\frac{1}{\rho} \frac{\partial}{\partial y}(p + \gamma h) + \frac{1}{3} \frac{\mu}{\rho} \frac{\partial}{\partial y} \left(\frac{\partial v_x}{\partial x} + \frac{\partial v_y}{\partial y} + \frac{\partial v_z}{\partial z} \right) \\ & + \frac{\mu}{\rho} \left(\frac{\partial^2 v_y}{\partial x^2} + \frac{\partial^2 v_y}{\partial y^2} + \frac{\partial^2 v_y}{\partial z^2} \right) \quad (70y) \end{aligned}$$

$$\begin{aligned} \frac{f_z}{\rho} = & -\frac{1}{\rho} \frac{\partial}{\partial z}(p + \gamma h) + \frac{1}{3} \frac{\mu}{\rho} \frac{\partial}{\partial z} \left(\frac{\partial v_x}{\partial x} + \frac{\partial v_y}{\partial y} + \frac{\partial v_z}{\partial z} \right) \\ & + \frac{\mu}{\rho} \left(\frac{\partial^2 v_z}{\partial x^2} + \frac{\partial^2 v_z}{\partial y^2} + \frac{\partial^2 v_z}{\partial z^2} \right) \quad (70z) \end{aligned}$$

Again recognizing the fact that the divergence of the velocity vector must be zero, the second term at the right side of each equation may be dropped. Then by writing the last term in shorthand fashion and replacing the force per unit mass by the equivalent expression for acceleration, one obtains these general relationships:

¹ Refer to LAMB, "Hydrodynamics," pp. 579-581, for a more comprehensive treatment than has been deemed necessary in the foregoing discussion.

$$\frac{\partial v_x}{\partial t} + v_x \frac{\partial v_x}{\partial x} + v_y \frac{\partial v_x}{\partial y} + v_z \frac{\partial v_x}{\partial z} = -\frac{1}{\rho} \frac{\partial}{\partial x}(p + \gamma h) + \frac{\mu}{\rho} \nabla^2 v_x \quad (71x)$$

$$\frac{\partial v_y}{\partial t} + v_x \frac{\partial v_y}{\partial x} + v_y \frac{\partial v_y}{\partial y} + v_z \frac{\partial v_y}{\partial z} = -\frac{1}{\rho} \frac{\partial}{\partial y}(p + \gamma h) + \frac{\mu}{\rho} \nabla^2 v_y \quad (71y)$$

$$\frac{\partial v_z}{\partial t} + v_x \frac{\partial v_z}{\partial x} + v_y \frac{\partial v_z}{\partial y} + v_z \frac{\partial v_z}{\partial z} = -\frac{1}{\rho} \frac{\partial}{\partial z}(p + \gamma h) + \frac{\mu}{\rho} \nabla^2 v_z \quad (71z)$$

Known as the equations of Navier-Stokes, these differ from the Euler equations of acceleration only through the addition of the operator $\mu/\rho \nabla^2$, which vanishes, of course, as the viscosity approaches the limit zero. Since these are exact mathematical statements of dynamic conditions within a viscous fluid, they may be expected to apply correctly to every type of viscous flow.

Nevertheless, it has been shown that the very general character of the Euler equations quite limits their usefulness in specific problems unless the nature of such problems either permits considerable simplification or provides an additional relationship which incorporates in convenient form the essence of these basic statements. Although such a relationship was often available in the form of a velocity potential, the reader will realize that the existence of a velocity potential depends entirely upon the absence of rotation, with the possible exception of isolated vortex lines. Not only are the Navier-Stokes equations of more complex form than those of Euler, but a glance at the additional terms will show that irrotational motion of a viscous fluid is generally out of the question unless fluid and boundaries move bodily through space. Indeed, the fact that in viscous flow the velocity of the fluid at a boundary must be identical with the velocity of the boundary itself (quite contrary to the conditions of fundamental hydromechanics) should be sufficient indication of this important fact.

With the convenient introduction of the velocity potential generally impossible, it is evident that actual application of the Navier-Stokes equations will depend entirely upon the extent to which these equations may be simplified for specific problems. While in fundamental hydromechanics dynamic conditions were of primary interest, it is evident that in an elementary study of viscous phenomena one must perforce consider dynamic effects negligible and concentrate upon the investigation of viscous resistance.

CHAPTER VIII

PROBLEMS IN LAMINAR MOTION

38. Steady Flow between Parallel Boundaries. Strictly speaking, the assumption of steady movement of a viscous fluid precludes any possibility of local fluctuation in velocity; in the absence of such local variation, the fluid will, in effect, move in layers—or laminae—whence the expression “laminar flow.” Such will generally be the case if a characteristic flow parameter composed of the product of mean velocity, density, and the spacing of the boundaries, divided by the dynamic viscosity of the fluid (*i.e.*, a Reynolds number, $R = V\rho L/\mu$), has a magnitude not greater than a certain limiting value which is roughly of the order of 10^3 . Generally speaking, this requires that the velocity of flow and the spacing of the boundaries be relatively small.

Consideration of steady laminar flow confined in the z direction by closely spaced parallel surfaces will permit extensive simplification of the basic Navier-Stokes equations. Since the local acceleration in each of the coordinate directions is then zero, and since the velocity vector has no component in the z direction, the following relationships must hold:

$$\begin{aligned}v_x \frac{\partial v_x}{\partial x} + v_y \frac{\partial v_x}{\partial y} &= -\frac{1}{\rho} \frac{\partial}{\partial x}(p + \gamma h) + \frac{\mu}{\rho} \left(\frac{\partial^2 v_x}{\partial x^2} + \frac{\partial^2 v_x}{\partial y^2} + \frac{\partial^2 v_x}{\partial z^2} \right) \\v_x \frac{\partial v_y}{\partial x} + v_y \frac{\partial v_y}{\partial y} &= -\frac{1}{\rho} \frac{\partial}{\partial y}(p + \gamma h) + \frac{\mu}{\rho} \left(\frac{\partial^2 v_y}{\partial x^2} + \frac{\partial^2 v_y}{\partial y^2} + \frac{\partial^2 v_y}{\partial z^2} \right) \\0 &= -\frac{1}{\rho} \frac{\partial}{\partial z}(p + \gamma h)\end{aligned}$$

A very important conclusion may be drawn from inspection: The pressure is hydrostatically distributed in a direction normal to the boundaries; as a result, at any point the gradient of the quantity $(p + \gamma h)$ in either of the remaining two directions is completely independent of the actual magnitude of z . In other words, however much the velocity may vary from one boundary to another, the distribution of $(p + \gamma h)$ must be the same in

every plane parallel to the boundary surfaces. It is then only reasonable to conclude that the pattern of stream lines in the xy plane will not vary across the flow, despite change in the magnitude of the velocity itself; that is to say, v will depend upon z in magnitude, but not in direction, a conclusion that is vindicated in the following development.

The fact has already been mentioned that the actual velocity of flow at any stationary boundary must be zero, owing to the viscous qualities of the fluid. It then follows that the magnitude of the velocity must vary rapidly with distance from the boundary, this velocity gradient, for a given rate of flow, being inversely proportional to the distance from one boundary to the other. If the boundaries are very close to one another, the gradient of the velocity in either of the other two coordinate directions will be relatively insignificant, under which conditions the terms $\partial v_x/\partial x$, $\partial v_x/\partial y$, $\partial v_y/\partial x$, and $\partial v_y/\partial y$, and the corresponding second derivatives, may safely be dropped from the foregoing equations. These will then reduce to

$$\begin{aligned}\frac{\partial}{\partial x}(p + \gamma h) &= \mu \frac{\partial^2 v_x}{\partial z^2} \\ \frac{\partial}{\partial y}(p + \gamma h) &= \mu \frac{\partial^2 v_y}{\partial z^2}\end{aligned}$$

Each of these may be integrated with respect to z , whereupon

$$\begin{aligned}z \frac{\partial}{\partial x}(p + \gamma h) &= \mu \frac{\partial v_x}{\partial z} + C_1 \\ z \frac{\partial}{\partial y}(p + \gamma h) &= \mu \frac{\partial v_y}{\partial z} + C_2\end{aligned}$$

If the center of coordinates is located midway between the boundaries, when $z = 0$, $\partial v_x/\partial z = 0 = \partial v_y/\partial z$, whence

$$C_1 = 0 = C_2.$$

A second integration then yields:

$$\begin{aligned}v_x &= \frac{z^2}{2\mu} \frac{\partial}{\partial x}(p + \gamma h) + C_3 \\ v_y &= \frac{z^2}{2\mu} \frac{\partial}{\partial y}(p + \gamma h) + C_4\end{aligned}$$

If the boundaries lie the distance $2b$ apart, when $z = \pm b$, $v_x = 0 = v_y$; hence,

$$C_3 = -\frac{b^2}{2\mu} \frac{\partial}{\partial x}(p + \gamma h), \quad \text{and} \quad C_4 = -\frac{b^2}{2\mu} \frac{\partial}{\partial y}(p + \gamma h).$$

Finally,

$$v_x = \frac{z^2 - b^2}{2\mu} \frac{\partial}{\partial x}(p + \gamma h) \quad (72x)$$

$$v_y = \frac{z^2 - b^2}{2\mu} \frac{\partial}{\partial y}(p + \gamma h) \quad (72y)$$

The curves of velocity distribution indicated by these parallel equations are parabolic in form (refer to Fig. 67), the velocity components having a maximum value at the point $z = 0$:

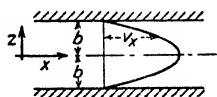


FIG. 67.—Laminar flow between parallel boundaries.

$$(v_x)_{\max} = -\frac{b^2}{2\mu} \frac{\partial}{\partial x}(p + \gamma h); \quad (73x)$$

$$(v_y)_{\max} = -\frac{b^2}{2\mu} \frac{\partial}{\partial y}(p + \gamma h) \quad (73y)$$

It follows from the geometry of the parabola that the mean component in either direction will be two-thirds the maximum, which result may also be obtained by integrating across the section (thus yielding the unit rate of discharge q) and dividing by the spacing of the boundaries; or, more simply,

$$V_x = \frac{1}{b} \int_0^b v_x dz = -\frac{b^2}{3\mu} \frac{\partial}{\partial x}(p + \gamma h) \quad (74x)$$

$$V_y = \frac{1}{b} \int_0^b v_y dz = -\frac{b^2}{3\mu} \frac{\partial}{\partial y}(p + \gamma h) \quad (74y)$$

Evidently the negative gradient of the sum $(p + \gamma h)$, indicating the rate at which energy is lost through viscous shear, will be directly proportional to the dynamic viscosity and to the component of mean velocity in the corresponding direction, and inversely proportional to the square of the spacing of the boundaries. Thus, in the direction of the mean velocity vector,

$$-\frac{\partial}{\partial s}(p + \gamma h) = 3 \frac{V\mu}{b^2} \quad (75)$$

A glance at Eqs. (72) will suffice to show that under these boundary conditions the velocity components in the xy plane are the derivatives of a function of two-dimensional space; that is, there exists a velocity potential having the form

$$\phi_z = \frac{(z^2 - b^2)(p + \gamma h)}{2\mu} \quad (76)$$

the subscript restricting the velocity potential to a single plane the distance z from the plane of the axes x and y . Moreover, Eqs. (74) and (75) indicate the existence of another velocity potential for the mean flow:

$$\phi_m = -\frac{b^2(p + \gamma h)}{3\mu} \quad (77)$$

While this would appear to contradict the general statement made on page 149, it will be recalled that the foregoing equations were derived by assuming negligible velocity gradients in the x and y directions. In other words, a velocity potential can exist in viscous flow only if there is no appreciable acceleration in the direction of motion.

In the latter part of the last century there was developed in England by Hele-Shaw¹ a method of simulating stream-line patterns of two-dimensional potential motion, as discussed in Chapter V, through application of the foregoing principles of viscous flow between parallel plates. It will be recalled that any potential flow pattern depends solely upon the geometrical form of the boundaries, regardless of the acting forces. Hele-Shaw took advantage of this fact by inserting various boundary profiles between closely spaced glass plates, passing a low flow of water through the system, and coloring an arbitrary number of stream filaments by injecting dye at equal intervals across the entrance (a schematic diagram of the apparatus is shown in Fig. 68). By this means he was able to reproduce not only the patterns of potential flow around elementary profiles, but also those of various source-sink combinations. Such patterns are identical with those determined analytically for similar boundary conditions, with the exception of a slight distortion in the neighborhood of the boundary itself. But since the distance the zone of boundary influence extends into the flow is approximately equal to the spacing of the plates, it is obvious that this effect may be reduced as much as desired simply by bringing the plates closer together.

¹ HELE-SHAW, H. J. S., Investigation of the Nature of the Surface Resistance of Water and of Stream-line Motion under Certain Experimental Conditions, *Trans. Inst. Naval Architects*, vol. 40, 1898.

Since these elementary patterns may easily be obtained analytically, a more practical use of the apparatus lies in the determination of flow patterns in cases too complex to handle through conformal transformation, in particular for conditions of flow through, rather than around, fixed boundaries. In this way, flow patterns have been obtained for discharge through siphons, over spillways (prior knowledge of the form of the free surface then being essential), and even in the pervious soil formations beneath hydraulic structures.

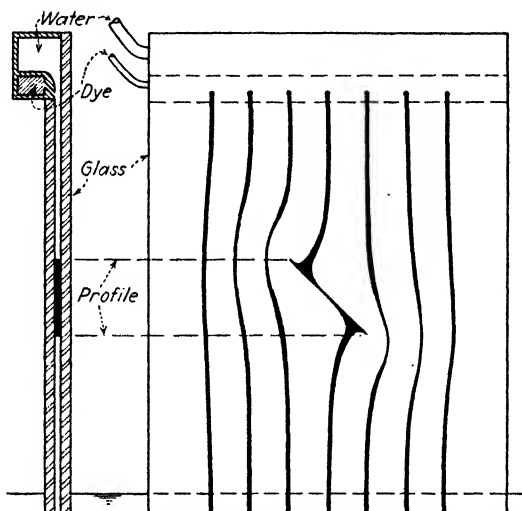


FIG. 68.—Hele-Shaw apparatus for visual study of potential flow.

Variation in the sum $(p + \gamma h)$ with distance is fundamentally a measure of the rate at which energy of flow is dissipated in viscous shear, from which it follows that if this quantity shows no variation in the direction of motion, then flow as such will not occur. For instance, if the potential energy is made constant in Eqs. (72) or (74), the velocity at every point must become zero.

Assume now that the only motion of the enclosed fluid is that resulting from shearing stresses due to relative displacement of the two boundaries. Since there can be no change in $(p + \gamma h)$ in any direction, conditions of equilibrium require that the intensity of shear be the same at every point—in other words, the velocity gradient with respect to z [refer to Eqs. (65)] must be a

constant for any values of x and y . If the upper boundary is moved with the velocity v_0 in the x direction, then at the moving boundary $v_x = v_0$, and at the fixed boundary $v_x = 0$, whence,

$$v_x = v_0 \frac{b+z}{2b} \quad (78)$$

The velocity now varies linearly between the plates, and the energy dissipated in the form of heat comes from the work done in moving the one boundary. The total force that must be exerted is simply the product of the area of either boundary and the intensity of shear caused by the relative motion:

$$F = \frac{A \mu v_0}{2b} \quad (79)$$

Indeed, this simple principle is often used as a means of determining fluid viscosity, through measurement of the force necessary to displace two plates in a given fluid at a known relative velocity. These plates are most conveniently arranged in the form of nested cylinders (the Couette apparatus), one of which is supported on a torsion balance and the other rotated at a known angular speed. Owing to the small clearance between the cylinders, the relatively great magnitude of the radius of curvature

of the boundaries often permits treatment of the motion as approximately planar.

It must be remarked, however, that an exact solution must include the effects of curvature and centripetal acceleration; thus, if the inner cylinder is rotated, the higher velocities at the inner boundary may lead to instability of flow; on the other hand,

rotation of the outer cylinder will always have a stabilizing influence.¹

If conditions described by Eqs. (72) and (78) are combined, in the x direction the resulting velocity distribution will have the form

$$v_x = v_0 \frac{b+z}{2b} + \frac{z^2 - b^2}{2\mu} \frac{\partial}{\partial x}(p + \gamma h) \quad (80)$$

¹ TAYLOR, G. I., Stability of a Viscous Fluid Contained between Two Boundaries, *Phil. Trans.*, A, vol. 223, 1922.

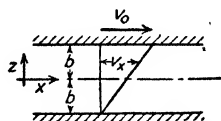


FIG. 69.—Velocity distribution resulting from the motion of one boundary parallel to another.

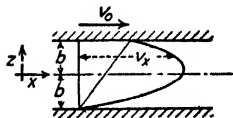


FIG. 70.—Laminar flow between two parallel boundaries, one of which is in motion.

As shown in Fig. 70, the parabolic distribution curve is displaced by an amount varying directly with the velocity of the moving boundary and with the relative distance from the boundary at rest. The mean velocity component in the x direction will now have the magnitude

$$V_x = \frac{v_0}{2} - \frac{b^2}{3\mu} \frac{\partial}{\partial x}(p + \gamma h) \quad (81)$$

while it should be evident that the maximum velocity no longer occurs midway between the boundaries.

39. Elements of Lubrication. Theories of bearing lubrication are so closely related to other problems of laminar motion as to warrant a brief discussion in this text, despite their limited application to general hydraulic engineering. No attempt will be made to present more than a partial review of the essential methods of approach, the sole endeavor being to correlate the characteristics of viscous flow in bearings with the basic principles of fluid motion.

The layman's conception of lubrication would probably undergo a radical change were he to witness the operation of a small mechanical model produced by a prominent manufacturing concern. This model consists of a polished circular disk mounted on a vertical shaft and capable of rotating upon several polished rocker plates serving as horizontal bearings. The shaft and disk are electrically insulated from the mountings of the rocker bearings, but placed in series with a battery and a small lamp in such manner that the latter will glow when the disk is actually in contact with the bearings that support it. If the disk is set in motion by spinning the shaft, the lamp will at once cease to glow; the apparatus has been constructed so carefully that the rotating disk will lose speed very slowly, yet the lamp will not light again until motion is almost completely at an end—which thus indicates that the bearings do not come in contact with the disk so long as appreciable movement occurs.

The observer can only conclude that air, being a viscous fluid, may on occasion serve as a very capable lubricant, and that so long as a lubricant functions properly there will be no direct contact between properly finished bearing surfaces. It is in this connection that the mathematical principles of lubrication are of tremendous importance, for through them may be determined the degree to which a bearing surface must be finished, the clear-

ances that must be allowed, the point of application of the resultant force, and the viscosity and rate of flow of the lubricant that will prevent both metal-to-metal friction and excessive heating through viscous shear.

From the foregoing discussion of flow between parallel boundaries, the reader will realize that under uniform conditions the pressure gradient must remain constant in the direction of motion—that is, the second derivative of the pressure intensity must be zero, regardless of distance along the x axis [refer to Eq. (80)]. If the fluid movement results entirely from the displacement of one boundary, the pressure gradient will then be zero. It then follows that if one boundary is of finite length and the fluid is at atmospheric pressure at either end, no resultant force normal to the boundaries may be exerted as a result of the movement. In other words, parallel bearing surfaces are incapable of supporting any load unless they are actually in physical contact with one another; it is obvious that such contact would defeat the purpose of lubrication.

Consider now a plane boundary of finite length which, similar to the rocker bearings in the model already described, may be inclined slightly with respect to a horizontal boundary a short distance above, as shown in Fig. 71. It must be noted that the proportions of the illustration are necessarily distorted, for both the mean spacing and the difference in spacing at the two ends are extremely small in comparison with the length of the lower plate. Equation (80) or (81), therefore, will describe the conditions of flow with negligible error if the upper boundary is moved to the right with the constant velocity v_0 . The lower boundary is so inclined that the spacing decreases in the direction of motion, the distance between the boundaries for a given value of x being expressed by the relationship

$$b = b_1 - \frac{x}{L} (b_1 - b_2) = b_1 - \alpha x \quad (82)$$

If h is assumed constant, integration over the cross section of flow will yield the rate of discharge q through a section of unit width:

$$q = \int_0^b v \, dz = \frac{v_0 b}{2} - \frac{\partial p}{\partial x} \frac{b^3}{12\mu}$$

Introducing Eq. (82) and treating the pressure gradient as the dependent variable

$$\frac{\partial p}{\partial x} = \frac{6 \mu v_0}{(b_1 - \alpha x)^2} - \frac{12 \mu q}{(b_1 - \alpha x)^3}$$

Then integrating with respect to x ,

$$p = \frac{6 \mu v_0}{\alpha (b_1 - \alpha x)} - \frac{12 \mu q}{2\alpha (b_1 - \alpha x)^2} + C$$

The constant C , as well as the constant unit discharge q , may be determined from the fact that the pressure intensity must be atmospheric (or, more generally, $p = p_0$) at $x = 0$ and at $x = L$; thus,

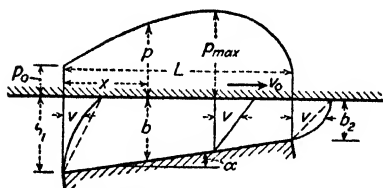


FIG. 71.—Distribution of pressure and velocity in a lubricated bearing.

$$C = p_0 - \frac{6 \mu v_0}{\alpha b_1} + \frac{12 \mu q}{2\alpha b_1^2}$$

$$q = \frac{v_0 b_1 b_2}{b_1 + b_2} \quad (83)$$

The pressure intensity at any point along the boundary may then be expressed as follows:

$$p = p_0 + \frac{6 \mu v_0 x (L - x) (b_1 - b_2)}{L b^2 (b_1 + b_2)} \quad (84)$$

The resulting curve of pressure distribution is shown schematically in Fig. 71. It will be noted that the maximum ordinate lies to the right of the midpoint of the bearing, its position being found by placing equal to zero the derivative of p with respect to x :

$$b = \frac{2q}{v_0} \quad \text{for which} \quad x = \frac{b_1 L}{b_1 + b_2}$$

Integration of the pressure intensity over the length L yields the following pertinent expression for the resultant normal force per unit width of bearing:¹

$$P = \frac{6 \mu v_0 L^2}{b_2^2 (c - 1)^2} \left(\ln c - 2 \frac{c - 1}{c + 1} \right) \quad (85)$$

in which c represents the ratio b_1/b_2 . It is evident from this equation that P will have a value of zero when the two surfaces

¹ Intermediate steps in this and succeeding developments may be found in KAUFMANN, W., "Hydromechanik," vol. 2, Springer, Berlin, 1934, from which the foregoing derivations of lubrication equations have been taken.

are parallel, and will become negative once c is less than unity. Its maximum positive magnitude may be found by setting equal to zero its derivative with respect to c , under which conditions c is approximately equal to 2.2 and

$$P_{\max} = \frac{0.41 \mu v_0 L^2}{b_m^2} \quad (86)$$

in which b_m is the mean spacing of the boundaries. Of great importance is the fact that the point of action of this resultant force is not at the midpoint of the bearing. A trial computation will convince the reader of the tremendous loads which may be supported by a thin film of oil once the bearing surfaces are given their proper slope.

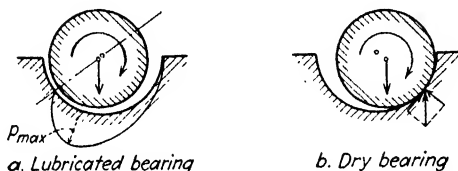


FIG. 72.—Displacement of rotating shaft with and without lubrication.

By expressing the intensity of shear along the upper boundary as a function of the velocity gradient and integrating over the distance L , an equation may be obtained for the tangential force per unit width that resists the motion of the upper boundary; this will be, for the case of maximum normal force,

$$T = -1.21 \frac{\mu v_0 L}{b_m} \quad (87)$$

The foregoing equations for the forces involved in the two-dimensional problem of lubrication merit careful study, in that they indicate—at least qualitatively—the characteristics of any lubricated bearing. Nevertheless, quantitative solution of actual bearing problems requires considerable extension of this development, for seldom may a case be regarded as truly two-dimensional. For instance, plane bearings are of finite width as well as of finite length, and generally involve rotation about a central axis, as in the model first described; moreover, lubrication of cylindrical bearings entails radial displacement of the shaft, as shown in Fig. 72 (it is to be noted that the resultant action of normal and tangential stresses produces a displacement in the

opposite direction from that caused by mechanical friction). For further study of this specialized branch of fluid mechanics, the reader must turn to other sources.¹

40. Uniform Flow in Circular Tubes. The basic equations of Navier-Stokes may be simplified still further in the treatment of steady, laminar motion in circular tubes of uniform diameter. Assuming that the x axis is coincident with the center line of the tube and positive in the direction of flow, it follows that v_y and v_z are both zero, and that v_x is identical with the velocity vector; moreover, the velocity remains constant in the x direction, owing to the uniformity of the flow section. Under these conditions,

$$\begin{aligned}\frac{\partial}{\partial x}(p + \gamma h) &= \mu \left(\frac{\partial^2 v_x}{\partial y^2} + \frac{\partial^2 v_x}{\partial z^2} \right) \\ \frac{\partial}{\partial y}(p + \gamma h) &= 0 \\ \frac{\partial}{\partial z}(p + \gamma h) &= 0\end{aligned}$$

Evidently, the pressure intensity will vary in the axial direction as the result of viscous shear and change in elevation, but it must be hydrostatically distributed over every normal cross section of the flow; this conclusion cannot be too highly stressed.

Because of the symmetry of the flow about the longitudinal axis, the flow picture in every plane through the axis must be the same. It is therefore convenient to change from the rectangular to the cylindrical coordinate system, in which a point in the flow is established by the distance x along the central axis from some arbitrary zero point, by the normal distance r from this axis, and by the central angle θ from some arbitrary axial plane.

As may be seen by expressing the equilibrium of viscous, pressure, and gravitational forces upon a fluid element having the volume $dx dr r d\theta$, the equations of Navier-Stokes in cylindrical coordinate notation, simplified for the problem now under consideration, will have the form:

$$\begin{aligned}\frac{\partial}{\partial x}(p + \gamma h) &= \frac{\mu}{r} \frac{\partial}{\partial r} \left(r \frac{\partial v}{\partial r} \right) \\ \frac{\partial}{\partial r}(p + \gamma h) &= 0 = \frac{\partial}{r \partial \theta}(p + \gamma h)\end{aligned}$$

¹ THOMSEN, G. C., "The Practice of Lubrication," McGraw-Hill Book Company, Inc., 3d ed., 1937; or HERSEY, M. D., "Theory of Lubrication," John Wiley & Sons, Inc., 1936.

As in the case of flow between parallel boundaries, these may be integrated directly to provide the distribution of velocity across the section of flow. However, the same result may be obtained in a more graphic way by proceeding directly from the relationship

$$\tau = \mu \frac{\partial v}{\partial y} \quad (88)$$

in which y differs from r only in that it is measured from the flow boundary rather than from the longitudinal axis. As has already been noted, the potential energy may vary only in the direction of flow, and by an amount directly proportional to the viscous resistance to motion. Thus the longitudinal force per unit volume, $-\frac{\partial}{\partial x}(p + \gamma h)$, multiplied by the volume of any isolated portion of the flow, must equal the total shearing force exerted upon the surface of that volume. If this isolated portion of the flow is bounded by the walls of the tube (where $r = r_0$ and $\tau = \tau_0$) and by two planes normal to the axis and the distance L apart,

$$\pi r_0^2 L \frac{\partial}{\partial x}(p + \gamma h) = -2 \pi r_0 L \tau_0$$

and

$$\tau_0 = -\frac{r_0}{2} \frac{\partial}{\partial x}(p + \gamma h) \quad (89)$$

Since the potential energy per unit volume is constant over any normal section, a similar expression must hold for any coaxial cylinder of fluid:

$$\tau = -\frac{r}{2} \frac{\partial}{\partial x}(p + \gamma h) \quad (90)$$

Hence,

$$\tau = \tau_0 \frac{r}{r_0} = \tau_0 \left(1 - \frac{y}{r_0}\right) \quad (91)$$

an equation of basic importance.

From Eqs. (88) and (91),

$$\mu \frac{\partial v}{\partial y} = -\mu \frac{\partial v}{\partial r} = \tau_0 \frac{r}{r_0}$$

which becomes, through integration,

$$v = -\frac{\tau_0 r^2}{2 \mu r_0} + C$$

At the wall of the tube the velocity of flow must be zero, whence

$$C = \frac{\tau_0 r_0}{2\mu}$$

The distribution of the velocity will then be

$$v = \frac{\tau_0}{2\mu r_0} (r_0^2 - r^2) \quad (92)$$

As this equation is evidently that of a paraboloid of revolution, symmetrical about the longitudinal axis, the maximum velocity of flow may be found by setting r equal to zero:

$$v_{\max} = \frac{\tau_0 r_0}{2\mu} = -\frac{r_0^2}{4\mu} \frac{\partial}{\partial x}(p + \gamma h)$$

Similarly, one may derive an expression for the rate of discharge through the tube by integrating the velocity over the entire cross section of flow:

$$Q = \int_0^{r_0} v 2\pi r dr = \frac{\pi r_0^4 \tau_0}{4\mu}$$

Expressed in terms of the diameter and the potential gradient, this will have the form

$$Q = -\frac{\pi D^4}{128\mu} \frac{\partial}{\partial x}(p + \gamma h) \quad (93)$$

and division by the area of the cross section will then yield an expression for the mean velocity of flow:

$$V = \frac{Q}{A} = -\frac{D^2}{32\mu} \frac{\partial}{\partial x}(p + \gamma h) \quad (94)$$

As may also be seen from the geometry of the paraboloid of revolution, the mean velocity is exactly one-half the maximum. Finally, upon rewriting Eq. (94), a fundamental relationship is obtained for the rate of energy loss in steady, laminar flow through a uniform circular section:

$$-\frac{\partial}{\partial x}(p + \gamma h) = 32 \frac{\mu V}{D^2} \quad (95)$$

Equation (95) states that the rate of loss of potential energy is directly proportional to the dynamic viscosity and the first power of the mean velocity, and inversely proportional to the

area of the cross section. These essential facts were discovered independently by Hagen and by Poiseuille, shortly before the middle of the nineteenth century, through experiments on capillary tubes.

41. Percolation. That phase of laminar motion which is probably of greatest importance to hydraulic engineers involves the passage of water through pervious material—whether in the relatively simple sand filters of sanitary installations, or in the more complex soil formations underlying hydraulic structures,¹ or even in the materials of the structures themselves. In any case, the interstices of the pervious matter form countless little con-

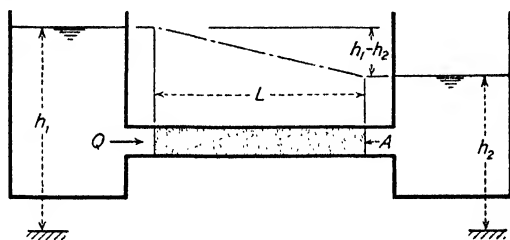


FIG. 73.—Percolation through a uniform column of pervious material.

duits of ever-changing section; but these tiny channels are so complex and innumerable that any attempt to treat each as an individual—even if a typical one could be imagined—would be quite futile. It thus becomes essential to disregard the devious course of each fluid passage, and to look upon the pervious mass simply as a space through which the fluid moves. The impervious boundaries then define the limits of the movement, and the effective cross section of flow is determined by the area enclosed by these boundaries without regard to that portion of the area actually occupied by the grains of solid matter.

Consider, for instance, a tube filled with sand and connecting two tanks of water of unequal surface elevation (Fig. 73). If the sand is relatively fine and if the difference in pressure intensity is not excessive between the beginning and end of the sand column, not only should the motion of the fluid through the interstices be laminar, but the rate of discharge Q through the column,

¹ For a general treatment of percolation through soils the reader is referred to NEMÉNYI, P., "Wasserbauliche Strömungslehre," Johann Ambrosius Barth, Leipzig, 1933; and to TOLMAN, C. F., "Ground Water," McGraw-Hill Book Company, Inc., 1937.

divided by the cross-sectional area of the tube, will yield an effective velocity that is exceedingly small. Indeed, the magnitude of the effective kinetic energy, proportional to the square of this small quantity, is quite negligible, so that the effective energy of flow may safely be considered entirely potential. That is, since the velocity head may be ignored, the total head must consist wholly of pressure head and elevation:

$$E_w = \frac{p}{\gamma} + h$$

The reader has already seen that in laminar flow the rate of energy loss (indicated by the slope of the energy line) varies directly with the first power of the mean velocity across the actual flow section. Evidently, the ratio of the mean velocity through an average interstice to the effective velocity for the cross section of the tube will depend entirely upon the characteristics of the given pervious material, and owing to the fineness of this material the ratio will remain essentially the same from one section to another. Hence, the effective velocity of flow must also be directly proportional to the difference between the surface elevations in the two tanks and inversely proportional to the length of the soil column. Introducing the factor k as the coefficient of proportionality,

$$V = k \frac{h_1 - h_2}{L} \quad \text{and} \quad Q = kAS \quad (96)$$

in which $\frac{h_1 - h_2}{L} = S$, the slope of the energy line. Evidently k must have the dimension of a velocity, which relegates it to the class of dimensional coefficients, varying in magnitude from one dimensional system to another. This factor is commonly known as the permeability of the given material.

Obviously, such a coefficient is not alone a function of material characteristics, which its name implies, for it must also vary with the reciprocal of the dynamic viscosity of the fluid. With regard to properties of the material, it will depend in magnitude upon the grading, the form and diameter of the average grain, and the degree of compaction under flow conditions. Determination of k still depends upon experimental measurement¹ or the use of

¹ BAKHMETEFF, B. A., and FEODOROFF, N. V., Flow through Granular Media, *Trans. A. S. M. E., Applied Mechanics Division*, vol. 4, no. 3, p. A-97, 1937.

unsatisfactory empirical relationships, for though it is a simple matter to introduce μ as a separate variable and thus make k a true permeability coefficient dependent upon material properties alone, as yet no one has succeeded in the analytical derivation of its functional relationship with these properties.

If the boundaries of flow are not straight and uniformly spaced, as in the foregoing illustration, but generally curved and non-parallel, it should be apparent that the resistance to flow will still be basically the same. However, the effective velocity no longer represents a mean over an appreciable cross section, for it will now vary in magnitude and direction from one point to another (and from instant to instant, if the flow is an unsteady one). Still proportional to the factor k , this velocity vector will now depend in magnitude and direction upon the rate of change of the total head E_w as a general function of space and time. Evidently E_w must have the maximum gradient in the direction of flow s , whence, for steady motion,

$$v = -k \frac{\partial E_w}{\partial s} \quad (97)$$

Furthermore, since the total head is generally a function of three-dimensional space, the components of the effective velocity vector may be written as follows:

$$v_x = -k \frac{\partial E_w}{\partial x}; \quad v_y = -k \frac{\partial E_w}{\partial y}; \quad v_z = -k \frac{\partial E_w}{\partial z} \quad (98)$$

As the reader will recall, if the velocity is the space derivative of a continuous space function, then the flow must be a potential one; in this case the velocity potential is simply

$$\phi = -kE_w = -k \left(\frac{p}{\gamma} + h \right) \quad (99)$$

This fact at once opens the way for a graphical solution of a multitude of percolation problems, in particular if the flow is purely a two-dimensional one. For given geometrical boundary conditions, construction of a flow net will yield a comprehensive picture of pressure and velocity distribution, the scale of which depends only upon the total loss of head and the magnitude of k for the given fluid viscosity and the given soil conditions.

Figure 74 shows, for example, a typical problem involving seepage through a pervious stratum of sand underlying a low

dam. The orthogonal lines of the flow net represent lines of constant potential head, the loss of head between each successive pair of lines being constant. The stream lines indicate the direction of the velocity vector at every point and, relatively speaking, the effective lengths of the paths the fluid particles must travel. Owing to the square construction of the net, the magnitude of the effective velocity will vary inversely with the sides of the squares—this approximate relationship becoming exact as the squares approach the infinitesimal.

The slope of the energy line at any point may now be replaced, for all practical purposes, by the change in head from one poten-

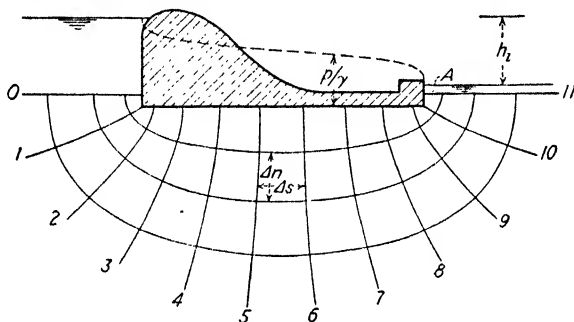


FIG. 74.—Determination of pressure distribution due to seepage under a masonry dam.

tial line to the next divided by the spacing of potential lines at that point: $S = -\Delta E_w / \Delta s$. Thus, if there are N_s divisions of any stream line in the net, and if the total loss of head is equal to $h_1 - h_2 = h_t = -\Sigma \Delta E_w$, the loss between each pair of orthogonal lines will be $-\Delta E_w = h_t / N_s$. The latter fraction, multiplied by k , is equal to the change in velocity potential $\Delta \phi$, which, divided by the distance between potential lines Δs , in turn is equal to the magnitude of the velocity in the given region: $v = \Delta \phi / \Delta s = k h_t / N_s \Delta s$. But since the spacing of stream lines and the spacing of potential lines are identical at any point ($\Delta s = \Delta n$), the quantity $k h_t / N_s$ must also equal the rate of discharge (per unit width of effective flow section) between any neighboring pair of stream lines; that is,

$$\Delta q = v \Delta n = k \frac{h_t}{N_s} \frac{\Delta n}{\Delta s} = k \frac{h_t}{N_s} \quad (100)$$

Thus the total rate of discharge through the sand stratum

is found by multiplying this ratio by N_n , the number of parts into which the stream lines divide any line of constant potential head, and by b , the width of the stratum. This relationship will then be as follows:

$$Q = kb \int^n v_s dn = -kb \int^n \frac{\partial E_w}{\partial s} dn \approx kb h_i \frac{N_n}{N_s} \quad (101)$$

The approximate expression at the right, of course, becomes more exact as the divisions in the flow net are increased in number.

Comparison of Eq. (99) with expressions developed in Chapter II for the force potential will show that the effective velocity of percolation is directly proportional to the force exerted by the flow upon the pervious material. If the velocity vector has a downward direction, the flow tends to cause further compaction of the material. If flow is upward, on the other hand, the opposite effect is produced; and unless the material is heavy (or cohesive) enough to withstand such uplift, the phenomenon known as piping will take place, whereby the downstream portion of the material is carried out by the flow. Danger points of this nature are generally marked by excessive concentration of the flow lines, for the smaller the relative spacing in any locality, the greater the local velocity will be—and hence the greater the force tending to move the material. For example, a condition such as that at point *A* in Fig. 74 must be avoided by more careful design, or else the soil must be protected by a layer of rocks that are individually heavy enough to remain in place, fine enough to form an effect blanket for the underlying material, and yet coarse enough to offer little additional resistance to flow.

So long as the soil particles are reasonably round and uniformly deposited, the permeability factor k will be independent of direction. Appreciable stratification, however, or the presence of flat grains deposited in parallel fashion, will result in a lower resistance to flow in one direction (generally the horizontal) than in another, and hence variation of the quantity kE_w with space is no longer dependent solely upon the form of the impermeable boundaries. Under such circumstances the flow net will be deformed, since the spacing of the stream lines—for a given loss in potential—must then change inversely with k . Similar

conditions are encountered at the boundary of two sediments of different permeability, in which region there is a sharp discontinuity in the energy gradient. The solution of such problems simply through adjustment of the stream lines in accordance with assumed or measured variation of k requires considerable experience; where experience is lacking, model studies in a glass-walled tank are of great value, for the stream lines in the artificially deposited material may be made visible along one trans-

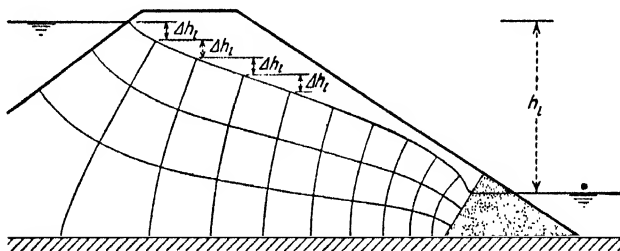


FIG. 75.—Flow net for percolation through an earth embankment

parent wall through injection of dye at various points on the upstream surface of the stratum, with simultaneous piezometric measurement of pressure distribution along the lines of flow.

Less difficult is the case in which there is no impervious upper boundary. As indicated in Fig. 75, the free water surface within the soil must take a form that is in hydrodynamic equilibrium with the forces involved—that is, the pressure must be atmospheric at all points along the topmost stream line, discounting the height of capillary rise in the interstices of the material. The surface profile may therefore be found by so adjusting the flow net that the uppermost stream line drops the same distance Δh_l between every pair of potential lines.

CHAPTER IX

FLUID TURBULENCE

42. The Transition from Laminar to Turbulent Motion. In the foregoing chapter certain elementary examples of steady viscous flow were shown to be subject to solution through application of the Navier-Stokes equations in greatly simplified form. In each case the simplification restricted the essential variables to pressure, weight, and viscous shear, to the exclusion of all dynamic effects of acceleration. Lest the reader draw the erroneous conclusion that laminar flow is basically one in which inertia plays no role, the fact must be made very clear that numerous problems of laminar flow exist in which the differential terms for local and convective acceleration can by no means be ignored. It is only because of the complexity of the resulting differential equations that rigorous analysis of such problems has not yet been accomplished.

Nevertheless, one may conveniently classify problems in viscous motion according to the relative magnitude of the terms for acceleration and the terms for viscous force per unit mass in the Navier-Stokes equations. The preceding chapter dealt with cases of predominant viscous action, in which the accelerative terms were negligible; on the other hand, the entire first part of this book proceeded on the assumption that viscous action was non-existent, the dynamic effects of acceleration then being all-important. Between these two limits of the realm of fluid motion there lies a vast range of problems in which neither dynamic nor viscous effects can be ignored. It is here that the majority of engineering problems are to be found.

A very significant parameter may be developed to designate the relative magnitude of the dynamic (or inertial) characteristics with respect to the viscous characteristics of a given steady motion. Any one of the Navier-Stokes equations may be reduced to the following essential terms:

$$\frac{\partial}{\partial x}(p + \gamma h) = \mu \nabla^2 v_x - \rho a_x$$

It is evident that in non-viscous motion the potential gradient will depend entirely upon the mass acceleration, whereas in non-accelerative motion it will be entirely a function of viscous shear. In general, the extent to which each of these factors will control the potential gradient will depend entirely upon the relative magnitude of the terms ρa_x and $\mu \nabla^2 v_x$. If the flow is a steady one, the velocity at any point will be proportional to the mean velocity of flow, while the velocity gradient at any point will vary with the mean velocity and with the reciprocal of some length characteristic of the boundary conditions. Thus, the product of density and convective acceleration for any typical region of the flow must be proportional to $\rho v^2/L$, whereas in the same region the term $\mu \nabla^2 v_x$ must be proportional to $\mu V/L^2$. The ratio of these two pertinent quantities will then take the form,

$$\frac{\rho V^2/L}{\mu V/L^2} = \frac{VL\rho}{\mu}$$

This is seen to be identical with the dimensionless parameter called the Reynolds number, which was obtained in Chapter I from purely dimensional considerations. It is apparent that the greater the relative magnitude of the numerator of R , the more the dynamic aspects of the problems will predominate; on the other hand, the greater the denominator, the greater the role played by viscosity.

So long as the dynamic aspects of a given flow are negligible, there can be no question but that the motion must be extremely stable; such conditions are marked by very low values of the Reynolds number. Once dynamic effects become appreciable, as indicated by higher values of R , although the flow may still continue in a laminar state, the stability of the laminar motion becomes entirely a relative matter. That is, any momentary disturbance in the flow (a local pressure or velocity fluctuation due to one cause or another), if sufficiently small, will be effectively damped out by viscous action. But the same flow may be unstable to a larger disturbance, which will then grow in magnitude and spread to other regions of the moving fluid. It is apparent that the stability of laminar motion depends in part upon the magnitude of the disturbance and in part upon the relative magnitude of inertial and viscous qualities of the flow;

the larger the Reynolds number, the smaller the disturbance necessary to produce instability.

The growth of such instability may easily be followed by injecting dye into the flow upstream from the disturbance. So long as the motion remains laminar, the filament of dye will remain intact; but the slightest fluctuation will cause it to waver, and if the disturbance is not damped by viscous action, the filament will disrupt and rapidly diffuse across the flow section. Osborne Reynolds first demonstrated this phenomenon in connection with flow through a glass tube,¹ the series of photographs in the Frontispiece illustrating effects similar to those which he obtained. From Fig. 76 may be seen the essential

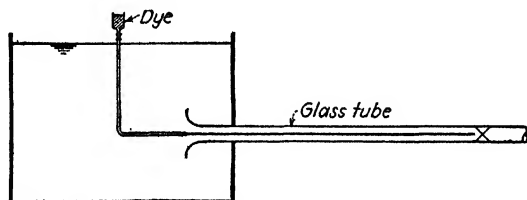


FIG. 76.—The Reynolds apparatus.

features of the Reynolds apparatus. The entrance to the glass tube should be well rounded and the liquid in the supply tank must be stilled for several hours if one is to obtain good results; colored fluid is introduced through a fine jet at the mouth of the tube, while the discharge is controlled by a valve at the exit. As the valve is slowly opened, the flow will be so steady that at first glance the ribbon of color will appear to be stationary, as may be seen from the uppermost photograph. If no disturbance is generated through careless handling, the valve may be opened wider and wider without any noticeable change in the character of the flow. But since disturbance is a relative matter, with increasing discharge the movement will eventually reach a stage at which the filament of dye will begin to fluctuate, and finally break up completely.

Experimentation with the Reynolds apparatus will show that the initial disturbance may result from such widely varied

¹ REYNOLDS, OSBORNE, An Experimental Investigation of the Circumstances Which Determine Whether the Motion of Water Shall Be Direct or Sinuous, and of the Laws of Resistance in Parallel Channels, *Phil. Trans. Roy. Soc.*, vol. 174, 1883; Papers, vol. 2, pp. 51–105.

causes as vibration of the apparatus, insufficient stilling of the water before flow begins, too great an influx of dye from the jet, poor rounding of the bellmouth, or abrupt adjustment of the valve, in particular if the latter is partially closed after flow has been established. Reynolds found that instability generally occurred at a value of the parameter $\frac{VD}{\mu/\rho}$ varying from 10,000 to 12,000, but considerable care on the part of more recent investigators has led to results which would indicate that the limit of the critical Reynolds number is indeterminate, depending primarily upon the extent to which disturbances may be eliminated.¹

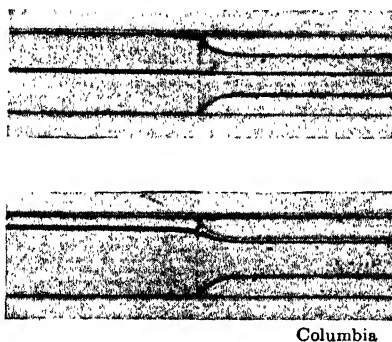


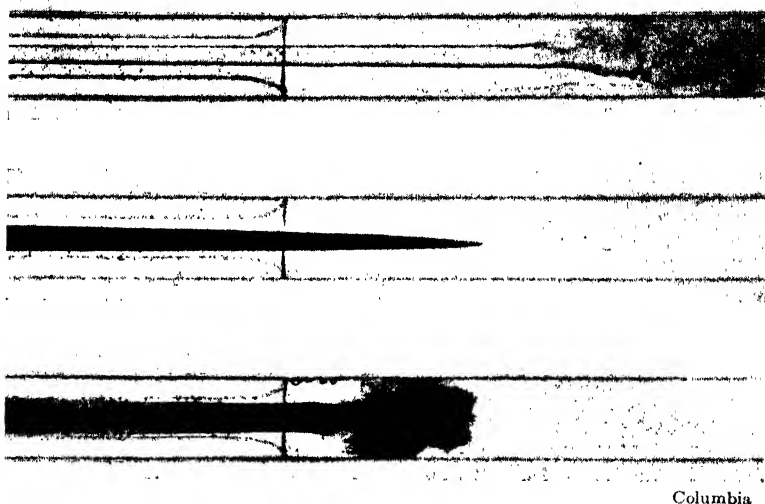
FIG. 77.—Stability of laminar flow at a boundary contraction.

Experience has shown, however, that a very definite lower limit of R exists, below which all disturbances will be effectively damped out by viscous action. This lower critical value of R will depend entirely upon the boundary conditions of the flow; for example, in the case of circular pipes it will be approximately 2000. Although within the range of this lower critical limit the influence of viscosity is predominantly stabilizing, the reader must not conclude that this is the sole function of viscous action; reference to the discussion on the dissipation of energy in Chapter VII will recall to his mind that viscous shear is also a factor involved in changing the kinetic energy of the flow. 'Indeed, in the motion of fluids with low relative viscosity, viscous

¹ With Reynolds' original equipment, for instance, a value of R of more than 40,000 has been reached; see EKMAN, V. W., On the Change from Steady to Turbulent Motion of Liquids, *Arkiv mat., astron. fysik*, vol. 6, no. 12, 1911.

influences are often the cause of the initial disturbance producing instability.

It has been seen that a disturbance too great to be quelled will rapidly increase in magnitude and spread to neighboring regions in the form of eddies, this complex pattern of secondary motion appreciably modifying the basic pattern of flow. Such secondary motion, once established, is known as fluid turbulence. It is characterized primarily by the continuous mixing action of the eddies, whereby small fluid masses are constantly being carried



Columbia

FIG. 78.—Instability of laminar flow at a boundary expansion, the point of disruption moving upstream with increasing Reynolds number. The form of the dye cloud in the center photograph is evidence of parabolic velocity distribution.

into regions of different velocity. This produces, in effect, a transport of kinetic energy from central regions of high velocity toward the boundary regions of low velocity, and vice versa. The obvious result is that in turbulent flow the velocity distribution is more uniform than in laminar, except in the immediate vicinity of the boundaries; here the velocity must again approach the limit zero.

As must be concluded from the foregoing discussion, the intensity of the turbulent eddies will increase with the Reynolds number. It then follows that the higher the magnitude of R , the more uniform the velocity distribution, as is shown schemat-

ically in Fig. 79 for the case of a circular pipe.¹ Moreover, the higher velocity gradient at the boundary would indicate, for the same mean velocity as in laminar flow, a much higher boundary resistance. That this is actually the case is proved by experiment, for in turbulent motion the intensity of shear at a smooth boundary is proportional to a power of the mean velocity ranging from 1.75 to 2, depending upon the magnitude of R . The relation of τ_0 to V in the critical region is indicated in the logarithmic plot of Fig. 80.

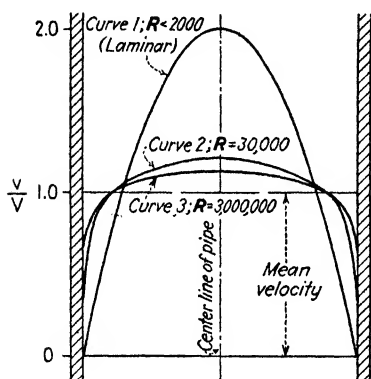


FIG. 79.—Distribution of velocity for laminar and turbulent flow in a circular pipe.

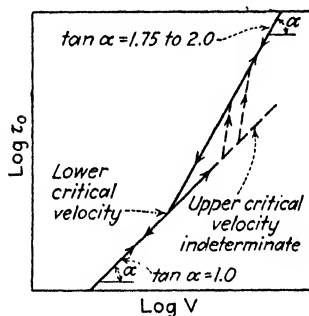


FIG. 80.—Boundary shear versus mean velocity in the critical region.

The point has already been stressed that viscous action is the only means by which flow energy may be transformed into heat. It is evident that no change in fluid characteristics occurs with the onset of turbulence (that is, "impact" between fluid particles is still physically impossible), so that the Navier-Stokes equations may be expected to apply to laminar and turbulent flow alike. In the case of turbulence the rate of energy dissipation is obviously increased, but this becomes fully understandable if the reader visualize the complex curve of velocity distribution that must exist across the flow at any instant, each one of the countless eddies then being the source of additional viscous shear. In other words, for any value of R above the critical there exists

¹ As R becomes infinitely great, the energy of flow will then be constant across any normal section; this corresponds to the case of non-viscous flow as treated in Part One, for the condition $R = \infty$ is satisfied when $\mu = 0$.

a definite average state of viscous equilibrium within the eddying fluid.

Nevertheless, the turbulent pattern is not only exceedingly complex but ever changing in detail. However correctly the Navier-Stokes equations may describe conditions at any point at any instant, it is obviously futile to attempt to use them in investigating a finite portion of the flow for a finite length of time—unless it is found possible so to modify them that the complexity of the secondary fluctuations will not conceal the basic essentials of the flow.

43. Reynolds' Modification of the Navier-Stokes Equations.

While casual observation of the turbulent mixing process would seem to indicate complete lack of system, investigators have attacked the general problem with fair success through use of statistical methods, based upon the following point of view. If one imagine a single vortex filament and its surrounding velocity field, it is evident that the transit of this filament past a point of observation will produce a rapid change in the velocity vector. At any instant during transit the magnitude and direction of the recorded velocity will depend upon the strength and sense of rotation of the filament, and upon the proximity of its path to the actual point of observation. If many such filaments of different strengths are distributed through the flow, not only will the velocity record at the fixed point display continuous fluctuation, but the actual pattern of stream lines surrounding each individual filament will be influenced by the velocity fields of all other filaments in the immediate vicinity. As a matter of fact, vortex lanes (such as those shown in Fig. 99) are often the initial stage in the development of turbulence; however, by the time the turbulent motion has become fully established, the eddies bear little or no resemblance to the original picture of flow, for individual vortices are no longer recognizable as such. From the observer's viewpoint, nevertheless, the transit of irregular eddies will differ from the transit of regular vortices only in the complexity of the velocity record.

Some semblance of order will be brought into this record if one first differentiate between velocities involved in the secondary movement and those pertaining to the basic translation of the fluid as a whole through space. One may thus consider the instantaneous velocity vector at any fixed point to represent

the vector sum of two different velocities, \bar{v} and v' , the first referring to the basic movement and the second to the fluctuation. Schematically, then, v' might be thought of as the relative velocity within an eddy at the point of observation, and \bar{v} as the velocity with which the eddy is carried past this point by the flow. Since each of these vectors, as well as their vector sum, will generally have components in each of the three coordinate directions, the following relationships will be seen to hold:

$$\begin{aligned}
 v &= \bar{v} + v' \\
 v_x &= \bar{v}_x + v'_x; \quad v_y = \bar{v}_y + v'_y; \quad v_z = \bar{v}_z + v'_z \quad (102) \\
 v &= \sqrt{\bar{v}_x^2 + \bar{v}_y^2 + \bar{v}_z^2} \\
 \bar{v} &= \sqrt{\bar{v}_x^2 + \bar{v}_y^2 + \bar{v}_z^2} \\
 v' &= \sqrt{v'_x{}^2 + v'_y{}^2 + v'_z{}^2}
 \end{aligned}$$

The vector of fluctuation v' varies continuously in magnitude and direction, so that turbulent flow can never be steady in the strict sense of the word. The three components of v' will sometimes be positive, sometimes negative, while the numerical magnitude of each may vary from zero as a minimum to a maximum that is still relatively small when compared with the components of \bar{v} .

In order to compute the instantaneous rate of discharge through any cross section of the flow, one must integrate over this section the normal component of the instantaneous velocity vector; assuming the cross section parallel to the yz plane,

$$Q = \int^A v_x dA = \int^A \bar{v}_x dA + \int^A v' dA$$

If conditions of continuity are still to hold, it is evident that the rate of discharge through every successive cross section of the flow at any instant of time must be the same. Such a condition is possible, however, only if the total flow past a section is independent of the secondary fluctuations in velocity—in other words, the second integral in the above expression must always equal zero. More generally, it may be said that the average of any component of fluctuation over a normal area must be zero, so long as the magnitude of the area is great in comparison with the scale of the secondary movement:

$$\frac{1}{A} \int^A v'_x dA = 0, \text{ etc.} \quad (103)$$

In order to determine the temporal mean value of any component of the instantaneous velocity, one must integrate this component at a given point with respect to time and divide by the corresponding time interval:

$$\frac{1}{t} \int^t v_x dt = \frac{1}{t} \int^t \bar{v}_x dt + \frac{1}{t} \int^t v'_x dt$$

From statistical considerations, since v'_x is restricted neither in numerical magnitude nor in sign, the last term in the above expression must have a value of zero, provided only that the time of observation be sufficiently long. It then follows that

$$\bar{v}_x = 0; \quad \bar{v}_y = 0; \quad \bar{v}_z = 0 \quad (104)$$

under which conditions the vector \bar{v} must equal the temporal mean value of the instantaneous vector v . It is therefore possible to treat the vector \bar{v} as a general function of space in describing the underlying flow pattern, just as in the earlier chapters of this book; \bar{v} may also be considered a general function of time, so long as the rate of variation of the mean motion is sufficiently small to be distinct from the more rapid changes of the secondary pattern. In this sense, turbulent flow may now be characterized as steady or unsteady, uniform or non-uniform, with respect to the temporal mean vector alone, without regard to variation of v' as a special function of space and time.

Fully established turbulent motion is not merely a heterogeneous agitation of the moving fluid, for, as has been shown by experience, an essential characteristic of true turbulence is a certain average correlation of the three components of v' at any typical point in the flow.¹ That is, limiting the illustration to the xy plane, the components v'_x and v'_y will not display the random distribution indicated in Fig. 81a, since a positive value of v'_x , let us say, will more often than not be associated with a negative

¹This applies to turbulence produced by flow along a boundary—the type most commonly encountered in hydraulic engineering. In isotropic turbulence—that forming in the wake of a grid—there will necessarily be a random distribution of the components at any point, but correlation of similar components at two neighboring points.

value of v'_y , and vice versa, as illustrated by Fig. 81b. Owing to the existence of such correlation, although the temporal average of any component of fluctuation must be zero, the mean product of any two components will always have a finite value. If one

define the coefficient of correlation by the ratio¹ $\frac{\overline{v'_x v'_y}}{(\overline{v'^2_x})^{1/2} (\overline{v'^2_y})^{1/2}}$,

in which the bars denote mean values, random distribution would then correspond to zero correlation, whereas the perfect correlation shown in Fig. 81c would have the maximum coefficient, unity. Measurements with the hot-wire anemometer² indicate a practically constant degree of correlation throughout the greater

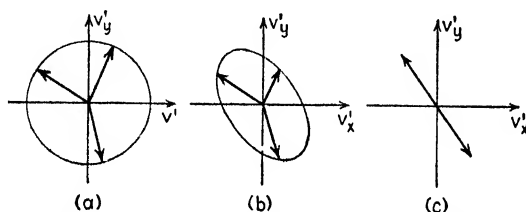


FIG. 81.—Schematic representation of correlation.

part of flow between parallel boundaries. The actual magnitude of the coefficient appears to depend upon the boundary conditions of motion. From these considerations, it would seem that the character of the turbulent mechanism might well be described through use of the following essential terms: $\overline{v'^2_x}$, $\overline{v'^2_y}$, $\overline{v'^2_z}$, $\overline{v'_x v'_y}$, $\overline{v'_y v'_z}$, $\overline{v'_z v'_x}$.

Returning to the basic equation of Navier-Stokes, for each component of the instantaneous velocity vector may be substituted the equivalent sum of the components of \bar{v} and v' ; for the x direction the result will have the general form,

$$\rho \frac{d\bar{v}_x}{dt} + \rho \frac{dv'_x}{dt} = -\frac{\partial}{\partial x}(p + \gamma h) + \mu \nabla^2 \bar{v}_x + \mu \nabla^2 v'_x$$

In addition, the equation of continuity may now be written in terms of both the temporal mean velocity and the velocity of fluctuation:

¹ KÁRMÁN, TH. VON, Turbulence and Skin Friction, *J. Aeronautical Sci.*, vol. 1, no. 1, p. 1, 1934.

² WATTENDORF, F. L., Investigation of Velocity Fluctuations in a Turbulent Flow, *J. Aeronautical Sci.*, vol. 3, no. 6, p. 200, 1936.

$$\frac{\partial \bar{v}_x}{\partial x} + \frac{\partial \bar{v}_y}{\partial y} + \frac{\partial \bar{v}_z}{\partial z} = 0 \quad (105)$$

$$\frac{\partial v'_x}{\partial x} + \frac{\partial v'_y}{\partial y} + \frac{\partial v'_z}{\partial z} = 0 \quad (106)$$

The total derivative dv'_x/dt may now be expressed as the sum of partials with respect to time and space; to these are added the quantity $v'_x \left(\frac{\partial v'_x}{\partial x} + \frac{\partial v'_y}{\partial y} + \frac{\partial v'_z}{\partial z} \right)$ (which, for reasons of continuity, must equal zero), with the following result:

$$\rho \frac{dv'_x}{dt} = \rho \frac{\partial v'_x}{\partial t} + \rho \left(\frac{\partial (v'^2_x)}{\partial x} + \frac{\partial (v'_x v'_y)}{\partial y} + \frac{\partial (v'_x v'_z)}{\partial z} \right)$$

Owing to the complexity of the secondary motion, such an equation cannot be of practical value unless it is made to indicate the average—rather than the instantaneous—effect of the mixing process. Under such conditions, only those terms which have a temporal mean value of finite magnitude will be significant. Such quantities as $\partial v'_x/\partial t$ and $\nabla^2 v'_x$, for instance, may then be dropped, for the mean values of the components of v' , and hence their mean rates of change with time or distance, must always equal zero. If such operations are performed for each of the coordinate directions, the three Navier-Stokes equations will assume the following modified form, first developed by Osborne Reynolds:¹

$$\begin{aligned} \rho \left(\frac{\partial \bar{v}_x}{\partial t} + \bar{v}_x \frac{\partial \bar{v}_x}{\partial x} + \bar{v}_y \frac{\partial \bar{v}_x}{\partial y} + \bar{v}_z \frac{\partial \bar{v}_x}{\partial z} \right) &= -\frac{\partial}{\partial x}(\bar{p} + \gamma h) \\ + \mu \left(\frac{\partial^2 \bar{v}_x}{\partial x^2} + \frac{\partial^2 \bar{v}_x}{\partial y^2} + \frac{\partial^2 \bar{v}_x}{\partial z^2} \right) &- \rho \left(\frac{\partial \overline{v'^2_x}}{\partial x} + \frac{\partial \overline{v'_x v'_y}}{\partial y} + \frac{\partial \overline{v'_x v'_z}}{\partial z} \right) \end{aligned} \quad (107x)$$

$$\begin{aligned} \rho \left(\frac{\partial \bar{v}_y}{\partial t} + \bar{v}_x \frac{\partial \bar{v}_y}{\partial x} + \bar{v}_y \frac{\partial \bar{v}_y}{\partial y} + \bar{v}_z \frac{\partial \bar{v}_y}{\partial z} \right) &= -\frac{\partial}{\partial y}(\bar{p} + \gamma h) \\ + \mu \left(\frac{\partial^2 \bar{v}_y}{\partial x^2} + \frac{\partial^2 \bar{v}_y}{\partial y^2} + \frac{\partial^2 \bar{v}_y}{\partial z^2} \right) &- \rho \left(\frac{\partial \overline{v'^2_y}}{\partial y} + \frac{\partial \overline{v'_y v'_x}}{\partial x} + \frac{\partial \overline{v'_y v'_z}}{\partial z} \right) \end{aligned} \quad (107y)$$

$$\begin{aligned} \rho \left(\frac{\partial \bar{v}_z}{\partial t} + \bar{v}_x \frac{\partial \bar{v}_z}{\partial x} + \bar{v}_y \frac{\partial \bar{v}_z}{\partial y} + \bar{v}_z \frac{\partial \bar{v}_z}{\partial z} \right) &= -\frac{\partial}{\partial z}(\bar{p} + \gamma h) \\ + \mu \left(\frac{\partial^2 \bar{v}_z}{\partial x^2} + \frac{\partial^2 \bar{v}_z}{\partial y^2} + \frac{\partial^2 \bar{v}_z}{\partial z^2} \right) &- \rho \left(\frac{\partial \overline{v'^2_z}}{\partial z} + \frac{\partial \overline{v'_z v'_x}}{\partial x} + \frac{\partial \overline{v'_z v'_y}}{\partial y} \right) \end{aligned} \quad (107z)$$

¹ REYNOLDS, OSBORNE, On the Dynamical Theory of Incompressible Fluids and the Determination of the Criterion, *Phil. Trans. A*, vol. 186, 1894; *Papers*, vol. 2, p. 535.

The reader must not lose sight of the fact that these modified expressions of Reynolds apply no more accurately to conditions of turbulence than do those of Navier-Stokes; their particular merit lies principally in the opportunity they afford to differentiate between the primary and secondary characteristics of the motion.

44. Stress Intensity in Terms of Momentum Transport.

Through the foregoing adaptation of the basic equations of acceleration, it is evident that the magnitudes of the terms for viscous stress are greatly reduced. Since a quantity such as $\mu \nabla^2 \bar{v}_x$ involves only the temporal mean component of velocity, the further effect of viscous action in the complex secondary motion of the eddies is now implicitly expressed by quantities such as $-\rho \left(\frac{\partial \overline{v_x'^2}}{\partial x} + \frac{\partial \overline{v_x' v_y'}}{\partial y} + \frac{\partial \overline{v_x' v_z'}}{\partial z} \right)$. In other words, the actual stress due to viscous action is replaced by the viscous stress in terms of the mean velocity gradient plus the apparent stress due to the exchange of momentum in the mixing process. Such apparent stress results from the fact that fluid masses carried from one region into another—the velocity generally being different in the two regions—will thereby either gain or lose a small amount of momentum; if they gain momentum through being carried into a region of higher velocity, they will exert a corresponding retarding force upon the flow in the latter region, and vice versa. Expressions for the magnitude of such forces may be obtained by the following elementary considerations.

Owing to the mixing process in turbulent motion, small fluid masses are continually carried back and forth across any imaginary plane. The temporal rate of flow per unit area due to this secondary movement will equal simply the component of v' normal to the plane, while the difference between the mean velocity of any fluid mass and that of the region into which it comes on crossing the plane will appear as a momentary velocity fluctuation. If the wandering fluid mass then adapts itself to the velocity conditions of its new surroundings, the change in momentum per unit volume of fluid must be equal to the product of the fluid density and the velocity of the fluctuation, v' . It is evident that the momentum change per unit volume, multiplied by the volume passing a unit area per unit time, must equal

the rate of transport of momentum per unit area as a result of the secondary flow. The force per unit area necessary to produce such inertial reaction must then be equivalent to the stress intensity caused by the momentum transport.

With reference to Fig. 82, momentary flow across the line $a-a$ as the result of the component v'_y will exert a normal force in the y direction and a tangential force in the x direction, the stress intensities having the following magnitudes:

$$p'_y = \rho v'^2_y; \quad \tau'_{yx} = -\rho v'_x v'_y$$

If these are now written as average values, and similar expressions are obtained for the remaining coordinate directions, they will have the form

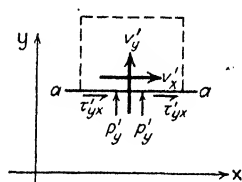


FIG. 82. - Apparent stresses resulting from momentum transport.

$$\overline{p'_x} = \rho \overline{v'^2_x}; \quad \overline{p'_y} = \rho \overline{v'^2_y}; \quad \overline{p'_z} = \rho \overline{v'^2_z} \quad (108)$$

$$\overline{\tau'_{xy}} = -\rho \overline{v'_x v'_y}; \quad \overline{\tau'_{yz}} = -\rho \overline{v'_y v'_z}; \quad \overline{\tau'_{zx}} = -\rho \overline{v'_z v'_x} \quad (109)$$

In addition to such stresses resulting from momentum transport, one must not fail to consider those of viscous action in terms of the temporal mean velocity gradient:

$$\bar{p} - \overline{p_x} = 2\mu \frac{\partial \bar{v}_x}{\partial x}; \quad \bar{p} - \overline{p_y} = 2\mu \frac{\partial \bar{v}_y}{\partial y}; \quad \bar{p} - \overline{p_z} = 2\mu \frac{\partial \bar{v}_z}{\partial z} \quad (110)$$

$$\overline{\tau_{xy}} = \mu \left(\frac{\partial \bar{v}_x}{\partial y} + \frac{\partial \bar{v}_y}{\partial x} \right); \quad \overline{\tau_{yz}} = \mu \left(\frac{\partial \bar{v}_y}{\partial z} + \frac{\partial \bar{v}_z}{\partial y} \right); \quad \overline{\tau_{zx}} = \mu \left(\frac{\partial \bar{v}_z}{\partial x} + \frac{\partial \bar{v}_x}{\partial z} \right) \quad (111)$$

The total intensity of normal and tangential stress in the several directions will finally be given by the sums of the respective quantities in Eqs. (108-111). These expressions correspond to the equations formerly developed for general viscous flow (refer to Chapter VII), and which apply fully as well to turbulent as to laminar motion. The sole difference lies in the fact that the latter refer to instantaneous conditions, whereas the relationships just obtained apply to an interval of time of sufficient length to yield the average effect of the mixing process. It will be apparent to the reader that the Reynolds equations should also be obtainable without recourse to those of Navier-Stokes, by proceeding directly from the foregoing expressions for normal and tangential stress. That identical results may

be found in this way merely substantiates these elementary considerations.

45. Kinetic Energy of Turbulence. Any general statement for the total energy per unit volume at a given point in a moving fluid must include terms for kinetic and potential energy; that is,

$$E = \frac{\rho v^2}{2} + (p + \gamma h)$$

This statement is independent of the force properties of the fluid, for it refers to conditions at a single point at a single instant, without regard to change with time or space; again, it is as valid for turbulent as for laminar motion, since the kinetic energy is expressed in terms of the instantaneous velocity. However, instantaneous conditions in turbulent flow are of little practical significance, for they can provide no clue as to the mean effect of the fluctuations. If, for purposes of convenience, the measurable temporal mean velocity is incorporated in such an expression, it must be remembered that merely substituting a parallel term, $\rho \bar{v}^2/2$, for the kinetic energy of the mean flow, completely ignores the existence of the kinetic energy involved in the secondary motion. In order that the quantity E may truly represent the total energy of the flow, it is essential to add a further term for the kinetic energy of the turbulent fluctuation; thus, for average conditions at any point,

$$\bar{E} + \bar{E'} = \frac{\rho \bar{v}^2}{2} + (\bar{p} + \gamma h) + \frac{\rho \overline{v'^2}}{2} \quad (112)$$

in which

$$\bar{E'} = \frac{\rho \overline{v'^2}}{2} = \rho \frac{(\overline{v_x'^2} + \overline{v_y'^2} + \overline{v_z'^2})}{2} \quad (113)$$

If the turbulence is not fully established, the kinetic energy of the secondary movement will either increase or decrease with time. In other words, the quantity

$$\frac{d\bar{E'}}{dt} = \rho \frac{d}{dt} \left(\frac{\overline{v_x'^2} + \overline{v_y'^2} + \overline{v_z'^2}}{2} \right)$$

will then have a finite numerical value. There are, however, only two ways in which the energy of turbulence may vary. Evidently, the viscous stresses within the eddies must entail

a continuous drain of energy at a rate depending only upon the dynamic viscosity of the fluid and the existing intensity of the turbulent motion. In the course of such loss, the kinetic energy of the eddies must gradually decrease unless energy is supplied by the basic flow at an equivalent rate. On the other hand, if the intensity of the turbulent fluctuations increases, it is because energy is being transmitted to the secondary movement faster than the existing state of viscous stress within the eddies can dissipate it in the form of heat. Under no circumstances can energy of turbulence be restored to the mean motion. Thus, unless the flow is in a state of stable equilibrium, the rate of dissipation of turbulent energy will differ from the rate at which energy is supplied by the mean flow, with the result that the intensity of the secondary motion must change accordingly.

In Chapter VII a very fundamental relationship was obtained for the rate of dissipation of flow energy as a result of viscous stress. It should hardly be necessary to remind the reader at this point that such a general relationship must apply fully as well to turbulent flow as to laminar. However, similar operations performed in terms of \bar{v} and v' will yield expressions that are particularly significant in the case of turbulence. With respect to the mean motion alone, the rate of increase of kinetic energy and the rate of viscous loss will be identical with those discussed in Chapter VII, provided that \bar{v} is substituted for v throughout each of the two expressions. The work done by the apparent stresses of the momentum transport, however, represents a further drain upon the energy of the mean flow. As first shown by Reynolds,¹ the average rate at which the energy of the mean flow is thus reduced may be written in the form:

$$\rho \bar{M} = \rho \left[\bar{v}_x^2 \frac{\partial \bar{v}_x}{\partial x} + \bar{v}_y^2 \frac{\partial \bar{v}_y}{\partial y} + \bar{v}_z^2 \frac{\partial \bar{v}_z}{\partial z} \right. \\ \left. + \bar{v}_x \bar{v}_y \left(\frac{\partial \bar{v}_x}{\partial y} + \frac{\partial \bar{v}_y}{\partial x} \right) + \bar{v}_y \bar{v}_z \left(\frac{\partial \bar{v}_y}{\partial z} + \frac{\partial \bar{v}_z}{\partial y} \right) + \bar{v}_z \bar{v}_x \left(\frac{\partial \bar{v}_z}{\partial x} + \frac{\partial \bar{v}_x}{\partial z} \right) \right]$$

This expression, evidently, must also represent the mean rate at which energy is supplied to the secondary motion.

At any instant, the rate of dissipation of the turbulent fluctuations through viscous action must be as follows:

¹ Compare with LAMB, "Hydrodynamics," p. 674.

$$\mu N = \mu \left[2 \left(\frac{\partial v'_x}{\partial x} \right)^2 + 2 \left(\frac{\partial v'_y}{\partial y} \right)^2 + 2 \left(\frac{\partial v'_z}{\partial z} \right)^2 + \left(\frac{\partial v'_x}{\partial y} + \frac{\partial v'_y}{\partial x} \right)^2 \right. \\ \left. + \left(\frac{\partial v'_y}{\partial z} + \frac{\partial v'_z}{\partial y} \right)^2 + \left(\frac{\partial v'_x}{\partial z} + \frac{\partial v'_z}{\partial x} \right)^2 \right]$$

The mean rate of such dissipation is then denoted by $\mu \bar{N}$.

These two quantities may now be combined to yield the temporal rate of change of turbulent energy per unit fluid volume:

$$\frac{d\bar{E}'}{dt} = \rho \bar{M} - \mu \bar{N} \quad (114)$$

Although \bar{E}' will change with time in the most general case, once the motion is fully established the following condition of equilibrium must obtain,

$$\rho \bar{M} = \mu \bar{N}$$

whereby the intensity of the turbulence remains constant.

In order to describe conditions over a finite region of the flow, the quantity \bar{E}' must be integrated with respect to the volume of the region under investigation; thus,

$$\frac{d}{dt} \left(\int \bar{E}' dV \right) = \rho \iiint \bar{M} dx dy dz - \mu \iiint \bar{N} dx dy dz \quad (115)$$

Unless terms are added for the rate of transport of turbulent energy into and out of this region, this equation is strictly correct only if the intensity of the fluctuations around the boundaries of the region is either zero or so distributed as to produce a net transport of zero magnitude.

In addition to the instructive nature of these relationships¹ they also have a decidedly practical value, for it is through them that conditions of instability of motion are investigated. Reynolds adopted the method of seeking that case of existing turbulent motion in which the velocity fluctuations would gradually disappear; more recent studies proceed from an initial state of laminar motion, and determine whether or not local disturbances

¹ Prandtl has developed the basic expression in such a way as to include a Reynolds number of the flow; see his *Mechanics of Viscous Fluids*, vol. 3, Division G, p. 182, of DURAND'S "Aerodynamic Theory," Springer, Berlin, 1935.

can grow in magnitude under the given boundary conditions. Considerable success has resulted from the latter method of attack, although the general problem has not yet yielded to exact solution.

46. Quantitative Analysis of the Turbulence Mechanism. As yet no mention has been made of the actual magnitude of the intensity of turbulence, aside from its dependence upon the mean products of the velocity components of the secondary motion. Although these quantities correctly define the character of the fluctuations, they are in themselves of little practical significance unless they can be related to flow characteristics that are more readily measurable.

Even before Reynolds published his classic analysis of the secondary fluctuations, Boussinesq introduced a coefficient of "molar" (as distinguished from "molecular") viscosity, by means of which the intensity of apparent stress due to the momentum transport might be expressed in terms of the mean velocity gradient.¹ This coefficient, henceforth denoted by the symbol η , is dimensionally the same as the dynamic viscosity of the fluid, and has come to be known generally as the eddy viscosity; it is, in effect, a dynamic coefficient of turbulence. After the method of Boussinesq, Eqs. (108-111) will have the following form:

$$\bar{p} - \bar{p}_x - \bar{p}'_x = 2(\mu + \eta) \frac{\partial \bar{v}_x}{\partial x} \quad (116x)$$

$$\bar{p} - \bar{p}_y - \bar{p}'_y = 2(\mu + \eta) \frac{\partial \bar{v}_y}{\partial y} \quad (116y)$$

$$\bar{p} - \bar{p}_z - \bar{p}'_z = 2(\mu + \eta) \frac{\partial \bar{v}_z}{\partial z} \quad (116z)$$

$$\bar{\tau}_{xy} + \bar{\tau}'_{xy} = (\mu + \eta) \left(\frac{\partial \bar{v}_x}{\partial y} + \frac{\partial \bar{v}_y}{\partial x} \right) \quad (117xy)$$

$$\bar{\tau}_{yz} + \bar{\tau}'_{yz} = (\mu + \eta) \left(\frac{\partial \bar{v}_y}{\partial z} + \frac{\partial \bar{v}_z}{\partial y} \right) \quad (117yz)$$

$$\bar{\tau}_{zx} + \bar{\tau}'_{zx} = (\mu + \eta) \left(\frac{\partial \bar{v}_z}{\partial x} + \frac{\partial \bar{v}_x}{\partial z} \right) \quad (117zx)$$

If, as Boussinesq assumed, the factor η is constant for a given state of flow, the equations of Navier-Stokes written in terms

¹ BOUSSINESQ, J., *Essai sur la théorie des eaux courantes, Mémoires présentés par divers savants à l'Académie des Sciences*, vol. 23, 1877.

of the mean velocity gradients would differ only to the extent that the sum $(\mu + \eta)$ would replace the term μ . Actually, however, η varies widely in magnitude, not only with the general conditions of motion but from point to point in a given flow; thus, while μ represents a fluid property that is independent of the state of motion, η depends as well upon the fluid density [compare Eqs. (116–117) with (108–111)] as upon the intensity of the secondary movement.

While the relation of η to the basic flow pattern is still undetermined, the Boussinesq equations lend themselves to the following significant comparison. At any Reynolds number below the critical, η obviously has a magnitude of zero. As R increases beyond the critical range, the eddy viscosity becomes increasingly important, and, as shown by experiment, eventually acquires such magnitude as to dwarf the dynamic viscosity completely. In other words, at high Reynolds numbers the viscous stresses in terms of the mean velocity gradient are negligible in comparison with the apparent stresses due to momentum transport. Under such conditions, all terms containing μ in either the Boussinesq or the Reynolds equation may then be dropped. Evidently, the magnitude of the Reynolds number may be considered a direct indication of the ratio between the eddy viscosity and the viscosity of the fluid; that is $R \sim \eta/\mu$.

In the effort to relate the rate of momentum transport to the pattern of the mean flow, Prandtl¹ introduced a characteristic linear dimension called the mixing length, roughly similar to the mean free path in the kinetic theory of gases. Such a length may be considered to represent the average distance a small fluid mass will travel before it loses its increment of momentum to the region into which it comes. As in the case of the components of v' , it is apparent that the magnitude of the mixing length will not only change from point to point, but at a given point will also vary with direction.

Prandtl, however, restricted his analysis to the case of essentially uniform motion, defining the mixing length as a distance normal to the direction of mean flow. He then referred the components of fluctuation to the transverse velocity gradient by reasoning that a fluid mass traveling the distance l across the

¹ PRANDTL, L., Bericht über Untersuchungen zur ausgebildeten Turbulenz, *Z. angew. Math. Mech.*, vol. 5, no. 2, p. 136, 1925.

flow before changing its momentum would cause a fluctuation at the end of its journey (Fig. 83) proportional to the product of l and the mean velocity gradient—i.e., to the difference in mean velocity between beginning and end of its course. Thus, if the flow is in the x direction and if \bar{v} varies only with y , the following average proportionality may be written,

$$|\overline{v'_x}| \sim l \frac{\partial \bar{v}_x}{\partial y}$$

in which the vertical bars denote numerical magnitude, regardless of sign. Furthermore, Prandtl concluded, if two fluid masses approach each other in a direction parallel to one axis, from reasons of continuity the resulting secondary flow normal to this axis must depend upon their velocity of approach. In other words, further proportionality must exist between the components of fluctuation in the two normal directions. Thus,

$$|\overline{v'_x}| \sim |\overline{v'_y}|$$

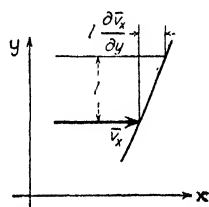


FIG. 83.—The mixing length.

Evidently a positive fluctuation v'_x will generally accompany a negative fluctuation v'_y , and vice versa, which is merely another way of admitting the existence of correlation.

Since the intensity of turbulent shear may also be expressed in terms of these components,

$$\overline{\tau'} = -\rho \overline{v'_x v'_y} \sim \rho |\overline{v'_y}| l \frac{\partial \bar{v}_x}{\partial y} \sim \rho l^2 \left| \frac{\partial \bar{v}_x}{\partial y} \right| \frac{\partial \bar{v}_x}{\partial y}$$

Inasmuch as both l and the factor of proportionality are still unknown quantities, it would seem expedient to combine the two into a single term. Thus, if l is considered to absorb the proportionality factor, the following significant relationship will be obtained:

$$\overline{\tau'} = \rho |\overline{v'_y}| l \frac{\partial \bar{v}_x}{\partial y} = \rho l^2 \left| \frac{\partial \bar{v}_x}{\partial y} \right| \frac{\partial \bar{v}_x}{\partial y} \quad (118)$$

The coefficient η may now be given added significance through comparison of Eqs. (117) and (118), from which it will be seen that

$$\frac{\eta}{\rho} = |\overline{v'_x}| l = \epsilon \quad (119)$$

Just as the ratio μ/ρ represents a quantity that is independent of both force and mass characteristics and called the kinematic viscosity, ν , the ratio η/ρ is a kinematic turbulence factor, ϵ (epsilon), sometimes known as the kinematic eddy viscosity. This factor is a direct measure of the transporting capacity of the mixing process, regardless of whether the transport refers to momentum, as in the Prandtl development, or to vorticity, salinity, sediment, or heat. As shown by von Kármán,¹ such engineering problems as heat transfer due to turbulent convection or the transportation of silt as suspended load in rivers may be studied conveniently in terms of the kinematic turbulence coefficient. This may be seen from the following generalization of the Prandtl concept.

Assume again that due to cross fluctuations having the mean numerical value $|\overline{v_y}|$, fluid masses are carried an average transverse distance l before losing their identity; moreover, let u represent the local magnitude per unit volume of any flow characteristic or fluid property, or the local concentration per unit volume of any substance carried in solution or suspension. The rate of lateral transport of u as a result of the mixing process will depend upon the change in u over the distance l (i.e., approximately $l \partial u / \partial y$) and upon the general rate of flow per unit area $|\overline{v_y}|$ in this direction. But if l is again assumed to absorb the proportionality constant, the product $|\overline{v_y}| l$ becomes the kinematic turbulence factor ϵ , whence the rate of transport of u across the flow can be written simply as

$$U = -\epsilon \frac{\partial u}{\partial y} \quad (120)$$

the minus sign indicating that the net transport will be in the direction of decreasing u . If this equation is written in terms of the average momentum per unit volume $\rho \bar{v}$,

$$M = -\epsilon \frac{\partial(\rho \bar{v})}{\partial y} = -\epsilon \rho \frac{\partial \bar{v}}{\partial y} \quad (120M)$$

which is, of course, the same as Eq. (118). Similarly, if n represents the number of silt particles per unit volume at any point in the flow, the rate of silt transport in the direction y will be

¹ KÁRMÁN, TH. VON, Some Aspects of the Turbulence Problem, *Proc. Fourth Intern. Congress Appl. Mech.*, Cambridge, 1934.

$$N = -\epsilon \frac{\partial n}{\partial y} \quad (120N)$$

Again, letting $c\theta$ denote the heat per unit fluid volume (*i.e.*, the product of specific heat and temperature), the rate of heat transfer may then be expressed as

$$H = -\epsilon \frac{\partial(c\theta)}{\partial y} = -\epsilon c \frac{\partial \theta}{\partial y} \quad (120H)$$

Other applications should be obvious to the reader. Some question remains, however, as to whether the factor ϵ is the same in each of the above equations—for instance, whether the velocity of fluctuation for the silt particles can be considered identical with that of the fluid, and whether the proportionality constant for the mixing length will also be the same.

As a matter of fact, while the Prandtl mixing-length concept obviously has great schematic value, upon closer investigation it will be found to be far from rigorous either mathematically or physically—if only for the fact that one can scarcely visualize fluid masses traveling a certain transverse distance and then abruptly changing in momentum. Taylor¹ attempted to eliminate such fallacies through use of an expression for vorticity transfer to replace Prandtl's model of momentum transfer. Denoting by ω'_z the vorticity fluctuation, from the basic equations of uniform two-dimensional flow Taylor obtained:

$$\frac{\partial \bar{p}}{\partial x} = -\rho \frac{\partial}{\partial x} \overline{v'_x v'_y} = -\rho \overline{v'_y \omega'_z} \quad (121)$$

Assuming a length l denoting the transverse path in the vorticity transfer, there will result the general expression,

$$-\frac{\partial \bar{p}}{\partial x} = \rho \overline{|v'_y|} l \frac{\partial \overline{\omega'_z}}{\partial y} = \rho \overline{|v'_y|} l \frac{\partial^2 \overline{v_x}}{\partial y^2} \quad (122)$$

which was intended to replace Prandtl's Eq. (118).

Perhaps the most satisfactory approach is that embodied in von Kármán's hypothesis of turbulent similitude,² based upon

¹ TAYLOR, G. I., The Transport of Vorticity and Heat through Fluids in Turbulent Motion, *Proc. Roy. Soc. (London)*, A, vol. 135, 1932.

² First announced in 1930, the similarity hypothesis is discussed at length by VON KÁRMÁN in "Turbulence and Skin Friction," and in "Some Aspects of the Turbulence Problem."

these two reasonable assumptions: (1) The mechanism of turbulence is independent of viscosity except in the immediate neighborhood of the flow boundaries; (2) the pattern of the secondary flow is statistically similar from point to point, varying only in time and length scales. The first assumption is in accord with experimental data on the relative magnitude of η and μ . The second assumption simply entails a constant factor of correlation at all points in the flow, a condition also indicated by experiment. Schematically, the time and length scales may be thought of in connection with the mean frequency and the mean amplitude of the velocity fluctuations. More conveniently, the length scale may be represented by a quantity l , similar to the mixing length of Prandtl but not requiring the latter's special concept of the mixing process, whereas the time scale is then related to the mean velocity gradient.

If this hypothesis is applied to the case of two-dimensional uniform motion, as shown by von Kármán, the following three conclusions will be reached:

a. The components of fluctuation will be proportional to the length l and to the gradient $\partial \bar{v}_x / \partial y$.

b. The intensity of shear will be proportional to $\rho l^2 (\partial \bar{v}_x / \partial y)^2$.

c. The length l will be proportional to $\partial \bar{v}_x / \partial y \div \partial^2 \bar{v}_x / \partial y^2$.

Each of these conditions depends upon a length scale of the secondary motion that is small in comparison with the scale of the mean flow. In *c*, for instance, derivatives higher than the second have been ignored. Actually, the relative scale of the turbulent process is greater than assumed, so that these proportionalities must be considered as first approximations. Nevertheless, experimental evidence substantiates these conclusions to a very satisfactory degree, and indicates that the factor of proportionality, κ (kappa), under *c* has the nature of a universal constant, with a magnitude of approximately 0.40. Through these relationships the mixing length may at last be eliminated from Eq. (118), leaving a simple expression for shear in terms of the mean velocity gradient:

$$\sqrt{\frac{\tau}{\rho}} = -\kappa \frac{(\partial \bar{v}_x / \partial y)^2}{\partial^2 \bar{v}_x / \partial y^2} \quad (123)$$

Still dissatisfied with the approximate qualities of this hypothesis and its failure to yield a complete picture of the turbulence mechanism, von Kármán has recently made a radically different

attack upon the problem, neither assuming the relative scale of turbulence to be smaller than it actually is, nor ignoring the fact that viscous stresses play an essential role within the secondary movement. Proceeding from the basic mechanism of energy and vorticity dissipation, and extending the basic concept of correlation, after eliminating terms of negligible value von Kármán obtained the following salient expressions:¹

$$-\frac{\partial}{\partial y} \left[v'_y \left(\frac{\rho v'^2}{2} + p \right) \right] + \tau \frac{\partial v_x}{\partial y} = \mu \sum_{m=x,y,z} \sum_{n=x,y,z} \overline{\left(\frac{\partial v'_m}{\partial n} \right)^2} \quad (124)$$

$$-\frac{\partial}{\partial y} \left(v'_y \frac{\omega'^2}{2} \right) = \nu \sum_{m=x,y,z} \sum_{n=x,y,z} \overline{\left(\frac{\partial \omega'_m}{\partial n} \right)^2} \quad (125)$$

The sigmas indicate the sum of the mean squares of the derivatives of the three velocity or vorticity components, each taken with respect to each of the three coordinate directions.

The first term of Eq. (124) represents the net rate of increase in turbulent energy per unit volume as a result of turbulent convection; the second term represents the rate of work done per unit fluid volume by the apparent shearing stress; the third term denotes the rate of energy dissipation through viscous action within the eddies. Similarly, the left side of Eq. (125) is a measure of the net rate of increase in eddy vorticity, whereas the right side represents the rate of dissipation of eddy vorticity through viscous shear.

Not only do these two fundamental equations yield excellent results for those elementary cases of flow already treated by means of the Prandtl and Taylor methods and von Kármán's similarity hypothesis, but present indications are that they will provide a general means of investigating such conditions of turbulence as are encountered in converging, diverging, and curvilinear flow, as well as the diffusion and decay of turbulence in the wake of an immersed body, and the motion of a fluid of variable density. Nevertheless, until the method of each individual application becomes clear and the analytical results are verified experimentally, the engineer must remain content with such solutions as are possible by means of the earlier theories, as described in the remaining chapters of Part Two.

¹ KÁRMÁN, TH. VON, *The Fundamentals of the Statistical Theory of Turbulence*, *J. Aeronautical Sci.*, vol. 4, no. 4, p. 131, 1937.

CHAPTER X

CHARACTERISTICS OF THE BOUNDARY LAYER

47. Boundary Influence in Non-uniform Motion. Throughout the first part of this book emphasis was placed upon the effect of the geometrical boundary conditions upon the pattern of the velocity field. It was shown that fluid motion proceeding from a state of rest must begin as one of constant energy, under which conditions the pressure and velocity distribution may be determined through the principles of potential flow. Although such principles were developed without regard to the effect of viscosity, it so happens that in rapidly accelerated flow the zone of appreciable viscous action is limited to the immediate neighborhood of the boundary itself. Under these circumstances, the general flow picture as determined by the given geometrical boundary conditions will remain essentially the same, viscous shear producing a marked modification of the potential pattern only in the boundary region. Recognition of this fact by Prandtl¹ early in the present century remains one of the most important contributions that has been made to modern fluid mechanics.

While Prandtl restricted his analysis to fluids of "low viscosity," it should be apparent that the actual magnitude of the viscosity is not a satisfactory criterion unless the velocity, density, and characteristic linear dimensions of the flow are also specified. That is to say, if velocity, kinematic viscosity, and length are combined in the dimensionless form $R = VL/\nu$, a given value of this parameter may represent a wide range in the absolute magnitudes of all three variables. Only if the numerator of this fraction is large in comparison with the denominator will those conditions assumed by Prandtl actually exist; otherwise, the boundary influence may extend an appreciable distance into the flow, whereupon the problem becomes primarily one of viscous shear, as treated in Chapter VIII.

¹ PRANDTL, L., *Über Flüssigkeitsbewegung bei sehr kleiner Reibung, Verhandlungen des III. Intern. Mathematiker-Kongresses, Heidelberg, 1904.*

At the boundary itself the velocities of boundary and fluid must always be identical. If the viscous action is confined to the boundary vicinity, the fluid velocity must then change from this limiting value to that of the surrounding flow over a relatively short distance, while within this zone the work done by the viscous stresses opposing the relative motion will entail dissipation of energy in the form of heat. As may readily be seen, however, continued reduction of energy as the flow progresses along the boundary must be accompanied by a steady growth in thickness of the layer that is noticeably affected by the viscous action. Moreover, it should be possible to express

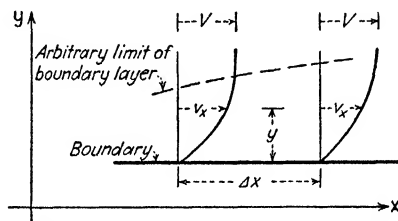


FIG. 84.—Boundary-layer growth in the direction of flow.

the rate of change of momentum involved in this process in terms of the boundary resistance and the pressure gradient.

In Eq. (17) there is already available a general statement of the momentum principle applicable to a finite region of the flow, in terms of the velocity distribution around the borders of this region. If the fluid is assumed to move past a stationary boundary, it is evident that the velocity at the boundary itself must always be zero, increasing outward to the velocity V of the undisturbed flow, as shown in Fig. 84. Equation (17), written for the direction x parallel to the boundary, may be applied to two successive normal sections a distance dx apart by expressing the differential rate of discharge dQ as the product of the variable velocity component v_x , the increment of distance dy normal to the boundary, and some width of flow b . Moreover, the change in velocity over the distance dx may be related conveniently to the velocity of the undisturbed flow by writing $\frac{\partial v_x}{\partial x} dx = -\frac{\partial}{\partial x}(V - v_x) dx$. Then the force producing this rate of change of momentum will have the form .

$$dF_x = -\rho \int_0^\delta \frac{\partial}{\partial x} (V - v_x) dx b v_x dy$$

in which δ (delta) signifies the normal distance to the undisturbed flow. This expression may be written more significantly as follows, the force per unit area being placed equal to the combined effect of pressure gradient and viscous shear at the boundary:

$$-\frac{dF_x}{b dx} = \frac{\partial p}{\partial x} dx + \tau_0 = \frac{\partial}{\partial x} \left[\rho \int_0^\delta v_x (V - v_x) dy \right] \quad (126)$$

Mathematically speaking, the effect of viscous shear along a boundary surface must always extend an infinite distance into the flow—that is, $\delta = \infty$ at every normal section, the magnitude of the viscous influence at any distance y being indicated by the difference between the velocity of the undisturbed flow and the actual velocity at the point in question. Nevertheless, as pointed out by Prandtl, the zone of appreciable variation in v_x is, under certain conditions, relatively narrow; this region is generally known as the boundary layer, and the symbol δ is used to denote its apparent thickness.

It is often of practical significance to express the magnitude of the boundary resistance in terms of the kinetic energy of the undisturbed flow, through use of a coefficient of local “friction” c_f —that is,

$$\tau_0 = c_f \frac{\rho V^2}{2}$$

whence

$$c_f = \frac{\tau_0}{\rho V^2/2} \quad (127)$$

Again, if the total resistance over a given portion of the boundary is divided by the corresponding boundary area, the resulting average intensity of shear may be referred to the kinetic energy of the undisturbed flow through a mean coefficient C_f :

$$\frac{F_x}{bx} = C_f \frac{\rho V^2}{2} \quad (128)$$

Equations (126), (127), and (128) are obviously quite general in form. Nevertheless, evaluation of the intensity of shear or the magnitude of either the mean or the local coefficient of resistance will require further knowledge of the velocity distribu-

tion. Such information should be available from the basic equations of motion.

48. The Laminar Boundary Layer. From inspection of the Navier-Stokes equations one may at once draw certain important conclusions as to the relative order of magnitude of the several terms in the case of laminar motion in a thin boundary layer.¹ Again assuming the x axis parallel to the boundary and in the direction of flow, and the y axis normal to the boundary, these equations—together with that of continuity—will have the form

$$\overset{1 \cdot 1}{v_x} \frac{\partial v_x}{\partial x} + \overset{\delta \cdot \frac{1}{\delta}}{v_y} \frac{\partial v_x}{\partial y} = -\frac{1}{\rho} \frac{\partial p}{\partial x} + \nu \left(\overset{1}{\frac{\partial^2 v_x}{\partial x^2}} + \overset{\frac{1}{\delta^2}}{\frac{\partial^2 v_x}{\partial y^2}} \right) \quad (129x)$$

$$\overset{1 \cdot \delta}{v_x} \frac{\partial v_y}{\partial x} + \overset{\delta \cdot 1}{v_y} \frac{\partial v_y}{\partial y} = -\frac{1}{\rho} \frac{\partial p}{\partial y} + \nu \left(\overset{\delta}{\frac{\partial^2 v_y}{\partial x^2}} + \overset{\frac{1}{\delta}}{\frac{\partial^2 v_y}{\partial y^2}} \right) \quad (129y)$$

$$\frac{1}{\delta} \frac{\partial v_x}{\partial x} + \frac{\partial v_y}{\partial y} = 0$$

Since the thickness of the boundary layer is relatively small, it is evident that linear characteristics of the flow in the directions x and y will be definitely of a different order of magnitude.

For instance, if v_x and $\frac{\partial v_x}{\partial x}$ are considered to be numerically of the order 1, then $\frac{\partial v_x}{\partial y}$ must be of the order $\frac{1}{\delta}$. Writing such

relative orders of magnitude as simple proportionalities, $\frac{\partial v_x}{\partial x} \sim 1$,

$\frac{\partial v_x}{\partial y} \sim \frac{1}{\delta}$, whence $\frac{\partial^2 v_x}{\partial x^2} \sim 1$ and $\frac{\partial^2 v_x}{\partial y^2} \sim \frac{1}{\delta^2}$. From the equation

of continuity, $\frac{\partial v_y}{\partial y} \sim \frac{v_x \partial}{\partial x} \sim 1$, whereupon $v_y \sim \delta$, $\frac{\partial^2 v_y}{\partial y^2} \sim \frac{1}{\delta}$,

$\frac{\partial v_y}{\partial x} \sim \delta$, $\frac{\partial^2 v_y}{\partial x^2} \sim \delta$.

Inasmuch as no single term of either of the two equations may be of greater order than the greatest of the other terms in that equation, it will be seen that the kinematic viscosity must be

¹ BLASIUS, H., *Grenzschichten in Flüssigkeiten mit kleiner Reibung*, *Z. Math. und Physik*, vol. 56, 1908.

of the same order as the square of the boundary-layer thickness. That is to say, $\delta \sim \sqrt{\nu}$, from which it follows that the lower the kinematic viscosity of the fluid, the smaller should be the effect of a laminar boundary layer upon the flow; the limit $\nu = 0$ then denotes the type of motion discussed throughout Part One. Moreover, since the largest terms in Eq. (129y) are of lesser order than the largest in Eq. (129x), the pressure gradient $\partial p/\partial y$ must be insignificant in comparison with $\partial p/\partial x$; in other words, the pressure intensity at the surface of the boundary cannot differ appreciably from that outside of the boundary layer. Under such circumstances, the boundary flow conditions are fully described by the momentum relationship [Eq. (126)], the equation of continuity, and the following modified form of Eq. (129x):

$$v_x \frac{\partial v_x}{\partial x} + v_y \frac{\partial v_x}{\partial y} = - \frac{1}{\rho} \frac{\partial p}{\partial x} + \nu \frac{\partial^2 v_x}{\partial y^2} \quad (130)$$

These equations apply correctly to curvilinear—as well as rectilinear—motion so long as the radius of curvature of the boundary is great in comparison with the boundary-layer thickness. If the boundary is planar, moreover, it is obvious that since the pressure intensity in the undisturbed flow must be constant, there can be no pressure gradient in the boundary layer in either direction. Such conditions are well illustrated by flow of an otherwise undisturbed fluid parallel to a thin flat plate, for a laminar boundary layer will form at the leading edge of the plate, growing steadily in thickness with distance from the point of formation. The distribution of velocity and the intensity of shear at any section of this boundary layer may be found through solution of the foregoing differential expressions for the following boundary conditions: $v_x = 0 = v_y$ at $y = 0$; $v_x = V$ and $v_y = 0$ at $y = \delta$. The exact solution is, however, rather complex, but a significant first approximation may be obtained through two simplifying assumptions.

The first assumption, substantiated by experimental data, is that the curves of velocity distribution at successive normal sections of the flow may be represented by a single analytic function of the form

$$\frac{v_x}{V} = f\left(\frac{y}{\delta}\right)$$

The second assumption must determine the form of this function. Since a parabolic distribution curve is typical of uniform laminar motion, it would seem the most logical one to choose for this first approximation. Thus, if the vertex is presumed to lie a distance $y = \delta$ from the boundary,

$$\frac{v_x}{V} = \left[1 - \left(1 - \frac{y}{\delta} \right)^2 \right] = 2 \frac{y}{\delta} - \frac{y^2}{\delta^2}$$

Then, from Equation (126),

$$\tau_0 = \frac{\partial}{\partial x} \left[\rho V^2 \delta \int_0^1 \frac{v_x}{V} \left(1 - \frac{v_x}{V} \right) d \left(\frac{y}{\delta} \right) \right] = \frac{\partial}{\partial x} \left(\frac{2}{15} \rho V^2 \delta \right)$$

But τ_0 must also equal the product of μ and the velocity gradient at the wall, whence

$$\tau_0 = \mu \left. \frac{\partial v_x}{\partial y} \right|_{y=0} = 2 \mu \frac{V}{\delta}$$

After eliminating τ_0 , integration will yield the thickness δ for any cross section of the boundary flow; thus,

$$\delta = 5.47 \sqrt{\frac{\nu x}{V}}$$

from which the intensity of shear at the boundary may now be obtained:

$$\tau_0 = 0.365 \sqrt{\frac{\rho \mu V^3}{x}}$$

Owing to the fact that the second assumption gave the quantity δ a definite finite magnitude, and since $v_x = V$ at the point $y = \delta$, the foregoing approximate equations must be expected to provide values which deviate somewhat from those obtained through either rigorous analytical solution or experimental measurement. Actually, v_x will equal V only as δ becomes infinitely great, despite the fact that practically the entire growth of v_x will take place within a short distance of the boundary. The exact solution, first obtained by Blasius, provides the curve of velocity distribution shown in dimensionless form in Fig. 85; the approximate curve has been added for purposes of comparison.

If δ in the exact solution must have a magnitude of infinity, it is evident that some other definition of effective boundary-

layer thickness must be found. One may, for instance, choose as δ that value of y at which the ratio v_x/V has attained some arbitrary magnitude close to unity (for instance, 0.99). Again, one may define δ in terms of the velocity gradient at the wall, by extending the tangent from this point of the curve until

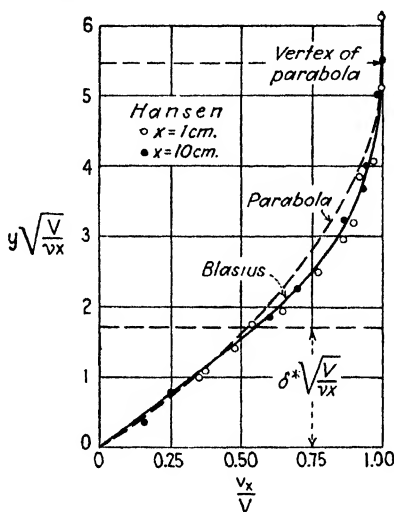


FIG. 85.—Dimensionless plot of velocity distribution in the laminar boundary layer.

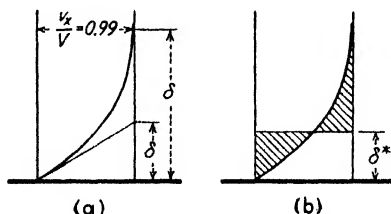


FIG. 86.—Definitions of boundary-layer thickness.

it intersects the vertical $v_x = V$, as indicated in Fig. 86a. By far the most significant result is obtained by using the mean ordinate of the velocity curve; designating this parameter by the symbol δ^* ,

$$\delta^* = \int_0^\infty \left(1 - \frac{v_x}{V}\right) dy \quad (131)$$

Since the shaded areas in Fig. 86b are therefore equal, δ^* thus represents the distance the stream lines of the surrounding flow

are shifted away from the boundary as a result of the redistribution of velocity in the region of appreciable viscous shear. Blasius found for this characteristic parameter the magnitude

$$\delta^* = 1.73\sqrt{\frac{\nu x}{V}} \quad (132)$$

and for the intensity of boundary resistance

$$\tau_0 = 0.332\sqrt{\frac{\rho \mu V^3}{x}} \quad (133)$$

Two essential facts are to be noted in these equations:¹ The boundary-layer thickness is directly proportional, and the intensity of boundary shear is inversely proportional, to the square root of distance from the leading edge, as shown schematically in Fig. 87. It must be recalled, nevertheless, that such relationships are not valid in the immediate neighborhood of the leading edge itself, for here the dimensions δ and x approach the

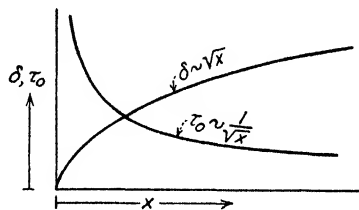


FIG. 87.—Variation of δ and τ_0 with x for the laminar boundary layer.

same order of magnitude—a condition contrary to that upon which the entire solution was based.

Since boundary-layer development involves both mass acceleration and viscous shear, designation of the conditions of motion by means of a characteristic Reynolds number is most appropriate. The velocity of the undisturbed flow and the kinematic viscosity of the fluid are pertinent variables, while either the boundary-layer thickness or the distance from the leading edge is a suitable linear dimension. If the latter length is chosen, Eq. (132) may be written in the form

$$\delta^* = \frac{1.73x}{\sqrt{R_x}} \quad (134)$$

Evidently, $R_{\delta^*} = 1.73\sqrt{R_x}$, whence

¹ For experimental verification of Blasius' solution see BURGERS, J. M., *Proc. First Intern. Congress Appl. Mech.*, Delft, 1924; HANSEN, N., *Die Geschwindigkeitsverteilung in der Grenzschicht an einer eingetauchten Platte*, *Z. angew. Math. Mech.*, vol. 8, no. 3, 1928.

$$\tau_0 = \frac{0.332}{\sqrt{R_x}} \rho V^2 = \frac{0.574}{R_{\delta^*}} \rho V^2 \quad (135)$$

from which the coefficients of local and mean boundary resistance may be obtained as follows:

$$c_f = \frac{0.664}{\sqrt{R_x}} = \frac{1.149}{R_{\delta^*}} \quad (136)$$

$$C_f = 2c_f = \frac{1.328}{\sqrt{R_x}} = \frac{2.298}{R_{\delta^*}} \quad (137)$$

It is evident that both c_f and C_f decrease as the boundary layer develops, owing to the fact that the velocity gradient at the wall (and hence the intensity of boundary shear) becomes smaller as the layer grows in thickness.

49. The Turbulent Boundary Layer. Laminar flow at a Reynolds number greater than a certain minimum critical value, readers will recall, may be unstable in the presence of disturbances of one magnitude, yet stable for disturbances of lesser magnitude; the disturbance capable of producing instability decreases with increasing values of R . In the case of uniform motion cited at the time this fact was discussed, both the kinematic viscosity and the characteristic linear dimension of the boundaries remained constant, while the change in R was produced by varying the mean velocity of flow. In the development of the laminar boundary layer, on the other hand, V and ν do not vary, the change in the Reynolds number resulting from a steady increase in the values of δ and x . As the region of appreciable viscous influence steadily grows in thickness with distance from the leading edge, such motion will eventually become unstable for disturbances of magnitude varying inversely with R_x or R_{δ^*} . If such disturbances occur, in the neighborhood of the corresponding critical section secondary fluctuations will develop, spreading rapidly throughout the boundary layer with increasing values of x . After a relatively short transition zone the boundary layer will display the characteristic velocity pattern of true turbulence, and further growth of δ must be described according to a different functional relationship.

Experimental investigations indicate that the lower critical Reynolds number for the boundary layer is by no means so

clearly defined as in the case of uniform flow in circular tubes. Indeed, the transition has been found to begin at values of R_x ranging between approximately 10^5 and 10^6 , whereas if the leading edge of the plate is not well sharpened, or if the approaching flow is not truly undisturbed, the boundary layer may be a turbulent one from the outset.

Under any circumstances, mean conditions at a given section can no longer be described satisfactorily by the equations of Navier-Stokes. Although the equation of momentum written in terms of \bar{v} is still very useful, the Reynolds equations introduce such additional complexities that exact solution of the turbulent boundary layer has not yet been accomplished. Moreover, since the temporal mean velocity, as well as the components of fluctuation, must still be zero at the boundary, it is to be expected that a very thin laminar sublayer will exist at the boundary surface; careful measurements indicate that this is actually the case. It is therefore apparent that the velocity-distribution curve (Fig. 88) must include a film of purely laminar flow, a region in which the turbulent process is fully developed, and a transition zone between the two in which the motion is neither laminar nor yet completely turbulent.

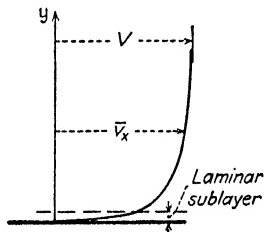


FIG. 88.—Velocity distribution in the turbulent boundary layer.

Nevertheless, it is not unreasonable to assume once again that the velocity-distribution function is the same over successive cross sections of the boundary layer. In the very thin laminar sublayer, the velocity may be considered, with negligible error, to be directly proportional to the normal distance from the boundary; that is,

$$\bar{v}_x \sim y \quad (138)$$

Laboratory data indicate that the velocity profile for the turbulent region may be approximated by the exponential function

$$\bar{v}_x \sim \sqrt[n]{y} \quad (139)$$

Of even more importance, it has been found that the intensity of boundary shear may be written in the exponential form

$$\tau_0 = \frac{C}{(V\delta/\nu)^n} \frac{\rho V^2}{2} = \frac{C}{R_\delta^n} \frac{\rho V^2}{2} \quad (140)$$

in which C is simply a constant of proportionality. The exponents m and n are found to bear the relationship

$$m = \frac{2 - n}{n}$$

a fact which might be surmised after noting that in Eq. (140), for constant values of τ_0 and ν ,

$$\delta \sim V^{\frac{2-n}{n}}$$

Without regard to the actual velocity function, it will readily be seen that the momentum integral $\rho \int_0^\delta \bar{v}_x (V - \bar{v}_x) dy$ may be written in the form $\alpha \rho V^2 \delta$, in which α is a dimensionless constant depending in magnitude upon the curve of velocity distribution.¹ Introducing the foregoing expression for τ_0 into the momentum equation,

$$\alpha \rho V^2 \frac{d\delta}{dx} = \frac{C}{(V\delta/\nu)^n} \frac{\rho V^2}{2}$$

If the factor α and the constant of proportionality are combined in the term C' , this relationship will then have the simplified form:

$$\delta^n d\delta = C' \left(\frac{\nu}{V} \right)^n dx$$

Integrating, and assuming $\delta = 0$ when $x = 0$,

$$\frac{\delta^{n+1}}{n+1} = C' x \left(\frac{\nu}{V} \right)^n$$

or

$$\delta = C'' x \left(\frac{\nu}{Vx} \right)^{\frac{n}{n+1}} = \frac{C'' x}{R_x^{\frac{n}{n+1}}} \quad (141)$$

If this value for δ is substituted in Eq. (140), the following three essential relationships are obtained;

$$\tau_0 = \frac{C'''}{R_x^{\frac{n}{n+1}}} \frac{\rho V^2}{2} \quad (142)$$

¹ This development closely follows that presented by von Kármán in "Turbulence and Skin Friction."

$$c_f = \frac{C'''}{R_x^{\frac{n}{n+1}}} \quad (143)$$

$$C_f = (n+1) c_f = (n+1) \frac{C'''}{R_x^{\frac{n}{n+1}}} \quad (144)$$

In the case of laminar flow, n will have the value unity, under which conditions Eqs. (141-144) will become identical in form with those just discussed in connection with the laminar boundary layer. Numerous laboratory measurements of velocity distribution and boundary shear in the case of turbulence indicate that n will have a magnitude of $\frac{1}{4}$ for Reynolds numbers just above the critical, in which case δ will vary with the four-fifths power of the distance from the leading edge (Fig. 89), while

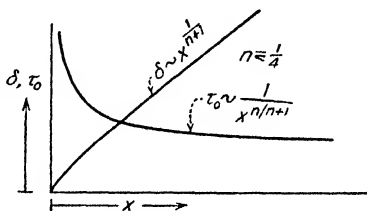


FIG. 89.—Variation of δ and τ_0 with x for the turbulent boundary layer.

$$\tau_0 = \frac{0.059}{R_x^{1/2}} \frac{\rho V^2}{2} \quad (145)$$

$$c_f = \frac{0.059}{R_x^{1/2}} \quad (146)$$

$$C_f = \frac{0.074}{R_x^{1/2}} \quad (147)$$

As indicated in Fig. 88, the turbulent fluctuations produce a marked change in the velocity curve, \bar{v}_x becoming more uniformly distributed throughout the greater part of the boundary layer. Consequently, in the boundary vicinity the gradient must be much steeper, particularly in the laminar sublayer. And since the gradient at the boundary itself, which actually determines the magnitude of τ_0 , is within the region of purely laminar motion, one can readily understand the reason for the increase in τ_0 when turbulence sets in. Furthermore, the intensity of the turbulence will increase with the Reynolds number; as a result, the greater the value of R_x , the more uniform will be the relative velocity distribution in the region of turbulent mixing. Yet since δ also increases with R_x , the velocity gradient at the boundary actually grows smaller; τ_0 thereby varies.

inversely with $x^{1/2}$. However, if the form of the velocity curve is thus to change with the Reynolds number, it is apparent that n cannot remain constant; although it is still approximately equal to $1/4$ well beyond $R_x = 10^7$, it gradually decreases with ascending values of R_x . The limit $n = 0$, therefore, would correspond to a Reynolds number approaching infinity.

Dissatisfied with the empirical nature of this development, in 1930 von Kármán extended his investigations leading to Eq. (123)

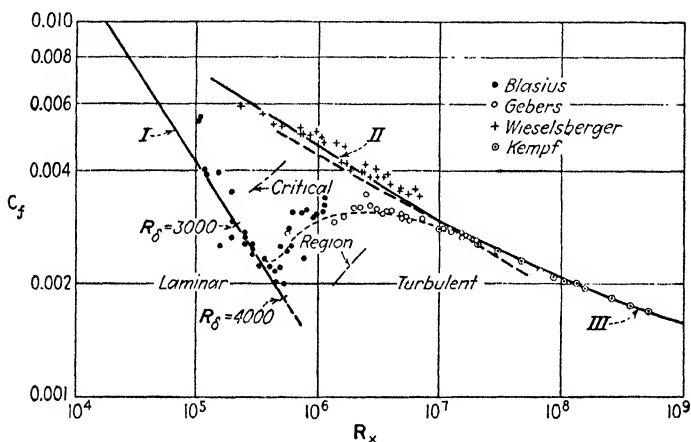


FIG. 90.—Coefficient of resistance for smooth plates as a function of the Reynolds number.

to the case of the turbulent boundary layer, obtaining the general expression

$$\sqrt{\frac{2}{C_f}} = \text{constant} + \frac{1}{\kappa} \ln (R_x C_f) \quad (148)$$

which applies equally well to the coefficient C_f . With numerical constants found experimentally, this becomes, for C_f ,

$$\frac{1}{\sqrt{C_f}} = 1.7 + 4.15 \log (R_x C_f) \quad (149)$$

Although the essential details of this derivation will be discussed in a later chapter on pipe flow, in Fig. 90 the reader will find comparative plots of Eqs. (137), (147), and (149) (Curves I, II, and III, respectively), from which may be obtained a general picture of boundary-layer development.

50. Separation and the Turbulent Wake. Three general characteristics of the boundary layer have been discussed in the foregoing pages: (1) within a very small distance normal to the boundary the velocity increases from zero to practically that of the corresponding potential motion; (2) the pressure intensity throughout the boundary layer is governed by the surrounding flow; (3) curvature of the boundary is of no consequence if the radius of curvature is great in comparison with the boundary-layer thickness. To these must now be added a fourth characteristic, the importance of which cannot be overemphasized.



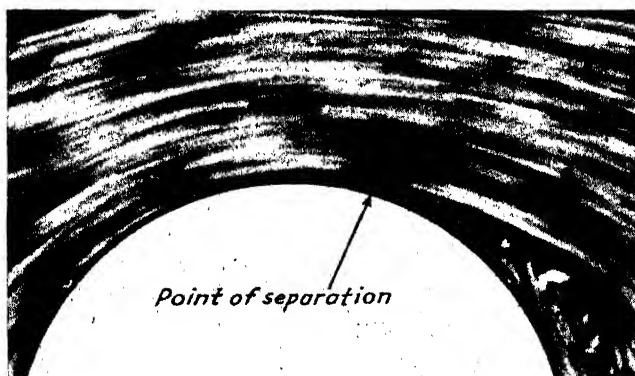
Columbia

FIG. 91.—Departure from pattern of potential flow at the edge of a thin plate.

So long as the pattern of the corresponding potential motion indicates either a constant or a steadily increasing velocity at the outer border of the boundary layer, the boundary pressure gradient in the direction of flow will be equal to or less than zero. Growth of the boundary layer will then proceed as described, energy dissipation taking place at the expense of the kinetic energy of the boundary flow. If, on the other hand, the potential pattern requires deceleration along the boundary, the decrease in velocity must be accompanied by a corresponding increase in pressure intensity, according to the basic principle of energy. Needless to say, this positive gradient would have to exist within the boundary layer as well as in the surrounding region of potential flow.

Nevertheless, energy once dissipated in the form of heat cannot be regained by the flow, from which it follows that the

kinetic energy lost in the growth of the boundary layer is no longer available for restoration of pressure; obviously, such restoration is essential if the potential motion is to continue. In other words, the existence of a boundary layer must tend to prevent any deceleration in the boundary region normally indicated by the pattern of potential motion. From this conclusion it would seem clear that flow under given geometrical boundary conditions is physically possible only if the potential pattern so modifies itself that no deceleration is required. This seemingly paradoxical statement merely signifies that the potential flow net must detach itself from the boundary at the



Columbia

FIG. 92.—Departure from pattern of potential flow at the boundary of a cylinder.

point where deceleration becomes appreciable, and beyond that point enclose a region of discontinuity instead of a solid boundary.

Separation of the flow from a boundary surface necessarily involves a complete change in the velocity distribution within the layer. This is indicated schematically in Fig. 93, in which conditions within the boundary layer are clarified by enlarging the scale of normal distance y . The point at which separation takes place is seen to be a point of stagnation on that stream line which divides the oncoming flow from the reverse flow of the region of discontinuity. As this point is approached, the velocity profile displays a gradual change in shape, the velocity gradient in the y direction becoming zero at the actual separation point. That the change in direction of curvature of the velocity profile is definitely connected with the pressure gradient may be seen

from Eq. (130), written for the boundary (*i.e.*, $v_x = 0 = v_y$ when $y = 0$):

$$\mu \frac{\partial^2 v_x}{\partial y^2} = \frac{\partial p}{\partial x}$$

Since $\partial v_x / \partial y$ indicates the slope of the velocity profile, $\partial^2 v_x / \partial y^2$ must show the rate of change of this slope with distance normal to the boundary. A reversal in curvature of the profile will then occur when $\partial^2 v_x / \partial y^2$ changes sign—simultaneous with a like change in sign of the pressure gradient.

It must not be concluded, however, that separation will invariably take place at the point at which the pressure gradient of the original potential motion becomes positive. Since separation produces a complete modification of the potential

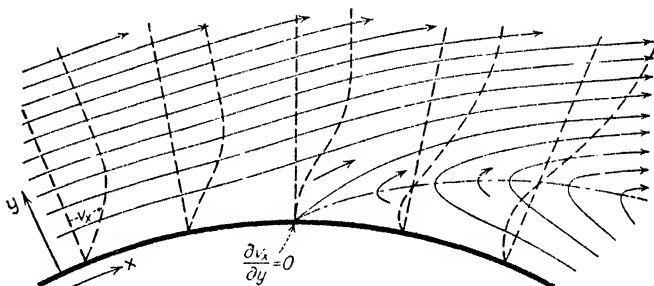


FIG. 93. - Separation of flow from a curved boundary; vertical scale is enlarged.

pattern, the force distribution in the resulting state of motion cannot be found directly from the geometry of the boundary surface—indeed, it depends to a considerable extent upon the stage of development already attained by the boundary layer in the upstream region. Owing to the more uniform velocity distribution in the turbulent layer, moreover, the latter is far less susceptible to separation than a layer in which the motion is still laminar; that is, a laminar boundary layer would lead to separation at an earlier point than a turbulent layer. Regardless of the exact point at which separation may be expected, it may definitely be stated that a region of appreciable deceleration is certain to cause separation if a boundary layer of either sort has formed. That the existence of a boundary layer actually is essential to separation was proved experimentally by Prandtl, who eliminated the effect in a diverging conduit by carefully drawing off the fluid of low velocity at the boundary.

The pattern of stream lines in Fig. 93 is typical of separation at relatively low values of the Reynolds number—in fact, the lower R , the more orderly and steady the flow in the region of discontinuity. While at low Reynolds numbers reverse flow displays the essential characteristics of laminar motion, as R increases, this region becomes even more susceptible to disturbing influences than the boundary layer itself. Once instability occurs in the wake of the boundary, the vortex that forms in the zone of reverse flow is swept downstream, whereupon another quickly forms and the process repeats itself. The rapidity of this intermittent action, as well as the speed of rotation of the vortex filament, increases with the Reynolds number. It is evident that such unsteady vortex motion in the region of separation must further modify the pattern of the surrounding flow. And since the interaction of these vortices rapidly produces true turbulent motion in the wake, the energy transfer of the turbulent process must lead to continuous growth of the wake with distance from the point of formation, the fluctuations thereby “decaying” as a result of viscous action.

Similar to conditions within the thin boundary layer, the mean pressure intensity within the turbulent wake is essentially the same as that of the surrounding flow, although the instantaneous magnitude of p depends upon the instantaneous velocity distribution within the vortex. Since the initial point of separation occurs in the region of lowest boundary pressure, it follows that the pressure intensity will remain at this low value along those portions of the boundary in contact with the wake. Furthermore, it is evident that the continual formation of vortices at the beginning of the region of discontinuity must represent a steady drain on the energy of flow. Thus, the phenomenon of separation not only modifies the force distribution along the boundary, but also results in energy loss to a marked degree.

CHAPTER XI

FLOW AROUND IMMERSED BODIES

51. Fundamental Concept of Drag. So long as the flow remains irrotational, a submerged body moving steadily through a fluid of constant density will experience no resistance to motion, for the resultant of the pressure distribution over the surface of any body in potential flow can never have a component in the direction of motion. Since the equations describing such motion involve only those forces due to fluid pressure, the resistance actually encountered in the movement of immersed bodies is evidently due either directly or indirectly to the influence of fluid viscosity.

From foregoing chapters, it will be apparent to the reader that viscous action may produce three essentially different types of resistance. At very low Reynolds numbers inertial effects caused by steady movement of a body are completely secondary to those of viscous stress, the latter then extending a great distance into the surrounding flow and causing more or less widespread distortion of the flow pattern; this type of resistance is known as "deformation drag." At much higher Reynolds numbers the region in which appreciable deformation occurs is limited to a thin fluid layer surrounding the body, the resulting shear along the boundary surface (regardless of whether the boundary layer is laminar or turbulent) then producing what is called "surface drag." Finally, if the form of the body is such that separation occurs, the low intensity of pressure in the wake leads to a resultant force which opposes the motion; since the magnitude of this force varies with the shape of the body, it is customarily termed "form drag." The latter is, however, a somewhat misleading expression, for the form and position of a body also determine to some extent the magnitude of the other two types of resistance.

Under favorable conditions form drag itself may reach such proportions as to reduce viscous stresses to relative insignificance. So far as form drag alone is concerned, one may distinguish

three different—though progressively related—types of body contour: (1) That in which the point of separation is determined almost wholly by angularity of profile, a thin flat plate normal to the flow being the simplest illustration of this case. (2) That in which the surface curvature is appreciable, yet gradual enough for the actual point of separation to be determined in part by conditions within the boundary layer; the sphere is an elementary example of this type. (3) That of such very easy curvature that the point of separation occurs close to the rear, the size of the wake thereby being reduced to a minimum as in the case of the streamlined body. Evidently, there must exist a gradual transition from one type to the next. It should also be obvious that form alone is not a sufficient geometrical criterion, for orientation with respect to direction of motion can play an important role; for instance, a thin flat plate moving parallel to its own plane represents the ideal limit of streamlining, although it presents extreme boundary angularity when turned through 90° .

If a boundary of the fluid exists in the neighborhood of the relative motion, additional complexities may be expected. A solid boundary, for example, will increase deformation drag through transmitted shear, or will alter the pressure distribution when inertial effects are involved. If the boundary is a free surface, wave motion may be produced, and thereby require additional expenditure of energy; such wave resistance is an essential part of the total resistance encountered by a moving ship. On the other hand, elastic waves will be propagated if a body moves through a fluid with a velocity greater than that of sound, again augmenting the drag. Such phenomena as these must be excluded from the following presentation.

The actual resistance encountered by an immersed body will then depend only upon the Reynolds number characterizing the motion and upon the geometrical form and orientation of the body. Dimensional analysis of the several variables involved in the general phenomenon will lead to the following expression for the resultant force opposing motion:

$$F = \varphi\left(\frac{VL}{\nu}, \text{form}\right) L^2 \rho V^2$$

The general form of this equation was first determined by

Newton, although through imperfect analysis of the actual mechanism of drag. Newton reasoned that the resisting force must be proportional to the rate at which the momentum of the fluid is increased by the passage of the body; φ would then necessarily be constant for a given body form. Moreover, such conditions would require a steady increase in the momentum of the fluid—a condition possible in non-viscous flow only if the body undergoes continuous acceleration. Actually, the only quantity which increases in steady motion is the amount of flow energy which has been transformed into heat through viscous shear.

The basic drag relationship is generally written in the more convenient form

$$F = \varphi(\mathbf{R}, \text{form}) A \frac{\rho V^2}{2} = C_D A \frac{\rho V^2}{2} \quad (150)$$

in which A represents the projected area of the body on a plane normal to the direction of motion, whereas C_D is a variable coefficient of drag:

$$C_D = \varphi(\mathbf{R}, \text{form}) = \frac{F}{A\rho V^2/2} \quad (151)$$

Only in the most elementary cases of deformation drag has it been possible to determine C_D analytically for certain basic body forms, although application of the boundary-layer equations to problems of surface drag of streamlined bodies has yielded quite satisfactory results. Cases of motion involving separation and the formation of a wake have been attacked from various angles, but such methods have provided at best only qualitative indications. Quantitative study of drag, therefore, has remained largely experimental, although analytical methods are still needed to systematize, explain, and extrapolate laboratory measurements.

Widespread interest in drag first arose among ship designers, since surface and form resistance account for an appreciable part of the total resistance of surface craft. Aeronautical engineers further stimulated drag investigation, for a knowledge of resistance plays an even more important role in the design of craft in which only very small "factors of ignorance" are permissible. In recent years the magnitude of wind action on such

stationary structures as buildings and bridges has been the subject of further resistance investigations, while the hydraulic engineer is beginning to realize that drag phenomena are to be encountered in practically every type of flow with which he deals.

Since the mechanism of drag is essentially the same in all of these fields, the methods of approach to the general problem vary only slightly. The magnitude of the total resistance for a given body form is usually determined experimentally as a function of R , either in the wind tunnel or the towing tank, the body being held stationary in the first case, and moved with constant velocity in the second; needless to say, bodies may be moved through still air, or suspended in moving water, with similar results. Practical considerations have limited fluid media to air and water, except in special instances, although the variable-density wind tunnel has enabled greater latitude in the parameter R by using air under high pressure. In any case, the total resistance is measured by some form of balance, the pressure distribution over the surface of the body being determined piezometrically whenever desired; velocity distribution is generally of secondary importance. From these data the mechanics of the drag phenomenon may be studied in detail.¹

Since the fundamental variation of C_D may best be understood through analysis of the elementary profiles, in the following pages considerable attention will be paid to the drag of spheres, cylinders, flat plates, and airfoil sections, followed by a limited discussion of the more complex cases. Application to problems of flow in closed and open conduits will be found in succeeding chapters.

52. Resistance of Spherical Bodies. Stokes was the first to determine analytically the deformation drag encountered by a sphere falling steadily through a fluid as a result of its own weight.² Proceeding from the Navier-Stokes relationships, and assuming that the terms for convective acceleration could be ignored completely in comparison with those for viscous shear, he ultimately obtained the equation

¹ The reader will find abundant experimental material in the numerous Technical Reports and Memoranda of the National Advisory Committee for Aeronautics.

² STOKES, G. G., *Cambridge Trans.*, vol. 9; "Collected Papers," vol. III. See LAMB, "Hydrodynamics," pp. 597-604, or PRANDTL, "Aerodynamic Theory," vol. 3, pp. 71-75.

$$\frac{2}{9}(\gamma_s - \gamma_f) = \frac{\mu V}{r^2} \quad (152)$$

in which r is the radius of the sphere and $(\gamma_s - \gamma_f)$ the difference between the specific weights of sphere and fluid.

Since the resultant force upon the body must equal the specific-weight difference times the volume of displaced fluid, Stokes' expression may be given the following form, corresponding to that of Eq. (150):

$$F = \frac{4\pi r^3}{3}(\gamma_s - \gamma_f) = 6\pi\mu rV = \frac{24}{\frac{VD\rho}{\mu}} A \frac{\rho V^2}{2} \quad (153)$$

Evidently, introduction of ρ is merely a convenient means to an end, since true deformation drag is independent of fluid density (inertial effects being negligible) and varies with the first power of the velocity. It is now apparent, however, that under these circumstances the coefficient of drag will have the magnitude

$$C_D = \frac{24}{R} \quad (154)$$

The Stokes relationship has found extensive application in the study of the rate of settlement of very small particles of solid matter through liquids and gases. Nevertheless, it must be noted that in the case of deformation drag the proximity of boundary surfaces will markedly augment the resistance—such effects being measurable even for boundary distances of considerably greater order than the diameter of the particle. These effects may be taken into account through use of a correction factor determined analytically by Ladenburg;¹ with slight modification of the second numerical term, as noted by Faxén,² this factor is of the form

$$\left(1 + 2.1 \frac{D}{L}\right)$$

for a sphere moving along the axis of a cylinder of diameter L .

¹ LADENBURG, R., Ueber den Einfluss von Wänden auf die Bewegung einer Kugel in einer reibenden Flüssigkeit, *Ann. Physik*, vol. 23, 1907.

² FAXÉN, H., "Einwirkung der Gefäßwände auf den Widerstand gegen die Bewegung einer kleinen Kugel in einer zähen Flüssigkeit." Uppsala 1921.

It has been pointed out by Oseen and others that the accelerative terms neglected by Stokes are actually of lower order than those for viscous stress only in the neighborhood of the body, whereas at a considerable distance the situation is quite the reverse. Oseen, therefore, attempted an improvement¹ upon the Stokes analysis by retaining certain of the neglected terms, with the approximate result:

$$C_D = \frac{24}{R} \left(1 + \frac{3}{16} R \right) \quad (155)$$

Goldstein,² in turn, obtained the following exact solution of Oseen's analysis:

$$C_D = \frac{24}{R} \left(1 + \frac{3}{16} R - \frac{19}{1280} R^2 + \frac{71}{20,480} R^3 - \dots \right) \quad (156)$$

It is evident that both the Oseen and the Goldstein equations approach that of Stokes as R becomes less than about 0.1. Indeed, the Stokes relationship has been proved valid experimentally up to this limit. Oseen's expression yields good results somewhat beyond that of Stokes, whereas Goldstein's is trustworthy to approximately $R = 2$.

With increasing values of R , marked deviation from experimental evidence is shown by all three equations. Although slight discrepancies at lower Reynolds numbers may be attributed to the simplifying assumptions regarding inertial effects, the latter become of paramount importance as the region of appreciable viscous deformation is gradually restricted to the immediate neighborhood of the boundary surface. But at the same time that a true boundary layer develops, the rapid deceleration of flow toward the rear of the sphere also tends to produce boundary-layer separation. The resulting wake behind the body is at first laminar; but as the Reynolds number increases, flow in the wake becomes unstable, and finally the body leaves in its course an expanding trail of eddies. Under such circumstances, the boundary resistance over the front surface of the sphere is

¹ OSEEN, C. W., "Neuere Methoden und Ergebnisse in der Hydrodynamik," Akademische Verlagsgesellschaft, Leipzig, 1927. See LAMB, pp 608-617, or PRANDTL, pp. 75-80.

² GOLDSTEIN, S., The Steady Flow of Viscous Fluid past a Fixed Spherical Obstacle at Small Reynolds Numbers, *Proc. Roy. Soc. (London)*, A, vol. 123, 1929.

comparatively slight, from which it may be expected that the drag coefficient will then be practically independent of R —hence, directly proportional to the square of the velocity.

Such progressive developments in the resistance of the sphere may be followed closely in a plot of the drag coefficient against the Reynolds number, logarithmic coordinate scales showing the successive stages to best advantage. In Fig. 94 the Stokes relationship is indicated by a straight line with the slope -1 ,

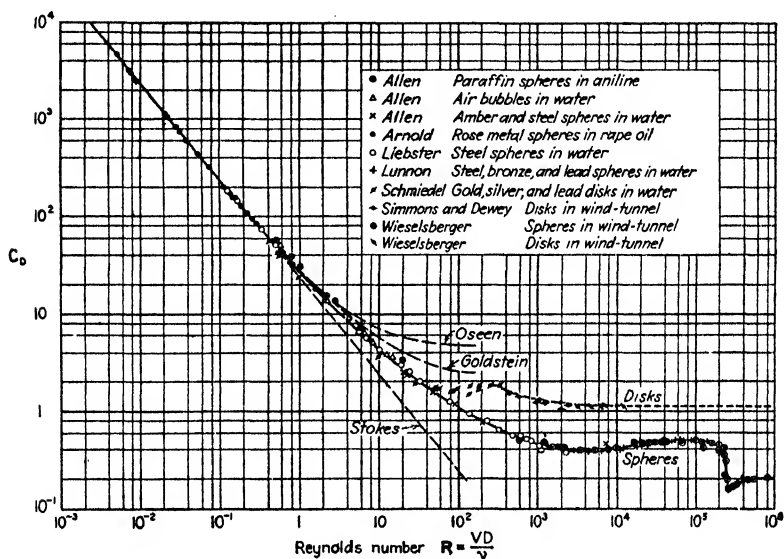


FIG. 94.—Drag coefficients for spheres and disks as functions of the Reynolds number.

while the upper curves correspond to the equations of Oseen and Goldstein. Experimental data obtained by a great many investigators under a wide variety of conditions¹ form the basis for the full line, which is seen to lie between Stokes' and Goldstein's plots as the region of deformation drag is passed. Development of the true boundary layer, as the inertial qualities of the motion become important, leads to the gradual upward trend

¹SCHILLER, L., Fallversuche mit Kugeln und Scheiben, "Handbuch der Experimentalphysik," vol. IV-2, Akademische Verlagsgesellschaft m. b. H., Leipzig, 1932; ROUSE, H., Nomogram for the Settling Velocity of Spheres, *Annual Report, Committee on Sedimentation*, National Research Council, 1937.

in the experimental curve, whereas the growth of eddies in the wake produces the more abrupt rise. Once the wake is fully turbulent, the curve becomes essentially horizontal, indicating almost complete independence of the drag from the Reynolds number.

Although surface resistance is then quite secondary to that of form, it must not be assumed that the boundary layer has no further influence upon the flow. So long as flow in the boundary layer remains laminar, the point of separation will lie somewhat ahead of the plane of maximum cross section; once the boundary layer becomes turbulent, however, the energy transfer within the turbulent region abruptly reduces the tendency toward reversal of flow, whereupon the point of separation is shifted toward the rear of the sphere. The accompanying reduction in size of the turbulent wake decreases the area of low pressure at the rear of the sphere, the change in the pattern of the surrounding flow also reducing the magnitude of the pressure intensity, with a corresponding drop in the resistance to motion. Under normal conditions this change will occur at the value of R indicated in Fig. 94, but Prandtl has caused this to take place much earlier by fastening a wire around the front of the sphere to produce artificial turbulence in the boundary layer.¹

The fact must be emphasized that if such experiments are conducted with a stationary body and a moving fluid (as in the case of a wind tunnel), initial turbulence of the approaching flow will have a marked effect upon the measured drag, the magnitude of this effect depending upon the degree of turbulence and the Reynolds number of the mean flow. Moreover, surface roughness may also produce an earlier transition from the laminar to the turbulent boundary layer, and thus further influence conditions in the wake. These factors have not yet been investigated so systematically as to warrant more than general comment at this time.

53. Drag Characteristics of the Cylinder. As will be seen from Fig. 95, the resistance coefficient for an extremely long circular cylinder, with axis normal to the direction of motion, varies with the Reynolds number in much the same way as that for a sphere. The differences in numerical values, as well as

¹ The change in size of the wake may be seen from the photographs in Plate 14, of PRANDTL-TIETJENS' "Applied Hydro- and Aeromechanics."

slight local changes in the function, merely distinguish parallel cases of two-dimensional and three-dimensional motion. Owing to mathematical difficulties, solution for the deformation drag of the cylinder at low values of R after the manner of Stokes has not proved possible, but Lamb¹ has succeeded in obtaining an equation corresponding to that of Oseen, the form of which is shown by the broken line in the illustration. It is apparent,

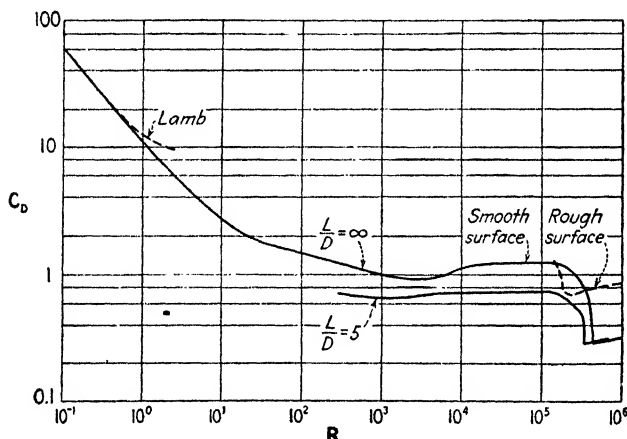


FIG. 95.—Drag coefficients for circular cylinders.

however, that the curve for very small values of R is asymptotic to a straight line with the slope $-\frac{3}{4}$.

Because of the two-dimensional symmetry of the cylinder, the initial separation is evidenced by the formation of two symmetrical vortices directly behind the profile; these vortices grow in size with increasing Reynolds number, and eventually reach such a stage of development that they pass off together into the wake, whereupon two more form to replace them. Under such circumstances, the wake will consist of a series of vortex pairs, as shown schematically in Fig. 96*a*, the velocity of the vortex system relative to that of the body being less than that of the surrounding fluid.

Such a system is unstable, however, and at higher values of R the vortices begin to alternate in formation and in departure into the wake. Two-dimensional vortex trails of this nature

¹ LAMB, "Hydrodynamics," pp. 614-616.

were studied analytically by von Kármán,¹ without regard to the viscous stresses involved; he not only proved that the symmetrical series of vortex pairs must be unstable to small oscilla-

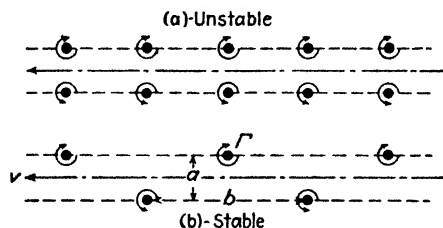


FIG. 96.—Vortex trails.

tions, but showed that alternate vortices (Fig. 96b) will be stable if arranged according to the expression

$$\frac{a}{b} = \frac{1}{\pi} \cosh^{-1} \sqrt{2} = 0.2806$$

He obtained in addition an equation for the velocity of the vortex system,

$$v = \frac{\Gamma}{b\sqrt{8}}$$

Although these expressions are in close accord with experimental measurement, it is apparent that they contain no reference either to the dimensions of the body producing the wake or to the relative velocity between the body and the undisturbed fluid.



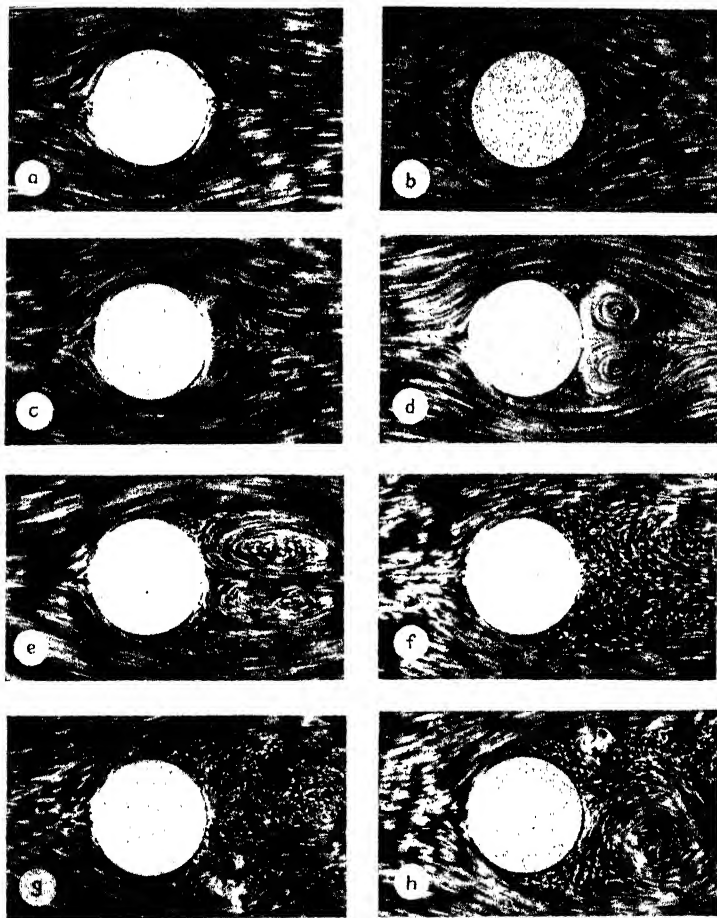
FIG. 97.—Instantaneous stream lines of the Kármán vortex trail.

It has been found, however, that if the magnitudes of the ratios b/D and v/V are determined experimentally, these relationships may be used to compute the drag of the long cylinder (and of other “two-dimensional” bodies as well) with a fair degree of accuracy.

The cylindrical body lends itself very conveniently to visual and photographic studies of vortex behavior in the wake, the

¹ KÁRMÁN, TH. VON, Über den Mechanismus des Widerstandes, den ein bewegter Körper in einer Flüssigkeit erfährt, *Nachr. Ges. Wiss. Göttingen*, 1911-1912.

flow pattern being made visible through introduction of finely divided particles of solid or fluid matter, such as aluminum flakes or drops of an immiscible oil. With satisfactory illumination, a short time exposure of relative motion at any Reynolds number



Columbia

FIG. 98.—Development of the wake behind a cylinder.

will yield excellent instantaneous flow patterns, the direction of the stream lines and the relative magnitudes of the velocities being indicated by the short paths of the brilliantly lighted particles during the interval of exposure. In Fig. 98 are repro-

duced a series of photographs made in this way, which are qualitatively indicative of the conditions at various magnitudes of R . It must be remarked, however, that these pictures represent the sequence of events as a body is accelerated from a state of rest, conditions in the wake then depending in part upon

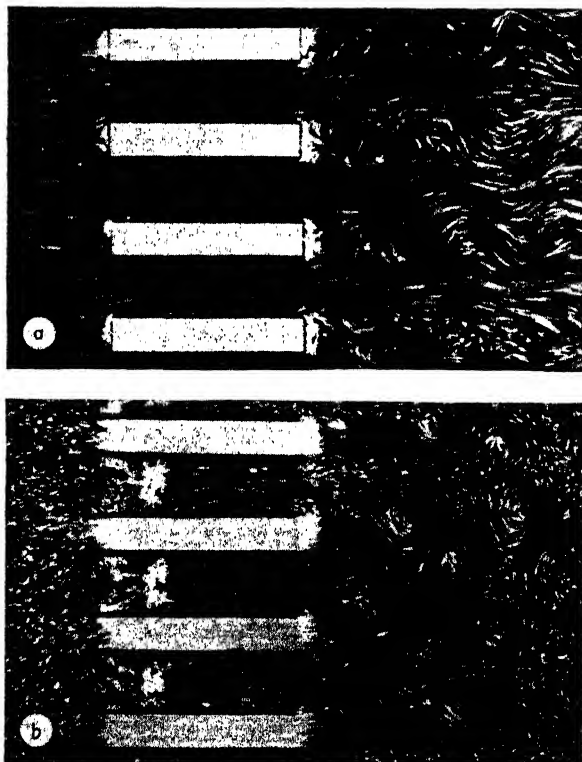


FIG. 99.—Kármán vortex trails in the wake of a grid.

development of the boundary layer with time. In Fig. 99, furthermore, the reader will find photographs of the vortex trails produced by the parallel bars of a grid. In one case (a) the camera moved with the grid, in the other case (b) remained at rest with respect to the undisturbed fluid; since the velocity of any such vortex system differs from that of either body or fluid, in neither case do the vortices yield patterns of steady motion. However, the relationship of the two velocity fields is clearly visible, as

well as the gradual dissolution of the vortex motion into true turbulence as the distance from the grid increases.

Such unsymmetrical vortex development behind the cylinder must evidently give rise to a side thrust that continually reverses its direction. If the cylinder is not rigidly supported, it will tend to oscillate from one side to the other, in particular if its natural period of vibration is in resonance with the frequency

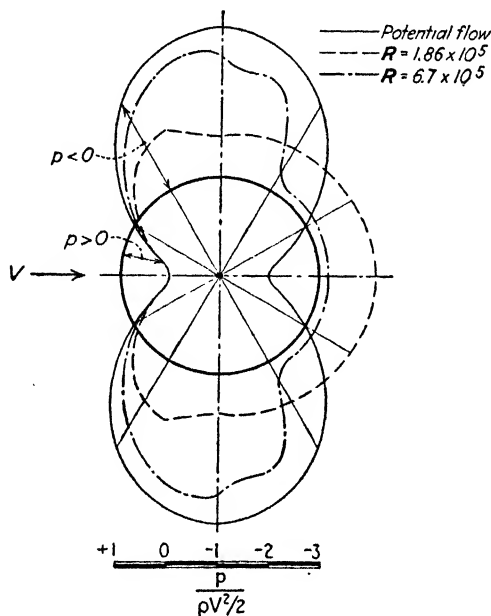


FIG. 100.—Pressure distribution around a circular cylinder.

of the vortex formation (witness the tendency of telephone wires to “sing” at certain wind velocities).

If one consider only the mean distribution of pressure intensity, a very illuminating portrayal of the forces involved in the form drag itself is to be found in the accompanying reproduction of pressure measurements made by Eisner¹ (Fig. 100). The relative pressure curve—the dimensionless parameter $\frac{p}{\rho V^2/2}$ representing the ratio of actual pressure to the stagnation pres-

¹ EISNER, F., “Widerstandsmessungen an umströmten Zylindern,” Mitteilungen der Preussischen Versuchsanstalt für Wasserbau und Schiffbau, Springer, Berlin, 1929.

sure of the oncoming flow—under conditions of potential motion is seen to be symmetrical about both axes. In the subcritical range (*i.e.*, for a laminar boundary layer) the relative pressure in the fully developed wake is very low and extends over more than half the boundary. In the supercritical range, turbulence

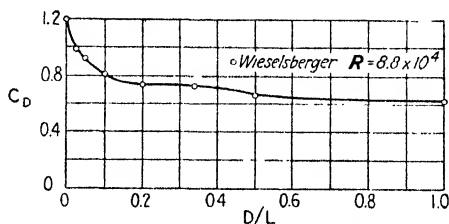


FIG. 101.—Coefficients of drag for cylinders of finite length.

within the boundary layer has not only made the wake effectively smaller, but raised the relative pressure in this region.

At either end of a cylinder of finite length the motion will necessarily be three-dimensional. In the end zones there will

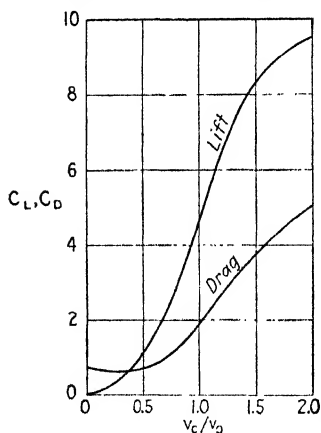


FIG. 102.—Coefficients of lift and drag for a rotating cylinder.

no longer be a region of high stagnation pressure in front of the cylinder, for the fluid tends to “leak” around the end into the region of low pressure in the wake. Evidently, the extent to which end effects modify the drag of the cylinder as a whole will depend largely upon the relative magnitudes of length and diameter. The larger the ratio D/L , the lower the value of C_D (refer to Fig. 101); on the other hand, as D/L approaches zero, conditions become more nearly those already discussed.

In Chapter V it was shown that the combination of circulation and parallel flow around a cylinder would produce a resultant pressure action normal to the direction of parallel motion. Such circulation may be effected in the neighborhood of an immersed cylinder by viscous shear if the cylinder is rotated about its axis, although the surrounding velocity field will not be identical with that of potential motion. Nevertheless, simultaneous

translation and rotation of a cylinder in a viscous fluid will actually result in a force vector having components both parallel and normal to the direction of translation. Needless to say, the drag and side thrust are by no means independent of one another, indeed, the point of separation is shifted considerably on either side, since the fluid in the boundary layer tends to rotate with the body. Experimental measurements of the two force components are customarily plotted as indicated in Fig. 102, C_L denoting the coefficient of side thrust or "lift."

54. Lift and Drag of the Airfoil. Although lift can be produced on a symmetrical body such as the cylinder or sphere only by actual rotation of the body (note the tendency of a

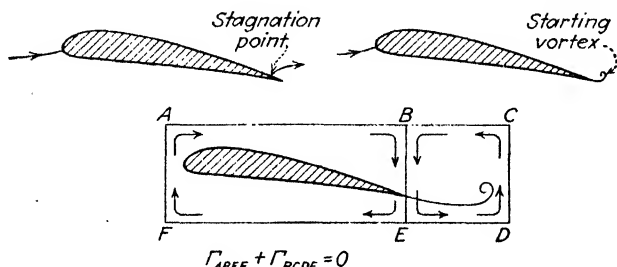


FIG. 103.—Circulation around an airfoil starting from rest.

spinning ball to curve in flight), separation at one side of an unsymmetrical body will also result in circulation, and thus give rise to a very useful normal force component. Since such lift is the very basis of performance in the case of an airplane wing or the blade of a turbine or propeller, efforts have long been made to develop body profiles having the maximum lift and the minimum drag coefficients for the given conditions of flow. Proceeding with the Joukowski profile, the airfoil has gradually been perfected, until today abundant information exists for a wide variety of shapes.

A brief description has already been given of the Joukowski transformation and the accompanying pattern of flow, mention having been made of the fact that the region of high velocity at the sharp trailing edge could be avoided by superposing upon the parallel motion a circulation of such magnitude that the flow would leave the trailing edge in a tangential direction. This is, in effect, what actually occurs. While the flow around an airfoil is truly potential at the instant motion begins, the very high

velocity at the trailing edge immediately causes the formation of a "starting vortex." As the vortex develops, the point of stagnation on the upper boundary surface moves toward the rear and finally vanishes at the trailing edge, yielding a velocity distribution around the foil (higher above, lower below) that is fully

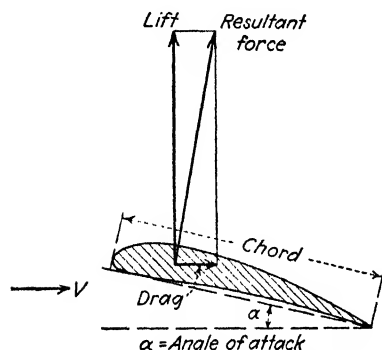


FIG. 104.—Airfoil characteristics.

characteristic of circulation. Moreover, the circulation of the starting vortex is exactly equal and opposite, so that around a closed curve including both vortex and airfoil (Fig. 103) the circulation will continue to have a magnitude of zero—in perfect accord with Thomson's law (refer to page 80).

It is evident that the lift and drag of the airfoil will depend upon the Reynolds number of the flow as well as upon the form and position of the profile. But since such foils are normally used at relatively high values of R , viscous resistance within the boundary layer is generally secondary to the influence of form and position upon the point of separation—and hence upon the lift and drag.

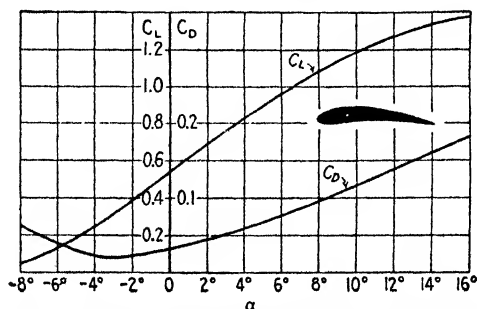


FIG. 105.—Coefficients of lift and drag for a typical airfoil.

From Fig. 104 may be seen the essential characteristics of a typical foil profile. Since the projected area as normally defined would change with angle of attack, it is customary to regard A as the product of chord and span. The coefficients C_D and C_L then become

$$C_D = \frac{\text{drag}}{A\rho V^2/2}; \quad C_L = \frac{\text{lift}}{A\rho V^2/2} \quad (157)$$

Unless these coefficients are considered to apply to an infinite width of foil (or to conditions at a given cross section), the fact that end effect may have a considerable influence upon the total lift and drag of a foil of finite span makes it essential to specify the aspect (span-chord) ratio for the airfoil so described. In Fig. 105, for instance, will be found plots of C_L and C_D as functions of angle of attack for a typical foil with an aspect ratio of 5:1. The same information is presented more compactly in Fig. 106 in the form of a polar diagram, with C_L a function of C_D .

From either diagram it will be apparent that increasing the angle of attack will at first increase the coefficient of lift—because of increased circulation—but at the same time the wake also becomes larger, and thus causes greater drag. Eventually, however, the point of separation will have moved so far forward

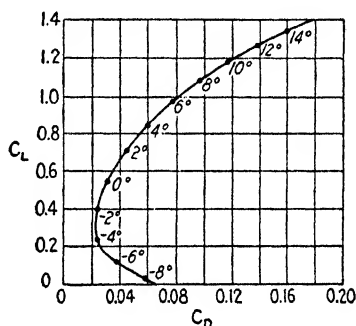
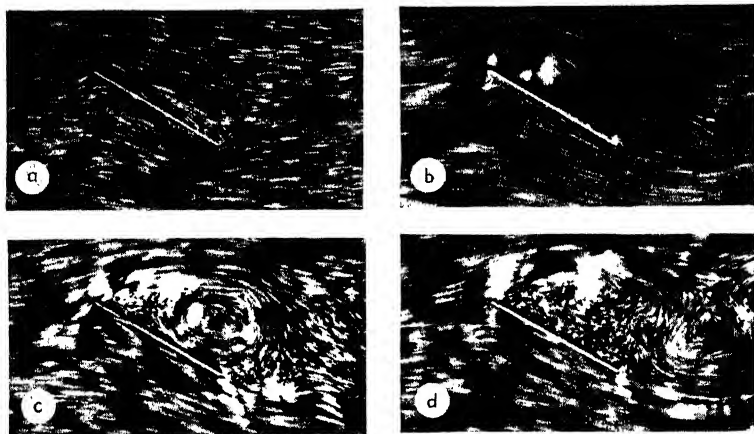


FIG. 106.—Polar diagram corresponding to Fig. 105.

on the foil that further increase in the angle of attack can only serve to reduce the lift, the drag coefficient at the same time increasing rapidly. The relative magnitudes of lift and drag may be controlled over a wide range, through variation of the airfoil shape to meet the particular requirements of a given problem. Application of these elementary principles to aeronautics and to such hydraulic fields as propeller, pump, and turbine design may be found in standard references.¹

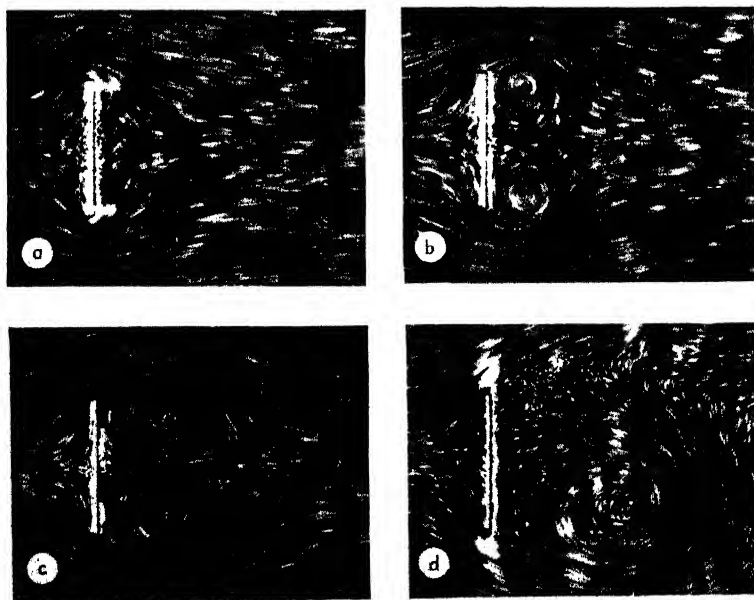
55. Relative Drag of Miscellaneous Profiles. Since development of the airfoil proceeded from the simpler case of a flat plate held at an angle to the flow, it is evident that such plates must also encounter both lift and drag. Owing to the size of the wake (Fig. 107) the lift is relatively small, and it was soon found that if the plate is given both camber and properly varied

¹ N.A.C.A. Technical Reports; PRANDTL-TIETJENS, "Applied Hydro- and Aerodynamics," Chap. VI; KAUFMANN, "Hydromechanik," vol. 2, Chap. VII.



Columbia

FIG. 107.—Flow past an inclined plate.



Columbia

FIG. 108.—Development of the wake behind a plate held at right angles to the flow.

thickness (as in the Joukowski transformation) the lift-drag ratio may be greatly increased. For such reasons, the problem of inclined plates has become largely an academic one.

In Fig. 108 will be found a number of photographs of the wake produced by a thin flat section, the sequence again proceeding from a state of rest. In each case it will be noted that the actual point of separation lies at the edge of the plate. Indeed, if the

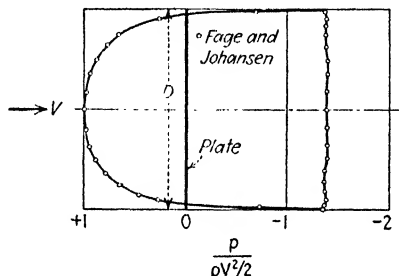


FIG. 109.—Mean pressure distribution over a plate of infinite length.

plate is normal to the flow, surface drag is of no consequence whatever, as may be seen from the diagram of mean pressure intensity in Fig. 109. It is obvious, however, that the length, as well as the width, of a rectangular plate must play an appreciable role in determining the over-all form resistance, the coefficient of drag approaching a constant limit only as the length

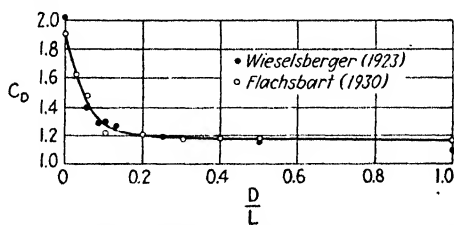


FIG. 110.—Drag coefficients for plates of finite length.

becomes very great—the problem thereby becoming essentially two-dimensional. From Fig. 110 may be seen the trend of the drag coefficient as the width-length ratio varies.

Inasmuch as two-dimensional flow past an infinitely long plate corresponds to three-dimensional flow around a circular plate, it is apparent that the foregoing general conclusions must apply equally well to the latter case of motion. Measurements of

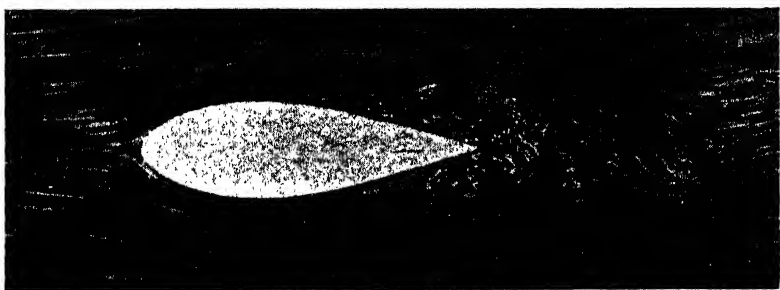
TABLE III.—APPROXIMATE VALUES OF DRAG COEFFICIENT AND DISK RATIO FOR VARIOUS BODY FORMS

Form of body	L/D	R	C_D	Disk ratio
Circular disk		$>10^3$	1.12	
Tandem disks (L = spacing)	0	$>10^3$	1.12	1.0
	1		0.93	0.83
	2		1.04	0.93
	3		1.54	1.37
Rectangular plate (L = length)	1	$>10^3$	1.16	
	5		1.20	
	20		1.50	
	∞		1.95	
Circular cylinder (axis \parallel to flow)	0	$>10^3$	1.12	1.0
	1		0.91	0.81
	2		0.85	0.76
	4		0.87	0.78
	7		0.99	0.88
Circular cylinder (axis \perp to flow)	1	10^5	0.63	
	5		0.74	
	20		0.90	
	∞		1.20	
	5	$>5 \times 10^5$	0.35	
	∞		0.33	
Streamlined foil (1:3 airplane strut)	∞	$>5 \times 10^4$	0.10	
Hemisphere: Hollow upstream		$>10^3$	1.33	1.19
Hollow downstream			0.34	0.30
Sphere		10^5	0.47	0.42
		$>3 \times 10^5$	0.20	0.18
Ellipsoid (1:3, major axis \parallel to flow)		$>2 \times 10^5$	0.06	0.054
Airship hull (model)		$>2 \times 10^5$	0.042	0.038

the drag encountered by such a disk held normal to the flow indicate that the coefficient of drag is practically constant over a wide range of R — $C_D = 1.12$ —a value so obviously a convenient

reference that it is frequently accepted as such. Thus, the "disk ratio" of a given body represents the ratio of its drag to that of a disk having the same projected area. Only if the body is circular in cross section will its disk ratio—numerically equal to the ratio of its drag coefficient to the value 1.12—be significant.

In Table III the reader will find disk ratios for a number of elementary body forms. Since these ratios will vary with the Reynolds numbers in the majority of cases, the given values should serve only as a basis for comparison, an actual plot of C_D as a function of R always being preferable. One may see at a glance, however, the essential effect of change in form, proper



Columbia

FIG. 111.—Flow around a streamlined body. The wake is further reduced in size when the boundary layer becomes turbulent.

streamlining reducing the wake—and hence the drag—to a surprisingly low relative magnitude. While the recent vogue of streamlining almost every possible type of body has often produced results more ornamental than practical, the fact remains that reduction in size of the wake behind a moving body not only lowers the rate of energy loss but makes the problem more susceptible to analytical solution.

56. Wind Pressure. Although airplane and propeller designers are primarily concerned with total lift and drag, and hydraulicians with the energy loss caused by separation, there are certain problems which require a knowledge of the pressure distribution over the surface of a body exposed to fluid motion; in particular is this true in the design of structures to be erected in regions subject to winds of appreciable magnitude.

Certain structural forms are so similar to the elementary bodies already discussed that the corresponding drag relationships may be expected to yield quite satisfactory results. For instance,

such cylindrical structures as chimneys, oil and gas tanks, masts, pipes, and conduits differ from the elementary cylinder of finite length only in that they are generally in contact with a plane boundary (such as the earth) at one or both ends. But at the same time that this reduces or completely eliminates the end effect of "leakage," the reduced velocity near the plane boundary will have an influence of approximately the same order of magnitude. It must be noted, however, that the effect of boundary roughness may be appreciable, and hence laboratory experiments on smooth models are not properly transferable.

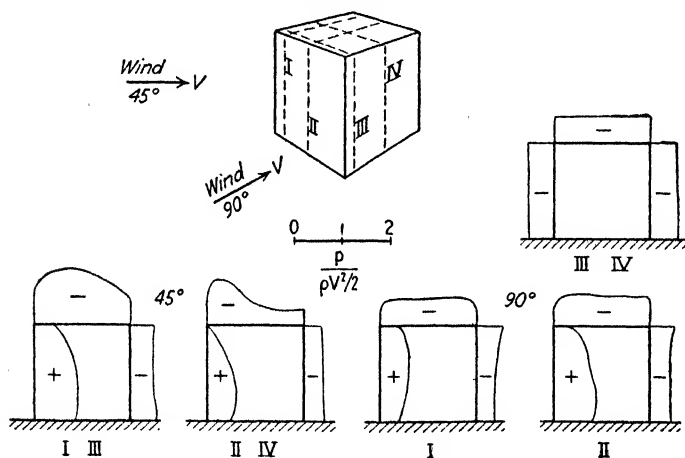


FIG. 112.—Distribution of wind pressure on an elementary building.

The majority of structural forms are by no means so simply handled. Yet so far from streamlined are present-day buildings that one fact can safely be asserted: wind pressure on the average structure may be considered a function of form and position alone, without regard to the magnitude of the Reynolds number. Evidently, early practice of computing the force of wind on the basis of the stagnation effect on the windward side was not in error because of neglect of viscous influence; in fact, such structures were amply strong to resist positive pressure of any probable magnitude. The fallacy in these methods lay rather in widespread ignorance of the fact that the more effective negative pressures on the leeward side are always distributed over a far greater area, with the result that buildings that failed through improper design usually blew out instead of in.

So complex and unsymmetrical are the forms of buildings and their orientation with regard to variable wind direction that analytical solution of pressure distribution is still completely out of the question. However, wind-tunnel tests on building models are satisfactory and economical means of investigation, although it should be apparent to the reader that such studies might just as well be conducted in the towing tank or in a channel of flowing water. Results of such experiments on a simple type of building are presented in dimensionless form in Fig. 112. It is quite apparent that negative pressures may produce resultant forces far greater than the positive—a situation particularly dangerous if the structural members have been designed for exactly the opposite type of stress.

Needless to say, the accompanying diagram can give at best merely an indication of the complex distribution of wind force on office buildings, factories, railroad stations, and the like, partially open as many are, and located in close proximity to others of different form. Only laboratory investigation can provide adequate quantitative information, although sound knowledge of flow principles may prevent many a serious blunder in design.

CHAPTER XII

FLOW IN CLOSED CONDUITS

57. General Aspects. Essential as the closed conduit has become to civilization, the engineer has been forced to depend to a great extent upon formulas for discharge and energy loss developed many decades ago, with only slight modification from time to time in acknowledgment of fresh experimental data. Fortunately for the practical engineer, the subject of pipe resistance has been well suited to empirical investigation, for the one-dimensional method of treatment is simple to an extreme, and a well-chosen coefficient is all that is needed to make the engineering adaptation of the Bernoulli theorem a handy tool. On the other hand, this apparent simplicity of the phenomenon has tended to confine hydraulic advancement to a course set long ago—for recent developments of vast importance to the hydraulic engineer have come largely from outside the hydraulic world. Far from being as simple as it appears, flow in closed conduits actually involves every phase of confined motion that has been discussed in the foregoing chapters of this book.

By far the most elementary type of conduit is straight, smooth, and of uniform circular cross section; similarly, the most elementary type of fluid movement through this conduit is uniformly laminar. From the analysis of Chapter X, it is evident that the resistance to such motion corresponds generally to deformation drag in the case of immersed bodies at low Reynolds numbers, for inertial effects are completely absent and the viscous influence extends to the innermost region of the flow. From the point of view of establishment of motion, however, it should be clear that at the very beginning of the conduit—if the latter leads from a large reservoir—the motion must be essentially one of constant energy; it follows that a laminar boundary layer must commence to develop over the entire inner surface at the entrance, growing in thickness with distance in the direction of flow as indicated by Eq. (132). Evidently, the uniform motion is fully established (Fig. 113) only as the effective

boundary-layer thickness becomes equal to the radius of the conduit. During this development the factor K_e will vary from 1 to 2, as indicated by the energy diagram.

If the Reynolds number of the flow is above the critical, and if initial disturbances of sufficient magnitude are present, the boundary layer will become turbulent before reaching the centerline of the conduit; further growth will then correspond to the conditions expressed by Eq. (141). It is apparent that such circumstances are displayed in the Reynolds apparatus

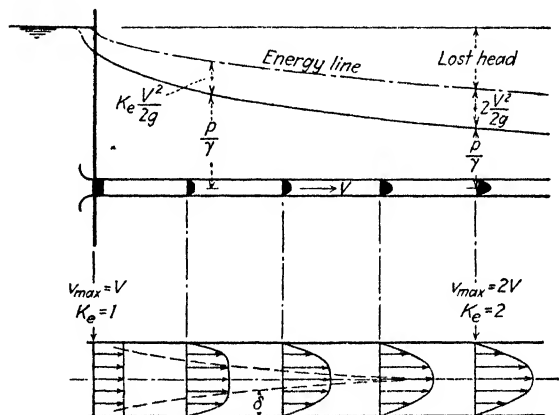


FIG. 113.—Establishment of laminar flow in a circular pipe.

previously described, in which the initial formation of eddies takes place outside of the central region of undisturbed flow. Moreover, the existence of a laminar sublayer is definitely indicated by traces of dye that persistently cling to the walls of the glass tube, moving forward comparatively slowly and without diffusing.

From this point of view, once flow is established the entire body of moving fluid might be regarded as the boundary layer. It will be realized, nevertheless, that conditions of motion differ from those discussed in Chapter X, in that the latter deals specifically with non-uniform flow, whereas in the case of the uniform conduit boundary-layer growth has reached an end at the section at which the flow is fully established. In the sense that established laminar flow was suggested as the counterpart of deformation drag, moreover, it has seemed more expedient to treat the laminar sublayer at the wall of the conduit as the effective bound-

ary layer, the high intensity of boundary shear in this layer thereby producing the counterpart of surface drag. From both dimensional and mechanical aspects, the characteristics of such established motion must depend entirely upon the magnitude of the Reynolds parameter.

Form drag, on the other hand, is primarily a function of geometrical boundary conditions. And while a straight pipe of circular cross section is nominally uniform in diameter, its boundary surface is actually covered with innumerable geometrical irregularities, the size, form, and distribution of which may vary between wide limits. It might be reasoned that the degree of roughness of a boundary surface is a relative quality, the effect of roughness of some characteristic linear dimension depending upon its magnitude in comparison with the diameter or radius of the conduit—that is, upon some relative-roughness parameter. Such reasoning is well vindicated by experiment. Further reflection might then lead to the conclusion that roughness influence could also depend upon the relative dimensions of the average roughness element and the boundary layer, since surface roughness that is wholly enveloped by the laminar film of the conduit must have a totally different influence from that which is coarse enough to disrupt the laminar boundary flow. Once again, laboratory measurements have thoroughly substantiated this conclusion.

Thus, form drag in straight circular conduits may be caused by geometrical irregularities in the boundary surface, the wake of an isolated body immersed in a flow being reproduced, in effect, behind each individual roughness projection. Needless to say, the net result must depend upon a complex process of mutual interaction and interference, but the mechanism is essentially the same. Moreover, just as certain angular body profiles show an influence that is nearly independent of viscous influence, certain types of roughness display identical characteristics at sufficiently high Reynolds numbers, whereas other types produce a boundary drag that varies continuously with increasing magnitude of R .

Although the ratio of boundary-layer and roughness dimensions has been stated to indicate the character of the roughness influence, it must be recalled that the relative thickness of the boundary layer itself is a function only of the Reynolds number.

Dimensionally, therefore, the mean intensity of boundary drag or shear may be expressed in the following form:

$$\tau_0 = \varphi\left(\frac{VD}{\nu}, \text{rel. roughness}\right) \frac{\rho V^2}{2} \quad (158)$$

This relationship is seen to be practically identical with that for the drag of an immersed body. In terms of rate of energy loss with distance in the direction of flow,

$$-\frac{\partial}{\partial x}(p + \gamma h) = f\left(\frac{VD}{\nu}, \text{rel. roughness}\right) \frac{\rho}{D} \frac{V^2}{2} \quad (159)$$

$$-\frac{\partial}{\partial x}\left(\frac{p}{\gamma} + h\right) = f\left(\frac{VD}{\nu}, \text{rel. roughness}\right) \frac{1}{D} \frac{V^2}{2g} \quad (160)$$

If the conduit is now presumed to vary in cross section, it is apparent that the analogy is even more apt. Non-uniformity of section indicates that—aside from the dynamics of the flow as a whole—further development within the boundary layer is to be expected, accompanied by a change in magnitude of the surface drag. If local deceleration occurs in the boundary regions, a wake will result, the effect of which is of far greater order than that of the boundary roughness. As in the case of a submerged body, form drag resulting from change in section will then be a function of the Reynolds number and the geometry of the conduit, as will the energy lost along the boundary and in the resulting turbulence of the wake:

$$-\Delta(p + \gamma h) = \zeta(\mathbf{R}, \text{form}) \frac{\rho V^2}{2} \quad (161)$$

The problem of change in direction of flow, as well as change in section, is again described by a parallel dimensionless relationship. The case of unsteady motion, however, introduces complexities of a different nature, for in addition to the dynamics of acceleration or deceleration of the flow as a whole, boundary-layer developments now become a function of time as well.

Dimensional treatment of this sort serves to provide a sound foundation for either experimental or analytical investigation. The case of uniform laminar flow, it has been seen, is readily solvable without recourse to laboratory measurements; analysis of turbulent flow has recently produced relationships of essentially correct form, only the constants of which depend upon experimental data. But although the analytical study of form

resistance in closed conduits has progressed rapidly so far as roughness itself is concerned, attempts at rigorous investigation of non-uniform flow have as yet met with negligible success. The case of unsteady flow in closed conduits remains approachable only through the simplifying assumptions of the one-dimensional method of attack.

Abundant experimental data have been obtained in the past decade or two, covering the essential phenomena encountered in steady flow in conduits, and in many instances investigators have appreciated the advantages of dimensionless presentation of results in terms of the essential parameters. These data, therefore, are not only applicable to a wide range of flow conditions, but give dependable indications of the physical mechanism involved in the phenomena. Nevertheless, since it is not the purpose of this text to provide the reader with an inclusive résumé of numerical results, the reader is referred elsewhere for such information.¹ The purpose of the following pages is rather to describe successful analytical methods of attack, and, in cases in which such methods have not yet succeeded, to seek the underlying mechanism of the phenomena through general principles now at hand.

58. Velocity Distribution in Uniform Flow.² First realized by Stanton,³ of fundamental importance is the fact that the form of the velocity-distribution curve in the central region of uniform turbulent flow is independent of the gradient at the boundary so long as the intensity of boundary shear remains the same. Since the velocity gradient at the wall of a conduit will vary with the Reynolds number and with the surface roughness, it is evident that the foregoing fact would indicate complete independence of the turbulence mechanism from viscous influence and wall effects.

This condition was described by Stanton in the following dimensionless form:

¹ DAUGHERTY, R. L., "Hydraulics," McGraw-Hill Book Company, Inc., 1937; FORCHHEIMER, P., "Hydraulik," B. G. Teubner, Leipzig and Berlin, 3d ed., 1930.

² A more extensive treatment of flow in pipes may be found in BAKHMETEFF, B. A., "The Mechanics of Turbulent Flow," Princeton University Press, 1936, or ROUSE, H., *Modern Conceptions of the Mechanics of Fluid Turbulence*, *Trans. A.S.C.E.*, vol. 102, 1937.

³ STANTON, T. E., *Proc. Roy. Soc. (London)*, A, vol. 85, p. 366, 1911.

$$\frac{v_{\max} - v}{\sqrt{\tau_0/\rho}} = \varphi_1\left(\frac{r}{r_0}\right) \quad (162)$$

The term $(v_{\max} - v)$ represents a so-called "velocity defect," or the difference between the velocity at the centerline and that at the point in question, a quantity which must then vary as a function of relative distance from the center. (The bar denoting the temporal mean velocity is henceforth omitted.) Thus, the dimensionless velocity curves taken from measurements by

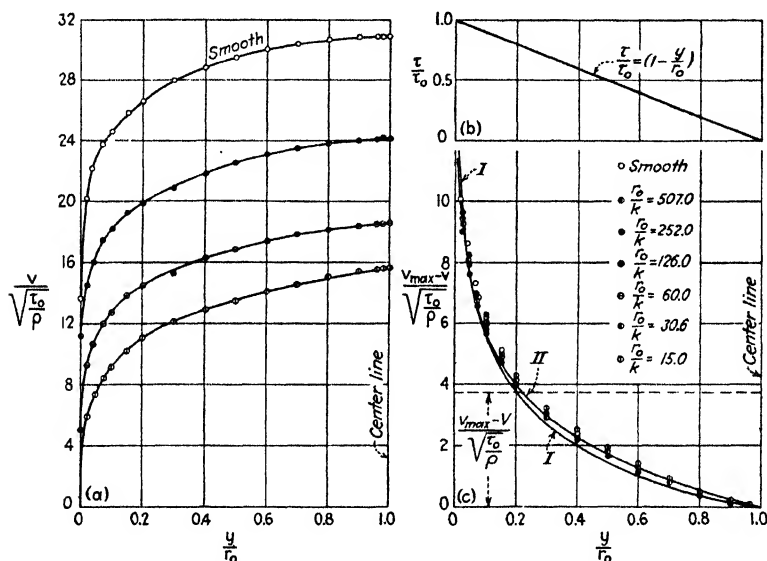


FIG. 114.—Dimensionless plots of velocity distribution for various degrees of relative roughness.

Nikuradse¹ (Fig. 114a), for both smooth and rough pipe, should, when the points of maximum velocity are superposed, yield a single curve in the central region of flow—as shown in Fig. 114c.

The fact was pointed out in Chapter IX that at high values of the Reynolds number any term for viscous shear as a function of the mean velocity gradient becomes quite negligible in comparison with the apparent stress of momentum transport. This fact is strikingly portrayed in Fig. 115, showing dimensionless

¹ NIKURADSE, J., *Gesetzmässigkeiten der turbulenten Strömung in glatten Röhren*, VDI Forschungsheft 356, 1932; *Strömungsgesetze in rauen Röhren*, VDI Forschungsheft 361, 1933.

plots of the mixing length as a function of relative distance from the pipe wall. Nikuradse computed the various magnitudes of l from measurements of velocity distribution and wall resistance, not only for smooth pipes at different Reynolds numbers, but for various degrees of relative roughness, at high values of R , through use of Eq. (118). As may be seen at once, the ratio l/r_0 becomes independent of viscous influence once R is greater than about 100,000, indicating that Eq. (118) is then applicable.

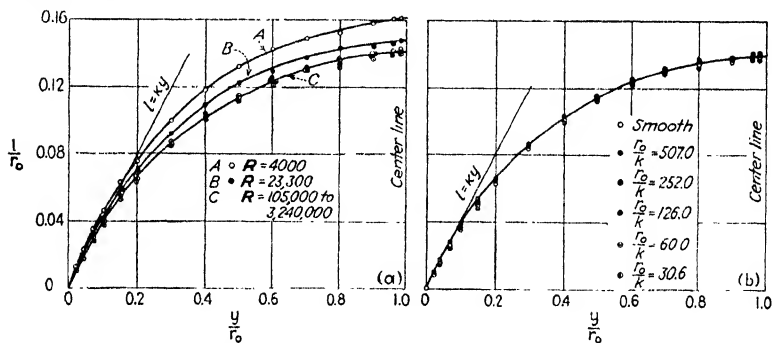


FIG. 115.—Dimensionless plots of the mixing length for (a) smooth pipes and (b) rough pipes.

Under such circumstances, von Kármán's universal relationship for the intensity of turbulent shear [Eq. (123)] should also be applicable—that is,

$$\sqrt{\frac{\tau}{\rho}} = -\kappa \frac{(\partial v / \partial y)^2}{\partial^2 v / \partial y^2} \quad (163)$$

It remains only to express the variation of τ with relative distance from the center of the conduit in order to determine the function φ_1 in Eq. (162).

If the equations of Reynolds are written for the case of steady, uniform motion in which the terms $\mu \nabla^2 v_z$, etc., are negligible, it will be seen that

$$\begin{aligned} \frac{\partial}{\partial x}(p + \gamma h) &= -\rho \frac{\partial}{\partial y} \overline{v_z v_y'} - \rho \frac{\partial}{\partial z} \overline{v_z v_z'} \\ \frac{\partial}{\partial y}(p + \gamma h) &= -\rho \frac{\partial}{\partial y} \overline{v_y^2} - \rho \frac{\partial}{\partial z} \overline{v_y v_z'} \\ \frac{\partial}{\partial z}(p + \gamma h) &= -\rho \frac{\partial}{\partial y} \overline{v_z v_y'} - \rho \frac{\partial}{\partial z} \overline{v_z^2} \end{aligned}$$

It is at once evident that the quantity $(p + \gamma h)$ may be expected to vary in each of the three directions, whereas in uniform laminar flow it was seen that the pressure must be hydrostatically distributed over any normal section. However, differentiation of each of these equations with respect to x will yield

$$\frac{\partial^2}{\partial x^2}(p + \gamma h) = \frac{\partial^2}{\partial y \partial x}(p + \gamma h) = \frac{\partial^2}{\partial z \partial x}(p + \gamma h) = 0$$

from which it is apparent that the potential gradient at any point of the cross section will not change with distance in the direction of flow. Furthermore, since the order of differentiation with respect to two quantities may be reversed, it is also apparent that the potential gradient with respect to x will not vary from point to point over the section. Thus, although the pressure may not be hydrostatically distributed over a normal cross section, the rate of change of $(p + \gamma h)$ will be the same at all points within the uniform flow. It follows at once that Eqs. (89-91) are fully applicable to the present case (see Fig. 114b):

$$\tau = -\frac{r}{2} \frac{d}{dx} (p + \gamma h) = \tau_0 \frac{r}{r_0} = \tau_0 \left(1 - \frac{y}{r_0}\right) \quad (164)$$

Combining Eqs. (163) and (164) through elimination of τ

$$\frac{d^2 v / dy^2}{(dv/dy)^2} = -\frac{\kappa}{\sqrt{\tau_0/\rho}} \frac{\sqrt{r_0}}{\sqrt{r_0 - y}}$$

This expression may readily be integrated, the constant of integration being determined through assuming an infinite velocity gradient at the boundary; this is obviously only a convenient means to an end, for conditions in the boundary region have no further bearing upon this phase of the problem. The resulting equation

$$\frac{dv}{dy} = -\frac{1}{2\kappa} \frac{\sqrt{\tau_0/\rho}}{\sqrt{r_0}} \frac{1}{\sqrt{r_0 - y} - \sqrt{r_0}}$$

may now once again be integrated, the second constant being evaluated through use of the fact that $v = v_{\max}$ at $y/r_0 = 1$:

$$\begin{aligned} \frac{v_{\max} - v}{\sqrt{\tau_0/\rho}} &= -\frac{1}{\kappa} \left[\ln \left(1 - \sqrt{1 - \frac{y}{r_0}} \right) + \sqrt{1 - \frac{y}{r_0}} \right] \\ &= -\frac{1}{\kappa} \left[\ln \left(1 - \sqrt{\frac{r}{r_0}} \right) + \sqrt{\frac{r}{r_0}} \right] \end{aligned} \quad (165)$$

A plot of this function, first obtained by von Kármán, may be found in Fig. 114c (Curve I) for a magnitude of the universal constant $\kappa = 0.36$. It may be seen at a glance that the experimental data obtained by Nikuradse follow the trend of the curve with good approximation, even well into the boundary region.

For the boundary region itself—exclusive of the laminar boundary film—von Kármán reasoned that in the case of a smooth wall the velocity distribution must depend upon the intensity of wall shear, the fluid density and viscosity, and the absolute distance from the wall; in other words, conditions in this region should be independent of the state of flow in the central portion for which Eq. (165) is valid. He thereby obtained the general function

$$\frac{v}{\sqrt{\tau_0/\rho}} = \varphi_2\left(\sqrt{\frac{\tau_0}{\rho}} \frac{y}{\nu}\right) \quad (166)$$

Further reasoning¹ led to the conclusion that the functional relationship must again be logarithmic, and of the form

$$\frac{v}{\sqrt{\tau_0/\rho}} = C_1 + \frac{1}{\kappa} \ln \left(\sqrt{\frac{\tau_0}{\rho}} \frac{y}{\nu} \right) \quad (167)$$

It must be noted that the quantity at the right has the nature of a Reynolds number, for $\sqrt{\tau_0/\rho}$ is dimensionally equivalent to v , and is commonly called the “friction velocity.”

In the case of wall roughness of appreciable magnitude, the intensity of turbulence resulting from form drag will be so great as to render mean viscous shear relatively insignificant. Under such circumstances the velocity distribution should depend only upon wall roughness and distance from the wall. Assuming that roughness characteristics may be defined in terms of a linear dimension k , the general function will then become

$$\frac{v}{\sqrt{\tau_0/\rho}} = \varphi_3\left(\frac{y}{k}\right) \quad (168)$$

Again reasoning that the function must be logarithmic, von Kármán obtained for the velocity distribution in the neighborhood of rough walls the expression

¹ See “Turbulence and Skin Friction” for a résumé of this derivation.

$$\frac{v}{\sqrt{\tau_0/\rho}} = C_2 + \frac{1}{\kappa} \ln \left(\frac{y}{k} \right) \quad (169)$$

Systematic investigation by Nikuradse of the velocity distribution in both smooth and rough pipes over a very wide Reynolds-number range has yielded extensive data with which the validity of Eqs. (167) and (169) may be tested. In Fig. 116 the plotted points for smooth pipes are seen to fall along a single curve—regardless of the magnitude of R —if the

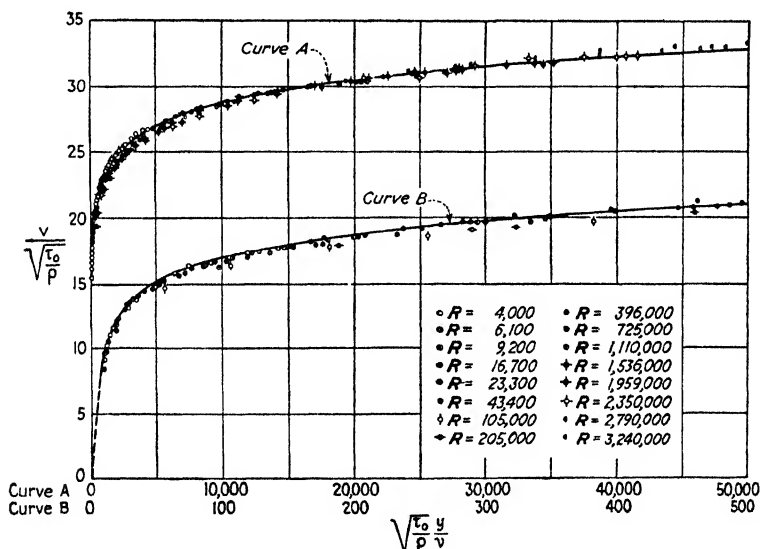


FIG. 116.—Dimensionless plot of the velocity distribution in smooth pipes.

quantities $\frac{v}{\sqrt{\tau_0/\rho}}$ and $\sqrt{\frac{\tau_0}{\rho}} \frac{y}{v}$ are used as ordinate and abscissa of the plot. The single curve is shown at two different scales in order to emphasize the continuity of the function over an extreme abscissa range. If the same data are plotted to semilogarithmic scale, as shown in Fig. 117, the trend becomes the more significant. It is seen that the points all lie essentially upon a straight line, and thus validate Eq. (167); sensible deviation becomes apparent only as the laminar boundary film is approached, whereas the function remains linear well into the central region. From the slope and position of this straight line Nikuradse obtained

the following constants for von Kármán's basic equation:

$$\frac{v}{\sqrt{\tau_0/\rho}} = 5.5 + 5.75 \log \left(\sqrt{\frac{\tau_0}{\rho}} \frac{y}{\nu} \right) \quad (170)$$

The constant 5.75 corresponds to $\kappa = 0.40$ and includes the conversion factor 2.30 between the natural and common logarithmic systems.

Under conditions of turbulent motion the laminar boundary layer is extremely thin in comparison with the pipe radius, so

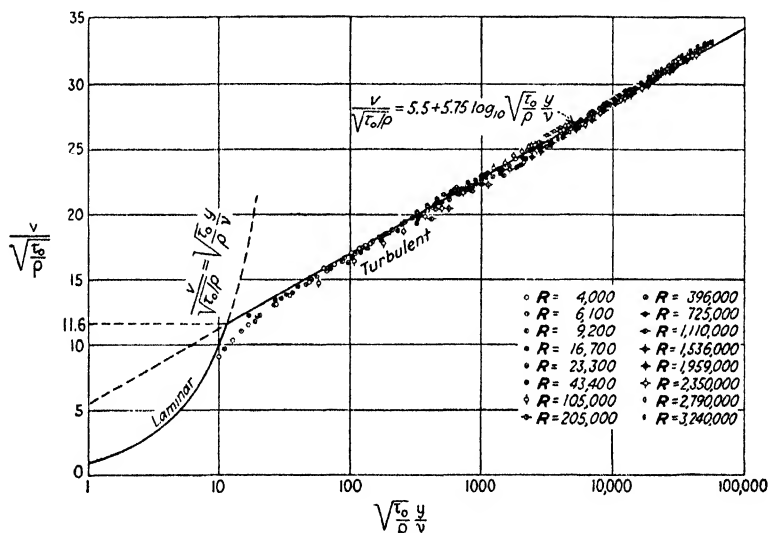


FIG. 117.—Universal velocity distribution for smooth pipes.

that the variation of τ over the thickness δ may be ignored without appreciable error; in other words, the actual parabolic velocity distribution within this narrow zone of laminar motion is so close to linear that the velocity gradient is essentially constant—that is, $v = y \tau_0/\mu$. Under such conditions it is evident that the velocity distribution within the laminar film may be plotted in Fig. 117 according to the equation

$$\frac{v}{\sqrt{\tau_0/\rho}} = \sqrt{\frac{\tau_0}{\rho}} \frac{y}{\nu}$$

Although there is obviously no definite border between the zone of pure laminar flow and that of fully developed turbulence,

a convenient arbitrary limit of the boundary layer is represented by the intersection of the two plotted curves in Fig. 117, at which point

$$\frac{v}{\sqrt{\tau_0/\rho}} = \sqrt{\frac{\tau_0}{\rho}} \frac{y}{v} = 11.6$$

Writing $y = \delta$ at the intersection, it follows that

$$\delta = 11.6 \frac{v}{\sqrt{\tau_0/\rho}} \quad (171)$$

It is to be noted that the only fixed point in the semilogarithmic plot is this arbitrary limit of the boundary layer. Owing to the

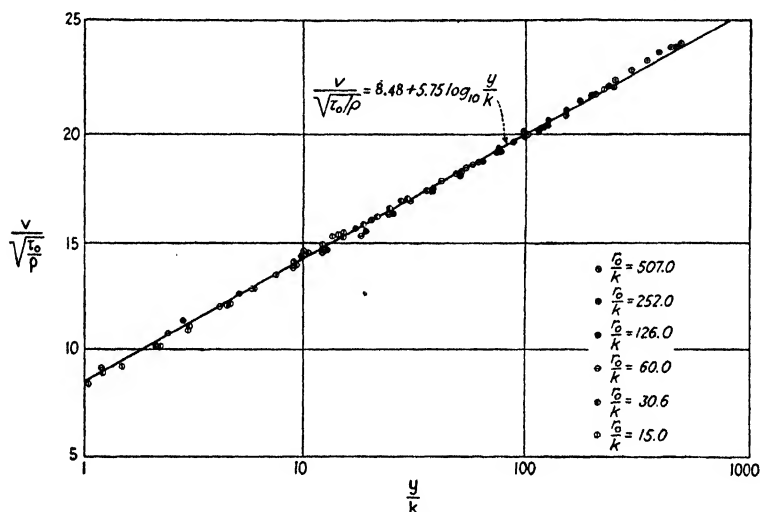


FIG. 118.—Universal velocity distribution for rough pipes.

nature of the logarithmic scale, the boundary itself lies an infinite distance to the left, whereas the location of the centermost point ($y = r_0$) varies with the Reynolds number of the flow.

Nikuradse extended his pipe research to the case of artificial roughness, controlling the relative magnitude of the roughness by cementing sand grains of uniform diameter to the inner wall of the pipe. Through judicious selection of grain size with respect to pipe diameter, he was able to vary the relative roughness r_0/k between limits of 507 and 15, the grain diameter being used to represent the roughness dimension k . A semilogarithmic plot of his measurements is shown in Fig. 118; the linear character

of the plot validates von Kármán's Eq. (169), constants determined by Nikuradse from the slope and position of the straight line yielding the expression

$$\frac{v}{\sqrt{\tau_0/\rho}} = 8.48 + 5.75 \log \left(\frac{y}{k} \right) \quad (172)$$

It is evident from the trend of the measured values that no trace of a laminar boundary layer exists along the pipe wall, the points following a linear course practically to the extremities of the roughness projections.

From the form of Eqs. (165), (170), and (172), it will be seen that the corresponding curves still have finite slopes dv/dy at the central axis. This is contrary to actual circumstances, although the error thus introduced is of small magnitude. Moreover, while Eqs. (170) and (172) were developed specifically for the boundary regions, experimental evidence indicates that they yield satisfactory results well into the central regions of flow, deviating only slightly as the axis of the conduit is approached. If each is written for the point $y = r_0$,

$$\frac{v_{\max}}{\sqrt{\tau_0/\rho}} = 5.5 + 5.75 \log \left(\sqrt{\frac{\tau_0}{\rho}} \frac{r_0}{v} \right) \quad (173)$$

$$\frac{v_{\max}}{\sqrt{\tau_0/\rho}} = 8.48 + 5.75 \log \left(\frac{r_0}{k} \right) \quad (174)$$

and Eqs. (170) and (172) are subtracted therefrom, the two results will have the identical form

$$\frac{v_{\max} - v}{\sqrt{\tau_0/\rho}} = 5.75 \log \frac{r_0}{y} = -\frac{1}{\kappa} \ln \left(1 - \frac{r}{r_0} \right) \quad (175)$$

Eq. (175) not only embodies the general functional relationship of Stanton's original expression [Eq. (162)], but for the universal constant $\kappa = 0.40$ yields a distribution curve for the central regions in very close accord with experimental findings (Curve II in Fig. 114c). Moreover, its simplicity in comparison with von Kármán's fundamental equation (165) is an obvious advantage in succeeding developments.

Since this relationship permits determination of the velocity defect with good approximation for all values of r from the central axis to the limit of the laminar film, it should also enable direct computation of the difference between the maximum and mean velocities of the flow for any values of fluid density and boundary

shear. Indeed, the quantity $\frac{v_{\max} - V}{\sqrt{\tau_0/\rho}}$ is nothing more than the mean ordinate of the velocity defect curve over the entire flow section, and hence may be evaluated (as shown by Bakhmeteff) by the following operation:

$$\frac{v_{\max} - V}{\sqrt{\tau_0/\rho}} = \frac{1}{\pi r_0^2} \int_{r_0}^0 2\pi (r_0 - y) \frac{1}{\kappa} \ln \frac{r_0}{y} dy = \frac{3}{2\kappa} = 3.75 \quad (176)$$

Although Nikuradse found that the value 4.05 would better correspond with experimental measurement of v_{\max} and V , the former value will be retained in this discussion. If Eq. (176) is now subtracted from Eqs. (173) and (174), the following expressions will result for the mean velocity in terms of the friction velocity, the universal constant, and the corresponding boundary parameters, for smooth and rough pipes, respectively:

$$\frac{V}{\sqrt{\tau_0/\rho}} = 1.75 + \frac{1}{\kappa} \ln \left(\sqrt{\frac{\tau_0}{\rho}} \frac{r_0}{\nu} \right) \quad (177)$$

$$\frac{V}{\sqrt{\tau_0/\rho}} = 4.73 + \frac{1}{\kappa} \ln \left(\frac{r_0}{k} \right) \quad (178)$$

59. Universal Laws of Resistance. Aside from Eqs. (177) and (178), as yet no means are at hand for determining the intensity of boundary shear in terms of readily measurable characteristics of flow and fluid. From dimensional considerations it has been seen that τ_0 must depend upon mean velocity, viscosity, density, pipe diameter, and boundary roughness, with the following general functional relationship of these variables:

$$\tau_0 = \varphi \left(\frac{VD}{\nu}, \frac{k}{r_0} \right) \frac{\rho V^2}{2}$$

Intensity of boundary shear, however, is not directly measurable without extensive apparatus, and it is more expedient to express boundary resistance in terms of the corresponding rate of energy loss. From Eq. (89), which has been shown to apply alike to laminar and turbulent flow,

$$\tau_0 = -\frac{D}{4} \frac{d}{dx} (p + \gamma h) \quad (179)$$

substitution of which in the foregoing functional relationship will yield

$$-\frac{d}{dx}(p + \gamma h) = \varphi\left(\frac{VD}{\nu}, \frac{k}{r_0}\right) \frac{4}{D} \frac{\rho V^2}{2}$$

The function $4\varphi(\mathbf{R}, k/r_0)$ is commonly given the symbol f , and is called the coefficient of pipe resistance:

$$f = f\left(\mathbf{R}, \frac{k}{r_0}\right) = -\frac{D \frac{d}{dx}(p + \gamma h)}{\frac{\rho V^2}{2}} \quad (180)$$

Many generations of hydraulic engineers have produced a wealth of empirical data, all of which pointed definitely to the

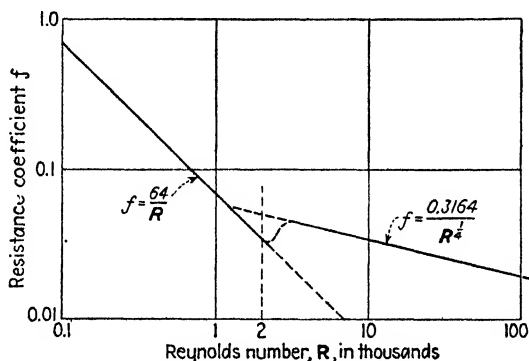


FIG. 119.—Logarithmic plot of f as a function of \mathbf{R} for smooth pipes.

variability of f , but it was not until Blasius¹ analyzed an extensive series of measurements made by Saph and Schoder that the significance of Eq. (180) was fully appreciated. Blasius found that the Saph-Schoder data for turbulent flow in smooth pipes lay along the straight line shown in the logarithmic plot of Fig. 119, the slope and position of the line indicating that f might be expressed in the following exponential form:

$$f = \frac{0.3164}{\mathbf{R}^{1/4}} \quad (181)$$

That the curve in the region of laminar motion must vary simply as $f = 64/\mathbf{R}$ may be seen by writing Eq. (94) in the form of Eq. (180).

¹ BLASIUS, H., Das Aehnlichkeitsgesetz bei Reibungsvorgängen in Flüssigkeiten, *Forschungsarbeiten auf dem Gebiete des Ingenieurwesens*, 131, 1913.

Although the data upon which Blasius based his analysis extended to a Reynolds number of approximately 100,000, it was not long before Eq. (181) was assumed capable of considerable extrapolation—despite the fact that it was dimensionally sound but otherwise entirely empirical. More recent investigations by Stanton and Pannell, Lees, Hermann, and Nikuradse (Fig. 120) proved conclusively that the function is not a linear

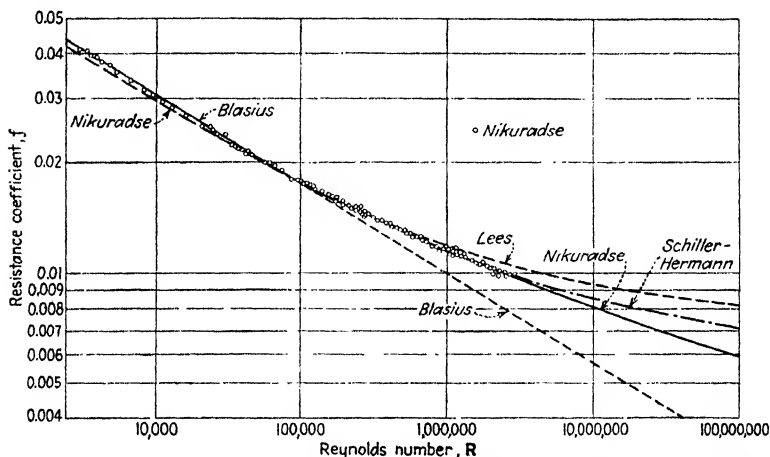


FIG. 120.—Resistance coefficients for smooth pipes at high Reynolds numbers.

one beyond the Blasius range, and therefore may not be considered exponential unless the exponent is also treated as variable with R . As in the case of the turbulent boundary layer, the exponent n is equal to $\frac{1}{4}$ in the range immediately following the transition from laminar flow to turbulent, but with ascending values of R this exponent asymptotically approaches the limit zero. Although various empirical expressions have been offered to apply over a greater range than that of Blasius, each of these is limited to the region of the actual experimental measurements, and extrapolation beyond this region is no more warranted than in the case of Eq. (181).

From Eqs. (179) and (180) it will be apparent that

$$\frac{V}{\sqrt{\tau_0/\rho}} = \sqrt{\frac{8}{f}} \quad \text{and} \quad \sqrt{\frac{\tau_0}{\rho}} = V\sqrt{\frac{f}{8}}$$

If these values are now introduced into Eq. (177), it will be seen that

$$\begin{aligned}\frac{\sqrt{8}}{\sqrt{f}} &= 1.75 + \frac{1}{\kappa} \ln \left(\frac{\sqrt{f}}{\sqrt{8}} \frac{VD}{2\nu} \right) \\ &= 1.75 + \frac{1}{\kappa} \ln \frac{1}{4\sqrt{2}} + \frac{1}{\kappa} \ln (R\sqrt{f})\end{aligned}$$

Finally,

$$\frac{1}{\sqrt{f}} = -0.91 + 2.03 \log (R\sqrt{f})$$

Thus, a very simple relationship for the resistance factor in terms of the universal constant and the Reynolds number has

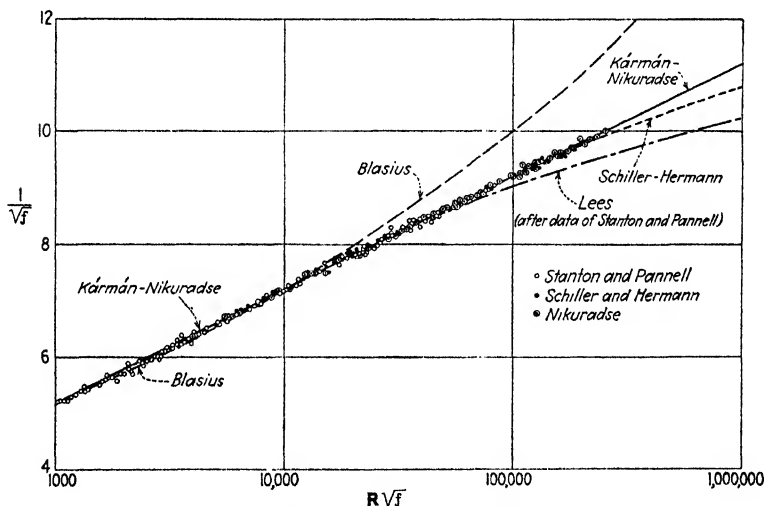


FIG. 121.—Universal resistance function for smooth pipes.

been developed directly from the general expression for the velocity distribution in smooth pipes. This basic relationship was first derived by von Kármán in 1930 in terms of the maximum velocity, and later put into the more convenient form above by Prandtl. With slight modification of constants to agree more closely with Nikuradse's experimental data, this becomes

$$\frac{1}{\sqrt{f}} = -0.8 + 2 \log (R\sqrt{f}) \quad (182)$$

Equation (182) is shown by the straight line in the semi-logarithmic plot of Fig. 121, from which it is seen that curves

corresponding to the several empirical relationships deviate markedly with ascending values of the Reynolds number. Owing to the nature of the basic von Kármán expression, however, solution for f for a given value of R must be found by graphical means. Nikuradse, therefore, has proposed the empirical relationship (Fig. 120)

$$f = 0.0032 + \frac{0.221}{R^{0.237}} \quad (183)$$

which follows closely the trend of Eq. (182) even for relatively high values of the Reynolds number. So far as extensive extrapolation is concerned, nevertheless, only the von Kármán expression possesses sufficient analytical foundation to be dependable to very high—if not to infinite—magnitudes of R . In the Blasius range, on the other hand, it is seen to deviate somewhat from the empirical curve of Eq. (181). This may be attributed to the fact that viscous shear in terms of the mean velocity gradient is not negligible for low Reynolds numbers, a region for which no satisfactory analytical solution as yet exists. Needless, to say, no single function has been obtained to describe the continuous variation of f over the entire Reynolds-number scale.

A parallel development proceeding from Eq. (178) will be found to yield a corresponding expression for the resistance coefficient in rough pipes; with slight modification of constants in accordance with Nikuradse's experimental data this will take the form

$$\frac{1}{\sqrt{f}} = 1.74 + 2 \log \frac{r_0}{k} \quad (184)$$

It is seen at once that the Reynolds number does not appear in this expression, indicating that the magnitude of f is totally independent of viscous influence. At this point the reader must recall to mind two assertions made at the beginning of this chapter: First, boundary roughness that is enveloped by a continuous laminar boundary layer cannot be expected to have the same influence upon resistance as roughness projections of sufficient relative magnitude to disrupt the laminar film. Second, unless the roughness is sufficiently angular, the resistance will always depend in part upon the Reynolds number of the flow.

The first of these two statements will be clarified by reference to the plot of Nikuradse's roughness data, shown in Fig. 122, in which variation with R is indicated by the abscissa scale, and variation with the ratio r_0/k by the sequence of curves, each for a constant relative roughness. It is quite evident from the several curves that the greater the relative roughness, the smaller the Reynolds number at which deviation from the curve

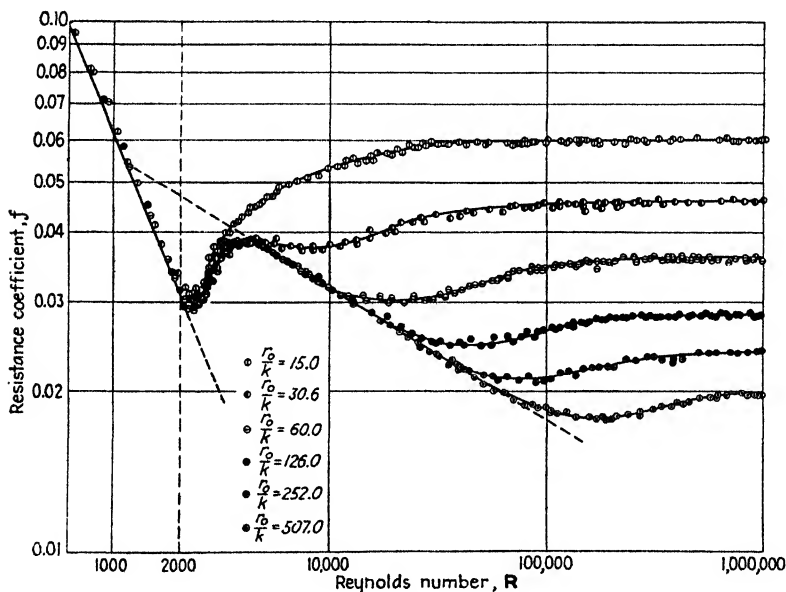


FIG. 122.—Resistance coefficients for artificially roughened pipes.

for smooth pipes begins. In other words, so long as the roughness projections are rendered ineffective by a surrounding laminar film, the resistance coefficient remains the same as that for a smooth boundary; but with increasing values of R , the laminar film decreases in thickness, and must eventually begin to yield to the roughness of the boundary. That this effect depends entirely upon the relative magnitudes of δ and k may be shown by replotting Nikuradse's data in terms of the parameters

$\frac{1}{\sqrt{f}} - 2 \log \frac{r_0}{k}$ and $\frac{k}{\delta}$. Use of the former as ordinate scale will bring all horizontal portions of the curves in Fig. 122 to the common ordinate 1.74, whereas use of the latter as abscissa

scale will align vertically all points for which the ratio of absolute roughness to boundary-layer thickness is the same. The magnitude of δ is found from Eq. (171), from which it will be seen that

$$\frac{k}{\delta} = \frac{1}{11.6} \sqrt{\frac{\tau_0}{\rho}} \frac{k}{\nu} = \frac{0.0152 R \sqrt{f}}{r_0/k}$$

As is obvious from Fig. 123, this procedure reduces the curves of Fig. 122 to a single composite function, regardless of the absolute magnitude of R or the relative magnitudes of δ and k .

Needless to say, only the horizontal portion of any resistance curve may be described by Eq. (184), and then only if the factor

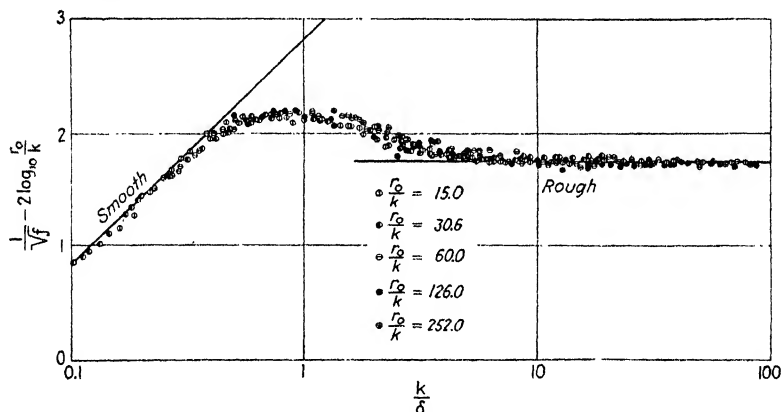


FIG. 123.—Variation in roughness effect with relative thickness of the boundary layer.

k is fully indicative of the roughness characteristics. That the relationship will then be valid is proven by the fact that Nikuradse's measurements yield a straight line in the semilogarithmic plot of Fig. 124. But it will also be apparent from Fig. 125, showing general trends in experimental data for commercial pipe, that not all roughness has the same characteristics as Nikuradse's—those curves marked "wavy" showing pronounced tendencies to vary continuously with R .

60. The Roughness Problem. Despite the fact that von Kármán's analysis of the resistance of rough pipes is a decided step forward, it is but the first of many steps that must be taken before the problem of roughness finds a satisfactory solution. First of all, designation of a single linear dimension k to describe

in full the roughness characteristics will have quantitative significance only so long as the roughness elements remain similar in form, as in the case of Nikuradse's sand grains. Once the same criterion is applied to the roughness of commercial surfaces, it is obvious that a single linear dimension cannot begin to include effectively the many types of roughness, unless k becomes merely

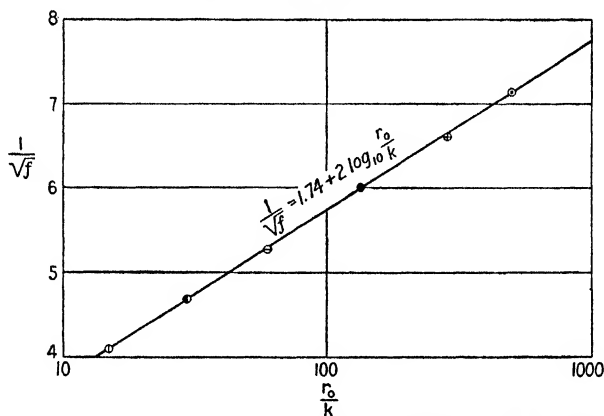


FIG. 124.—Universal resistance function for artificially roughened pipes.

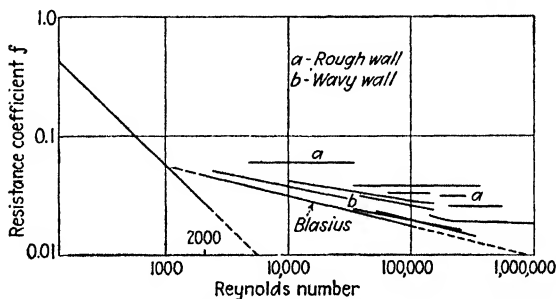


FIG. 125.—Typical resistance curves for commercial pipe.

an abstract parameter indicating relative performance rather than actual size. Furthermore, no satisfactory analysis has been made of the regime in which both roughness and viscous influences are of the same order of magnitude; so many data have been obtained indicating functional trends (Fig. 125) between the limits of Eqs. (182) and (184) that it is apparent that something more is involved than simply the relative magnitudes of δ and k as in Nikuradse's experiments. In other words, if k represents the height of the projections, there must be added a

factor indicating roughness form, and possibly a third characteristic dimension denoting the proximity of roughness elements—roughness effect at a given Reynolds number varying with each of these three parameters.

Schlichting¹ has developed a method of testing commercial surfaces for effective roughness, whereby it is possible to designate in terms of a parameter k the resistance of the surface in question in comparison with some arbitrary standard. He made use of a closed conduit of wide rectangular section, three walls of which were very smooth, the fourth being formed by the actual surface to be investigated. Provisions were made for piezometer measurements along the wide smooth wall opposite the test section, and for Pitot-tube traverses between the smooth and rough boundaries, no further experimental data being necessary. Essential, of course, was a sufficient length of conduit (including the rough wall under investigation) for establishment of uniform flow upstream from the zone of measurement.

Since the rate of energy loss—proportional to the negative pressure gradient if the conduit is horizontal—must be the same for the smooth and rough walls, it is evident that measurement of this gradient along the smooth wall alone will suffice. Owing to the essential equilibrium between pressure gradient and boundary shear,

$$(\tau_0)_s + (\tau_0)_r = -b \frac{dp}{dx} \quad (185)$$

in which b is the spacing of smooth and rough walls, to which the subscripts s and r refer, respectively. The velocity distribution in the neighborhood of the smooth wall must satisfy Eq. (170), since this relationship was developed for the boundary region, without regard to conditions beyond the central portion of the flow. From Fig. 126 it will be seen that a typical velocity traverse near both smooth and rough walls will plot as a linear function on semilogarithmic coordinates; preliminary tests by Schlichting indicated satisfactory accordance with Eqs. (170) and (172), despite essential asymmetry of the velocity diagram. From the velocity traverse near the smooth wall $(\tau_0)_s$ may at once be found, and substitution in Eq. (185) will then yield $(\tau_0)_r$.

¹ SCHLICHTING, H., *Experimentelle Untersuchungen zum Rauigkeitsproblem*, *Ingenieur-Archiv*, vol. 7, p. 1, 1936.

The velocity traverse in the neighborhood of the rough wall will finally permit solution for k through Eq. (172). Means are therefore at hand for determining the effective absolute roughness of the surface under investigation—"effective" in the sense that k is no longer an actual linear dimension of the roughness, but a parameter signifying behavior in comparison with Nikuradse's experiments for which the constants in Eq. (172) were chosen. It should be apparent to the reader, however, that this method of roughness "calibration" is possible only if the rough-

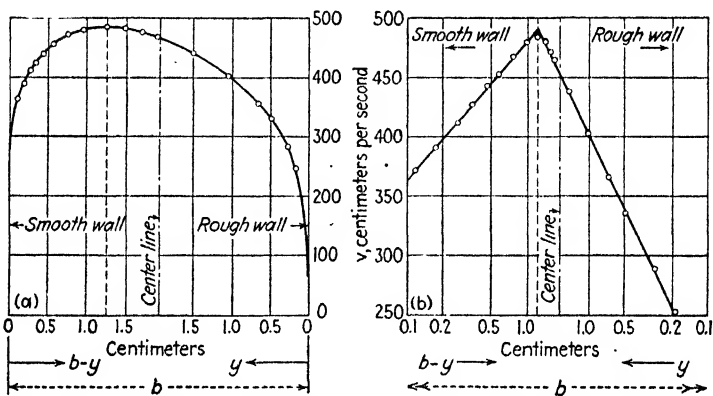


FIG. 126.—Velocity traverses between smooth and rough boundaries.

ness is of such form, and the Reynolds number of such magnitude, that viscous influence is not appreciable.

Further research by Schlichting deserves mention at this point. Instead of varying the relative roughness and thereby keeping the boundary geometrically similar, as did Nikuradse, Schlichting chose elementary shapes of constant elevation (such as small spheres, hemispheres, or plates) and varied their spacing with respect to one another. Since each such element produces its own tiny wake, and since the effectiveness of each such wake varies with the spacing of neighboring elements, the following results were obtained: With increasing proximity of the elements the mean intensity of wall shear first grew in magnitude, because of the additional turbulence as more elements were contained in a unit area. But a maximum value of τ_0 was finally attained, further concentration of the elements merely increasing the mutual interference and serving to decrease

the intensity of shear; the limit would be reached—ideally, of course—as the elements become so closely packed together as to produce, in effect, a smooth surface. Schlichting showed, moreover, that the resistance of each roughness element, when sufficiently removed from its neighbors, was essentially the same as though it moved as an individual body through the same fluid under the same velocity conditions.

The significance of this research must not be underestimated. Boundary roughness, whether natural or artificial, cannot be described only in terms of the magnitude of linear projection from a reference plane, for the form of the individual elements and their location with respect to one another are quite as important. If, for the present, practical considerations make it advisable to designate effective roughness action by a single linear parameter k , then it is far more desirable to select arbitrarily a definite basis for comparison, for Nikuradse's sand grains and method of application to the pipe walls are at best difficult standards to reproduce. Nevertheless, it is obvious that any such linear roughness scale, if internationally adopted, must suffer from the existence of more than one common dimensional system, for conversion factors rob any basic scale of its simplicity. Even though this problem of roughness designation should find an early solution, that type of surface irregularity which does not fully eliminate the influence of viscosity will probably trouble investigators for some time to come.

61. Symmetrical Section Changes. Closely analogous to the drag of immersed bodies, resistance to motion in non-uniform conduits will depend in part upon boundary shear and in part upon separation and the formation of a turbulent wake. The relative extent to which each of these will affect the flow must then vary with the Reynolds number and the geometry of the conduit boundaries. Nevertheless, two essential differences exist between flow around an immersed body of given form and flow through a conduit transition that is geometrically analogous (compare, for instance, a streamlined body and a Venturi meter, or a disk and a plate orifice): First, the immersed body is generally surrounded by a great expanse of fluid, whereas one wall of a conduit transition faces another wall not far removed; such confinement should cause noticeable differences in the corresponding dynamic patterns. Second, boundary-layer growth begins

at the leading edge of an immersed body, whereas a boundary layer already exists at the beginning of a change in conduit cross section owing to prior development in the region of approach; as a result, the velocity distribution of the approaching flow plays no small part in determining the flow pattern in the transition region.

The most representative example of a symmetrical boundary change is found in the plate orifice (Fig. 127), the analysis of which will apply in general to all transitions of this nature.

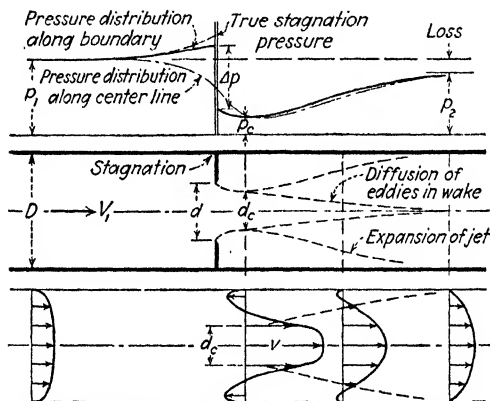


FIG. 127.—Distribution of pressure and velocity at a pipe orifice.

Customary hydraulic treatment of this case is doubtless familiar to the reader. The equation of mean energy is first written between a section in the approach and the section of maximum jet contraction, ignoring the magnitude of K_e at each section but assuming a small loss of energy:

$$E_1 = \frac{\rho V_1^2}{2} + p_1 = \frac{\rho V_c^2}{2} + p_c + \Delta E$$

The equation of continuity has the form

$$Q = AV_1 = C_c a V_c$$

C_c denoting the ratio of jet area to orifice area a . The energy lost between the two sections is expressed through introduction of a velocity coefficient C_v , such that

$$V_c = C_v \sqrt{\frac{2}{\rho} (E_1 - p_c)} = C_v \sqrt{\frac{2}{\rho} \left(\frac{\rho V_1^2}{2} + p_1 - p_c \right)}$$

whence

$$\Delta E = (1 - C_v^2) \left(\frac{\rho V_1^2}{2} + p_1 - p_c \right) = \left(\frac{1}{C_v^2} - 1 \right) \frac{\rho V_c^2}{2}$$

These equations are then solved for the rate of discharge:

$$Q = \frac{C_v C_c a}{\sqrt{1 - (C_v C_c a/A)^2}} \sqrt{\frac{2(p_1 - p_c)}{\rho}} \quad (186a)$$

In deriving this relationship, the hydraulician carefully includes the "correction for the velocity of approach," yet inconsistently ignores the fact that the velocity-distribution factor is decidedly different at the two sections. On the other hand, to simplify Eq. (186a) the product $C_v C_c$ is generally dropped from the radical, the coefficient in the numerator then bearing the burden of this change; thus,

$$Q = \frac{C_d a}{\sqrt{1 - (a/A)^2}} \sqrt{\frac{2(p_1 - p_c)}{\rho}} \quad (186b)$$

Measurements by Witte¹ indicate that the magnitude of the measured differential pressure $p_1 - p_c$ will vary considerably with the location of the two piezometer connections (see Fig. 127), and thereby change the magnitude of the discharge coefficient. If results of different investigators are to be comparable, therefore, it is essential that pressures be measured at geometrically similar points—the most logical position being the base of the orifice plate. Although this point on the upstream side is only nominally a point of stagnation (Fig. 127), and although the pressure at the base on the downstream side is not exactly the same as that within the contracted jet, such assumptions are justified if only for the fact that they greatly simplify the discharge equation. Thus

$$V_c = C'_v \sqrt{\frac{2(p_s - p_c)}{\rho}}$$

and

$$Q = C'_v C_c a \sqrt{\frac{2(p_s - p_c)}{\rho}}$$

Writing the differential pressure as Δp and the product $C'_v C_c$ as

¹ WITTE, R., Die Strömung durch Düsen und Blenden, *Forschung auf dem Gebiete des Ingenieurwesens*, vol. 2, no. 7, p. 245, 1931.

C_q , this equation becomes essentially the same as that obtained by dimensional analysis:

$$Q = C_q a \sqrt{2 \frac{\Delta p}{\rho}} \quad (186c)$$

From dimensional considerations one would expect the coefficient C_q to vary with the ratio of orifice and conduit diameters, with the Reynolds number of the flow, and with the relative



Columbia

FIG. 128.—Instantaneous flow pattern at a two-dimensional plate orifice.

roughness of the conduit boundaries—all other factors (such as sharpness of the orifice and proximity of upstream disturbances) thereby remaining constant. C_q is thus a function of three basic parameters:

$$C_q = \varphi \left(\frac{d}{D}, \frac{VD}{\nu}, \frac{k}{D} \right)$$

Needless to say, the Reynolds number may also be written in terms of the orifice diameter and the corresponding velocity.

Since the following relationship exists among the several coefficients (assuming the piezometers to have the same locations),

$$C_q = \frac{C_d}{\sqrt{1 - (d/D)^4}} = \frac{C_v C_c}{\sqrt{1 - (C_v C_c)^2 (d/D)^4}}$$

it follows that C_q , C_d , and $C_v C_c$ must all be related functions of the same three dimensionless parameters. Although C_v and C_c cannot be measured directly, as in the case of free efflux, visual

experiments such as those of Johansen¹ permit a definite insight into their mutual effect upon the discharge coefficient as the three basic parameters vary. At extremely low values of the Reynolds number ($vd/\nu < 10$) Johansen found the flow pattern to be essentially symmetrical about the plane of the orifice, the outermost stream lines closely following the boundary profile. As the parameter vd/ν increased beyond 10, the flow began to separate from the downstream side, the divergence of the jet gradually decreasing and a slight contraction becoming perceptible. At $vd/\nu = 150$ the outermost stream lines of the jet reached the pipe wall 5 or 6 diameters downstream, the jet then being surrounded by a region of slow reverse flow. A slight instability of the outer filaments of the jet was apparent at $vd/\nu = 250$, whereas at 1000 the jet was encircled by a succession of vortex rings, although the flow within the jet was still undisturbed. With the onset of turbulence in the wake of the orifice, the contraction of the jet gradually approached a maximum, observation through use of dye thereafter being extremely difficult.

These stages of development can be correlated with variation in the discharge coefficient through reference to the measurements of Johansen reproduced in Fig. 129. One must remember, first of all, that C_d is a coefficient of delivery, as opposed to the coefficient of resistance C_d for immersed bodies; the discharge coefficient must be looked upon, therefore, as a reciprocal function of the orifice drag, the latter yielding a curve essentially similar to that of Fig. 94. So long as the pattern of flow is symmetrical on both sides of the orifice, the phenomenon is purely that of deformation drag, an increase in the Reynolds number producing a decrease in the resistance coefficient and hence a rise in C_d ; the initial portion of the curve in Fig. 129 thus corresponds to the Stokes region for immersed bodies. By the time $vd/\nu = 100$ ($\sqrt{vd/\nu} = 10$), the effect of separation becomes noticeable, just as in the case of an immersed body, whereupon the upward trend in C_d is gradually offset by the contraction of the jet.

At this point, however, the essential difference between the immersed body and the conduit transition becomes readily apparent. Since the velocity of the approaching laminar flow

¹ JOHANSEN, F. C., Flow through Pipe Orifices at Low Reynolds Number, *Proc. Roy. Soc. (London)*, vol. 126, no. 801, p. 231.

is considerably higher in the central region than near the walls, the degree of jet contraction will vary with the relative size of the orifice opening. C_e (and hence C_d) will then increase with d/D , resulting in considerable deviation of the several curves as inertial effects come into play. Once turbulence sets in, the velocity distribution in the conduit becomes more uniform, resulting in

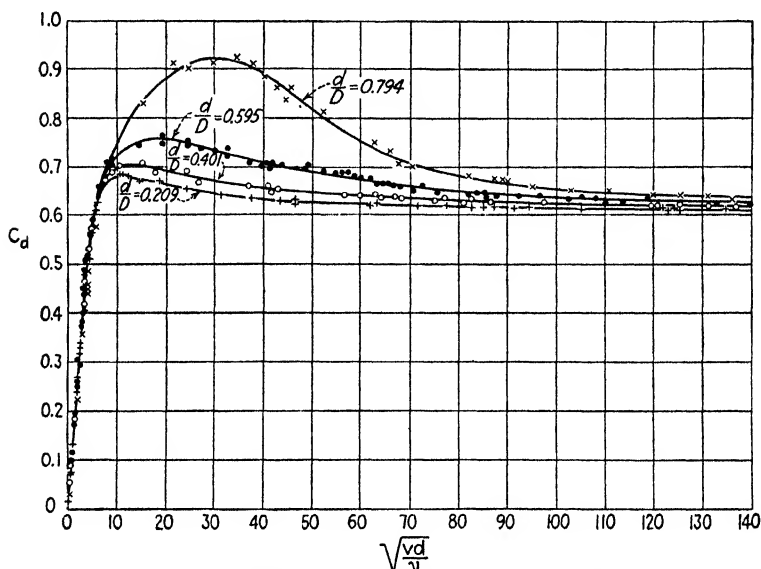


FIG. 129.—Discharge coefficients for the plate orifice.

further contraction of the jet, particularly for large values of d/D . With increasing turbulence, viscous effects decrease in relative magnitude, wherewith all curves begin to approach asymptotic limits. Such limits are actually reached, however, only when the Reynolds number is infinitely great, for not until then is the velocity of approach evenly distributed over the cross section.

The close relationship between the trend of the discharge coefficient and the growth of turbulence in the conduit may be seen by plotting the same experimental data against the Reynolds number of the conduit. Figure 130 thus shows C_d as a function of VD/ν for orifices in smooth pipes, generalized from the measurements of Johansen, and from those of Witte for high

values of R . The approximate limits of these curves are plotted in Fig. 131a against d/D , together with the corresponding values of C_d and $C_v C_c$.

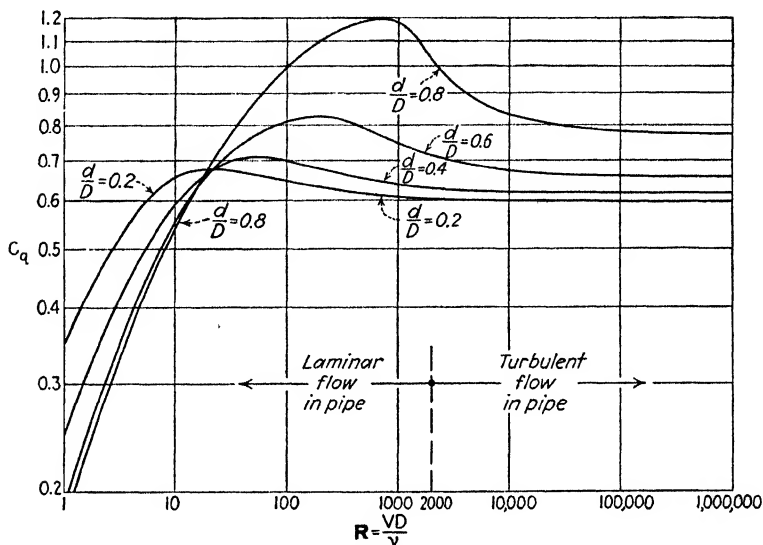


FIG. 130.—Generalized logarithmic plot of C_q as a function of R and d/D .

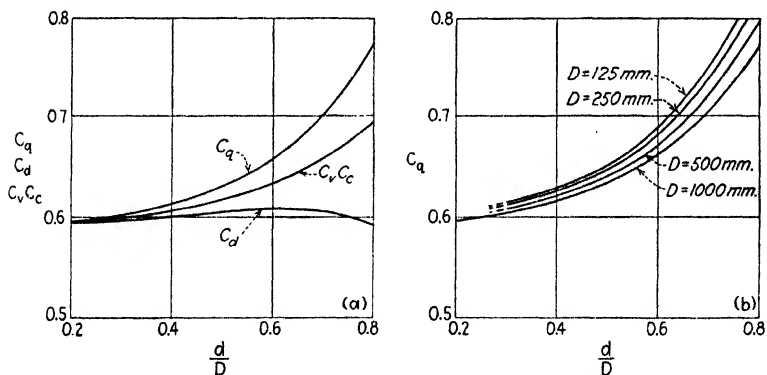
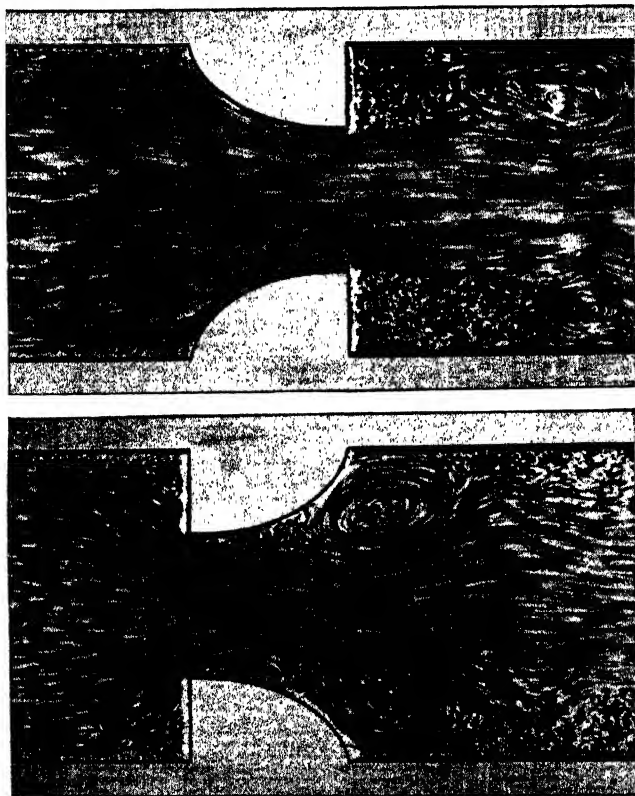


FIG. 131.—Variation in discharge coefficients with d/D and D .

As yet the influence of conduit roughness upon orifice discharge has not been analyzed quantitatively in accordance with known characteristics of flow in rough pipes. It is apparent, however, — that the greater the ratio of maximum to mean velocity in the approaching flow (increasing with the relative roughness of the

boundary), the smaller will be the contraction of the flow as it passes the orifice. Such effects are indicated by the measurements of Jacob and Kretzschmer¹ on orifices in pipes of different diameters but of essentially the same absolute roughness. As



Columbia

FIG. 132.—Flow through a rounded orifice, showing relative effect of gradual and abrupt boundary transition.

may be seen from the sequence of curves in Fig. 131*b*, the maximum value of C_v corresponds to the minimum pipe diameter, and hence to the maximum relative roughness.

In its general aspects the foregoing analysis is applicable to any conduit transition of related form, whether or not it is

¹ JACOB, M., and KRETZSCHMER, F., Die Durchflussszahlen von Normaldüsen und Normalstaurändern für Rohrdurchmesser von 100 bis 1000 mm, *Zeitschrift VDI*, vol. 73, no. 26, p. 935, 1929.

intended for flow measurement. In this category may be included flow nozzles and Venturi tubes, pipe inlets, abrupt contractions or enlargements, divergent or convergent sections, needle valves—in fact, all boundary changes that are symmetrical about a central axis. In the case of flow measurement, interest centers in the coefficient of discharge, but this may readily be converted into a coefficient of resistance when energy loss is of primary concern. Either of the two related coefficients

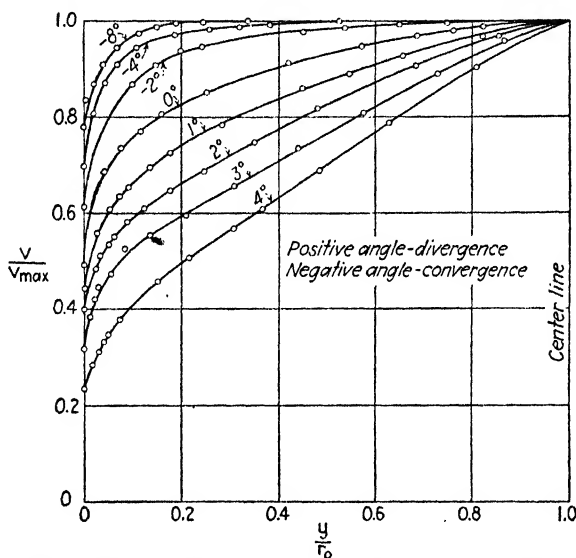


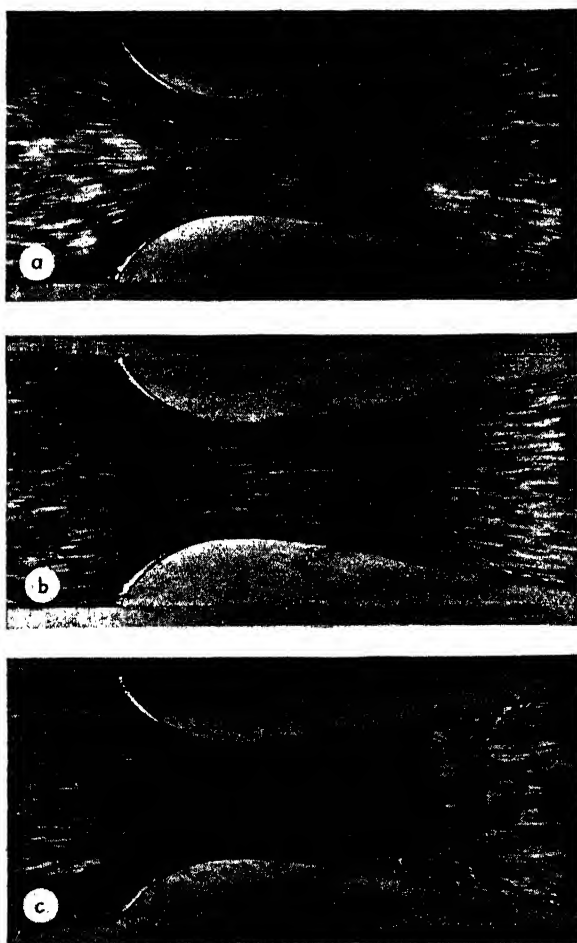
FIG. 133.—Velocity distribution in convergent and divergent flow.

will invariably be some function of the Reynolds number and the conditions of approach, the function varying from case to case with the geometry of the transition.¹

If, in distinction to the plate orifice, the boundary change is relatively gradual, the flow phenomenon will involve primarily the distribution of dynamic pressure and velocity, the energy loss then being of secondary importance. That convergence effectively modifies the velocity profile may be seen from Fig. 133, showing measurements of velocity distribution in con-

¹ For numerical data the reader is referred to such standard texts as DAUGHERTY'S "Hydraulics," and to the extensive bibliography given by KRETZSCHMER, F., in *Strömungsform und Durchflusszahl der Messdrosseln*, VDI Forschungsheft 381, 1936.

vergent throats of different central angles.¹ As is apparent from the same illustration, under sufficiently small angles of



Columbia

FIG. 134.—Establishment of flow through a Venturi throat; note beginning of separation as boundary layer develops.

divergence turbulent flow will not separate from the conduit walls, and very gradual enlargements of section may then also

¹ NIKURADSE, J., Untersuchungen über die Strömungen des Wassers in konvergenten und divergenten Kanälen, *Forsch.Arb. a. d. Geb. d. Ingenieurwesens*, 289, 1929.

be treated in similar fashion. More rapid deceleration, however, is certain to result in separation, conditions in the wake depending upon R and upon the form of the profile. At high values of the Reynolds number—in particular if the boundary curvature is abrupt—the coefficient of resistance will become independent of R , varying only with change in the boundary contours.

Figure 135 illustrates a study by Kröner¹ of energy loss in relation to the angle of divergence, all angles but the smallest

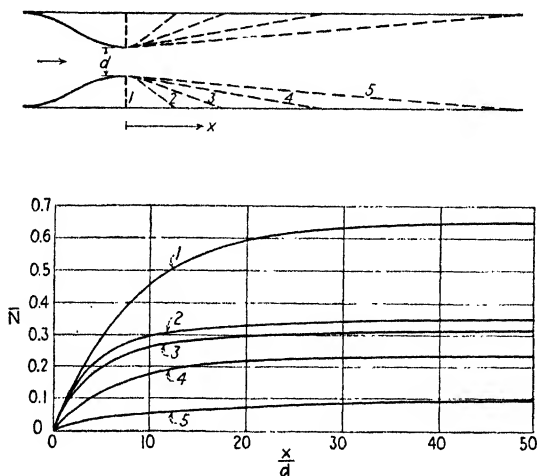


FIG. 135.—Loss of potential energy in diverging flow.

($10^{\circ} 46'$) being sufficiently great for separation to occur, and the Reynolds number being of such magnitude that viscous influences were negligible. In all cases the transition was two-dimensional. The dimensionless ordinate \bar{N} denotes the magnitude of the energy loss up to any section in its ratio to the kinetic energy at the throat. It is apparent that the loss of energy increases with angle of divergence, indicating a correspondingly greater intensity of the eddy motion in the region of discontinuity. In other words, the restoration of kinetic energy to potential energy decreases with angle of divergence. Moreover, as will be seen from the magnitude of the ratio x/d at which the

¹ KRÖNER, R., Versuche über Strömungen in stark erweiterten Kanälen, *Forsch. Arb. d. VDI*, 222, 1920.

curves approach a constant slope, the restoration (such as it is) does not reach completion until quite some distance downstream.

Reference to the velocity profiles indicated in Fig. 127 will show that the mixing process in the wake results in a transport of fluid with high velocity from the central region toward the walls, and thus tends to equalize the velocity distribution with distance downstream from the transition. At the same time, however, the eddies spread from the initial region of discontinuity toward the centerline. Since the energy of flow which is transformed into turbulence in this expanding wake cannot be abruptly dissipated in the form of heat, it follows that the degree of turbulence of the flow as a whole must be abnormally great by the time the wake has expanded to the axis of the conduit. Although the rate of energy dissipation within the eddies is high at this section, the intensity of the turbulent fluctuations is not reduced to a normal value before the flow has traveled many pipe diameters in the downstream direction. Not until this excess turbulence is completely dissipated will the velocity distribution and the longitudinal pressure gradient again correspond to established uniform motion.

62. Secondary Flow in Asymmetrical Conduits. Quite distinct from the secondary pattern of the velocity fluctuations in turbulence is a type of secondary movement resulting from asymmetry of conduit boundaries. So long as these boundaries are surfaces of revolution, the enclosed flow must be perfectly symmetrical about the longitudinal axis—with the possible exception of intermittent pendulation of the wake downstream from an abrupt enlargement. Such symmetry may be destroyed, however, in two different ways: either by changing the shape of the cross section or by curving the axis of the conduit. Either modification will result in a form of secondary flow that remains independent of time so long as the mean motion itself is steady. But it is then evident that the temporal mean velocity vector must be the resultant of primary and secondary components. If the primary flow is considered essentially longitudinal, it is apparent that the secondary flow must take place in the plane of the conduit cross section. In other words, the secondary movement is evidenced by the presence of circulation superposed upon the longitudinal translation of the fluid, the stream lines of the mean motion then assuming a spiral form.

The most penetrating investigation of secondary flow caused by cross-sectional form was undertaken by Nikuradse¹ at Prandtl's suggestion. Rectangular, triangular, and grooved circular conduits were studied with respect to longitudinal velocity distribution and circulation, the latter being determined

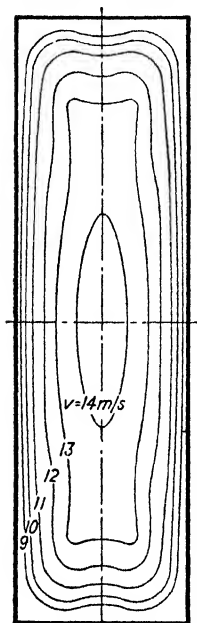


FIG. 136.—Velocity distribution in a narrow rectangular conduit.

photographically through injection of a milky fluid at numerous points over the section. In every case there was found to exist a definite secondary flow toward the corners of the section and away from the sides, with the result that the isovels—velocity contours—were transposed locally in the direction of the secondary motion. The measured velocity distribution in the case of a narrow rectangular conduit is reproduced in Fig. 136, from which it is seen that the velocity in the corner regions is far higher than would normally be expected, whereas points of inflection are to be found

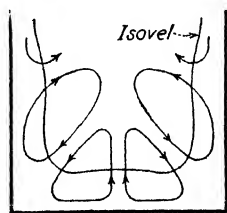


FIG. 137.—Secondary flow at the corners of a conduit.

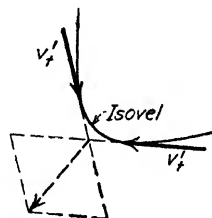


FIG. 138.—Resultant of tangential fluctuations.

in each isovel a short distance away. The pattern of circulation producing this effect is indicated in Fig. 137.

Prandtl offered an explanation of the phenomenon in terms of turbulent fluctuation.² In the case of a symmetrical cross section the isovels are necessarily concentric circles, the three components of fluctuation being directed longitudinally, radially, and tangentially. In the foregoing treatment of apparent shear, the

¹ NIKURADSE, J., Untersuchungen über turbulente Strömungen in nicht kreisförmigen Röhren, *Ingenieur-Archiv*, vol. 1, p. 306, 1930.

² PRANDTL, L., Über die ausgebildete Turbulenz, *Proc. 2d Int. Cong. for App. Mech.*, Zurich, p. 62, 1927.

tangential components were neglected—not because they were of lesser magnitude than the others, but simply because they were not effective in the mechanism of symmetrical pipe resistance. Once an isovel changes curvature, however, the tangential components of fluctuation are no longer in symmetrical equilibrium, but produce a resultant stress normal to the isovel in the region of maximum curvature, as shown schematically in Fig. 138. Inasmuch as the velocity decreases outward, the resultant force will also be outward, regardless of direction of the fluctuation. This force, reasoned Prandtl, tends to produce a mean secondary flow across the isovels in this region—toward the corners of the rectangular conduit—which, by reason of continuity, must be accompanied by an equivalent inward flow across adjacent parts of the isovels where the curvature is less pronounced.

Although the secondary flow occurring at a conduit bend is of essentially the same nature, its cause is quite different. Were the energy of the fluid the same at every point, the distribution of velocity would correspond to conditions of potential motion, the pressure intensity reaching a maximum along the outer boundary at the midpoint of the bend. Since viscous resistance actually reduces the boundary velocity, the energy in the boundary region is less than that in adjacent layers; it must follow that at the outside of the bend the pressure intensity falls away abruptly toward the boundary. Since this pressure gradient normal to the boundary is exactly opposite to that of potential motion, secondary flow takes place in the direction of the outer wall, continuity requiring an inward flow along the side walls to compensate, according to the diagram in Fig. 139a.

The resulting double spiral that is characteristic of flow at bends has long been observed, perhaps the most effective experimental studies being those of Hinderks.¹ By constructing long-radius elbows in split sections and coating the inside surfaces with a heavy paint, Hinderks was able to secure the actual pattern traced in the partially dry paint by the moving fluid.

The effect of this induced circulation at bends is threefold: In addition to the energy lost in normal boundary resistance, further energy is taken from the primary flow to produce the

¹ HINDERKS, A., *Nebenströmungen in gekrümmten Kanälen*, *Zeitschrift* n. 1779, 1927.

secondary movement. The velocity distribution at the bend is completely modified, for the spiral motion transposes the region of maximum velocity toward the outside of the bend. Finally, the circulation persists a considerable distance downstream from the bend (from 50 to 75 pipe diameters), and until it disappears, conditions of established, uniform motion will not prevail.

If the ratio of conduit diameter to radius of bend is large, it is evident that the rapid deceleration of the flow (before the mid-

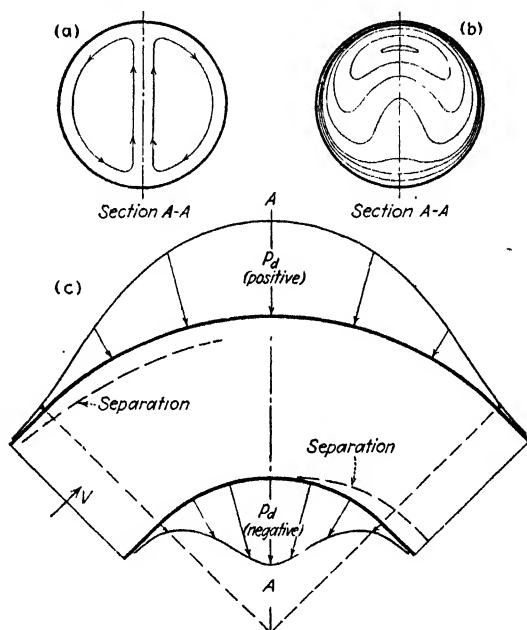


FIG. 139.—Flow at a conduit bend.

point of the bend along the outer wall and past the midpoint along the inner wall) will produce two regions of separation that further add to the energy loss. Measurements by Nippert¹ show that the effect of the secondary motion is still quite evident, even when separation occurs, as may be seen from the velocity distribution in Fig. 139*b*. Nippert found, however, that the pressure distribution does not differ appreciably from that of potential motion, despite the complete redistribution of velocity. Since in potential flow the pressure difference between the inside

¹ NIPPERT, H., *Über den Strömungsverlust in gekrümmten Kanälen*, *Forsch. Arb. a. d. Geb. d. Ingenieurwesens*, 320, 1929.

and the outside of a given bend depends only upon the quantity $\rho V^2/2$, it is then to be expected that the rate of discharge through a commercial pipe bend will vary directly with the square root of the pressure difference—the discharge coefficient remaining practically constant for high values of R . This fact has been utilized at the University of Illinois in adoption of the pipe elbow as a discharge meter.

Many attempts have been made to determine the energy loss at bends as a function of the Reynolds number and the bend

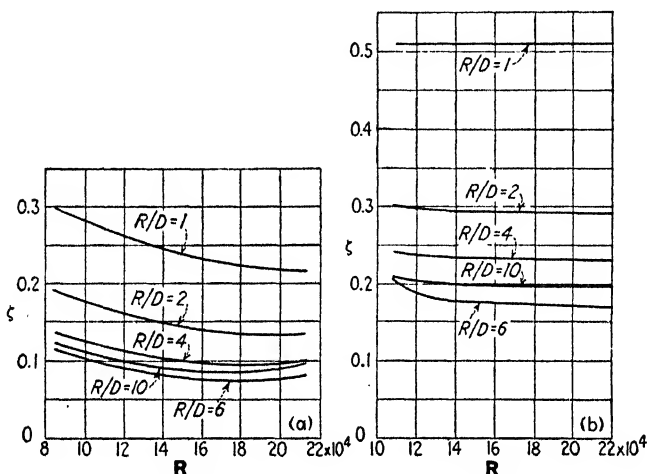


FIG. 140.—Resistance coefficients for 90° bends; (a) smooth pipes, (b) rough pipes.

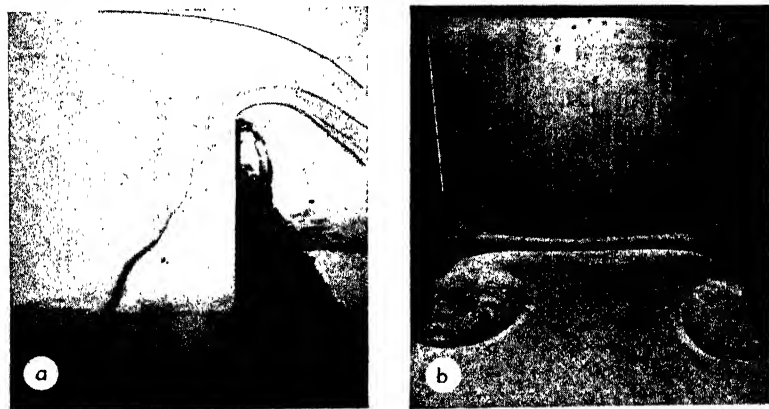
proportions, with results that are in general quite unsatisfactory—indeed, almost as many contradictory curves have been published as there have been investigators engaged in such research. Perhaps the most dependable of these are due to Hofmann,¹ whose generalized results are presented in Fig. 140. It is apparent that in smooth bends the resistance coefficient ζ in the expression

$$-\Delta p = \zeta \frac{\rho V^2}{2} \quad (187)$$

is greatest when the ratio of radius of bend to pipe diameter is very low, since the effect of separation is then the most pro-

¹ HOFMANN, A., Der Verlust in 90°-Rohrkrümmern mit gleichbleibendem Kreisquerschnitt, *Mitteilungen des hydraulischen Instituts der T. H. München*, no. 3, Oldenbourg, Munich, 1929.

nounced; even then, however, the viscous influence is still appreciable, as evidenced by variation with R . That the resistance coefficient again increases as the ratio R/D becomes great is due to the increasing length of surface along which shear would occur under any circumstances. The effect of roughening the boundary is apparent from the neighboring curves, the loss from separation at low values of R/D no longer varying with R .



M.I.T.

FIG. 141.—Secondary motion at the base of a weir. The vortex filament in *a* is colored by crystals of dye buried in the sand bed. In *b* is shown the pattern left in the sand.

A first approximation for the loss at bends of a central angle greater or less than 90° may be obtained by multiplying ζ by the ratio $\alpha^\circ/90^\circ$.

In the case of very abrupt changes in direction in conduits of rectangular cross section, the combined effect of separation and secondary spiral motion may give rise to intense, intermittent vortex motion in each of the outer corners. While the existence of a free surface is not essential to this phenomenon, similar effects may be observed directly upstream from a sluice gate or weir (Fig. 141). The reduction in velocity due to drag along the lower boundary produces a normal reversal of flow in the region of stagnation at the base of the weir, as shown by the sand pattern in Fig. 141*b*. However, the velocity defect is even more pronounced at the juncture between the floor and either wall, which considerably augments the tendency toward flow reversal at the sides and leads to the formation of a vortex normal to the floor near each corner (Fig. 141*a*). As soon as such a vortex is

established, the pressure gradient leading to its formation no longer exists, and the secondary motion abruptly ceases. Thereupon, the cycle begins once again. Since low pressures accompany the high tangential velocities, the vortex filament may be ventilated from the downstream side, a tube of air often penetrating the flow well past the plane of the weir. Ventilation from the upstream side of the sluice gate may also follow the formation of

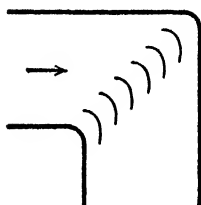


FIG. 142.—Guide vanes in a conduit bend.

depressions in the upper surface similar to those of Fig. 27.

A very successful method of eliminating practically every unwanted effect of the conduit bend has long been used in aeronautics, and is gradually finding favor among hydraulic engineers. The bend is made as abrupt as possible, the fluid being diverted through the corresponding angle by means of a series of properly designed guide vanes, as shown in

Fig. 142. If the form and spacing of these vanes¹ are correctly chosen, the resistance coefficient may be as low as 0.15, whereas the flow leaves the elbow free from secondary motion and with a practically uniform velocity distribution. Needless to say, such a method would be economically unsound in the case of small commercial pipe fittings, but in the larger sizes vaned elbows have been welded to order at a cost similar to that of standard products. Quite aside from the eventual probability of commercial recognition, the use of guide vanes in the experimental laboratory is extremely advantageous.

¹ Quantitative information is given in KROBER, G., *Schaufelgitter zur Umlenkung von Flüssigkeitsströmungen mit geringem Energieverlust*, *Ingenieur-Archiv*, vol. 3, p. 516, 1932.

CHAPTER XIII

FLOW IN OPEN CHANNELS

63. Survey of the General Problem. Fundamentally similar in every other respect, the open channel possesses one distinguishing characteristic that renders it considerably more difficult of investigation than the closed conduit—a free surface, the form of which introduces one further variable into any functional relationship. Open-channel flow thus displays almost the identical phenomena of velocity distribution, resistance, and secondary flow, described in the preceding chapter, but only in the case of established uniform motion does the free surface fail to introduce complexities of primary magnitude.

The form of the surface profile is determined by the fact that all forces involved in the motion must produce as upper boundary a stream line along which the pressure intensity is constant. Except in small-scale models, the effect of surface tension is negligible, so that weight and viscosity are the two force properties involved in open-channel flow. Although the most general case includes appreciable influence of both, solution of such problems is at best extremely difficult. For practical reasons, therefore, it has been found expedient to distinguish between two broad classes of motion: that in which the surface profile is determined primarily by boundary resistance, and that in which the surface curvature is the result of rapid or abrupt change in the boundary contour. The extreme case of the latter type of motion has been presented at length in Part One; on the other hand, the problem of resistance in established motion differs little from that in the closed conduit of uniform section, and a vast number of practical problems involve acceleration that is so gradual that inertial effects may be considered negligible in comparison with boundary drag.

Owing to similarity of conditions, analytical study of uniform flow in open channels is quite as far advanced as that of uniform flow in the closed conduit—so long as conditions of symmetry are

equivalent. In other words, the circular conduit finds its counterpart in the open channel of constant depth and infinite width, under which circumstances equations of velocity distribution and resistance are practically identical in the two cases. But the channel of finite width is equivalent to the conduit of non-circular cross section, the secondary flow which occurs in either case still awaiting satisfactory treatment in general terms. Needless to say, such difficulties in the treatment of uniform motion are equally in evidence in the investigation of non-uniform motion, and only in the case of two-dimensional flow can any approach to a rigorous analysis be hoped for at the present time. Both gradually varied flow and rapidly varied flow, in channels of finite width, have thus far yielded only to empirical investigation, although analytical methods are gradually eliminating many of the misinterpretations that seem to accompany pure empiricism, and are slowly throwing light upon a complex phase of fluid motion. It is the purpose of this chapter to clarify the basic aspects of the problem, in the effort to provide a sound background for further advancement.

64. Velocity Distribution and Resistance in Uniform Motion.

Hydraulic literature contains considerable evidence of the attempts that have been made to fit velocity measurements to a parabolic, ellipsoidal, or exponential distribution curve of one sort or another. It is noteworthy, therefore, that Krey¹ derived a logarithmic function both for pipes and for open channels at a time when exponential functions for pipe flow were much in favor—some years before von Kármán introduced his similarity hypothesis which led to the universal logarithmic equations. Krey's expression for a wide channel actually yields a curve that differs little from that of Eq. (175):

$$v = v_{\max} \frac{\log \left(1 + \frac{y}{a} \right)}{\log \left(1 + \frac{d}{a} \right)}$$

The factor y is a variable distance from the lower boundary, d is the total depth, and a is the very small distance between the

¹ KREY, H., Die Quer-Geschwindigkeitskurve bei turbulenter Strömung, *Zeit. angew. Math. Mech.*, vol. 7, no. 2, 1927.

Even earlier (1893) a logarithmic function was obtained by Jasmund; see FORCHHEIMER, "Hydraulik," p. 179.

boundary and the reference axis. The physical deductions that led Krey to formulate this expression, as well as the accuracy with which he found it to agree with experimental data, would lead one to conclude that Eqs. (170) and (172) should apply equally well to open channels as to pipes, so long as the problem is one of two dimensions.

A question remains, nevertheless, with regard to the mechanism of the mixing process in the neighborhood of the free surface. Nikuradse, it will be recalled, found indirectly from laboratory measurement that the mixing length invariably reached a maximum at the pipe axis (Fig. 115), a result which one would naturally expect in the case of pipe flow. But at a relatively smooth free surface, on the contrary, the length characteristic of the mixing process must approach the limit zero, for otherwise the surface would be the scene of violent agitation in the vertical direction. Visual observation would indicate that only the vertical component of the turbulent mixing is reduced at the free surface, for relatively large surface eddies are visible in any open-channel flow of appreciable velocity. In Chapter XII, however, brief mention was made of the fact that von Kármán's logarithmic velocity functions necessarily have a finite slope dv/dy at the pipe axis, a discrepancy accompanied by a curve for the mixing length that approaches zero at the centerline of flow. Although these circumstances are at variance with actual conditions in the case of pipe flow, they still appear to introduce no serious error; and since they are more nearly in accord with surface conditions in the open channel, there is no reason to question seriously their validity until definite experimental evidence is at hand.

Under normal conditions of flow in actual channels, geometrical dimensions are usually so great that not only is the motion definitely turbulent, but the Reynolds number is well above the range of appreciable viscous influence. Although artificially lined channels are sometimes so smooth that a laminar boundary film may still exist, more often than not it is boundary roughness that determines the magnitude of wall shear. Under such conditions, Eq. (172) is applicable once boundary roughness may be described in terms of a linear parameter k . It remains, however, to determine τ_0 in terms of suitable flow characteristics. From Fig. 143 it is evident that the following relationship must

hold for very wide channels, the factor $S = \sin \alpha$ denoting the identical slopes of energy line, water surface, and channel bottom:

$$\begin{aligned}\gamma b y dx \sin \alpha &= \tau_0 b dx \\ \tau_0 &= \gamma y S\end{aligned}\quad (188)$$

On the other hand, just as in the case of flow in a closed conduit, the intensity of boundary shear will vary according to the following functional relationship:

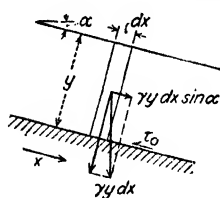


FIG. 143.—Definition sketch—boundary shear in an open channel.

$$\tau_0 = \varphi \left(\frac{Vy}{\nu}, \frac{k}{y} \right) \frac{\rho V^2}{2} \quad (189)$$

The function φ is the customary dimensionless resistance coefficient [compare with Eq. (158)] and is equal in magnitude to one-fourth the pipe coefficient f ; therefore, combining Eqs. (188) and (189),

$$S = \frac{f}{4y} \frac{V^2}{2g} \quad (190)$$

Just as the velocity distribution in the central regions of very wide channels of constant depth is fully described by Eqs. (170),

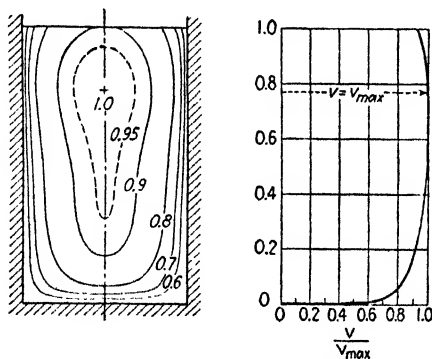


FIG. 144.—Velocity distribution in a narrow channel.

(172), and (175), the resistance coefficient may be determined by Eqs. (182) and (184).

Whereas the pipe of uniform circular cross section is that type of closed conduit most frequently encountered, its counterpart—the open channel in which side effects are negligible—plays only a

small role in engineering practice. To expect that the same relationships would be applicable to any channel, regardless of width and cross-sectional form, is at best optimistic—in particular if one recalls the secondary flow in a conduit of non-circular cross section. In Fig. 144, for instance, are plotted velocity measurements made by Nikuradse in a narrow open channel, corresponding approximately to the proportions of the closed

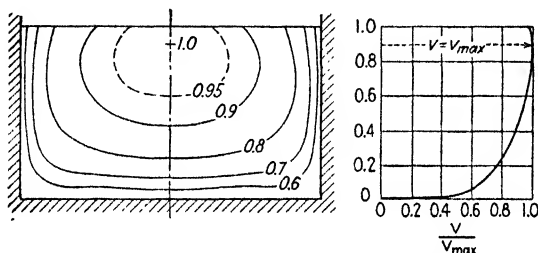


FIG. 145.—Velocity distribution in a wider channel.

conduit of Fig. 136. Comparison of these plots will show at once that the influence of the two boundary corners is essentially the same; but, in addition, the effect of the secondary flow in the upper regions is to depress the region of maximum velocity a considerable distance below the free surface. Figure 145, based on measurements by Bazin¹ in a channel of greater width, indicates that the maximum velocity occurs considerably nearer the free surface—a trend that approaches the limit already discussed as the width-depth ratio becomes very great.

In other words, the velocity distribution in an open channel is definitely dependent upon the relative magnitude of channel width and channel depth. Evidently, it will also depend upon cross-sectional form, for the secondary flow in a semicircular channel, for instance, must differ to some extent from that in one of trapezoidal form, although the width-depth ratio is the same. But even for a given channel section the magnitude of the roughness must influence the relative position, and hence the relative shape, of the isovels (a fact vindicated by experiment), under which circumstances it will be seen that the location of the region of maximum velocity is not dependent upon form alone. Inasmuch as the velocity gradient at the boundaries will therefore

¹ DARCY, H., and BAZIN, H., *Recherches hydrauliques, Mém. prés. par divers savants*, Paris, 1865.

vary from point to point of a cross section of finite width, it follows that the intensity of boundary shear cannot be assumed constant over the walls and floor of the channel. The distribution of τ_0 must then be a function of the Reynolds number of the flow, the geometry of the cross section, and the relative roughness of the boundary.

If, for convenience, τ_0 is nevertheless assumed to represent the mean intensity of boundary shear, in uniform motion the following equilibrium of forces must prevail,

$$\gamma A S dx = \tau_0 P dx$$

in which P represents the perimeter of the wetted boundary, whereas A refers to the area of the flow section. These two parameters are customarily combined in the form $A/P = R$, the so-called hydraulic radius of the cross section, whereupon

$$\tau_0 = \gamma R S \quad (191)$$

It is obvious, however, that the factor R does not fully describe the geometry of the cross section, for R may have the same magnitude for an infinite variety of cross-sectional forms. If, therefore, one seeks to express the mean boundary shear in terms of R in a manner parallel to that of Eq. (189), the resistance coefficient must be a function of three distinct parameters—a Reynolds number VR/ν , relative roughness k/R , and a form factor β :

$$\tau_0 = \varphi\left(\frac{VR}{\nu}, \frac{k}{R}, \beta\right) \frac{\rho V^2}{2} \quad (192)$$

Combining with Eq. (191),

$$S = \frac{f}{4R} \frac{V^2}{2g} \quad (193)$$

This is seen to yield Eq. (190) as R approaches the limit y ; moreover, it is identical with Eq. (180), since $R = D/4$ in the case of a circular pipe.

Existing experimental data are not sufficient to determine the characteristics of the factor β —indeed, the necessity of giving due weight to channel form has seldom been recognized by the hydraulician. On the other hand, variation of f with the Reynolds number is usually slight, owing to the negligible influence

of mean viscous shear at the high values of R which usually prevail. Relative roughness, therefore, has been the parameter which has received the principal attention.

Credit for the first comprehensive formulation of the effect of relative roughness is due von Mises,¹ who derived from experimental evidence the dimensionally correct expression applicable alike to closed and open conduits:

$$f = 0.0096 + 4\sqrt{\frac{k}{R}} + \frac{0.85}{\sqrt{R}} \quad (194)$$

At high values of R , or for high magnitudes of k/R , the last term becomes of negligible value. The factor k , evidently, must have the dimension of length, so that tables of this parameter will necessarily vary in numerical magnitude from one dimensional system to another. Table IV, indicates the variation of this factor with boundary material, after von Mises, the foot being used as the length unit.

Equation (193) is more commonly written in the form derived in 1775 by de Chézy,

$$V = C\sqrt{RS} \quad (195)$$

in which the Chézy coefficient C is neither dimensionless nor constant, as formerly considered, for

$$C = \sqrt{\frac{8g}{f}} \quad (196)$$

The magnitude of C , in turn, is generally computed through use of the empirical relationships of Ganguillet and Kutter, Manning, or Bazin; these are, respectively, as follows:

$$C = \frac{41.65 + \frac{0.00281}{S} + \frac{1.811}{n}}{1 + \left(41.65 + \frac{0.00281}{S}\right) \frac{n}{\sqrt{R}}} \quad (197)$$

$$C = \frac{1.486R^{1/6}}{n} \quad (198)$$

$$C = \frac{157.6}{1 + \frac{m}{\sqrt{R}}} \quad (199)$$

¹ MISES, "Elemente der technischen Hydromechanik," p. 62.

The factor n appearing in the first and second expressions is the same (refer to Table IV), and is presumed to incorporate the

TABLE IV.—CHARACTERISTIC VALUES OF THE ROUGHNESS FACTORS k , m , AND n

Boundary surface	von Mises k (ft. $\times 10^4$)	Bazin m (ft. ^{1/2})	Manning n (ft. ^{1/6})
Smooth brass.....	0.3-1.6	0.007-0.009
Planed wood.....	4-8	0.109	0.010-0.014
Unplaned wood.....	8-16	0.290	0.011-0.015
Finished concrete.....	1.2-2.4	0.109	0.011-0.013
Unfinished concrete.....	3.3-6.6	0.290	0.013-0.016
Cast iron.....	16-33	0.013-0.017
Riveted steel.....	33-82	0.017-0.020
Brick.....	33-90	0.290	0.012-0.020
Rubble.....	150-600	0.833	0.020-0.030
Earth.....	1600-3300	1.54	0.020-0.030
Gravel.....	2.35	0.022-0.035
Earth with weeds.....	3 17	0.025-0.040

absolute roughness of the boundary; as will be seen, however, it has three different dimensions in the two equations. Bazin's m , on the other hand, appears as numerator in a fraction having $R^{1/2}$ as denominator; dimensionally, therefore, it is the square root of a length, the ratio m^2/R evidently being a true relative roughness parameter.¹ Although these several expressions are in general use in many countries, and give fairly satisfactory results over the normal range of practice, they are at best empirical relationships with scarcely a trace of analytical foundation. Nevertheless, until methods which have proved so fruitful in the case of closed conduits are extended to the more difficult problem of open-channel flow, they are the best available to the profession. So long as the engineer bears in mind their empirical nature, they will continue to yield results of practical value—in particular for channels which do not have extremely different cross-sectional forms. Altogether too often, however, they have been accepted as a foundation for analysis of a more advanced

¹ While the ratios $n/R^{1/2}$ and $n/R^{1/6}$ also indicate relative roughness, the numerical equality—but dimensional inequality—of the Kutter and the Manning n leaves their significance open to question. On the other hand, Eqs. (197) and (198) yield essentially the same results, while Eq. (199) will agree only if m (or n) also varies with R . The Manning formula is generally preferred.

nature—in particular in the field of sediment transportation. The danger in such methods should be self-evident.

65. Energy and Discharge Diagrams. At any point in a given flow the total head (energy per unit weight of fluid) has been shown to consist of velocity head, pressure head, and elevation. Strictly speaking, the velocity head should include the kinetic energy of the mean flow and the kinetic energy of turbulence; the latter, however, is not recoverable as energy of flow, and may now be omitted from the general statement. Similarly, while the pressure head at a given point must vary with direction as a result of the secondary stresses, such variation is not directly measurable, and hence may also be neglected. In the most general case both velocity head and pressure head will vary with elevation over a section normal to the flow—in part because of the dynamic effects of acceleration, in part because of the energy defect due to boundary resistance.

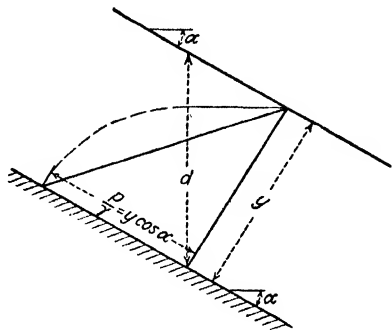


FIG. 146.—Pressure distribution in uniform flow on a steep slope.

If the discussion is restricted to cases of gradually varied flow, accelerative forces become quite negligible, under which circumstances the sum $\left(\frac{p}{\gamma} + h\right)$ must be constant over any normal section. It follows, therefore, that the pressure head at any point can equal neither the normal distance from the water surface nor the vertical distance, as is generally supposed, unless the water surface itself is horizontal. It may be seen from Fig. 146 that the pressure head at any vertical depth is equal to this depth multiplied by the square of the cosine of the angle between the vertical and the normal; a similar relationship may be found by equating the total floor pressure in Fig. 143 to the normal component of fluid weight. If the angle α is small, however, it is apparent that its cosine will differ only inappreciably from unity. For a channel having a slope of 1:10, for instance, $\cos^2 \alpha = 0.99$, which differs from unity by only 1 per cent. Under such circumstances, it makes little practical difference whether y is measured in the vertical or normal direction; simi-

larly, x may then represent distance in the horizontal direction or parallel to the channel bottom.

The velocity distribution, on the other hand, causes a definite variation in total head from the top to the bottom of the section, as well as from side to side. Since it is expedient to express the weighted mean total head in terms of the mean velocity, the quantity $V^2/2g$ must be multiplied by K_e , the velocity-head correction factor, whose value becomes unity only when the velocity is constant over the section. The magnitude of K_e may be as low as 1.05 in the case of very smooth boundaries and high velocities of flow, rising well beyond 1.20 if the relative roughness is great. Accurate investigations require due regard for this factor, in particular if the velocity distribution varies from one section to the next. On the other hand, in the development of methods of practical engineering value, inclusion of this variable as a function of other flow characteristic introduces needless complexities—a gesture not in keeping, for instance, with such inexact methods as are involved in the empirical expressions for resistance. K_e , therefore, is considered to have the value unity in the following developments.

The total head over a given vertical section will then be given by the simplified expression,

$$E_w = \frac{V^2}{2g} + \frac{p}{\gamma} + h \quad (200)$$

But since the potential head is constant over the section, and equal to the depth y plus the elevation h_0 of the lower boundary of the flow, the elevation of the energy line above the lower boundary may be written simply as the sum of velocity head and depth:

$$E_w - h_0 = H = \frac{V^2}{2g} + y \quad (201)$$

This quantity is commonly called the specific energy, H referring specifically to a datum which always coincides with the lowermost stream line.

In two-dimensional motion, the rate of discharge q per unit width of section is merely the product of depth and mean velocity; Eq. (201) then becomes

$$H = \frac{q^2}{2gy^2} + y \quad (202)$$

The foregoing expression is seen to involve only three variables (presuming g to remain constant), any one of which may be considered dependent upon the other two. In the most general case all three will vary, but in many types of motion one or another may change only slightly, if at all. Such states of flow may then be treated—at least as a first approximation—in terms of only two variables, in connection with which a plotted curve of the functional relationship is particularly helpful.

For instance, if q remains constant, according to Eq. (202) there will be two possible depths of flow y for every value of H . At some depth the specific energy must therefore reach a minimum value, which may be determined for any given q by differentiating Eq. (202) with respect to y and setting the result equal to zero; thus,

$$\frac{dH}{dy} = -\frac{2q^2}{2gy^3} + 1 = 0$$

whence

$$\left(\frac{q^2}{gy^3}\right)_{n_{\min}} = 1 \quad (203)$$

The depth and velocity corresponding to minimum specific energy are designated as critical and given the subscript c ; in terms of the constant rate of discharge,

$$y_c = \frac{2}{3} H_c = 2 \frac{V_c^2}{2g} = \sqrt[3]{\frac{q^2}{g}} \quad (204)$$

and

$$V_c = \sqrt[3]{gq}$$

As will be seen from Fig. 147, a convenient dimensionless plot of the function $y:H$ (the specific-energy diagram) may be constructed from the relationship

$$\frac{H}{y_c} = \frac{1}{2} \left(\frac{y_c}{y}\right)^2 + \frac{y}{y_c} \quad (205)$$

which is obtained by dividing the several terms of Eq. (202) by y_c or its equivalent.

Were H taken as the constant term in Eq. (202), it is apparent that for every value of q two depths of flow would again be possible. The rate of discharge must then have a maximum value for the given specific energy, which may similarly be

found by differentiating q with respect to y and setting the result equal to zero:

$$\frac{dq}{dy} = \sqrt{2g} \frac{2H - 3y}{2\sqrt{H - y}} = 0$$

whence,

$$\left(\frac{2H}{3y}\right)_{q_{\max}} = 1 \quad (206)$$

Evidently, the criterion for maximum discharge at a given specific

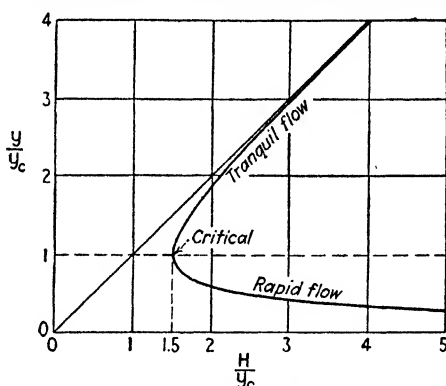


FIG. 147.—Dimensionless specific-energy diagram for two-dimensional flow.

energy is the same as that for minimum specific energy at a given rate of discharge. In other words, the terms maximum discharge and minimum energy both refer to conditions of critical flow. The maximum or critical discharge is seen to have the form

$$q_c = \sqrt{g} y_c^{3/2} = \sqrt{g} \left(\frac{2}{3} H\right)^{3/2} \quad (207)$$

As shown in Fig. 148, a dimensionless discharge diagram may be constructed from the equation

$$\frac{1}{2} \left(\frac{q}{q_c}\right)^2 = \frac{3}{2} \left(\frac{y}{y_c}\right)^2 - \left(\frac{y}{y_c}\right)^3 \quad (208)$$

FIG. 148.—Dimensionless discharge diagram. which may be derived in the same fashion as Eq. (205).

It now remains to examine the relationship that must obtain between H and q for constant depth. As may be seen from

inspection of Eq. (202), the minimum value of H is now reached when $H = y$ (that is, when the energy line coincides with the free surface), under which circumstances the rate of discharge will be zero; obviously, there is no upper limit to the magnitude of either q or H so long as y remains constant. The function $H:q$ may be plotted in the dimensionless form

$$\frac{H}{y} = \frac{1}{2} \left(\frac{q}{\sqrt{g} y^{3/2}} \right)^2 + 1 \quad (209)$$

as shown in Fig. 149.

A simple illustration of the use of the specific-energy diagram is seen in Fig. 150. It is assumed for simplicity that the energy line remains horizontal, the change in H resulting from the fact that the lower boundary rises the distance Δh_0 . Two surface profiles are possible, depending upon whether the depth of the approaching flow is greater or less than $y_c = \sqrt[3]{q^2/g}$; as seen from the figure, the surface will drop when $y_1 > y_c$ and will rise when $y_1 < y_c$, in accordance with the energy diagrams superposed on the boundary profile. In either case, both y_1 and y_2 are definitely established by the rate of discharge and

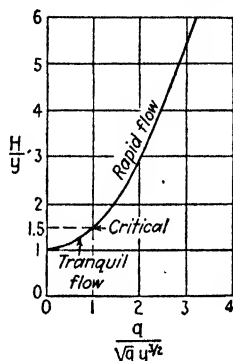


FIG. 149.—Dimensionless energy-discharge diagram.

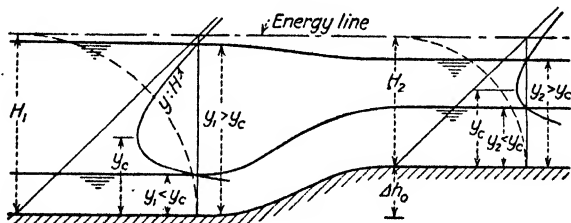


FIG. 150.—Application of the energy diagram to a change in channel elevation.

the energy-line elevation. Needless to say, the energy diagram cannot be applied to the intermediate region of curvilinear flow, where the pressure is not hydrostatically distributed, nor will it yield more than qualitative results if appreciable energy is lost at the transition.

Application of the discharge diagram may be illustrated by the case of a channel inlet at the side of a large reservoir. The energy line will coincide with the reservoir surface, whereas the

rate of discharge for constant H will vary with the depth of flow in the channel as governed by downstream conditions. Evidently, if the depth y is equal to H , no flow will take place. As y decreases, q will increase, until at some stage the flow profile will correspond to that in Fig. 151. The maximum rate of discharge will obtain when $y = y_c = \frac{2}{3}H$; no further increase in q is physically possible so long as H remains unchanged. If, instead, the flow is controlled by a sluice gate at the inlet, the discharge will obviously be zero when the gate is closed—i.e., when $y = 0$. As the gate is raised, q will increase with y

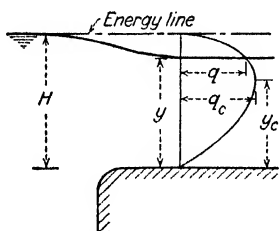


FIG. 151.—Use of the discharge diagram at a channel inlet.

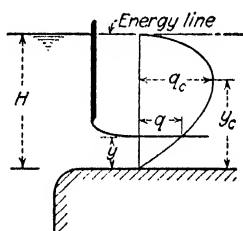


FIG. 152.—Use of the discharge diagram at a sluice gate.

according to the discharge diagram, passing through the intermediate stage shown in Fig. 152. The maximum rate of discharge under the gate must finally correspond with the foregoing case of free inflow at the depth y_c .

A somewhat different application of the discharge diagram may be seen in the case of flow between divergent or convergent vertical walls. For instance, if the flow passes between the plane boundaries shown in plan in Fig. 153, since Q necessarily remains constant from section to section, q will decrease in magnitude as the width of the flow section grows larger. If H is the same at all successive cross sections, it follows that y must either increase or decrease in the direction of flow, depending upon whether the depth is greater or less than y_c . Since q is inversely proportional to distance in the direction of flow, the surface profiles are given directly by the two arms of the discharge diagram reproduced to the appropriate scale. As will be seen from Fig. 153, flow with hydrostatic pressure distribution is physically possible—for the given magnitude of H —only after the width of the cross section has exceeded a certain minimum

magnitude. Similar conditions must obtain for flow in the opposite direction.

Use of the energy-discharge diagram may be shown in connection with the overfall, the depth y being held constant a

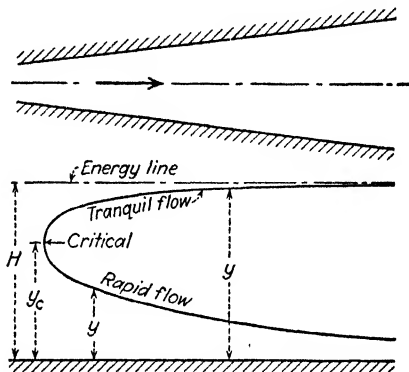


FIG. 153.—Surface profiles for divergent or convergent flow.

short distance upstream from the crest (Fig. 154). When the energy line coincides with the free surface, the discharge must be zero, which is possible only if the energy line coincides with the tailwater level. As the magnitude of H is increased, the discharge will also rise, the value of q being given by the inter-

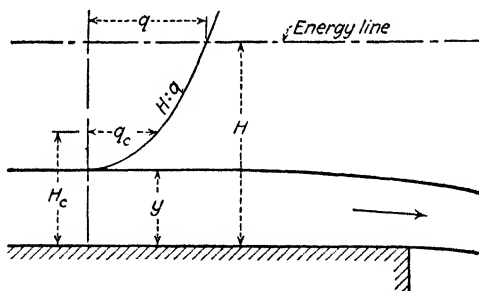


FIG. 154.—Application of the energy-discharge diagram to the free overfall.

section of the energy line with the energy-discharge curve. Once $q = q_c$, the tailwater elevation becomes immaterial, and the overfall may thenceforth be either submerged or free; q will continue to increase with H , as shown for the intermediate stage indicated in the illustration.

Evidently, the terms "maximum discharge" and "minimum specific energy" are significant only under conditions of constant

specific energy and constant discharge, respectively. In the case of constant depth of flow, H is limited only by the depth itself, while no upper limit exists for q . On the other hand, while maximum and minimum values take on entirely different aspects when the depth remains constant, conditions of critical flow still refer to very definite simultaneous values of q and H .

These simplified equations of two-dimensional flow will apply to a channel of finite width only if the side walls are vertical. For any other channel, since the rate of discharge Q is the product of V and the area A of the flow section,

$$H = \frac{Q^2}{2gA^3} + y \quad (210)$$

Since $dA = b \, dy$, in which b represents the surface width,

$$\frac{dH}{dy} = \frac{d}{dy} \left(\frac{Q^2}{2gA^3} + y \right) = -\frac{Q^2 b}{gA^3} + 1 \quad (211)$$

whence, under conditions of critical flow,

$$\left(\frac{A^3}{b} \right)_c = \frac{Q^2}{g} \quad (212)$$

The corresponding energy and discharge diagrams will be similar to the foregoing, although the exact forms of the curves and the accompanying numerical values will vary with the geometry of the channel section. The reader must again be cautioned that the use of such diagrams will yield more than a first approximation of flow conditions only so long as the pressure distribution is essentially hydrostatic over the section in question.

66. Equations of Gradually Varied Flow. Uniform motion is a limit that is approached only in very long channels of constant form, roughness, and slope. As a general rule, therefore, the depth of flow must be regarded as variable in the direction of motion, while for reasons of continuity the velocity head must change accordingly. Furthermore, as will be seen from the specific-energy diagram, variation in y and $V^2/2g$ under conditions of constant discharge will invariably result in a change in specific energy. It follows that the energy line, the water surface, and the channel bottom will all have different slopes, the rate of energy loss then differing from that in uniform motion.

Writing the mean total head at any cross section as the sum of velocity head, depth, and elevation of the channel floor,

$$E_w = \frac{V^2}{2g} + y + h_0 \quad (213)$$

A single differentiation with respect to distance in the direction of flow will yield the corresponding rate of change of each of these quantities:

$$\frac{dE_w}{dx} = \frac{d(V^2/2g)}{dx} + \frac{dy}{dx} + \frac{dh_0}{dx} \quad (214)$$

The first term evidently represents the rate of change of total head—a quantity which must always be negative in the direction of flow; $-\frac{dE_w}{dx}$, therefore, is proportional to the rate of energy loss, and as such should be expressible in terms of the essential flow characteristics and an appropriate coefficient of resistance. Unfortunately, such relationships have been developed only for the case of uniform motion, and their application to gradually varied flow would necessarily involve a certain amount of error. The fact has already been mentioned, for instance, that diverging flow is accompanied by a rate of loss that is greater than that in parallel flow, whereas convergence tends to produce just the opposite effect. Nevertheless, for want of a more satisfactory expression, one is forced to assume that the rate of energy loss in non-uniform motion is equivalent to that which would occur if the flow were uniform under identical conditions of depth, discharge, and boundary roughness. Thus, using the Chézy notation,

$$-\frac{dE_w}{dx} = \frac{V^2}{C^2 R}$$

The rate of change of velocity head, in turn, may be written more conveniently by introducing the quantity $V = Q/A$ and recalling that an increment of cross-sectional area dA is equal to the surface width b multiplied by the depth increment dy ; therefore,

$$\frac{d}{dx} \left(\frac{V^2}{2g} \right) = \frac{d}{dx} \left(\frac{Q^2}{2gA^3} \right) = -\frac{Q^2 b}{gA^3} \frac{dy}{dx}$$

The ratio A/b , moreover, is equal to the mean depth of flow y_m ; introducing this value, and again writing $Q/A = V$, the rate of change of velocity head will be simply

$$-\frac{V^2}{gy_m} \frac{dy}{dx}$$

The quantity dy/dx is obviously the rate of change of depth with distance, whereas dh_0/dx represents the slope of the channel bottom; since a downward slope is arbitrarily taken as positive, $dh_0/dx = -S_0$.

If these several equivalent terms are introduced into Eq. (214), the result will be as follows:

$$-\frac{V^2}{C^2R} = -\frac{V^2}{gy_m} \frac{dy}{dx} + \frac{dy}{dx} - S_0$$

Solution for dy/dx as the dependent variable then yields the differential equation of gradually varied flow in its most significant form:

$$\frac{dy}{dx} = \frac{S_0 - \frac{V^2}{C^2R}}{1 - \frac{V^2}{gy_m}} \quad (215)$$

67. Surface Profiles. Through Eq. (215) means are now at hand of evaluating the rate of change of depth with x for any point at which the depth itself is known. From inspection it will be seen that the depth will increase in the direction of flow if the numerator and denominator of the fraction at the right are both positive or both negative. Similarly, the depth will decrease in the direction of flow if the numerator is positive and the denominator negative, or if the numerator is negative and the denominator positive. Without integration, however, the differential expression can yield no quantitative information as to the actual depth at any arbitrary section. Nevertheless, further inspection of the fraction at the right will permit at least qualitative deductions as to the form of the surface profile.

Since the rate at which head is lost in the direction of motion determines the slope of the energy line, the numerator of the fraction is really the rate of change of specific energy with x :

$$S_0 - \frac{V^2}{C^2R} = S_0 - S_e = \frac{dH}{dx}$$

Evidently, if the flow is uniform, the numerator will be zero; if S_e is less than S_0 , H will increase with x and the numerator will be positive; if S_e is greater than S_0 , the numerator will be negative. But if dH/dx is positive, the energy line and the channel bottom diverge, indicating that the rate of loss is lower than in uniform flow; the velocity must therefore be lower than that for uniform motion (since the rate of loss varies with V^2), and the depth correspondingly greater than the uniform depth y_0 . Conversely, if dH/dx is negative, y must be less than y_0 . These essential relationships are therefore apparent:

$$\begin{aligned} S_0 > S_e & \quad \frac{dH}{dx} > 0 & y > y_0 \\ S_0 < S_e & \quad \frac{dH}{dx} < 0 & y < y_0 \end{aligned}$$

The denominator, upon comparison with Eq. (211), will be seen to represent the rate of change of specific energy with depth:

$$1 - \frac{V^2}{gy_m} = \frac{dH}{dy}$$

The denominator thus has a magnitude of zero at the critical depth, when H is a minimum. If the depth is greater than the critical, corresponding to a point on the upper arm of the energy diagram, H will increase with y and the denominator will be positive. For points on the lower arm, where the depth is less than the critical, H will decrease as y increases, and the denominator will accordingly be negative. In brief,

$$\begin{aligned} 1 > \frac{V^2}{gy_m} & \quad \frac{dH}{dy} > 0 & y > y_c \\ 1 < \frac{V^2}{gy_m} & \quad \frac{dH}{dy} < 0 & y < y_c \end{aligned}$$

Four limits of dy/dx are possible. The limit zero is approached as the numerator of the fraction becomes increasingly small; evidently, this limit must be approached asymptotically, for it corresponds to the case of uniform motion, wherein the energy line, the water surface, and the channel bottom are parallel. A second limit will be approached as the term $V^2/C^2R = S_e$ becomes increasingly smaller; since this condition indicates negligible loss of energy, the velocity of flow must also be inap-

preciable—in other words, dy/dx will then equal S_0 , signifying a horizontal water surface and a great depth of flow. The third and fourth limits, positive and negative infinity, correspond to flow at minimum energy, the denominator of the fraction then being equal to zero. This implies a free surface at right angles to the channel bottom—a situation that is physically impossible and is indicated by the equation only because the conditions specified earlier in the derivation are no longer fulfilled; that is, it was assumed that the pressure would be hydrostatically distributed over every normal section, whereas the stream lines in the region of critical depth become definitely curvilinear.

From the foregoing conclusions it will be seen that the surface profiles in gradually varied flow may be classified according to the relative magnitudes of actual depth, normal depth, and critical depth, for a given rate of discharge, a given boundary roughness, and a given channel cross section. Although the slope of the channel may in its own right be classed as sustaining (positive), horizontal (zero), or adverse (negative), sustaining slopes may be further grouped according to whether the normal or the critical depth is greater. If y_0 is greater than y_c , it is apparent that the corresponding uniform motion would be in the tranquil state; if y_0 is less than y_c , the uniform motion would be rapid. Slopes producing tranquil uniform flow are termed mild; similarly, slopes on which the uniform motion would be rapid are designated as steep. If y_0 exactly equals y_c , the slope is classed as critical, for the uniform motion would then take place at the critical depth, under conditions of minimum specific energy.

Adverse, horizontal, mild, critical, and steep slopes will henceforth be denoted by the appropriate letters A , O , M , C , and S , respectively. Furthermore, a surface profile for which the depth is always greater than both the normal and the critical is designated by the subscript 1; the subscript 2 is used if the depth is always between y_0 and y_c ; similarly, the subscript 3 applies to those profiles in which the depth is always less than both the normal and the critical. It should be possible, apparently, to obtain at the most fifteen distinct conditions of gradually varied motion, involving three different types of surface profile on each of the five classes of channel slope.

The trends of these several curves may be indicated diagrammatically after the method shown in Fig. 155, in accordance

with the foregoing discussion of Eq. (215). For convenient reference, imaginary lines of normal and critical depth are drawn parallel to the channel bottom. Considering, for example, a surface profile of the M_1 type, reference to the energy diagram will show that the depth must increase with x , since $y > y_0 > y_c$; from the discussion of limits, it is evident that the curve will be asymptotic to the normal-depth line at its upstream end, approaching the horizontal in the downstream direction. While

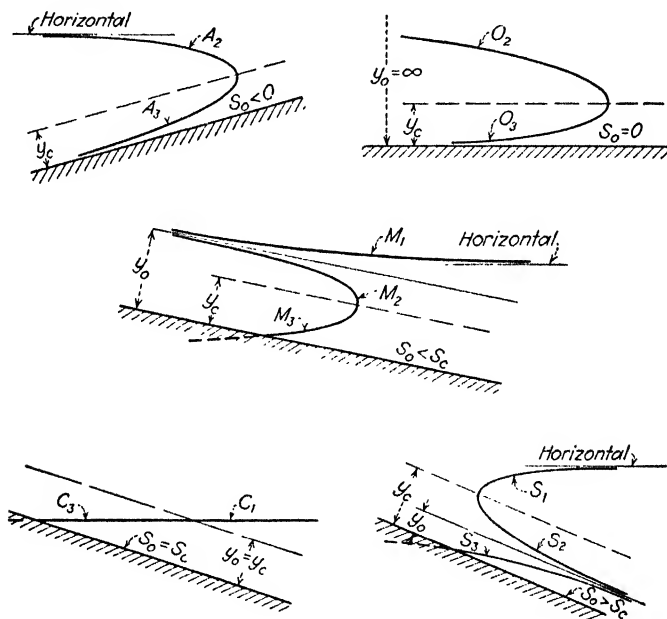


FIG. 155.—Surface profiles for channels of adverse, zero, mild, critical, and steep slopes.

the S_1 profile also approaches the horizontal for the same reason, it must be normal to the critical-depth line at its beginning, since $y_c > y_0$. Similar reasoning will justify the form of each individual curve as given in the composite diagrams, although certain singularities warrant further investigation.

For example, in the case of the critical slope, the C_2 profile will be identical with the superposed lines of normal and critical depth. That the C_1 and C_3 curves must be horizontal may be seen from the fact that they are the limits of the M_1 and S_1 curves, and the M_3 and the S_3 curves, respectively. The O_1

profile is not visible on the diagram, since it is a horizontal line an infinite distance above the channel, coincident with the energy line and the line of normal depth; only under conditions of zero velocity can the energy line be parallel to the horizontal floor of the channel. It follows that the O_2 curve must then also approach infinity in the upstream direction. The normal-depth line for adverse slopes, similarly, must again be parallel both to the channel bottom and to the energy line—conditions that can be satisfied only if the corresponding uniform flow is in the negative x direction. Obviously, then, the A_1 curve can have no practical significance, whatever academic interest it may arouse. The A_2 profile approaches the horizontal in the upstream direction, so that it is the one curve of type 2 which is not asymptotic to the line of normal depth. Curve A_3 thoroughly disproves the adage that water cannot flow uphill.

The reader must bear in mind the fact that the actual curvature of these profiles is very slight, except in the immediate vicinity of the critical depth; only because of the extreme reduction of horizontal scale do the composite diagrams tend to give a false impression. It must be noted, furthermore, that the relative length of the several curves, for a given rate of discharge, will vary with the relative depth of flow, since the rate of loss is proportional to the square of the velocity. Curves of type 3 are therefore the shortest, so far as the region of appreciable change in depth is concerned. It will be evident from Fig. 155, nevertheless, that only the C_3 and the M_3 profiles are actually limited in length, for all the other curves are asymptotic to the normal-depth line, to the bottom, or to the horizontal. The latter curves are then infinite in extent, mathematically speaking, although for practical purposes it is expedient to consider that a curve has reached its end when the depth is within 1 per cent or 0.1 per cent of its asymptotic limit.

68. Computation Procedure. These basic profiles are determined in form by the rate of discharge, the channel slope, the boundary roughness, and the geometry of the channel cross section. Which of these profiles will actually develop in a given channel will depend upon one further characteristic: a local change in the longitudinal profile of the channel itself. This may take the form of a sluice gate, a spillway, or some such structure causing backwater on the upstream side and flow at super-

critical velocity on the other; or it may be an abrupt change in slope, roughness, or channel section; under extreme conditions, the change may be in the rate of discharge, caused by the juncture of two channels or a partial diversion of the flow. A single

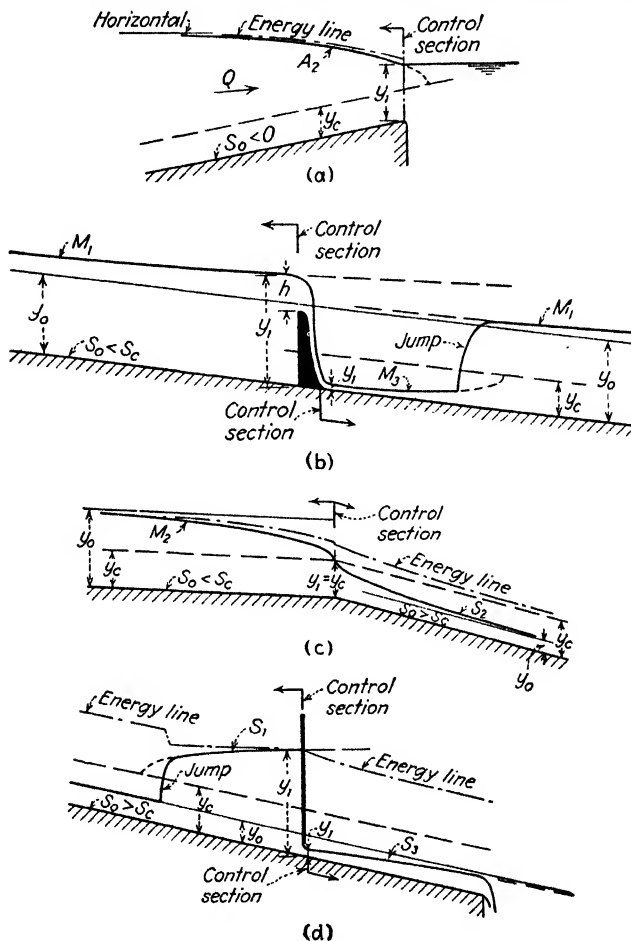


FIG. 156.—Typical profile combinations in gradually varied flow.

control section of this nature will determine whether the corresponding surface profile will be of type 1, 2, or 3; it will also definitely fix the profile with respect to the channel itself, in that the prescribed depth at that section will determine from which point on the basic curve the actual development will proceed

(Fig. 156). The extent to which development may continue obviously depends upon the proximity of the next control section in the upstream or downstream direction.

For example, an abrupt overfall at the end of a long adverse, horizontal, or mild slope is a control section at which conditions of minimum energy must prevail; the corresponding surface profile must then be of type 2, terminating at the fall with the depth $y = y_c$. Similar circumstances must hold true if any one of these slopes abruptly changes to a steep one; this also serves as a control section for the steep channel, at which point the S_2 profile will begin. Curves of type 1 are determined at the end of maximum depth, the magnitude of this depth being governed by the head required on a spillway or sluice to deliver the given flow, or by the surface elevation of a reservoir into which the channel discharges. Curves of type 3 are invariably controlled at their upstream end, by the depth at which water leaves a sluice gate or the apron of a dam.

With these points in mind, one may now proceed to the computation of surface profiles for various conditions of discharge and channel characteristics. The method of solution involves integration of the varied flow equation by steps, beginning with known conditions at the control section, the size of the steps determining the accuracy of the results. Equation (215) may be written in the more convenient form

$$\Delta x = \frac{\Delta H}{S_0 - (S_e)_m} \quad (216)$$

the magnitude of Δx being determined for the corresponding difference in depth Δy ; evidently, the slope of the energy line then represents a mean over the distance Δx . The change in depth from the control section to the limit which the curve approaches is first divided into an appropriate number of increments, thereby establishing a series of vertical sections along the curve for which the depths of flow are known quantities; the location of these sections is as yet unknown. For the given discharge it is then possible to compute for each section the cross-sectional area, the velocity, the velocity head, and the specific energy; ΔH then represents the change in specific energy between each successive pair of sections. Since the hydraulic radius of the flow section and the Chézy coefficient are also functions of the depth, the

quantity $S_e = V^2/C^2R$ may be computed for each value of y ; the mean slope of the energy line between any two sections may then readily be found, and evaluation of Δx is at once possible. This simple process is applicable to any type of surface curve, and to natural water courses as well as artificial channels. It is evident, however, that the ultimate accuracy of the solution will depend upon three factors: the extent to which assumptions leading to Eq. (215) are justified; the degree of accuracy with which the proper roughness parameter may be selected; and the shortness of the steps adopted for the integration. Since the method is not exact, it is futile to strive for greater accuracy in one respect than can be attained in either of the others.

Since early in the last century efforts have been made to integrate Eq. (215) analytically, in order that the somewhat bothersome process of integration by steps might forever be eliminated. Such success as these efforts have encountered has invariably been at the cost of further simplifying assumptions, with resulting functions that are usually more tedious to apply in individual cases than the method just presented. The true value of analytical integration, however, is found in the routine determination of flow characteristics for artificial channels of standardized dimensions, such as are encountered in extensive irrigation or power projects. This is particularly true in the construction of delivery curves for given channels under conditions of variable depth at one or both ends.

Any method of integration is based upon the fact that all variables in Eq. (215) are functions of the depth of flow; once these functions are expressible in simple form, there is at hand a differential equation for x in terms of y . For special cases the integration is then mathematically possible; otherwise the process must be graphical, the results in either case being compiled in the form of curves or tables for use in routine computation. The most recent of such endeavors is that by Mononobe,¹ who assumed both A and P to be monomial functions of y —an assumption that appears to introduce little error for the depth range of the M_1 and the M_2 curves in many types of channel. Applying his method specifically to these two types of surface profile, Mononobe submitted plots of his integration functions,

¹ MONONOBE, N., Back-Water and Drop-Down Curves for Uniform Channels, *Proc. A.S.C.E.*, vol. 62, no. 5, p. 643, 1936.

compared his results at length with those of nine earlier investigators, and presented a series of ingenious laboratory tests to substantiate his computations. One such measured profile is reproduced in Fig. 157. Since his experimental channel was considerably shorter than the surface curve in its entirety, for each succeeding run the water level at the downstream end was lowered sufficiently to provide an initial depth approximately equal to the smallest depth of the run before. Although com-

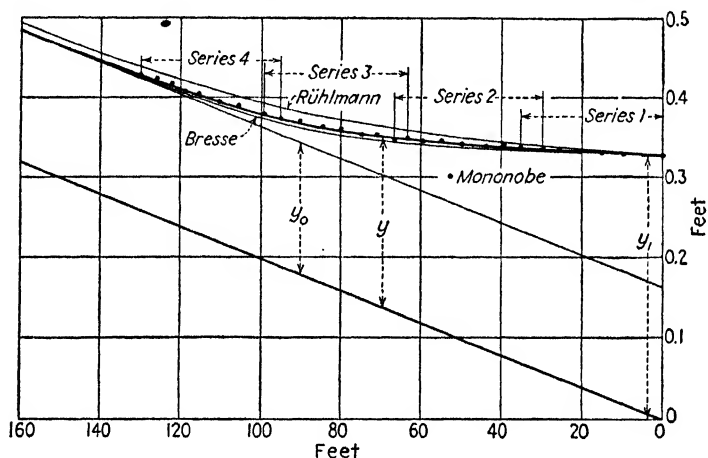


FIG. 157.—Experimental determination of a backwater profile.

parison with the curves obtained by the methods of previous investigators is an indication of progress during the past seventy-five years, it is to be noted that Stevens¹ checked the step-by-step method for this particular profile, with results scarcely discernible from the experimental data.

Mononobe's method differs little, however, from that perfected by Bakhmeteff²—a system which has met with widespread favor among hydraulic engineers. Finding that for prismatic channels the product A^2C^2R may satisfactorily be represented as a constant power of y over a considerable depth range, Bakhmeteff was able to develop by analytical and graphical means a series of integral tables, use of which greatly simplifies

¹ STEVENS, J. C., *Proc. A.S.C.E.*, vol. 62, no. 9, p. 1489, 1936.

² BAKHMETEFF, B. A., "Hydraulics of Open Channels," Engineering Societies Monograph, McGraw-Hill Book Company, Inc., 1932; see also, *Proc. A.S.C.E.*, vol. 63, no. 3, p. 556, 1937.

routine computation of surface profiles for sustaining slopes. Under Bakhmeteff's guidance, Matzke¹ recently extended this method to the case of adverse slopes, the nature of which requires a different set of tables. More detailed discussion of the procedure is pointless at this time, for it is ably presented in Bakhmeteff's text. Although the general principles of gradually varied flow have been developed over a period of many years, it has remained to Bakhmeteff to organize these principles for ready engineering use, and the writer is indebted to the latter for the form—if not the actual substance—of many of the concepts herein presented.

69. The Hydraulic Jump. On a preceding page the fact was mentioned that curves of the M_3 class are determined in position by an existing depth at their upstream end. However, such curves are definitely limited in extent; if the channel slope remains constant beyond this limit, it is evident that some change in regime must occur, for it is physically impossible for the M_3 profile to continue beyond the section of critical depth. Actually, in such a case the flow regime changes before the depth becomes equal to the critical, the surface rising abruptly to a depth greater than y_c , and then following a curve of type 1 or 2. This phenomenon is known as the hydraulic jump (Fig. 225), its location depending upon the existence of depths and velocities of flow which will satisfy the principle of momentum.

If one may assume, as in the foregoing pages, that use of mean velocities of flow will cause no appreciable error,² the momentum equation applied to the two cross sections of linear motion at beginning and end of the jump will have the following form:

$$\gamma z_2 A_2 - \gamma z_1 A_1 = \rho Q (V_1 - V_2) \quad (217)$$

The terms z_1 and z_2 , after Bakhmeteff, represent the depths of the centers of gravity of the respective sections below the free surface. It is apparent that boundary resistance as an essential force has been completely ignored; as a matter of fact, its effect is quite secondary, its omission introducing little error in results. On the other hand, the longitudinal component of weight may be of

¹ MATZKE, A. E., Varied Flow in Open Channels of Adverse Slope, *Trans. A.S.C.E.*, vol. 102, 1937.

² Note that K_m , the velocity-head correction factor for use in the momentum equation, is always smaller than K_e ; see p. 54.

appreciable magnitude on steep slopes; due regard for this factor, however, would require a knowledge of the approximate form of the jump and of the percentage of air contained within the violent eddies which it produces. These are factors so difficult to formulate¹ that the component of weight is generally ignored, or else the problem is restricted to channels of small slope.

Equation (217) may be rewritten in the form

$$\frac{Q^2}{gA_1} + A_1 z_1 = \frac{Q^2}{gA_2} + A_2 z_2 \quad (218)$$

each individual term of which is a function of y alone so long as Q remains constant. Bakhmeteff recommends plotting the

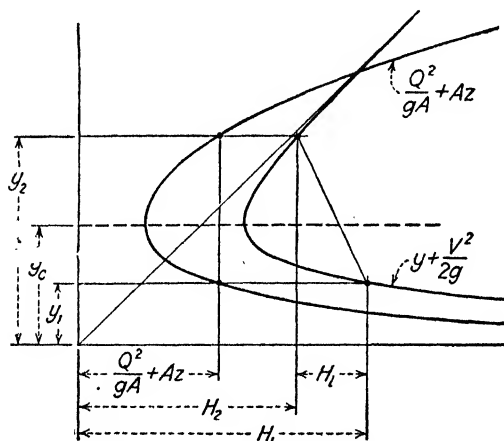


FIG. 158.—Plot of conjugate depths for the hydraulic jump.

quantity $\frac{Q^2}{gA} + Az$ against y for the given discharge and channel section. If this plot is superposed upon the energy diagram, as in Fig. 158, it will be seen that the function reaches a minimum at the critical depth. But it will also be apparent that for any two depths between which a jump will occur, the specific energy of flow is not the same; in other words, the hydraulic jump involves a definite loss of head depending in magnitude upon the ratio of the conjugate depths. The location of the jump along the channel profile is determined by Bakhmeteff as indicated in Fig. 159. Since for any depth y_1 on the lower sur-

¹ See p. 392.

face curve there is only one corresponding depth y_2 which will yield a stable jump, that section must be found at which the depths on the two surface profiles satisfy Eq. (218). The length of the jump—approximately four or five times y_2 —is so small in comparison with the length of the remaining surface profile that it may be neglected in all profile computations.

The reader must bear in mind the fact that the depth y_1 of the hydraulic jump must be less than y_c , and the depth y_2 greater than y_c . It is then possible for a jump to occur from profile

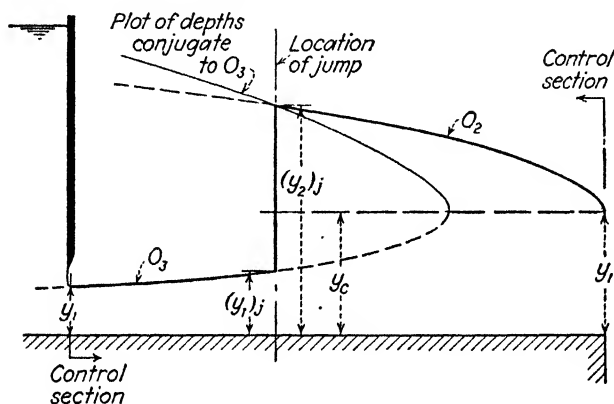


FIG. 159.—Location of the jump below a sluice.

M_3 to M_2 or M_1 ; from S_3 or S_2 to S_1 ; from O_3 to O_2 ; and from C_3 to C_1 . If a jump forms at any point on an adverse slope, on the contrary, it will generally advance upstream until the sluice-gate opening or spillway apron is completely drowned; there is no point on class A profiles at which stable conjugate depths may be found, unless the channel slope is relatively close to zero.

While such elementary knowledge of the jump is essential to the computation of surface profiles, further details of the inner mechanism of this phenomenon are unnecessary at this point. The jump is, in reality, closely related to the general field of wave motion, and as such will be discussed more fully in a later chapter.

70. Rapidly Varied Flow. Considerably more difficult of solution than the problem of gradually varied motion is that type of non-uniform flow in which accelerative forces are fully as important as boundary resistance. Curvature of the free surface is then so pronounced that the pressure distribution cannot be assumed hydrostatic, and the simplified methods

discussed earlier in this chapter are hence no longer applicable. Despite the efforts of many investigators—chief among these being Boussinesq¹—a satisfactory general analysis of this type of motion has not yet been obtained. Practical hydraulicians, therefore, have long since come to regard the various phenomena of rapid transition as a number of isolated cases of flow, each requiring its own particular empirical treatment. Not only does empirical hydraulics thus fail to establish a common physical background for all such problems, but the fundamental aspects of even the isolated problem are often so obscured that interpretation of experimental results is either superficial or definitely incorrect.

Local transitions of this nature as a general rule involve a change from the tranquil to the rapid stage of flow, and as such are quite distinct from the reverse process typified by the hydraulic jump. Moreover, while the jump may occur at some distance from a change in boundary form, rapidly accelerated flow is always the direct result of more or less abrupt variation of the channel cross section or slope. Since rapidly varied motion is thus definitely associated with the concept of the control section, knowledge of such motion is essential for a twofold reason: First, profile computations for gradually varied motion upstream and downstream from the control section are governed by depth conditions at beginning and end of the transition. Second, the control section is of great practical value as a flow meter if the rate of discharge is a known function of measurable flow characteristics.

From the dimensional point of view, the method of analysis presented in Chapter I will yield a significant expression for fluid motion of this nature, entirely without recourse to further analysis of the flow mechanism. Thus, the rate of discharge may be written as a general function of readily measurable characteristics of the motion, of the fluid, and of the boundaries:

$$Q = \varphi\left(\frac{l}{m}, \frac{l}{n}, \frac{l}{k}, \dots, \mathbf{F}, \mathbf{R}, \mathbf{W}\right) l^2 \sqrt{\frac{\Delta p}{\rho}} \quad (219)$$

The terms k , l , m , n , and so forth are simply linear boundary

¹ BOUSSINESQ, "Théorie des eaux courantes." Boussinesq's treatment merits careful study by those interested in this particular phase of fluid motion.

dimensions, k again referring specifically to boundary roughness. The factor Δp is the intensity of pressure (referred to atmospheric) at some definite point in the curvilinear motion—or the difference in pressure between two such points. Evidently, the dimensionless quantity $\frac{Q}{l^2 \sqrt{\Delta p / \rho}}$ is a general flow parameter dependent in magnitude upon the boundary geometry, and upon dimensionless parameters incorporating the three pertinent force properties of the fluid.

The basic significance of this relationship may be seen from the following illustration. Restricting the discussion, for convenience, to the case of two dimensions,

$$q = lV_0 = \varphi l \sqrt{\frac{\Delta p}{\rho}}. \quad (220)$$

For the boundary diagramed in Fig. 160*a*, the boundary conditions are amply described by the lengths l and m , by the angle α , and by the fact that the pressure intensity along all free surfaces must be atmospheric. Both m and α , evidently, describe the fixed boundaries, while l alone will vary with the flow. It would seem expedient to measure the dynamic pressure at the base of the sloping boundary, Δp then referring to atmospheric zero. Moreover, since the unit rate of discharge q is the product of a length and a mean velocity at some section, velocity must therefore be regarded as a dependent variable—and hence must not be included in the several independent parameters upon which q depends. As shown in Chapter I, the factor $\sqrt{\Delta p / \rho}$ is not only dimensionally equivalent to velocity, but is directly proportional to the velocity in the basic dynamic equations, and as such may properly appear in its place in the Froude, Reynolds, and Weber numbers. The coefficient φ , for the given state of motion, will then have the form

$$\varphi = \varphi\left(\frac{l}{m}, \alpha, \frac{\Delta p}{\rho g l}, \sqrt{\frac{\Delta p}{\rho}} \frac{l}{\nu}, \frac{\Delta p l}{\sigma}\right) \quad (221)$$

Assuming, to begin with, that \mathbf{F} , \mathbf{R} , and \mathbf{W} are infinitely great, the flow parameter $\frac{q}{l \sqrt{\Delta p / \rho}}$ will then vary only with the geometry of the boundary. In other words, the flow profile is uniquely

determined by the given boundary conditions, regardless of variation in the individual factors l , Δp , and ρ , upon which q then depends. As shown in Fig. 160b, the phenomenon in this elementary form is essentially the same as a two-dimensional jet striking an inclined plate.

The coefficient ϕ —and hence the flow profile and the parameter $\frac{q}{l\sqrt{\Delta p/\rho}}$ —must vary, however, once the force properties of the

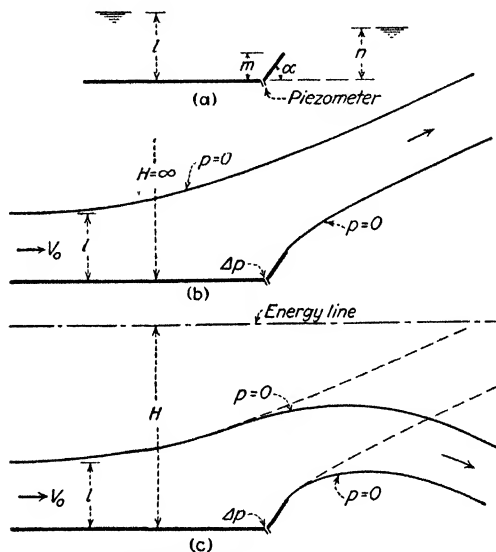


FIG. 160.—Rapidly varied flow at high values of F .

fluid begin to have appreciable influence. As indicated by the respective parameters, the absolute magnitudes of γ , μ , and σ are of no significance unless referred to the other essential variables of the given flow. The effect of specific weight, now the most important of these force properties, will serve to illustrate this point.

For a given depth of flow, it should be apparent that F may be great if γ (or g) is small, or if V (or Δp) is large; in either case the relative effect of weight will be the same. If F is sufficiently large, the force of gravity will have a negligible influence even if g is of normal magnitude, and the profile shown in Fig. 160b will be obtained. For lower values of the Froude number, the nappe will be deflected downwards (Fig. 160c), the degree of curvature

increasing as F grows smaller; needless to say, the entire flow pattern will be modified accordingly. Since the Froude number is dimensionally equivalent to the ratio of a velocity head and a depth of flow, its magnitude is, furthermore, a direct indication of the height of the energy line with respect to the flow profile. For the given boundary conditions (including complete aeration of the nappe), the energy line will reach its minimum elevation (corresponding to a minimum value of F) as the flow becomes equivalent to that normally encountered at a sharp-crested weir (Fig. 161a). Only if the tailwater is raised to a level sufficient to drown the nappe may F decrease below this value toward zero; this, however, would require the introduction of tailwater depth n as a further geometrical factor in the basic function.

Assuming now that R as well is no longer infinitely great, it will be apparent that for a given velocity of approach (indicated by Δp) the rate of energy loss will increase as R decreases. It is evident, moreover, that boundary roughness must now be included among the geometrical parameters, for the result of its influence is of the same nature as that of viscous shear. Boundary resistance will modify the conditions of motion in two distinct ways (refer to Fig. 161b): The flow will be characterized by a sloping energy line and a sloping surface, and the measurement of l some distance upstream from the crest will not in itself indicate energy conditions at the region of maximum curvature. In addition, the reduction in velocity near the lower boundary will modify the dynamic pattern in the region of appreciable curvature. The first effect tends to decrease the coefficient φ ; the second tends to increase it even more markedly.

The role of the Weber number is generally quite secondary, for capillary action becomes of importance in practical instances only when the radius of curvature of the free surface is relatively small. So-called surface tension then acts to decrease this

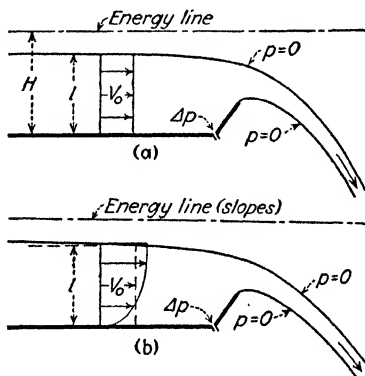


FIG. 161.—Rapidly varied flow at low values of F and R .

radius of curvature even more—and thus influences the pressure distribution and the flow profile; moreover; adhesion of the fluid at the point of separation from the fixed boundary tends to shift this point in the downstream direction as far as possible. The net result is to increase the discharge for a given depth of approach.

Although this method of analysis will seem quite unorthodox to the hydraulician, it yields a complete and systematic functional relationship that is dimensionally sound and extremely broad in application. The height of the sloping boundary, for instance, may vary from infinity to zero—a weir of zero height being simply a free overfall. The depth of approach may be greater or less than the boundary height; the latter case is an uncommon though quite conceivable state of motion at high Froude numbers, and is perfectly compatible with the function since the velocity of flow is not arbitrarily related to a measured head. The angle α may range from considerably greater than 90° , through zero (again the free overfall), to values much less than zero; the latter condition corresponds to the juncture between channels of mild and steep slope. Slight modification of geometrical parameters permits application to flow under (rather than over) an obstacle, as in the case of a sluice gate, whereas the addition of further linear dimensions will enable extension of the problem to three-dimensional phenomena of any desired type. In every case, F , R , and W are properly to be regarded as independent parameters, variable over an unlimited range.

Analytical determination of the coefficient is at best an arduous task; success has been attained in isolated instances, though only through ignoring all but the most essential variables. As explained in Chapter V, use of the concepts of potential motion, conformal mapping, and the Cauchy integral theorem will permit investigation of the flow profile as a function of boundary geometry and the Froude number, but only if the actual boundary resistance is negligible will such methods be practically applicable. Therefore, until it becomes possible to determine the form of the resulting function analytically, the engineer must remain content with empirical treatment—but not in the traditional manner, however, for the dimensional approach offers definite interrelationship of phenomena once considered quite

distinct from one another. Systematic experimental studies will then yield functional trends in graphical instead of analytical form—information quite as valuable to the practical engineer as to the investigator seeking a full understanding of the dynamic aspects of the problem. But only if experimenters duly recognize the significance of the pertinent dimensionless parameters will their results be of maximum value.

Methods of approach that are probably more familiar to the reader fail to consider the dynamic pressure as an essential variable. This is equivalent to assuming that a given discharge always occurs under conditions of minimum energy—in other words, that the elevation of the energy line is determined only by the boundary conditions. Under such circumstances, the dynamic pattern of the flow (as shown by lines of constant potential head) is also determined by the boundary geometry, whence $\Delta p \sim \gamma h$. This simplification obviously precludes the possibility of more than one rate of discharge for a given depth of approach, aside from the secondary variation due to boundary resistance and effects of capillarity.

Such limitations have seemed unimportant in the past; but with attention turning more and more to cases of flow in the rapid state, the more general analysis will soon be imperative. Suggestions have already been made to take account of energy-line elevation indirectly by introducing as an additional parameter a depth within the transition itself. This method is perfectly sound, for the form of the surface profile is definitely dependent upon the conditions of energy. But if one attempts to measure this depth piezometrically, as is the usual custom, such measurement in a region of non-hydrostatic pressure distribution will not yield the actual depth, but a head proportional to the dynamic pressure factor Δp exactly as required by Eq. (219).

71. Weirs and Sluice Gates. The vertical sharp-crested weir without side contractions has been the object of empirical treatment for well over two centuries. In 1716 Poleni proposed the formula

$$Q = \frac{2}{3} \sqrt{2g} b h^{3/2} \quad (222)$$

which he obtained by integration after assuming that the velocity over the vertical section at the crest must vary with the square root of the distance below the level of the approaching flow.

A correction factor C must be introduced, however, owing to the fact that conditions are by no means so simple as he assumed. Hydraulicians of this country, somehow prone to think of velocity of approach as an independent variable, favor Weisbach's extension of the Poleni formula, obtained in a similar fashion:

$$Q = C_c \frac{2}{3} \sqrt{2g} b \left[\left(h + \frac{V_0^2}{2g} \right)^{3/2} - \left(\frac{V_0^2}{2g} \right)^{3/2} \right] \quad (223)$$

The factor C_c is commonly known as the coefficient of contraction, although the weir nappe at no point reaches a minimum section equivalent to the *vena contracta* of the orifice.

Although C_c is frequently considered to be a constant, it actually varies over a considerable range, if only as a function of the boundary parameter $\frac{h}{h+w}$ (Fig. 164a). In reality, not only does the nappe contraction vary with boundary resistance, but C_c also includes perforce a velocity factor taking account of the energy loss in the approach and at the weir itself. On the other hand, if flow is assumed always to take place under conditions of minimum energy, it is evident that the elevation of the energy line is predetermined by the ratio of head to total depth of flow; in other words, the velocity of approach is not an independent variable, and need not be treated as such in a discharge relationship. The weir equation may then be given the more logical form,

$$Q = C_q \frac{2}{3} \sqrt{2g} b h^{3/2} \quad (224)$$

in which, if one will, the discharge coefficient C_q may be regarded as the product of C_c and a velocity-of-approach coefficient,

$$C_q = C_c \left[\left(1 + \frac{V_0^2/2g}{h} \right)^{3/2} - \left(\frac{V_0^2/2g}{h} \right)^{3/2} \right] \quad (225)$$

C_q is a function primarily of the boundary geometry, although varying to an appreciable degree with boundary resistance and the effects of capillarity.

For many decades efforts have been made to determine this functional variation of C_q both analytically and experimentally.

As has already been mentioned, Lauck proved that for potential flow over an infinitely high weir $\left(\frac{h}{h+w} = 0\right)$,

$$C_q = C_c = \frac{\pi}{\pi + 2} = 0.611,$$

whereas von Mises adapted the coefficient of the two-dimensional orifice to the weir, on the assumption that the influence of gravity upon the nappe would have no appreciable effect upon the coefficient of contraction. Others have attempted greatly simplified analyses of the general problem, but since curvilinear flow of this nature does not lend itself particularly well to simplified treatment, their results scarcely warrant mention. Far more practicable are several formulae based upon experimental data, although it must be recalled that the empirical process of curve fitting cannot be depended upon to reveal the true analytical form of the function.

Most formulas have been of the type proposed by Weisbach in 1844:

$$C_q = C_0 \left[A + B \left(\frac{h}{h+w} \right)^2 \right]$$

in which C_0 is the discharge coefficient for $\frac{h}{h+w} = 0$. Bazin,¹ for instance, expressed C_0 , A , and B as follows:

$$C_q = \left[0.6075 + \frac{0.0045}{h \text{ (cm)}} \right] \left[1 + 0.55 \left(\frac{h}{h+w} \right)^2 \right] \quad (226)$$

Rehbock,² on the other hand, has shown that the formula

$$C_q = 0.605 + 0.08 \frac{h}{w} + \frac{0.001}{h \text{ (cm)}} \quad (227)$$

may be expected to yield very accurate results under controlled conditions of the laboratory. Numerous other weir formulas may be found in hydraulic literature, but these are the most representative.

¹ BAZIN, H., "Expériences nouvelles sur l'écoulement par déversoir," Paris, 1898.

² REHBOCK, TH., *Trans. A.S.C.E.*, vol. 93, p. 1143, 1929.

Both Bazin and Rehbock introduce a term dimensionally inconsistent with the remainder of the relationship—a common empirical habit; this term appears to indicate the effect of capillarity at small heads, and—as Prandtl has shown—will be properly dimensionless if replaced with a form of the Weber number. Aside from this single term, however, both discharge coefficients are functions of the boundary geometry alone, and

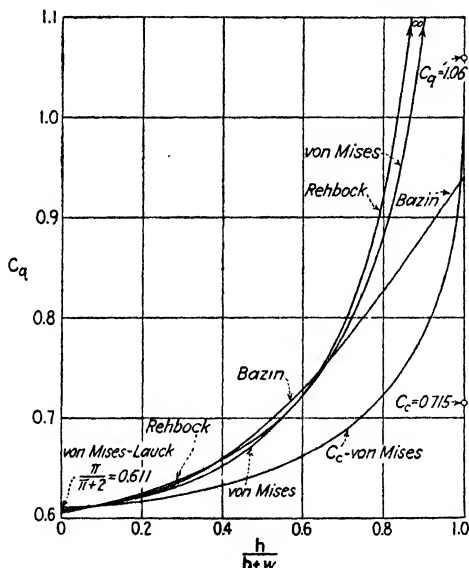
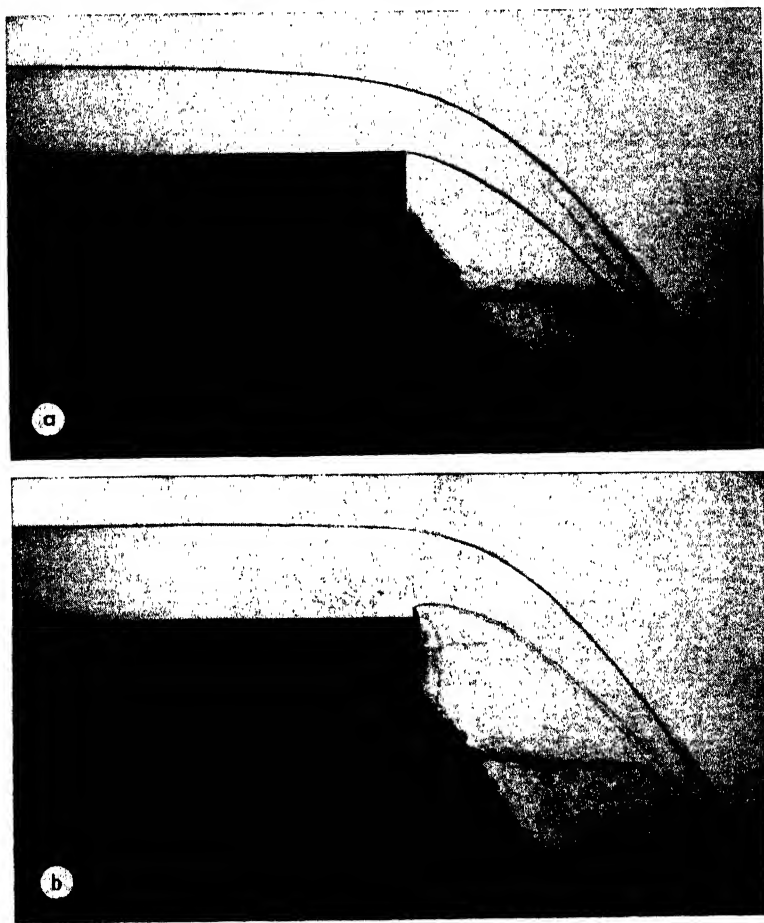


FIG. 162.—Coefficients of weir discharge as functions of $\frac{h}{h+w}$.

as such are plotted in Fig. 162, together with von Mises' adaptation of the contraction and discharge coefficients of the two-dimensional orifice. Von Mises' C_q curve becomes infinite as $\frac{h}{h+w}$ and C_c approach unity (the free overfall, a weir of zero height), owing to the fact that fluid weight was assumed to have no effect upon the nappe contraction. Rehbock's curve for C_q approaches the same limit, because of the nature of the assumed function. Bazin's expression does not indicate an infinite discharge for a very low weir, but does approach a limit somewhat lower than that actually obtained for the free overfall. As will be shown at a later point, this must have the magnitude 1.061, corresponding to a contraction coefficient of 0.715. Moreover,

the physical possibility of flow in the rapid state at relatively low weirs is not recognized by either of these relationships.



M.I.T.

FIG. 163.—Modification of flow profile as the weir height changes from zero to a finite value.

Needless to say, both the Bazin and the Rehbock formulas do not embody the true function for C_d —even so far as boundary geometry is concerned. It is probable that the Rehbock curve is the more nearly correct of the two, for the abrupt change in flow profile as the weir height becomes very small (Fig. 163) indicates a discontinuity in the function as C_d approaches the

limit 1.061. On the other hand, as $\frac{h}{h+w}$ becomes large, boundary resistance causes both energy line and water surface to slope appreciably in the channel of approach, the magnitude of h then varying with the point of measurement; the practical use of weirs, therefore, is ordinarily confined to

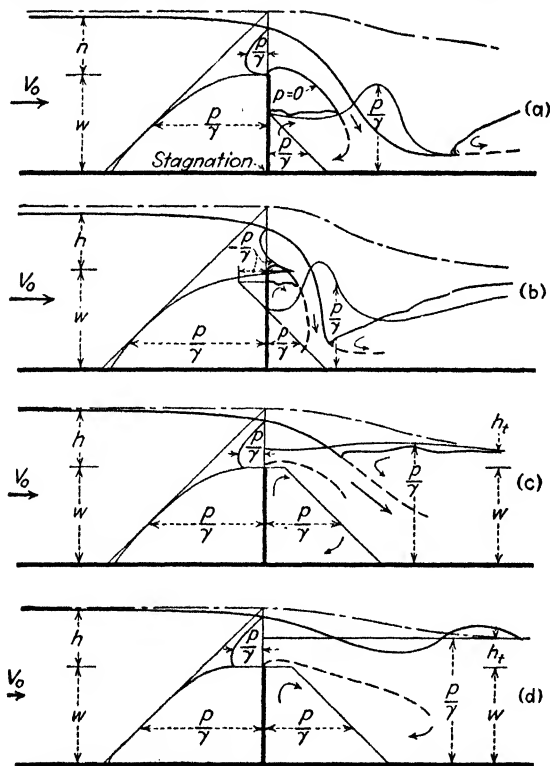


FIG. 164.—Variation of weir discharge with conditions downstream.

cases in which w is at least as great as h . Even then, Schoder¹ has shown, variation in the velocity distribution in the channel (caused, for example, by variation in relative roughness) may easily affect the rate of discharge for a given head by as much as 5 per cent. This is probably the reason why formulas developed from flow over weirs in short, smooth, laboratory flumes often fail to yield satisfactory results in the field.

¹SCHODER, E. W., and TURNER, K. B., *Precise Weir Measurements*, *Trans. A.S.C.E.*, vol. 93, p. 999, 1929.

Needless to say, the region beneath the nappe of a sharp-crested weir must be freely ventilated, in order that the pressure may be atmospheric along both free surfaces; otherwise, an additional variable must be included in the basic functional relationship, for the depression of the nappe (Fig. 164b) and the increase in velocity in the region of lowered pressure may produce a marked increase in C_d . Investigation of this effect might well be based upon the flow-net construction, although it has little other than academic interest because of the instability of flow under these conditions. The pressure below the nappe may be increased, however, if the tailwater level is sufficiently high. Influence upon the rate of discharge begins somewhat before the level of the crest is reached, owing to the fact that the pressure intensity within the nappe does not approach zero until well past the weir; moreover, the deflection of the nappe by the lower boundary always results in a backwater effect below the nappe, as shown in the several diagrams. When the tailwater elevation is considerably above the crest, the nappe abruptly changes in direction, no longer plunging below the surface but assuming a gently undular surface profile. The successive stages are indicated in the accompanying illustrations, taken from Koch¹ and from unpublished measurements by the author. While no general analysis of these conditions is available, it is a noteworthy fact that Bazin's weir investigations were extremely broad in scope, covering rate of discharge, pressure and velocity distribution, weirs of different slopes, and submergence of the nappe.

Although there is basically a close relationship between the weir and the sluice gate, the latter has received comparatively little attention from either the analytical or the experimental point of view. As indicated in an early chapter, the pressure distribution in the neighborhood of the sluice may be closely approximated by means of the flow net once the form of the free surface is known. Were such flow exactly comparable to the upper half of the two-dimensional orifice pattern (Fig. 16), the surface form would be the same and the coefficient of contraction would vary according to von Mises' curve in Fig. 162. However, not only is the pressure constant along the free surface, but owing to the effect of gravity the velocity head at the surface must

¹ KOCH, A., and CARSTANJEN, M., "*Bewegung des Wassers*," Springer, Berlin, 1926.

equal the distance below the energy line at every point. C_c is therefore identical with that of the orifice only when a/h (Fig. 165) equals zero. Through use of the hodograph method, Pajer¹ has obtained analytically the following relationship between C_c and a/h :

a/h	0	0.2	0.3	0.4	0.5
C_c	0.6110	0.6046	0.6036	0.6043	0.6066

In the actual case, there is a slight loss of energy between sections a short distance upstream and downstream, so that the coefficient

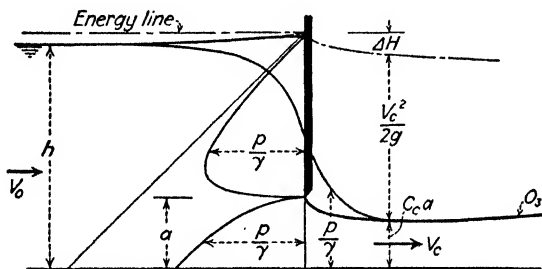


FIG. 165.—Flow under a sluice gate.

of contraction will depend not only upon the boundary geometry but upon boundary resistance as well.

From the notation in Fig. 165,

$$\frac{V_0^2}{2g} + h = \frac{V_c^2}{2g} + C_c a + \Delta H$$

Introducing a velocity coefficient,

$$V_c = C_v \sqrt{2g \left(h + \frac{V_0^2}{2g} - C_c a \right)}$$

while from continuity,

$$q = V_0 h = V_c C_c a$$

whence,

$$\Delta H = \left(\frac{1}{C_v^2} - 1 \right) \frac{V_c^2}{2g}$$

Substituting this latter value in the energy relationship, and

¹ PAJER, G., Über den Strömungsvorgang an einer unterströmten scharfkantigen Planschütze, *Zeit. angew. Math. Mech.*, vol. 17, no. 5, p. 259, 1937.

replacing the velocities by the ratios of unit discharge to depth,

$$\frac{q^2}{2gh^2} + h = \frac{q^2}{2g C_v^2 C_c^2 a^2} + C_c a$$

Solution for q will then yield the customary equation for discharge under the sluice gate:

$$q = \frac{C_v C_c a \sqrt{2g(h - C_c a)}}{\sqrt{1 - C_v^2 C_c^2 a^2/h^2}} \quad (228)$$

This relationship is perfectly general and correct as it stands—but useful only if one knows how C_c and C_v vary with the geometry and resistance of the boundaries. Although C_c may be taken from Pajér so long as C_v is approximately unity, little informa-

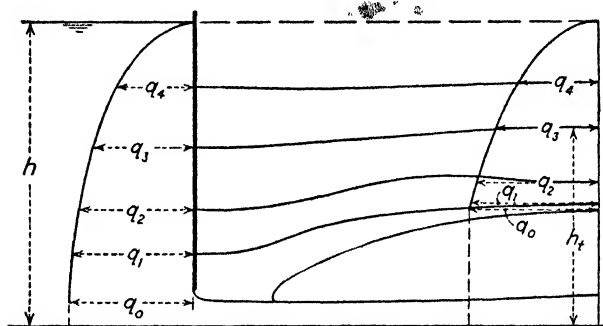


FIG. 166.—Sluice-gate discharge at various stages of submergence.

tion exists as to conditions actually to be expected in the field. From the dimensional point of view, it would seem more reasonable to write Eq. (228) in the elementary form,

$$q = C_q a \sqrt{2gh} \quad (229)$$

in which C_q is a single coefficient of discharge, varying as before with the usual boundary and fluid parameters. Introduction of a term Δp is not essential in this case, for the nature of the boundary conditions results in a close proportionality between Δp and γh . It is evident that in terms of the original coefficients C_q will be equivalent to

$$C_q = \frac{C_v C_c \sqrt{1 - C_c a/h}}{\sqrt{1 - C_v^2 C_c^2 a^2/h^2}} \quad (230)$$

For small values of the ratio a/h the discharge and contraction coefficients approach the identical value 0.611; as the ratio

becomes larger, C_q will increase, C_c changing very slowly; but at the limit $a/h = 1$, C_c must also equal unity, whereas C_q becomes indeterminate. In the latter region conditions are extremely unstable, and hence this limit is of little practical import.

The sluice gate is also subject to submergence, as indicated by the sequence of experimental results, after Koch, shown in Fig. 166; such conditions require a further variable h_t in the basic function. It is common practice to compute the rate of discharge on the basis of the effective head $h - h_t$, using the value

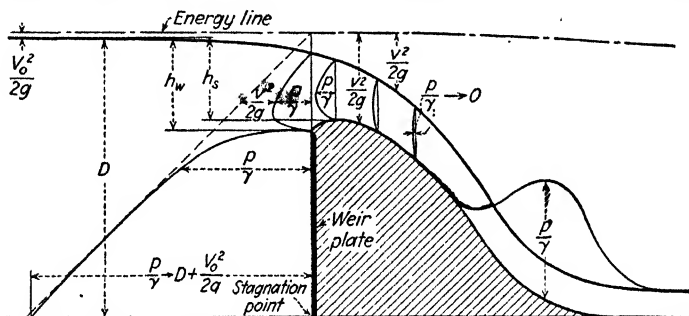


FIG. 167.—Pressure distribution at a spillway designed after the ventilated nappe of a weir.

of C_q determined for free efflux. The extent to which C_c and C_v are influenced by the effect of submergence upon the contracted section is not accurately known, but it is certain that such practice must introduce appreciable error.

72. Spillway Design. Spillways differ from weirs in two important respects. From the dynamic standpoint, the lower surface of the nappe is in contact with a fixed boundary along which the pressure intensity is not necessarily either constant or atmospheric. From the economic standpoint, a given length of spillway crest must safely deliver a peak discharge under the smallest possible head. American engineers usually pattern the spillway crest after the nappe profile of the sharp-crested weir, in order to obtain the maximum delivery without reducing the pressure below that of the surrounding atmosphere. Structural considerations have much to do with this practice, for although pressure distribution near the spillway crest is of little moment in designing for stability, it is feared that intermittent separation of the nappe might endanger the structure as a whole.

Experiments have shown¹ that a spillway so designed will produce a nappe that is not affected by the presence of a fixed lower boundary, so long as the spillway curve conforms exactly to that of the weir nappe for the same rate of discharge (Fig. 167). As may be seen from Fig. 168, however, the spillway profile must necessarily vary according to the parameter $\frac{h}{h+w}$, for the form of the weir nappe is definitely a function of the boundary geometry. Moreover, a spillway designed to produce zero pressure

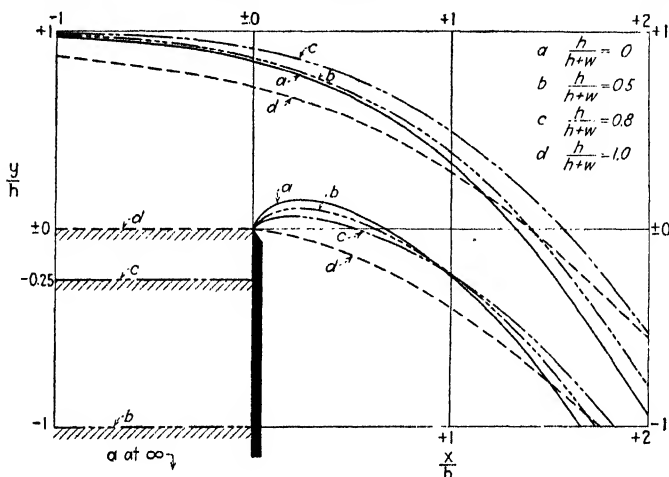


FIG. 168.—Variation in the weir nappe with $\frac{h}{h+w}$.

along the downstream face at one rate of discharge will no longer do so if the discharge changes. A lower head, for instance, will produce positive pressures at all points of the profile (since the weir nappe at that head would normally have a lower trajectory), whereas a greater head will produce negative pressures throughout the crest region.

Nevertheless, if the spillway profile is smoothly curved, according to a given nappe profile, the absence of abrupt changes in curvature at any point will permit considerable increase in head without danger of separation. Indeed, model studies²

¹ ROUSE, H. and REID, L., Model Research on Spillway Crests, *Civ. Eng.*, vol. 5, no. 1, p. 10, 1935.

² DILLMAN, O., Untersuchungen an Ueberfällen, *Mitteilungen des hydraulischen Instituts der T. H. München*, no. 7, Oldenbourg, Munich, 1933.

indicate that the design head may be exceeded by 300 per cent, flow still occurring in a perfectly stable state.¹ Abruptness of curvature is a relative matter, however, and separation must eventually occur, even though the nappe does not spring entirely

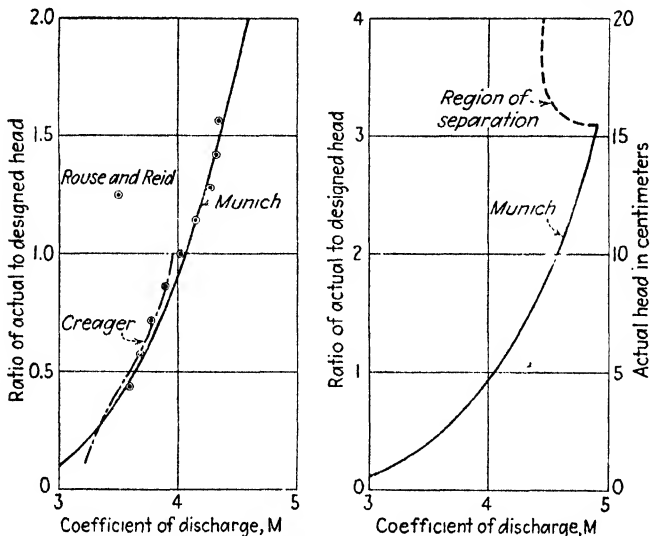


FIG. 169. Coefficient of spillway discharge as a function of relative head.

free. The Munich experiments, general results of which are plotted in Fig. 169, show an abrupt drop in the customary discharge coefficient

$$M = \frac{Q}{bh^{3/2}}$$

at the point of separation, a result that is to be expected with the accompanying change in nappe profile. It is apparent that the evil to be avoided is not necessarily underpressure, but rather a too-rapid change in curvature of the spillway face. Figure 170² is a good example of the latter danger, for separation is

¹ Needless to say, this applies solely to the two-dimensional case of flow. Abutment irregularities, or the presence of piers along the crest, would permit aeration of the nappe under far lower rates of discharge. To what extent the design head may then be exceeded will depend largely upon the distance the piers and end walls are continued smoothly down the spillway face.

² ESCANDE, L., "Étude théorique et expérimentale sur la similitude des fluides incompressibles pesants," Toulouse, 1929.

evident at two points of abrupt boundary transition, even under normal rates of discharge.

Although model studies are of inestimable value in spillway investigations of this nature, hydraulicians have come to expect flow measurements to be readily convertible to prototype scale solely through use of the Froude criterion for similitude. Indeed, within the last decade it has become quite customary to calibrate large-scale spillways by means of models often a hundredfold reduced in size. Eisner¹ has shown conclusively, however, through measurements on geometrically similar models at five different scales, that definite variation in the coefficient of discharge with the scale ratio is to be expected. Although the influence of viscosity could be noted, the essential factor was apparently the relative roughness of the boundary surface—the absolute roughness being the same in each of the several models. Moreover, so systematic was the variation of the discharge coefficient with relative roughness that

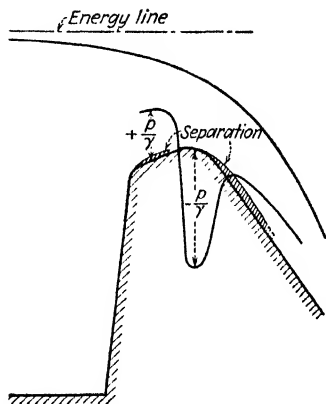


FIG. 170.—Separation at a spillway crest of poor design.

Eisner was able to extrapolate with a fair degree of certainty to conditions for the prototype itself. Though Eisner considered the discharge coefficient a function of the Froude number instead of the boundary geometry [compare with Eq. (219)], his general method warrants the attention of those engaged in such research.

73. Critical-depth Meters. Probably no phase of open-channel motion is so often misunderstood as flow under conditions of maximum discharge and minimum specific energy. So long as gradually varied flow is considered, the critical depth as previously*described is a very useful parameter—in particular since the regions of transition in which the flow is curvilinear are of relatively negligible length. But Eq. (204) applies specifically to rectilinear motion, and can have mere qualitative significance when otherwise used. Indeed, flow can pass from

¹ EISNER, F., Ueberfallversuche in verschiedener Modellgrösse, *Preussische Versuchsanstalt für Wasserbau und Schiffbau*, Berlin, 1933.

the tranquil to the rapid stage only as the result of surface curvature—under which circumstances it is seldom possible to assume hydrostatic distribution of pressure at the true critical section without introducing appreciable error.

A salient example of traditional practice is seen in the case of the broad-crested weir. It is usually presumed that for a given reservoir level (*i.e.*, energy-line elevation) upstream from the weir, the maximum possible quantity of water will be discharged per unit time. Still assuming parallel motion, the flow profile would have the form shown schematically in Fig. 171, after the

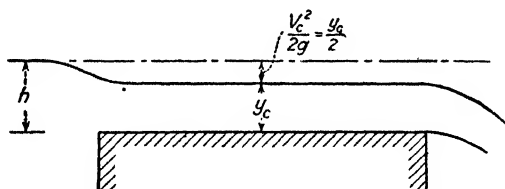


Fig. 171.—Customary treatment of the broad-crested weir.

usual textbook illustration. The rate of discharge should then be determinable from a single depth measurement:

$$q = \sqrt{g} y_c^{3/2} = \frac{2}{3\sqrt{3}} \sqrt{2g} h^{3/2}$$

Aside from the fact that this expression applies only to weirs of very great height, four essential discrepancies are involved in this elementary method of attack:

1. The regions of curvilinear motion at either end of the weir extend a considerable distance in each direction; unless the weir is very broad, at no section will the flow be truly parallel.
2. For a given specific energy, maximum discharge for parallel flow is not necessarily the same as maximum discharge for curvilinear flow.
3. If the weir actually is broad enough to eliminate effects of curvature near the midsection, the energy line (and hence the water surface) will have an appreciable slope; the section at which $y = y_c$ will wander along the weir with changing discharge.
4. The true section of minimum energy does not then lie at some intermediate point along the weir, but at the very end—which is a region of maximum curvature.

Since the rate of discharge is actually a function of boundary geometry and resistance (note, for instance, the various surface profiles in Fig. 172), it is evident that the discharge coefficient in the general expression

$$q = C_q \sqrt{2g} h^{3/2} \quad (231)$$

is by no means a constant. Use of an uncalibrated weir in the field is warranted, therefore, only when accuracy of measurement

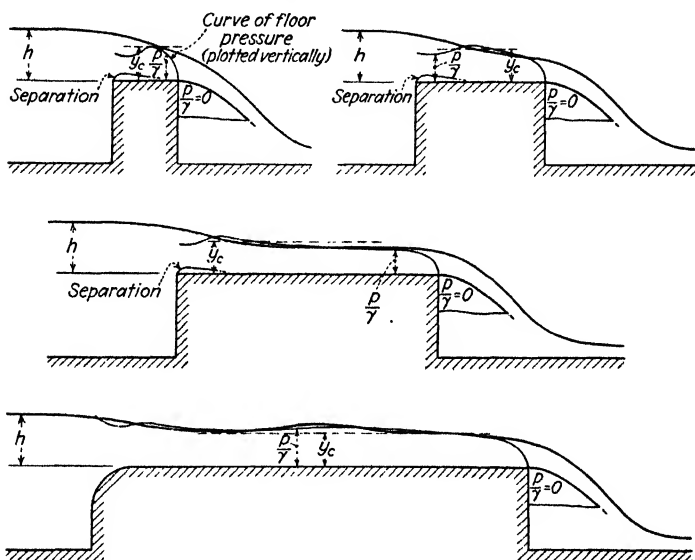


FIG. 172.—Variation in flow profile with form of weir, the head remaining constant.

is of no great consequence; in this respect it has the particular advantage of being relatively insensitive to conditions downstream, for the tailwater may rise at least the distance y_c above the crest without marked effect upon the rate of discharge.

The necessity of determining the functional form of the discharge coefficient for the broad-crested weir when used for more accurate measurement really defeats its purpose as a critical-depth meter. Efforts to develop such a meter through addition of side contractions (the Venturi flume) have been little more successful, for each such meter requires careful rating; even under the most fortunate conditions, C_q may be held approximately constant only over a limited range of head. One begins

to wonder, therefore, whether it is physically possible to devise a critical depth meter with a truly constant coefficient.

In order to answer this question capably, one must first investigate more thoroughly the general problem of critical flow. It follows from facts already discussed that a true critical

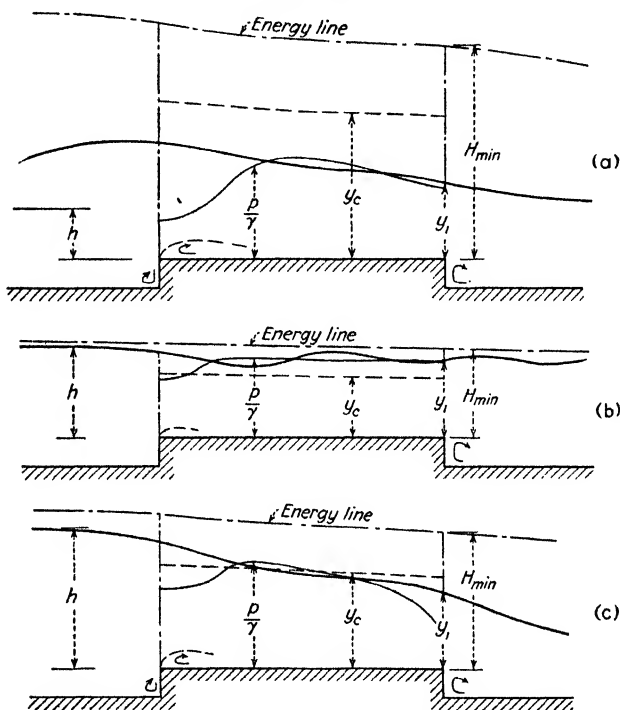


FIG. 173.—Variation in flow profile with Froude number, the crest depth remaining constant. Note that y_c corresponds to the local magnitude of H .

section for given boundary conditions must fulfill a two-fold requirement:

1. At that section the distance H between the sloping energy line and the lower boundary of the flow must be less than at any other point in the vicinity.
2. For this magnitude of the specific energy H , the rate of discharge must be the greatest that is dynamically possible under the given boundary conditions.

In Fig. 173 are shown schematically (after Koch) three types of flow over a relatively low broad-crested weir, all with the

same depth at the crest. Case *a* corresponds to a very high Froude number, Case *b* to a very low one. In every instance, the section at which the energy line lies nearest the boundary is located at the downstream end of the weir—at which section true critical conditions are to be sought. It may be seen by inspection, however, that for the magnitude of H at this section in

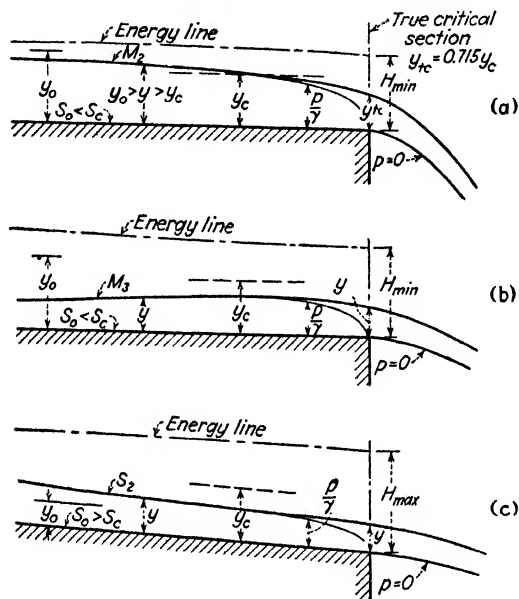


FIG. 174.—The free overfall as a true critical-depth meter.

Case *a* a greater depth would produce a greater rate of discharge; similarly the discharge for Case *b* would increase if for the same magnitude of H the depth were reduced. Evidently, neither of these cases represents true critical discharge, which will actually occur at some intermediate stage as shown by Case *c*.

Nevertheless, it is obvious that as H varies with respect to the dimensions of the weir, the flow profile for corresponding maximum discharge will also be modified. It is then apparent that although a true critical section has been found, the flow at this section is a definite function of the boundary geometry. A true critical-depth meter, on the contrary, must be of such form that the flow profile remains geometrically similar in the immediate vicinity of the crest, regardless of change in absolute depth.

Only then can the discharge coefficient be expected to remain essentially constant.

The free overfall at the end of a long, mild slope (Fig. 174a) is an excellent example of boundary conditions that satisfy this requirement. Since the curvilinear flow at the crest is marked by decidedly non-hydrostatic pressure distribution (refer to

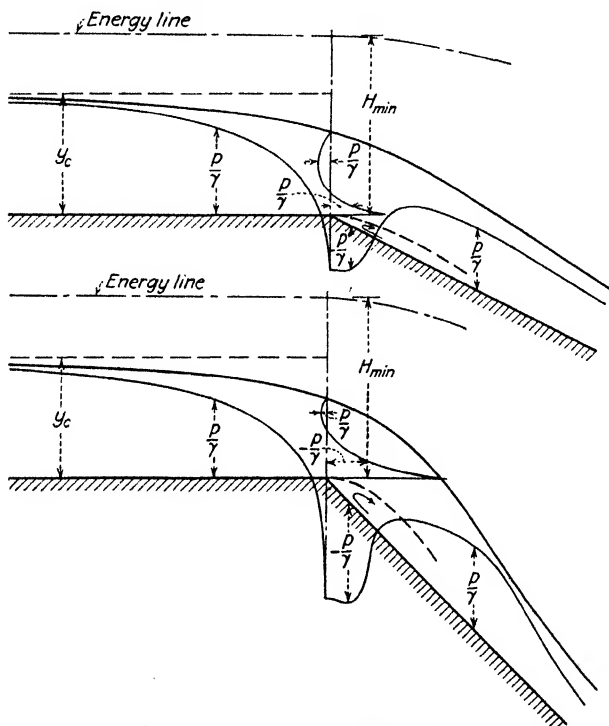


FIG. 175.—Variation in flow profile and pressure distribution with change in bottom slope.

Fig. 15), it is evident that the critical depth for parallel flow will be found a short distance upstream. The actual location of this section is indeterminate, however, for it will move upstream with increasing discharge, and downstream with increasing boundary roughness. The crest itself, however, is a true critical section; experiments indicate¹ that the ratio between the true critical depth at the crest and the nominal critical depth for parallel

¹ ROUSE, H., Discharge Characteristics of the Free Overfall, *Civ. Eng.*, vol. 6, no. 4, p. 257, 1936.

flow is 0.715—which happens to be exactly equal to the coefficient of contraction for the weir of zero height. A single measurement of depth at the crest will then permit immediate computation of the discharge:

$$q = \sqrt{g} y_c^{3/2} = \sqrt{g} \left(\frac{y_0}{0.715} \right)^{3/2} = 1.654 \sqrt{g} y_0^{3/2} \quad (232)$$

It should be apparent that if the flow approaches the overfall region in the rapid state, although the crest section is that at which H is less than at any point upstream, the rate of discharge is not a maximum for this specific energy (Fig. 174b). On the other hand, if the channel is steep, the energy line may or may not slope as rapidly as the channel bottom (depending upon whether the flow profile is of type 3 or 2), and H is therefore

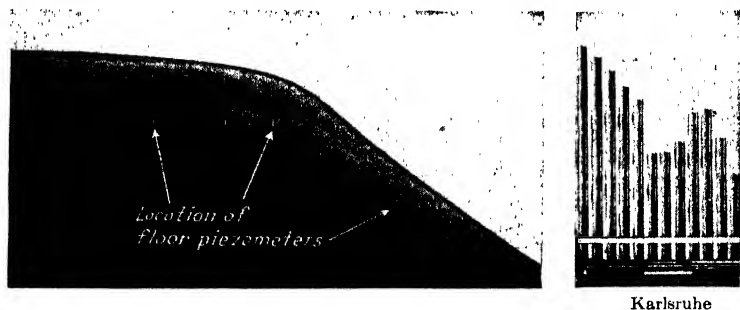


FIG. 176.—Abrupt change in channel slope, showing flow profile and distribution of floor pressure. Note region of separation colored by dye.

not necessarily a minimum at the crest (Fig. 174c). Even when the approaching flow is in the tranquil state, if a mild slope does not end in a free fall (or if the fall is not fully ventilated), it should be apparent that the constant factor in Eq. (232) will have a different value, depending in magnitude entirely upon the boundary conditions.

For instance, in Fig. 175 are shown two variations in the problem, after measurements by the author, representing the transition between mild and steep slopes. As will be seen, the entire flow profile—and hence the depth or pressure at the crest—varies appreciably with the downstream slope. As the latter becomes less and less, the crest depth gradually approaches y_c ; strictly speaking, of course, the entire surface profile should coincide with the line of normal depth when the downstream and upstream slopes become identical.

Since the ratio of depth to specific energy at the true critical section is so definitely a function of the curvature imposed by the fixed boundaries, it is almost futile to expect that a simple relationship may be found expressing this ratio in terms of the boundary geometry. It is to be hoped, nevertheless, that a broader understanding of true critical discharge may soon lead to definite progress in this essential field.

CHAPTER XIV

TRANSPORTATION OF SEDIMENT

74. Essential Aspects of the Problem. Strictly speaking, the phenomenon of sediment transportation does not rightfully belong in a treatise on the fundamentals of fluid mechanics, since the type of matter ordinarily treated in such a volume possesses the qualities of homogeneity and complete fluidity. Two closely related phenomena—the passage of fluid through a porous medium, and the movement of solid particles through a fluid—are obviously within the specified category, since each involves the relative motion between a fluid and solid boundaries. The transportation of such granular bodies by a fluid that moves with respect to other boundaries, on the contrary, not only combines the essential aspects of both phenomena, but through that combination produces a mixed substance that may no longer be regarded as either homogeneous or completely fluid.

Despite the complexity of the resulting problem, its eventual solution is of extreme importance to the hydraulic engineer. And remote as a general solution still appears to be, a careful examination of the present status of the problem seems pertinent at this time. Not only to the hydraulic engineer is the phenomenon of interest, for in such allied fields as meteorology, sanitary engineering, and geology the essential aspects of the problem are found to recur in one form or another. Hence, while the following review is presented in connection with open-channel flow, the principles outlined are applicable to other fields as well.

So far as the hydraulic engineer is concerned, the movement of solid matter in artificial and natural watercourses is of paramount importance. Under what circumstances will water scour the channel bed—and under what circumstances will material be deposited? How may a channel be forced to preserve a given conformation—and what amount of material will it discharge at its mouth under such conditions of equilibrium? By what means may reservoirs be prevented from filling with

silt over a reasonable period of years—and how can irrigation waters be relieved of suspended matter harmful to productive fields? With questions such as these demanding immediate answer, it is only to be expected that the first attempts at the analysis of such complex phenomena would be entirely empirical in nature, for even partial remedies for existing ills are better than none at all. In such investigations the hydraulic model has often proved its worth, despite the fact that model studies of this nature still yield purely qualitative indications.

Simultaneous with a concerted attack by empirical means, efforts have been made to comprehend the basic features of sediment transportation by reducing the problem to its barest

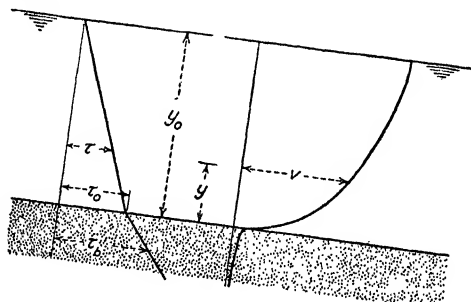


FIG. 177.—Distribution of velocity and shear in an open channel with bed material at rest.

essentials. To be sure, the ultimate application of the elementary principles thus discerned is by no means near at hand, but only in this way will eventual mastery of the problem be possible. Indeed, the slowness with which progress has been made is due in no small measure to the fact that the problem has often been approached in far too involved a form. It is the purpose of this chapter, therefore, to examine the phenomenon in as elementary a manner as possible, and then to review briefly the present status of our knowledge with an eye to future research.

Inasmuch as the physical analysis of open-channel flow is by no means well advanced, it follows that the analysis of sediment transportation by such flow is therefore handicapped at the outset. Although efforts have been made to permit the study of sediment transport in flumes of finite width, it seems advisable to restrict the following analysis to purely two-dimensional uniform flow. The problem thus proceeds from the state of

motion discussed at the beginning of the foregoing chapter. As indicated in Fig. 177, the limiting case of zero transport would correspond to parallel motion at a depth y_0 over a stationary bed of slope S and absolute roughness k . It will be recalled that the intensity of fluid shear will vary as a linear function of normal distance from the free surface,

$$\tau = \gamma (y_0 - y) S \quad (233)$$

with the limiting value at the lower boundary,

$$\tau_0 = \gamma y_0 S \quad (188)$$

whence,

$$\tau = \tau_0 \left(1 - \frac{y}{y_0}\right) \quad (234)$$

As has already been discussed, the shearing stress at any point in the flow may also be expressed statistically in terms of a mean viscous stress and an apparent stress resulting from the turbulent momentum transport across the flow. By this means it was possible to derive expressions both for the velocity distribution and for the boundary resistance in terms of the mean velocity. The former expression yields the curve shown schematically in the illustration, conditions near the bed depending upon whether the average surface irregularity or the boundary-layer thickness is of greater order of magnitude. The latter expression has been seen to have the form

$$\tau_0 = \frac{f}{4} \frac{\rho V^2}{2} \quad (189)$$

which may be combined at once with Eq. (188):

$$S = \frac{f}{4y_0} \frac{V^2}{2g} \quad (190)$$

The quantity f remains a bothersome factor, for the roughness problem is still far from solved—in particular for movable beds. One is sorely tempted to revert to an empirical relationship of the Manning form, but in so doing one must not lose sight of the fact that such practice at once incorporates every inherent weakness of the formula adopted.

Needless to say, a state of shear must also exist throughout the stationary bed. Although the intensity of shear at any point

in the flow is in equilibrium with the forces involved in the turbulent motion, within the bed a balance must exist between the longitudinal component of weight and the static friction of the sediment mixture. As shown in the diagram,

$$\tau_b = \tau_0 + \gamma_m (-y) S$$

γ_m representing the specific weight of the bed mixture (water plus sediment). It must be realized that the velocity of the fluid itself does not reach zero at the boundary, for a certain amount of percolation must take place through a porous material.

If one now consider the entire flow to consist of a mixture of water and sediment—whatever the mechanism of suspension may be—the picture becomes decidedly more complex. In Fig. 178 such conditions are indicated in a manner parallel to that of Fig. 177. So far as the intensity of shear at any point is

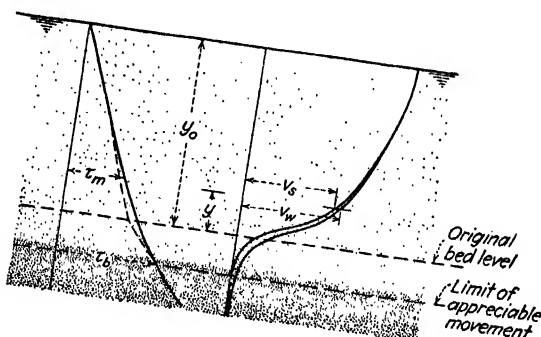


FIG. 178.—Distribution of velocity and shear for an advanced stage of sediment transportation.

concerned, Eq. (233) will have to be modified only through replacing γ by the specific weight γ_m of the mixture:

$$\tau_m = \gamma_m (y_0 - y) S \quad (235)$$

γ_m , however, must now be expected to increase with depth as the concentration gradually approaches a maximum at the bed. Although the function is necessarily continuous, the magnitude of τ no longer varies directly with depth, owing to the change in γ_m . Moreover, it is necessary to consider separate velocity curves for the fluid and the sediment, the two approaching one another in the upper region of the flow, but diverging toward the bottom as contact between particles becomes the more frequent. Owing to the mechanical friction resulting from

such contact, the sediment velocity is always less than that of the fluid.

It will be apparent that such a state of motion will, in general, represent some intermediate condition between the motion of a true fluid and that of a lubricated granular mixture, depending upon the sediment concentration. Evidently, the lower the concentration, the more nearly complete the fluidity and the greater the role of turbulence in producing the shearing stress; conversely, the greater the concentration, the greater is the probability of contact of neighboring particles and the more preponderant the effect of solid friction. It has seemed expedient to subdivide the vertical flow section according to these criteria—the upper region of relatively low concentration being considered the zone of suspended load, and the lower region that of bed load. Nevertheless, no fixed dividing line can be established between the two regimes. Indeed, turbulent mixing will occur well into the bed vicinity, whereas the effect of sediment concentration upon the apparent shear of the mixing process may extend nearly to the free surface. In the most general case, therefore, some complex function must be considered to apply to the entire flow section, the magnitude of τ_m depending upon both the intensity of the turbulent mixing and the internal friction of the sediment-water mixture—factors varying with the distribution of velocity and sediment. Unfortunately, neither is this complex function already known, nor has any approach been made toward treating the phenomenon as a whole. On the contrary, bed-load movement and sediment suspension are still treated perforce as two distinctly different phenomena. And although the ultimate solution of the problem must necessarily relate these two interdependent phases, the elementary method of attack remains for the present the only feasible one.

75. Bed-load Movement. If one arbitrarily restrict the zone of sediment transport to the immediate vicinity of the bed, it follows that the material in motion must roll along the bed or advance in a series of intermittent bounds (so-called saltation). Such restriction, however, limits the problem either to relatively low rates of discharge, or to material which is of sufficient size or weight to resist the tendency toward suspension resulting from the turbulent mixing. Although this has tended to confine the study of bed-load movement within narrow limits, from the standpoint of immediate applicability the restriction also has its

merits. Indeed, many streams transport material of appreciable size, in which suspended matter is quite negligible, whereas model studies must often, for practical reasons, simulate movable beds with material of low density and relatively large diameter. Nevertheless, the narrowness of such limitations is far too often ignored.

The process of rolling, as general movement of the bed begins, is due simply to the drag exerted upon individual particles more exposed to the boundary flow. Jeffreys¹ has shown that the initial rise of particles from the bed in the more advanced stage of motion called saltation may be explained by the resultant upward force due to the pressure distribution of the surrounding

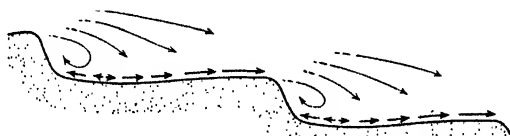


FIG. 179.—Longitudinal section through sand ripples.

curvilinear flow (low pressure just above a particle in the region of greater velocity, higher pressure below in the region of stagnation). Simultaneous with this lifting action, the development of skin and form resistance produces a forward translation; as the particle attains the velocity of the surrounding flow near the summit of its trajectory, such forces approach zero and the particle returns to the bed. Needless to say, the turbulence of the actual flow makes the general picture considerably more complex, and instead of investigating the movement from the standpoint of the individual particle, Einstein² has treated the problem statistically, according to probability criteria.

Perhaps the most troublesome feature of bed-load research within this restricted range is the tendency of the bed to develop surface ripples. Once such ripples exist (see Fig. 179), movement of the sediment is no longer general, for it varies from practically zero in the ripple troughs to a maximum at the crests. Moreover, if the material is not of uniform grain diameter, considerable sorting occurs, the distance a particle is carried past the crest

¹ JEFFREYS, H., On the Transport of Sediments by Streams, *Proc. Camb. Phil. Soc.*, vol. 25, pp. 272-276, 1929.

² EINSTEIN, A. H., Der Geschiebetrieb als Wahrscheinlichkeitsproblem, *Mitteilung der Versuchsanstalt der E. T. H.*, Zurich, 1937.

increasing with its size. And owing to the fact that a ripple advances in the downstream direction by a very slow "rolling" process, once a grain is buried beneath an advancing ripple, it must necessarily remain at rest until exposed in the succeeding trough.

For a given material, it has long been known¹ that ripples will develop gradually in size and rate of movement with increasing flow, reaching a maximum at approximately the critical velocity for the given depth of the stream. Under such conditions, however, the free surface is marked by pronounced undulations spaced according to the underlying ripples. When the discharge much exceeds the critical, the high local velocities will soon level off the ripple crests, the movement then becoming uniform at all points. At even higher rates of flow, bed irregularities will again form, but will now travel upstream as a series of long, low undulations.

Ripple formations of this nature are not limited to sand in water flowing at low depth, for they often accompany tidal phenomena, and are produced as well by the action of wind on sand and snow. In addition, ripple systems may be superposed upon bed undulations of a far greater order of magnitude, such as river bars or sand dunes. Although the present treatment must necessarily avoid such involved problems, the ripple question is not so easily dismissed even in a simplified study, for ripples are bound to develop at one time or another as well in the best as in the poorest of laboratory flumes. Their appearance is always marked by a rise in flow resistance, for the undulations cannot fail to increase the relative roughness of the bed. It is evident, however, that the scale of the ripple pattern in relation to the depth of flow is of considerable moment in determining this relative roughness; thus, although laboratory ripples are almost invariably quite large in proportion to the depth, one must remember that such conditions are not typical of all states of flow in nature. Moreover, consistent association of the critical velocity for ripples with that for open-channel flow is not fully warranted, for sand ripples are frequently leveled off in similar fashion by wind—to which the critical flow relationship $V_c = \sqrt{gy_c}$ cannot apply. To what extent ripple characteristics are gov-

¹ GILBERT, G. K., *The Transportation of Débris by Running Water*, U. S. Geol. Survey Prof. Paper 86, 1914.

erned by the characteristics of the sediment itself still remains to be determined satisfactorily—indeed, the mechanics of ripple formation is a most inviting subject for fundamental research.

Among the earliest attempts to analyze the rate of bed-load transportation was that of du Boys,¹ which warrants review at this point if only because of the considerable influence that it has had upon more recent endeavors: The bed is arbitrarily considered to move in a series of superposed layers, their thickness

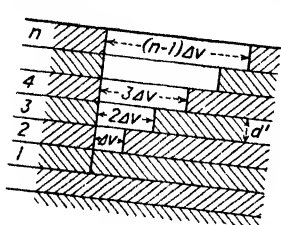


FIG. 180.—Analysis of bed movement. (After du Boys.)

d' presumably being of the same order of magnitude as the particles themselves. By assuming the velocity of the layers to vary linearly (by equal increments Δv) from zero to a maximum (Fig. 180), it is evident that if the n th layer from the top remains at rest, the topmost layer must have the velocity $(n - 1) \Delta v$. The weight discharge g of the sediment in motion, per unit width of bed, may then be found by multiplying the mean velocity of the layers $(n - 1) \Delta v / 2$ by the total thickness nd' and by the specific weight γ_s of the sediment in bulk:

$$g = \gamma_s n d' \frac{(n - 1) \Delta v}{2}$$

It now remains to relate one or another of these independent variables to known flow conditions. Du Boys assumed the longitudinal component of fluid weight $\gamma y_0 S$ to be counterbalanced by the friction of the sediment-water mixture at the bed. In this manner the intensity of boundary shear, already designated as τ_0 , becomes the so-called tractive force T —the force per unit area tending to move the bed. Evidently, reasoned du Boys, the frictional resistance between successive layers must depend upon the effective weight of the overlying material, the coefficient of friction ζ between layers arbitrarily being taken as a constant for the given material. It then follows that movement of successive layers will occur down to that level at which the weight of the overlying material produces a resistance equal

¹ Du Boys, P., *Études du régime du Rhône et l'action exercée par les eaux sur un lit à fond de graviers indéfiniment affouillable*. *Annales des Ponts et Chaussées*, Series 5, vol. 18, pp. 141–195, 1879.

in magnitude to the tractive force of the stream. At this point,

$$T = \gamma y_0 S = \zeta (\gamma_s - \gamma) n d'$$

If conditions of flow are such that the topmost layer of sediment will just resist motion, a critical value of T is reached, marking the limit of bed movement. Since n then equals unity, this critical force may be written

$$T_c = \zeta (\gamma_s - \gamma) d'$$

whereupon it is apparent that

$$T = n T_c$$

Introducing this expression into the equation for the rate of transport,

$$g = \frac{\gamma_s \Delta v d'}{2 T_c^2} T (T - T_c)$$

If the quantity $\gamma_s \Delta v d' / 2 T_c^2$ is considered to depend entirely upon sediment characteristics, the above relationship may be reduced to the form

$$g = \Psi T (T - T_c) \quad (236)$$

in which Ψ is the foregoing sediment parameter.

The general structure of the du Boys equation has been adopted in many a succeeding investigation. For instance, in the latest of these—that by Chang¹—the expression is used with practically no modification. Nevertheless, the extreme simplicity of du Boys' treatment of a very complex phenomenon is in itself reason for a certain amount of skepticism. The concept of sliding layers, as well as the failure to consider the weight component of the sediment itself in aiding the motion, are perhaps warranted simplifications, though surely open to question. But the velocity distribution within the sediment would hardly be linear, while ζ would certainly vary from layer to layer in all but the earliest stages of motion. O'Brien and Rindlaub² have sought to eliminate the latter objection by considering the bed

¹ CHANG, Y. L., Laboratory Investigation of Flume Traction and Transportation, *Proc. A.S.C.E.*, vol. 63, no. 9, 1937.

² O'BRIEN, M. P., and RINDLAUB, B. D., The Transportation of Bed-load by Streams, *Trans. Am. Geophysical Union*, pp. 593-603, 1934.

friction to vary exponentially with depth below the bed surface. The same method may also be applied to the velocity distribution within the moving sediment (note Fig. 178), the two developments yielding a relationship approximately of the form

$$\mathfrak{s} = \Psi' (T - T_c)^m \quad (237)$$

This type of equation has been selected by the United States Waterways Experiment Station,¹ but modified somewhat through introduction of the Manning n :

$$\mathfrak{s} = \frac{1}{n} \left(\frac{T - T_c}{K} \right)^m \quad (238)$$

The common assumption that the critical tractive force T_c depends alone upon sediment characteristics is thought to be justified by the fact that various investigators have noted a definite exponential relationship between particle diameter and critical force. Nevertheless, although the function appears to change slope more or less abruptly at a certain particle diameter, the experimental evidence is limited to a single fluid under approximately the same conditions of temperature. As shown by O'Brien,² the two portions of the curve doubtless apply to two different regimes of boundary motion, depending upon whether or not the surface particles of the bed lie within the laminar boundary film.* Under such circumstances the ratio between particle diameter and thickness of the boundary layer becomes an essential parameter, much as the ratio k/δ was found to be significant in the case of pipe roughness. Needless to say, boundary-layer thickness (a function of the Reynolds number) and average sediment diameter cannot be sufficient to determine T_c , since the specific weight, shape, and grading of the sediment are also of importance. Moreover, the stage at which movement begins over a uniformly flat bed cannot be expected to correspond to the point of cessation once ripples have developed.

Whether or not the boundary shear actually equals the true tractive force, it is not unreasonable to consider that some sort

¹ Studies of River Bed Materials and Their Movement with Special Reference to the Lower Mississippi River, *U. S. Waterways Experiment Station, Paper 17*, 1935.

² O'BRIEN, M. P., Notes on the Transportation of Silt by Streams, *Trans. Am. Geophysical Union*, pp. 431-436, 1936.

of functional relationship exists between \mathfrak{g} and τ_0 . On the other hand, this would imply that corresponding functions exist in terms of other flow characteristics, for through use of the Chézy relationship the quantity T (and, similarly, T_c) in any of the above expressions may be replaced by various combinations of depth, slope, and either velocity or the ratio of discharge and depth; thus,

$$T = \gamma y_0 S = \frac{\gamma V^2}{C^2} = \frac{\gamma q^2}{y_0^2 C^2} \quad (239)$$

Nevertheless, departures from the concept of tractive force are not in accord with the above transformation. Schoklitsch,¹ for instance, proposed the expression

$$\mathfrak{g} = \frac{A}{\sqrt{d}} S^{3/2} (q - q_c) \quad (240)$$

for sand of uniform grain diameter d , the beginning of bed movement being marked by a critical rate of discharge

$$q_c = \frac{Bd}{S^{1/2}}$$

MacDougall² used a relationship of the same general character for graded material. On the other hand, the laboratory of the Technische Hochschule at Zurich³ has adopted the expression

$$\frac{q^{3/2} S}{d} = a + b \frac{\mathfrak{g}^{3/2}}{d} \quad (241)$$

Herein both q and \mathfrak{g} have the same dimension of weight per unit time per unit width of bed. The critical discharge q_c (for $\mathfrak{g} = 0$) evidently has the value $(ad/S)^{2/3}$. This relationship is, nevertheless, specifically restricted to material of relatively large and uniform size, the investigators feeling that the ratio d/δ plays an essential role in determining not only the beginning

¹ SCHOKLITSCH, A., Der Geschiebetrieb und die Geschiebefracht, *Wasserkraft und Wasserwirtschaft*, p. 37, 1934. See also "Staurationverlandung und Kolkabwehr," Springer, Vienna, 1935.

² MACDOUGALL, C. H., Bed-Sediment Transportation in Open Channels, *Trans. Am. Geophysical Union*, pp. 491-495, 1934.

³ MEYER-PETER, E., FAVRE, H., and EINSTEIN, A., Neuere Versuchsergebnisse über den Geschiebetrieb, *Schweizerische Bauzeitung*, vol. 103, no. 13, 1934.

of movement but the form of the function once such motion is established. They show, moreover, that this form of bed-load function is particularly advantageous in comparison of model and prototype behavior, since the several factors are grouped in accordance with the Froude criterion for similarity.

Despite the abundance of experimental data upon which these several relationships were based, one fact remains apparent: the research world still cannot agree upon the actual form of the bed-load function. Indeed, continued efforts seem only to produce further variations in experimental trends, and the problem is far from a satisfactory end. Much of the discrepancy is undoubtedly due to differences in experimental technique, for bed-load measurement is not an easy matter. Experimental flumes are seldom of sufficient width to eliminate wall effect completely, and in many cases the material in motion is not completely trapped or the measurement is not continued for a sufficient length of time to average a series of ripple crests and troughs. Moreover, although sediment weight and mean grain diameter are generally given due heed, little attention has been paid to grading characteristics, except to note that uniform material never behaves the same as graded.

In all probability, many investigators have unknowingly dealt with different phases of the general problem, to which circumstance the lack of agreement in results may in part be attributed. That the Zurich studies show a relationship different from Eq. (241) for material of small size is evidence of this situation. On the other hand, apparently no investigation has included the more advanced stage of motion (Fig. 178) in which material is also carried in suspension and in which ripple formation probably plays no part.

If progress is to be made in this essential field, it would seem that two features must soon become essential: a satisfactory analysis of the general problem, at least from the dimensional point of view; and a truly extensive series of experimental measurements, conducted systematically and under conditions free from the usual sources of error. From the foregoing discussion, the Froude and Reynolds numbers, the slope, and the pertinent sediment properties ρ_s , d_m , and σ_g (discussed in Section 77) would appear to include all independent variables involved in the phenomenon. In order to obtain **F** and **R** as parameters

(refer to Chapter I), y_0 , V , and ρ must be selected as the three repeating variables, under which circumstances the bed-load function would have the dimensionless form

$$g = \varphi\left(F, R, S, \frac{\rho_s}{\rho}, \frac{d_m}{y_0}, \frac{\sigma_g}{y_0}\right) \rho V^3$$

Evidently, the resulting expression would be decidedly more involved than any of the empirical relationships already cited; indeed, although this function is perfectly sound dimensionally, it remains a moot question whether or not the parameters are in their most significant and convenient form. Whatever the final parametric arrangement, complete control of every pertinent variable—and not haphazard study of one or another over a small range—must be the ultimate experimental objective.

76. Sediment Suspension. Within the past one or two decades, progress in the statistical analysis of fluid turbulence has been so rapid that application of the resulting knowledge to problems other than that of fluid resistance has tended somewhat to lag. Thus, while the phenomenon of sediment suspension depends primarily upon the turbulent mixing process, for many years the study of this effect¹ retained the same empirical aspects still encountered in research on bed load. As a matter of fact, the attention paid to bed-load movement in the field and laboratory has far exceeded that given to material carried in suspension, and only recently has the latter begun to receive the notice merited by its importance to hydraulic engineering.

In discussing the essential aspects of bed-load transportation, it has been found expedient to consider at first only those conditions in which material is moved at or near the lower boundary. But although the turbulent suspension of sediment might be looked upon merely as an advanced stage of bed-load saltation, the problem of sediment suspension may best be approached by considering only those regions of flow that lie at some distance from the bed. Under such circumstances, boundary effects involved in the bed-load transport need not be taken directly into account, and the mixing process may then be analyzed according to the methods of Chapter IX. Indeed, Eq. (120m) is immediately useful, for it expresses in simple form the rate at

¹ JAKUSCHOFF, P., Die Schwebestoffbewegung in Flüssen in Theorie und Praxis, *Die Wasserwirtschaft*, vol. 25, nos. 5-8, 11, 1932.

which suspended material is carried across the flow as a result of the turbulent mixing. Since the present discussion is restricted to the case of fully established uniform motion, it follows that the normal curve of sediment distribution will, like the velocity profile, remain statistically the same at all successive flow sections. In other words, a state of equilibrium must exist between the rate at which sediment is raised by turbulence (*i.e.*, carried in the direction of decreasing concentration) and the rate at which it falls as a result of its own weight.

Designating by w the velocity of fall of a given type of particle, the product wc will then indicate the rate at which such material settles per unit horizontal area—the dimension of wc depending upon that of the concentration c (that is, c may represent the number, weight, or even volume of the particles per unit volume of the water-sediment mixture). If a state of equilibrium is to obtain, this rate of settling must exactly equal the rate at which the material is lifted by the turbulence; thus,

$$wc = -\epsilon \frac{dc}{dy} = -[\overline{v_y'}] l \frac{dc}{dy} \quad (242)$$

It is to be noted that this expression places no restriction upon the relative magnitudes of w and $[\overline{v_y'}]$. In this respect the reader must remember that the entire analysis is statistical, $[\overline{v_y'}]$, l , and c representing mean values about which considerable local variation will necessarily occur from instant to instant.

Integration of Eq. (242) leads at once to the general expression

$$\ln \frac{c}{c_a} = -w \int_a^y \frac{dy}{\epsilon} \quad (243)$$

which refers the concentration at any elevation y to a known concentration at the elevation a . Evidently, the final evaluation of the sediment distribution must depend upon knowledge of the variation of ϵ with y . The validity of the general expression, however, has been checked by making ϵ independent of y , through producing with some sort of stirring device a fairly constant degree of turbulence from bottom to top of a jar containing a mixture of water and sediment, and then determining the concentration of samples taken at various elevations. The experiments of Hurst,¹ conducted in this manner, yielded

¹ HURST, H. E., The Suspension of Sand in Water, *Proc. Roy. Soc. (London)*, vol. 124, p. 196, 1929.

results in good qualitative accord with Eq. (243), whereas more recent investigations by the author—as yet unpublished—indicate that the relationship is valid quantitatively as well.

In open-channel flow, however, ϵ must necessarily vary with y . Such variation may be written in terms of the mean velocity gradient by combining Eqs. (118) and (234):

$$\frac{dy}{\epsilon} = \frac{\rho}{\tau_0} \frac{dv}{dy} \frac{1}{(1 - y/y_0)} dy$$

Upon substitution in Eq. (243)

$$\ln \frac{c}{c_a} = - \frac{w y_0}{\tau_0 / \rho} \int_a^y \frac{dv/dy}{y_0 - y} dy \quad (244)$$

If the depth, the slope (since $\tau_0 = \gamma y_0 S$), and the velocity distribution are known, Eq. (244) may be used to determine by graphical integration the curve of sediment distribution referred to the concentration at some arbitrary level a . This method has been tested by Christiansen¹ for vertical distribution curves in a wide channel, with satisfactory agreement between measurement and calculation. It has, moreover, been adapted by Leighly² to the more general case of a relatively narrow cross section, through graphical analysis of plotted isovels.

If one assume that the velocity distribution in a very wide channel is of the universal logarithmic type (see page 275), it follows from Eq. (175) that

$$\frac{dv}{dy} = \frac{1}{\kappa} \frac{\sqrt{\tau_0 / \rho}}{y}$$

Substitution in Eq. (244) then yields an expression which may be integrated to give

$$\frac{c}{c_a} = \left[\frac{1 - \frac{y}{y_0}}{\frac{y}{y_0}} \times \frac{\frac{a}{y_0}}{1 - \frac{a}{y_0}} \right]^z = \left[\frac{1 - \frac{\eta}{\eta_0}}{1 + \frac{\eta}{a}} \right]^z \quad (245)$$

¹ CHRISTIANSEN, J. E., Distribution of Silt in Open Channels, *Trans. Am. Geophysical Union*, pp. 478-485, 1935.

² LEIGHLY, J., Turbulence and the Transportation of Rock Debris by Streams, *Geog. Rev.*, vol. 24, no. 3, 1934.

in which $\eta = y - a$ and

$$z = \frac{w}{\kappa \sqrt{\tau_0/\rho}} = \frac{w}{\kappa V \sqrt{f/8}}$$

It is apparent that the exponent z , for a given state of motion, will depend in magnitude upon the settling velocity of the sediment—and will, therefore, be different for the various particle sizes. In other words, the curve of total sediment distribution

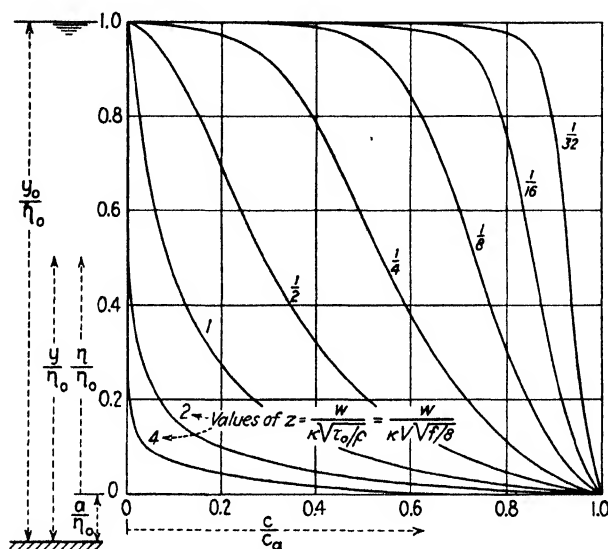


FIG. 181.—Dimensionless plot of suspended-load distribution.

must be considered as the summation of a series of individual curves for the particle sizes in the suspension. In Fig. 181 will be seen a number of these curves for various magnitudes of the exponent z , plotted from Eq. (245) on the assumption that the logarithmic velocity-distribution curve is valid between some arbitrary elevation a and the free surface of the flow.

The reader will realize that the foregoing development¹ is applicable only so long as the assumed conditions actually are fulfilled: First, the flow must be steady, uniform, two-dimensional motion, and hence free from the circulation encountered in channels of low width-depth ratio. Second, similarity of the turbu-

¹ ROUSE, *Modern Conceptions of the Mechanics of Fluid Turbulence*, pp. 534–536.

lence mechanism must obtain over the entire section considered; this excludes at once the region of the lower boundary, leaves open to question the immediate neighborhood of the free surface, and presumes that the presence of sediment will have no appreciable effect upon the mixing process. Mention has already been made of the fact that secondary motion in channels of relatively small width tends to bring the zone of maximum velocity below the free surface, which must necessarily influence the sediment distribution. Needless to say, the pronounced circulation at bends and in channels of irregular cross section will only magnify this effect. As for the boundary regions, little can be said at present as to conditions at the free surface, whereas the necessary exclusion of the zone near the bed may well afford a convenient basis for differentiating between bed load and suspended load. In this connection it is to be noted that Eq. (245) affords no means of determining the capacity of a stream, for the concentration at any point would seem to depend entirely upon the amount of material carried above the level a as the result of conditions in the bed region.

Analysis of the actual effect of sediment concentration upon the mixing process may eventually lead to a means of prophesying the capacity of a given flow, although at present only the following brief comment may be made. So long as the concentration is low, the density ρ_m of the water-sediment mixture will differ little from that of the water alone. Once the change in density becomes appreciable, however, it must be remembered that ρ_m can no longer be treated as a constant in determining the apparent shear due to the mixing process at any depth. That is, the stress resulting from the momentum transport will vary with the gradients of both density and velocity,

$$\tau = \epsilon \frac{d(\rho_m v)}{dy} = \epsilon \rho_m \frac{dv}{dy} + \epsilon v \frac{d\rho_m}{dy}$$

while ϵ will probably no longer be a function of the velocity gradient alone.

77. Sediment Characteristics.¹ In problems of sedimentation and percolation, as well as those of sediment transportation by a

¹ The methods discussed in the following pages were first brought to the author's attention by Mr. George H. Otto, to whom the author is also indebted for careful examination of this portion of the manuscript.

moving fluid, systematic and conclusive results cannot be expected without due regard to the characteristics of the material involved. In the past, all too little consideration has been given to this important aspect of the investigations, due in part to a regrettable lack of coordination among research men in the various fields of endeavor. Brief mention seems justified at this point, therefore, of certain methods of sediment analysis that may well prove of general value.

So far as the material itself is concerned, the essential properties may be listed as follows: density, or specific weight, commonly expressed in relation to the corresponding property of the fluid; average grain diameter, sometimes taken as the median, sometimes as the geometric mean;¹ characteristic shape of grain, which may be defined in terms of relative sphericity, and relative roundness of the surface irregularities; and, finally, size-frequency distribution, or the relative proportions by weight of the different grain sizes, determined by sieving in the coarser range and by hydraulic methods in the finer.

To these the reader may feel inclined to add the porosity or voids ratio of the sediment as a whole, and the velocity of fall of the individual particles. One must realize, however, that these qualities depend in part upon those already listed—and can seldom be used either as satisfactory substitutes or as independent parameters. To be sure, the velocity of fall was used exclusively in the foregoing treatment of sediment suspension, and replaces the sieve criterion for size in the hydraulic determination of grading in the finer range. But in either case this usage is tacitly limited to particles of fairly uniform density, for particle size would surely play a role (because of unequal interference) in a mixture of very light and very heavy materials. As for the voids ratio, knowledge of this factor is very essential in problems of percolation, in which it indicates the degree of compaction of the material. But in the case of sediment transportation over a bed whose other characteristics govern its porosity, laboratory determination of the voids ratio for an arbitrary degree of compaction will yield no information that is not available from the other sediment characteristics.

¹ The term "median" refers to the center of area of a distribution curve, the term "mean" to the center of gravity of that area; if the curve is symmetrical, the mean and the median will coincide.

The question of density needs no further comment. Determination of the shape factors¹ is a difficult matter, and for normal sands and silts the shape is fortunately a secondary characteristic. Average grain diameter and the grading of the material, on the other hand, are two properties of primary importance. Results by weight of sieve analyses were formerly plotted on ordinary coordinate paper against either mesh number or mesh size, a smooth curve through the plotted points yielding such diagrams as those shown in Fig. 182. Cumulative plots of the corresponding curves, also to arithmetic scale, would then have the form of the familiar percent-finer diagrams of Fig. 183. The average grain size expressed as the median is indicated on the cumulative curves by their intersection with the 50 per cent line.

This method, however, gives undue prominence to the coarse end of the distribution, and completely masks the distribution of the fines. Hence, plotting the results of mechanical analyses on semilogarithmic paper eventually gained favor, in particular since this method yields equal intervals on the abscissa scale for sieves of the Wentworth and Tyler series, which advance in mesh size by the factor $\sqrt{2}$. The added significance of the resulting diagrams is at once apparent from Figs. 184 and 185. They take on marked qualities of symmetry, and use of the geometric mean size embodies in this parameter a corresponding degree of emphasis for the distribution in the fine and coarse ends.

Although the curves shown as broken lines are taken from actual analyses of sediment, they differ little in character from the full line, which is the elementary curve of probability. Indeed, the deposition of sediment by natural causes is distinctly a matter of chance, the statistical treatment of which should yield a size-frequency distribution following a basic probability function so long as the conditions under which deposition occurs remain essentially constant. That distribution curves of other types are frequently encountered in practice is attributable to a great extent to improper methods of securing samples for mechanical analysis—for, in securing these samples, materials deposited under different conditions are often withdrawn together. On the other hand, if materials of a sufficient variety are combined,

¹ WADELL, H., Volume, Shape, and Roundness of Quartz Particles, *J. Geol.*, vol. 43, pp. 250-280, 1935.

the resulting grading characteristics should again approach the probability equation.

In movable bed material, segregation is bound to occur at various points, just as permeable soils are almost certain to

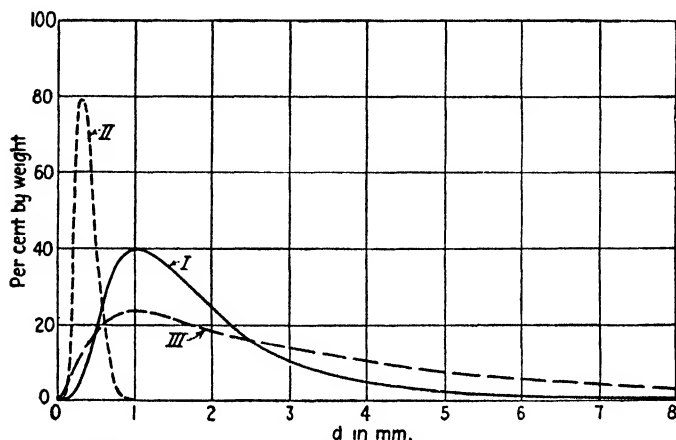


FIG. 182.—Size-frequency distributions of sediment—arithmetic coordinates.

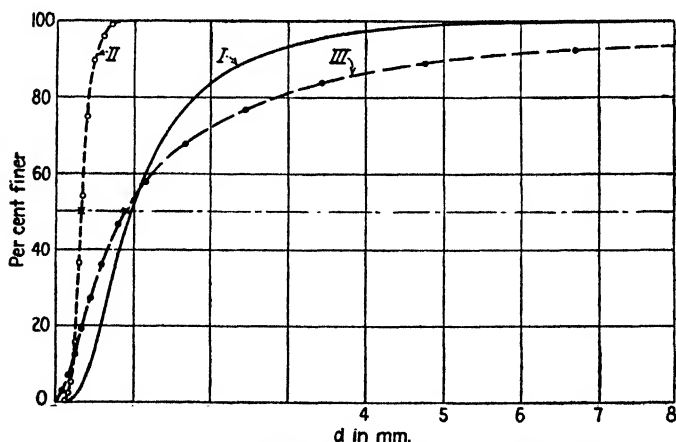


FIG. 183.—Cumulative curves of sediment distribution—arithmetic coordinates.

vary in composition from one zone to another. Nevertheless, in a given zone conditions should be essentially constant; as a result, the local grading of the sediment should follow the probability law. On the other hand, if a large number of such zones are represented in a single sample, the probability relation-

ship should again apply. In a word, treatment of the mechanical grading of sediment in this manner not only has definite bearing upon actual sediment characteristics, but permits a systematic

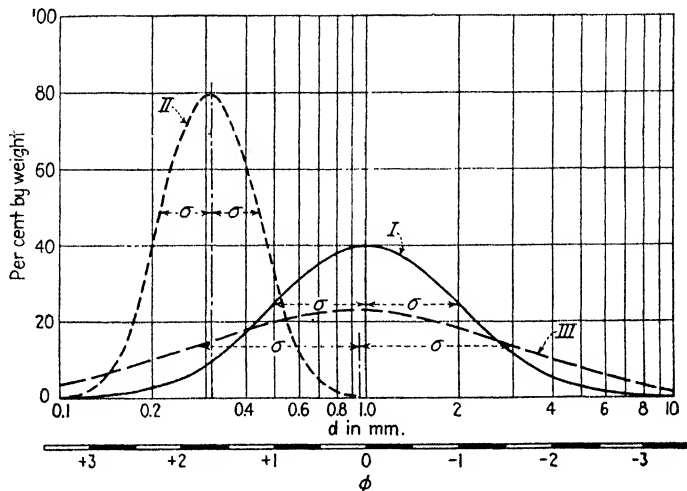


FIG. 184.—Semilogarithmic size-frequency curves.

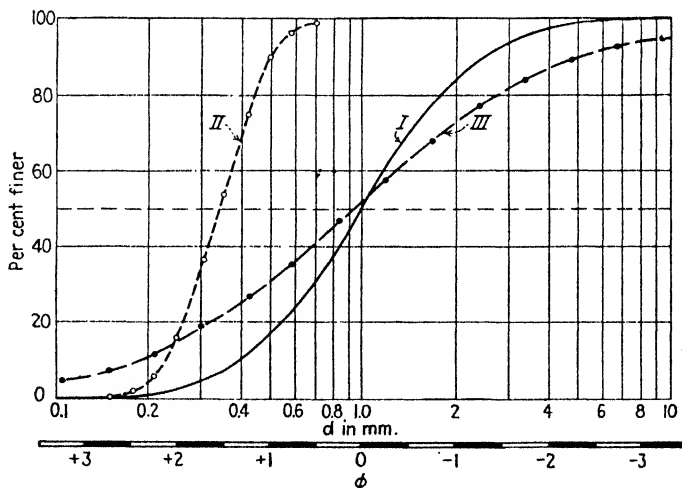


FIG. 185.—Semilogarithmic cumulative curves.

laboratory approach through the use of probability notation in the designation of typical size-frequency parameters.

• Selection of such parameters has been quite inconsistent in the past. Attempts have been made to define the cumulative

curve by its intercepts at, say, the 20 and 80 per cent ordinates, or by using the ratio of areas enclosed by certain arbitrary portions of the curve. By far the most useful method yet devised proceeds from the characteristics of the probability diagram of Fig. 184. The position of the curve is established by the geometric mean size d_m , which corresponds to the abscissa of the center of gravity of the enclosed area. The relative proportions of the curve are defined by the standard geometric deviation σ_g from this mean, which is equivalent to the radius of gyration of the enclosed area about a vertical axis through the center of

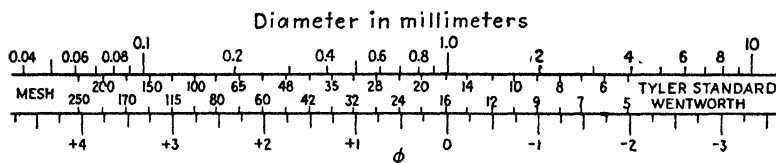


FIG. 186.—Relationship of Krumbein's ϕ scale to sieve mesh and nominal grain diameter.

gravity. If the curve is not symmetrical, a third parameter is necessary to define the skewness,¹ a characteristic that will not be discussed in these pages.

Krumbein² has further systematized such classification by replacing particle size by its logarithm to the base 2, arbitrarily selecting for this parameter ϕ the value of zero for the 1-mm. size and letting ascending values of ϕ correspond to descending magnitudes of grain diameter, and vice versa. The relation between ϕ and d will be evident from Fig. 186, in which it will be seen that the ϕ units correspond closely to the original Wentworth series, in which each size is twice the preceding. In terms of Krumbein's ϕ notation, the probability function may be expressed in the simple form

$$y = \frac{100}{\sqrt{2\pi} \sigma_\phi} e^{-\frac{1}{2}\left(\frac{\phi - \phi_m}{\sigma_\phi}\right)^2} \quad (246)$$

in which σ_ϕ represents the standard deviation—the radius of

¹ CAMP, B. H., "The Mathematical Part of Elementary Statistics," D. C. Heath & Co., 1931, Chapter II.

² KRUMBEIN, W. C., The Use of Quartile Measures in Describing and Comparing Sediments, *Am. J. Sci.*, vol. 32, pp. 98–111, 1936.

gyration about the mean ϕ_m —whereas the y scale (in per cent) is so chosen that the area under the curve is equal to 100 per cent.

Since the cumulative probability curve must plot a straight line on logarithmic probability paper, the diagrams should be the more significant in this form. Figure 187 thus shows the same three grading curves appearing in the other diagrams, each one of which may now be characterized in full by the position of the mean and by the slope—which is inversely proportional

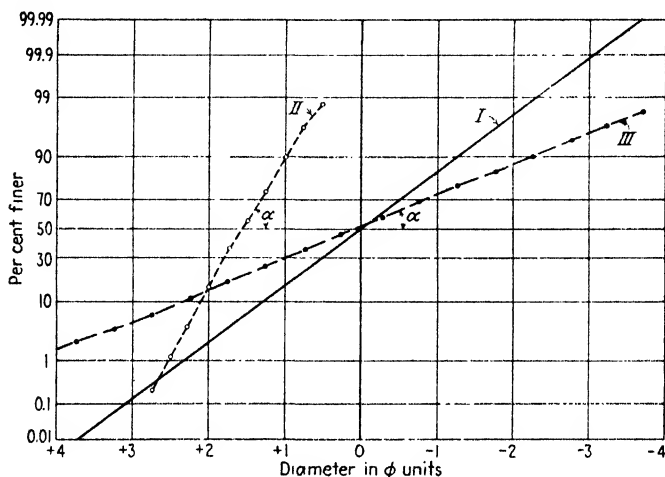


FIG. 187.—Logarithmic probability plot of cumulative curves.

to the standard deviation in ϕ units (that is, $\sigma_\phi \sim 1/\tan \alpha$). It is evident that any cumulative curve must be inclined at some angle between the vertical ($\sigma_\phi = 0$), corresponding to material of constant size, and the horizontal ($\sigma_\phi = \infty$), signifying the widest possible dispersion of sizes about the mean. Only one objection can be found to Krumbein's ϕ unit: since it is a logarithm, it is not a length; yet it is not truly dimensionless, for its magnitude depends upon the arbitrary selection of the millimeter scale, some question thus arising as to its significance in the process of dimensional analysis.

Not only is any grading curve that plots a straight line on logarithmic probability paper completely defined by the geometric mean size and the standard deviation, but departure from the rectilinear is in itself a measure of skewness. Reduction of mechanical-analysis results to the necessary form is not a

difficult matter,¹ whereas the general clarity and significance of the method well warrant its adoption. Indeed, perhaps the greatest engineering value of this probability relationship lies in the fact that means are now at hand whereby the characteristics of sediment used in controlled laboratory investigations may be varied over an extreme range in a logical and systematic fashion.

¹ KRUMBEIN, W. C., Application of Logarithmic Moments to Size Frequency Distributions of Sediments, *J. Sedimentary Petrology*, vol. 6, no. 1, pp. 35-47, 1936.

PART THREE
MECHANICS OF WAVE MOTION

CHAPTER XV

GENERAL CHARACTERISTICS OF WAVE PHENOMENA

78. Propagation of Disturbances in Fluid Media. In any pattern of fluid motion, variation of the velocity vector with either space or time represents, in effect, a disturbance of an otherwise steady, uniform state of flow. Such disturbances as those produced by the movement of an immersed body, by a pipe orifice, or by boundary roughness have already been discussed at length. In every case it was tacitly presumed that the effect of such disturbing factors was felt instantaneously throughout the surrounding fluid, the flow pattern thereby being governed primarily by the geometrical boundary conditions.

It is physically impossible, nevertheless, for such disturbing impulses to travel with an infinite velocity. Indeed, the velocity of propagation of any disturbance in a fluid medium has a definite, finite magnitude, depending upon the nature of the disturbance, the characteristics of the undisturbed flow, and the properties of the fluid in question. In many cases, to be sure, the velocity at which disturbances are propagated through a fluid medium is greatly in excess of the relative velocity between fluid and boundary; one may then conveniently assume that the velocity of propagation is infinitely great, and thereby avoid needless complication. If, however, these two velocities are roughly of the same order of magnitude, such an assumption will introduce appreciable error. And if the velocity of flow is actually greater than the velocity at which a disturbance can be propagated, the resulting pattern of flow will bear little resemblance to that assumed.

Needless to say, such phenomena involve the interplay of pressure intensity, density, and velocity, for the problem is essentially dynamic in its fundamental aspects. Yet the true nature of the fluid disturbance is determined by that force property which plays the predominant role in its propagation. Such force properties, as the reader will recall, include specific weight, dynamic viscosity, surface tension, and elastic modulus—

each of which is associated with a different type of disturbance.

For instance, a chapter or more has already been devoted to disturbances in which viscosity is the governing factor. In the case of deformation drag, it was pointed out that the movement of an immersed body would be felt throughout the fluid, provided the Reynolds number was of sufficiently small a magnitude; in other words, the disturbance caused by such motion through the action of viscosity would be propagated throughout the fluid at a velocity so much in excess of the velocity of the body that the slight time lag could be neglected entirely. At considerably higher Reynolds numbers, on the contrary, the relative velocity of the boundary was sufficiently great to confine the major part of the disturbance to a layer at the boundary—a layer growing in thickness, however, with distance from the leading edge. Evidently, the ratio of thickness to distance must then be a measure of the ratio between the velocity of propagation of a viscous disturbance and the relative velocity between boundary and undisturbed fluid. Needless to say, the spread of a viscous disturbance has its counterpart in the diffusion of turbulence, which again has a characteristic velocity of propagation.

Aside from this closely related phase of viscous action, disturbances of the type classed as waves are generally considered to proceed through the action of weight, surface tension, or elasticity; viscous action, however, is always present in waves of any of these three types, opposing the deformation of the fluid elements and gradually reducing the energy of the disturbance through dissipation in the form of heat. The nature of the several force properties determines to a large extent the conditions under which they play essential roles. Capillary waves (disturbances governed by surface tension) require the existence of a boundary surface between a liquid and a gas, or between two liquids; however, the radius of curvature of the surface disturbance must be relatively small if the capillary action is to be appreciable. Gravity waves (disturbances governed by fluid weight) are also restricted to liquids with a free surface, or to a liquid interface, but surface curvature is not the controlling factor. Elastic waves, on the other hand, may be propagated through liquid and gas alike, regardless of whether or not the fluid is confined by solid boundaries.

Unfortunately, wave motion is probably that branch of fluid mechanics which is least susceptible to rigorous mathematical treatment—except for certain limiting cases—for the general problem involves all the obstacles of steady, non-uniform flow, with one additional variable: time. In the following introductory treatment, therefore, the problem is reduced to its barest essentials in the effort to stress the fundamental mechanics of wave motion and the basic similarity of the several different wave types.

79. Relative Velocities of Wave and Fluid.

The steady movement of a body through a fluid might be imagined to proceed through a series of infinitesimal impulses; each of these then generates an infinitesimal disturbance or wave which moves outward with a celerity c , the velocity of wave propagation relative to the fluid under the existing conditions. The rapid sequence of these tiny impulses thus produces in the surrounding fluid a pattern of flow that depends in form upon the celerity of the wavelets in relation to the mean velocity of the body.

For convenience in illustration, one may imagine further that the source of the disturbances is represented by a single point advancing through the fluid. If the mean velocity of translation v is extremely small in comparison with the celerity of the wavelets, over a brief interval of time the source will move only imperceptibly and the series of impulses generated during this interval will appear to travel through space with the same velocity in every direction. Such a condition is shown in two dimensions in

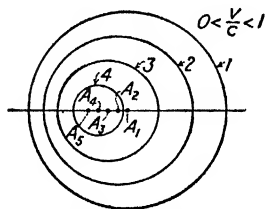


FIG. 189.—Wave source advances slowly through fluid.

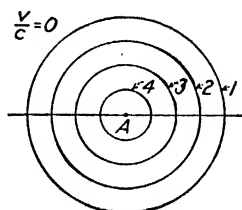


FIG. 188.—Waves generated at a stationary source.

Fig. 188 by a series of circles practically concentric with the body at point A . If, on the other hand, the velocity of translation approaches the magnitude of the celerity of wave propagation, each successive wavelet will be generated at a different point in space, owing to the continuous movement of the source. Thus, in Fig. 189, wavelets are generated at points A_1 , A_2 , A_3 , and A_4 ; by the time the source has reached

point A_5 , wavelets 1, 2, 3, and 4 have attained the proportions indicated in the illustration. Evidently, although the individual wavelet preserves a circular form (since the celerity c is measured relative to the fluid), the circles are no longer concentric.

Should the velocity of translation exactly equal the wave celerity, it is evident that the source will advance through the fluid at precisely the same rate as that portion of each wavelet lying in its path. Under such conditions an instantaneous picture of the wave pattern will consist of a series of circles tangent to one another at their intersection with the path of the

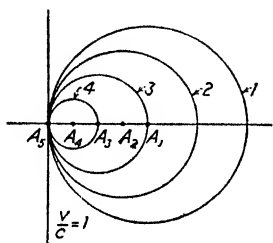


FIG. 190.—Velocity of wave source equals wave celerity.

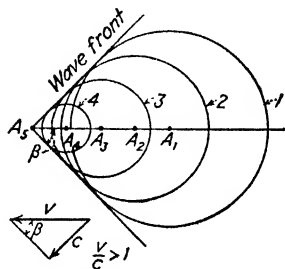


FIG. 191.—Velocity of wave source exceeds wave celerity.

source, as shown in Fig. 190. If the celerity of propagation is now exceeded by the velocity of translation, each succeeding wavelet will at once be left behind; lines tangent to the successive wavelet circles now represent the wave fronts of what is actually a continuous process of disturbance. As will be seen from Fig. 191, the wave angle β (commonly known as the Mach angle) is the following simple function of the celerity and the velocity of translation:

$$\sin \beta = \frac{c}{v} \quad (247)$$

Since the foregoing illustrations correspond to the motion of a body through a fluid originally at rest, the flow pattern must vary from instant to instant. Yet so long as the velocity of translation and the wave celerity retain their relative magnitudes, the unsteady pattern of flow may be transformed into a steady one simply by translating the coordinate system at a velocity equal to that of the moving body. Obviously, the resulting pattern of steady motion will be similar to that caused by fluid

moving with the same velocity past a stationary body, provided the coordinate system then remains at rest. But since the celerity c is invariably measured with respect to the fluid, the velocity of wave propagation with respect to the source of disturbance must always be considered as the vector sum of v and c .

If the flow pattern for given boundary conditions is determined on the assumption of an infinite velocity of propagation, it should now be apparent that the pattern actually obtained will differ from this limiting condition by an amount depending on the ratio of the mean velocity of flow to the celerity of an infinitesimal wave. For the condition of instantaneous propagation of fluid disturbances, presumed in classical hydromechanics and indicated by the wave pattern of Fig. 188, the parameter v/c obviously has the magnitude zero; for conditions typified by Figs. 189, 190, and 191 this parameter is less than, equal to, and greater than unity, respectively. As was mentioned in Chapter I, the Froude, Weber, and Cauchy numbers are none other than specific forms of this basic ratio, as is also the Reynolds number, in the light of the foregoing remarks. Thus, the dimensionless ratio v/c is a fundamental parameter not only of wave mechanics, but of fluid motion in general.

It is beyond the scope of this text to investigate more thoroughly the distortion of the basic flow pattern as this parameter gradually becomes of finite magnitude. Once it exceeds unity, however, the problem becomes primarily one of wave mechanics, a field that has direct bearing upon hydraulic engineering. It may not be unwise, therefore, to refresh the reader's memory on certain basic principles of wave geometry as taught in elementary physics, whereafter expressions for the celerity of the several wave types will be developed from the basic equations of fluid motion.

80. Wave Forms; Interference and Reflection. Needless to say, the original form of any disturbance in a fluid medium depends entirely upon the manner in which this disturbance is generated. Thus, if a moving piston at the end of a conduit acts as the generating mechanism, the temporal rate at which the piston changes its position will determine the form of the wave disturbance in the immediate vicinity of its source. For instance, if the piston were given a reciprocating motion, a continuous

train of similar waves would result, as indicated in Fig. 192. If, after a half cycle, the piston were to remain at rest, a solitary wave would be produced, like that in Fig. 193. In either case the diagram represents the change in flow conditions with time at a fixed section a short distance ahead of the piston. The abscissa scale therefore measures the passage of time, whereas the ordinate scale might properly indicate the total energy of the disturbance per unit fluid volume. More generally, however, it is the potential energy of the motion that is plotted, the wave form then representing the change in pressure intensity, in the

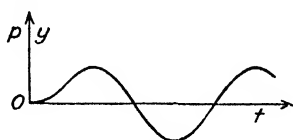


FIG. 192.—Generation of a wave train.



FIG. 193.—Generation of a solitary wave.

case of an elastic wave, or the change in elevation of the free surface, in the case of either gravity or capillary waves.

In the most general case—even of irrotational motion—the form of the wave must be considered to vary with time as it travels through space. Yet under certain conditions, to be discussed presently, the wave form may remain sensibly the same, the rate of energy loss due to viscous action and heat conduction being so slight as to produce a noticeable effect only after the wave has traveled a considerable distance. Under such circumstances, appropriate translation of the coordinate axes will transform the wave disturbance into a pattern of steady flow with constant energy. The Bernoulli equation then being fully applicable, velocity changes within the wave may readily be investigated through the basic equations of flow.

Should two wave systems approaching from opposite directions cross one another, it is evident that the energy of the individual elements of the two systems (and, similarly, the velocity components and increments of pressure intensity or elevation) must be added algebraically as the elements coincide in position. Assume two systems of simple harmonic motion, of equal amplitude and wave length, and equal and opposite celerity, as shown by broken lines in Fig. 194. Addition of the coincident elements of the two wave profiles will yield the curve

shown as a full line, which represents the resultant wave form at the given instant. As the two systems continue in their respective directions, the original profiles will eventually coincide, under which circumstances the resultant profile will attain its maximum proportions (Fig. 195). When the nodes next coin-

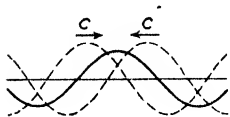


FIG. 194.—Wave interference.

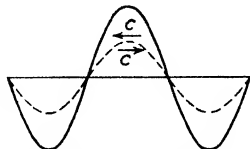


FIG. 195.—Coincidence of crests.

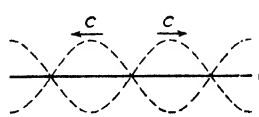


FIG. 196.—Coincidence of nodes.

cide, however, the resultant profile will simply be a straight line (Fig. 196). Under the given circumstances the resultant wave system will have the velocity of neither of its components, but will oscillate symmetrically with respect to a stationary coordinate system. The reason for this is simple: Although such scalar quantities as pressure intensity and elevation require only algebraic addition, the velocity fields of the two original wave systems must be combined vectorially—and since the celerities

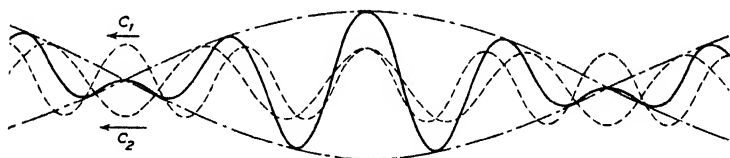


FIG. 197.—Formation of a wave group.

of the two component systems are of opposite direction, the resultant celerity must be of zero magnitude.

Had either wave system had a velocity of propagation other than that assumed, it is obvious that the celerity of the resultant motion would have been of finite magnitude. An interesting case is provided by two wave systems of equal amplitude but different wave length, traveling in the same direction with unequal celerities. As shown in Fig. 197, the resultant system will take the form of a series of wave groups quite distinct from one another. Upon closer investigation it will be found that the rate at which the wave groups appear to move through the fluid will differ from the celerity of the individual waves of the resultant system.

When a wave of any type strikes a solid boundary, each element is reflected positively by the boundary. The reflected wave elements, however, must be regarded as quite distinct from the remaining elements of the oncoming wave—the phenomenon of reflection giving rise to a new wave system, similar to the original in every respect save direction of propagation. Since the velocity component normal to the boundary must always remain equal to zero (Fig. 198), it follows that the angle of incidence will exactly equal the angle of reflection. Should a wave train approach a boundary at right angles (zero angles of incidence and reflection), the resultant system of oscil-

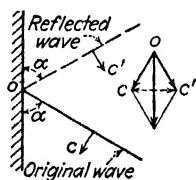


FIG. 198.—Reflection of a wave by a solid boundary.

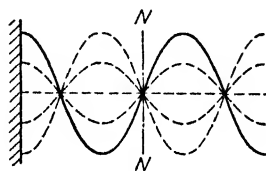


FIG. 199.—Oscillatory waves resulting from the reflection of a wave train.

latory waves will be that shown in Fig. 199, the reflecting boundary always coinciding with an antinode, or section of maximum amplitude, where the longitudinal velocity component is invariably zero.

The converse of a reflecting boundary must then be a section of flow at which the velocity may change without appreciable effect upon the pressure intensity or the elevation of the free surface, as the case may be. Such a section is illustrated by the juncture between a closed or open conduit and a large reservoir. The wave train is then reflected in the negative sense, the resultant wave system again being of the oscillatory type; the section of negative reflection, however, then coincides with a node (*NN* in Fig. 199).

It will be evident to the reader that such elementary rules of interference and reflection apply fully as well to solitary waves (note Fig. 200) as to wave trains—indeed, to any type of wave motion, regardless of form. The actual form of the wave, on the other hand, has a definite influence upon its stability and velocity of propagation. In general it may be said that wave celerity depends not only upon conditions within the undisturbed fluid, but also upon the extent of departure from these

original conditions within the wave itself. The celerity of a gravity wave, for instance, is a function of the amplitude of the wave as well as of the original depth of flow. It is obvious,

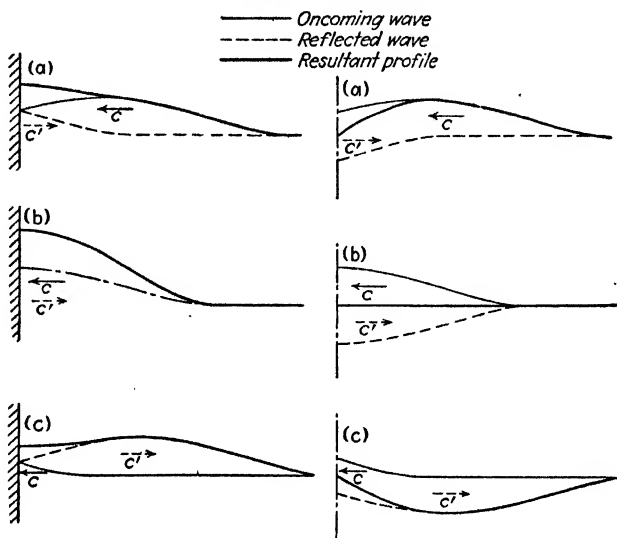


FIG. 200.—Positive and negative reflection of a solitary wave.

therefore, that in a wave of finite amplitude the departure from the original state of motion will vary from section to section of the wave profile. For example, the wave shown in Fig. 201 may be regarded as a series of superposed wavelets; the first wavelet will, on passing, change the velocity of the fluid relative to which the celerity of the next wavelet must be measured.

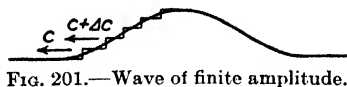


FIG. 201.—Wave of finite amplitude.

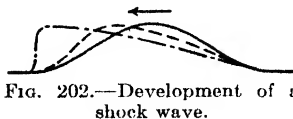


FIG. 202.—Development of a shock wave.

Relative to the undisturbed fluid, therefore, each element of the wave must then move somewhat more rapidly than that directly below. Under such circumstances the wave profile cannot preserve a constant form, for the front of the wave will tend to become progressively steeper, whereas the rear, on the contrary, will gradually flatten out.

As may be seen from the diagrammatic sketches of Fig. 202, the wave front must eventually take the form of an abrupt dis-

continuity in the flow characteristics—a condition that is physically impossible unless accompanied by appreciable loss of energy. Use of the term “shock wave” to characterize such conditions is therefore quite apt. Although waves in a gaseous medium are ordinarily adiabatic (constant heat), the sudden change in density caused by an elastic shock wave results in loss of heat through conduction, and adiabatic conditions then no longer hold. And whereas gravity waves may ordinarily be treated as cases of potential motion, a shock wave at the free surface of a liquid gives rise to a considerable degree of turbulence at the wave front.

A somewhat different aspect of shock-wave formation should throw further light upon this important phenomenon. In Fig. 203 is indicated the pattern of flow past a thin curved plate. For the sake of clarity the smooth curve has been replaced by a series of short tangents, each of which produces a small but finite disturbance in the flow. If the fluid approaches as shown with a velocity greater than the celerity c of wave propagation, the series of disturbances will give rise to a succession of wave fronts extending from the plate on either side.

For reasons of continuity (and as must follow from the geometry of the illustration) the stream lines will converge on the concave side of the plate, where the waves are positive, and diverge on the convex side, where the waves are negative—changing direction in every instance only as they cross a wave front. Moreover, it is apparent that the celerity of successive wavelets on the concave side must gradually increase, owing to the growth in amplitude of the wave proper along the plate; conversely, the wavelets on the convex side suffer a gradual reduction in celerity, as is indicated by the slight change in wave angle. Even were the wave celerity to remain sensibly constant, however, it will be seen that on the concave side the wave fronts will eventually intersect; it is because of the actual increase in c that the locus of successive intersections increases gradually in curvature. Such interference of wave fronts can only signify the existence of an abrupt discontinuity—in other words, a shock wave of steadily increasing magnitude must result.

Conditions within this shock wave may be more clearly visualized by investigating a series of cross sections normal to the wave front, shown schematically in Fig. 204. It would

appear from this that the shock wave must exist as such at the very beginning of the plate. It must be recalled, nevertheless, that the plate actually has the form of a smooth curve, and that

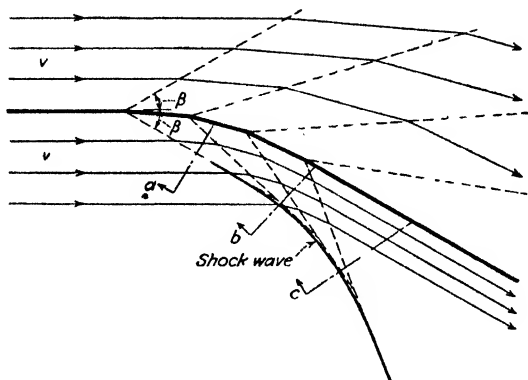


FIG. 203.—Wave pattern at a curved boundary.

the disturbance generated at the point of initial curvature is of infinitesimal amplitude. Only as the wave front attains finite proportions does it become truly of the shock type. Evidently, therefore, the proximity of the resulting shock wave to the boundary will increase with the degree of boundary curvature.

The obvious limit of such a trend is shown in the case of a plane boundary fixed at a finite angle to the oncoming flow. Under such circumstances (refer to Fig. 205) the resulting shock wave will be linear, the wave angle varying according to Eq. (247) with the velocity of the undisturbed flow and the celerity of the resulting wave—which is by no means that of an infinitesimal disturbance. As the angle of attack of the plate is increased, c will also grow in magnitude, and the wave angle will eventually approach 90° . Further change beyond this limit will cause the wave front to move away from the plate in the upstream direction, for the celerity of the wave will then have increased to such a magnitude that it exceeds the velocity of the oncoming flow.

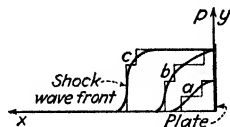


FIG. 204.—Sections normal to the wave front of Fig. 203.

81. Properties of Elastic Waves. The celerity of an elastic wave of very small amplitude may be determined directly through use of the fundamental equations of motion. Restricting the

discussion to the case of propagation in one direction, assume that an infinitesimal disturbance traveling through a fluid with the celerity c (to the left in Fig. 206a) produces a local

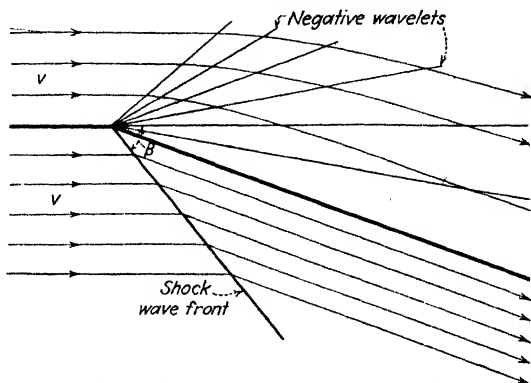


FIG. 205.—Wave pattern at a boundary angle.

change in pressure intensity dp . The picture may be reduced to a steady one by translating the coordinate system with the same velocity as that of the disturbance, resulting in an apparent flow from left to right as shown in Fig. 206b. The pressure differential dp then produces a slight velocity change $-dv$ as the fluid passes through the disturbance, in accordance with the differential equation for acceleration:

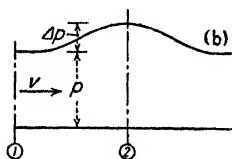
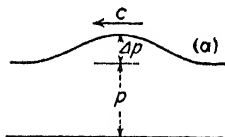


FIG. 206.—Elastic wave of small amplitude.

$$\rho v dv = -dp$$

In addition, conditions of continuity require that the rate of mass discharge be the same at all sections:

$$\rho v = \text{constant}$$

Writing the continuity equation in differential form,

$$\rho dv + v d\rho = 0$$

and combining with the above equation of acceleration,

$$v^2 = \frac{dp}{d\rho}$$

Recalling from Chapter I that $dp/d\rho = c/\rho$, the velocity of the steady flow may now be expressed in terms of the elastic modulus and the fluid density:

$$v = \pm \sqrt{\frac{e}{\rho}}$$

Since translating the coordinate axes with the disturbance to produce a pattern of steady motion is equivalent to superposing the velocity $-c$ upon every portion of the unsteady pattern, it is evident that v must equal $-c$, whereupon,

$$c = \mp \sqrt{\frac{e}{\rho}} \quad (248)$$

Owing to the method of derivation, the above expression for the celerity of an elastic wave applies only to disturbances of exceedingly small magnitude—whether positive or negative—such as those by which sound of normal intensity is transmitted through a fluid medium. The quantity $c = \sqrt{e/\rho}$ is, therefore, commonly known as the acoustic velocity. An elastic wave of finite magnitude, on the other hand, must be expected to have a velocity of propagation in excess of the acoustic velocity—the determination of which requires more detailed investigation.

In the case of liquids, it will suffice for the present to express the momentum relationship (refer to Sections 1 and 2 in Fig. 206b) in the form

$$p_2 - p_1 = \rho_1 v_1^2 - \rho_2 v_2^2$$

which, together with the equation of continuity,

$$\rho_1 v_1 = \rho_2 v_2$$

may then be written:

$$p_2 - p_1 = \rho_1 v_1^2 \left(\frac{\rho_2 - \rho_1}{\rho_2} \right)$$

Expressing the changes in density and pressure intensity as finite increments,

$$\Delta p = \rho v^2 \frac{\Delta \rho}{\rho + \Delta \rho}$$

and

$$v = \pm \sqrt{\frac{\Delta p}{\Delta \rho} \frac{\rho + \Delta \rho}{\rho}}$$

whence, neglecting quantities of the order $(\Delta \rho)^2$,

$$c \approx \sqrt{\frac{e}{\rho - \Delta \rho}}$$

According to this approximate relationship, c should increase with $\Delta \rho$. Nevertheless, if one recall that liquids are only slightly compressible, it will be apparent that under normal conditions the quantity $\Delta \rho$ will remain quite negligible in comparison with ρ , even for pressure differences of considerable magnitude. Not only is Eq. (248) thus applicable to practically all elastic waves in liquid media, but successive elements of any given wave will have sensibly the same celerity. Once such waves are generated, therefore, they will undergo no appreciable variation in form so long as other factors do not enter the problem.

Since gases, on the contrary, are readily compressible, it is quite possible that a finite density change $\Delta \rho$ may even exceed in magnitude the density of the undisturbed medium. Such variation in fluid characteristics must obviously involve thermodynamic principles, the most common assumption being that the density change caused by the disturbance takes place adiabatically—that is, without loss of heat. Eq. (248) will then have the form,

$$c = \sqrt{\frac{e}{\rho}} = \sqrt{k \frac{p}{\rho}}$$

Assuming, for the sake of argument, that Fig. 206*b* represents the pattern of steady motion for a finite disturbance, the momentum, continuity, and adiabatic relationships may be combined in the following manner:

$$\begin{aligned} p_2 - p_1 &= \rho_1 v_1^2 - \rho_2 v_2^2 \\ \rho_1 v_1 &= \rho_2 v_2 \\ \frac{p_1}{p_2} &= \left(\frac{\rho_1}{\rho_2} \right)^k \\ c = -v &= \sqrt{k \frac{p_1}{\rho_1}} \left\{ \frac{\frac{p_2}{p_1} - 1}{k \left[1 - \left(\frac{p_1}{p_2} \right)^{\frac{1}{k}} \right]} \right\}^{\frac{1}{2}} \end{aligned}$$

During the time dt the fluid $y_1 c dt$ (shown by single crosshatching) acquires the momentum per unit volume ρv of the disturbance, while the resultant force accomplishing this steady rate of change of momentum is produced by the difference in hydrostatic pressure over normal sections either side of the wave front. Equating resultant force and rate of momentum change,

$$\frac{\gamma}{2} (y_2^2 - y_1^2) = y_1 c \rho v$$

Introducing the continuity relationship and rearranging terms,

$$\frac{g}{2} (y_2 + y_1) (y_2 - y_1) = \frac{y_1}{y_2} (y_2 - y_1) c^2$$

from which it is apparent that

$$c = \sqrt{\frac{g y_2}{2 y_1} (y_2 + y_1)} = \sqrt{g y_1} \left[\frac{1}{2} \frac{y_2}{y_1} \left(\frac{y_2}{y_1} + 1 \right) \right]^{1/2} \quad (266)$$

This expression will be recognized as that for the celerity of a gravity shock wave, derived in a somewhat different manner in Chapter XIV. A disturbance of this type is aptly termed a

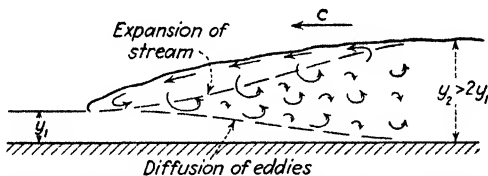


FIG. 220.—Source of eddies in a surge of the shock type.

surge, a basic type of gravity wave that is encountered in one guise or another in a wide variety of open-channel phenomena.¹

Mention has already been made of the fact that any true shock wave occasions a definite rate of energy loss. In the case of a gravity shock wave this loss apparently takes place at the wave front, which is generally a zone of violent eddy motion. To an observer looking down upon a passing surge, the front of the disturbance seems to be covered by a surface roller in a high state of agitation—a distorted vortex with horizontal axis, which to all outward appearances remains distinct from the fluid passing underneath. Nevertheless, careful observation through

¹ The word "bore," for instance, refers to a surge produced in large rivers or estuaries as the result of tidal action.

the glass wall of an experimental flume will establish beyond question the intimate relation of this roller to the flow beneath—for, as shown schematically in Fig. 220, small masses of rotating fluid are constantly being fed from the under side of the roller into the passing flow.

As is indicated in the illustration, the phenomenon closely parallels conditions in the wake of an immersed body, or at the abrupt enlargement of a closed conduit, for at the same time that the eddies spread downward across the flow section, the resultant mixing process accomplishes the necessary upward expansion of the mean flow. Just beyond this region of transition, therefore, the eddy motion will extend from top to bottom of the flow section. Needless to say, viscous dissipation of energy begins at once within the eddies, but the intense turbulent

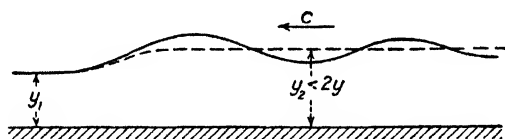


FIG. 221.—Profile of the undular surge.

agitation of the fluid is not reduced to a normal value for a considerable distance from the front of the surge. In other words, the apparent energy loss at the wave front itself does not represent immediate dissipation in the form of heat, and only the necessity of an independent expression for the kinetic energy of turbulence prevents analytical study of the surge by the simple energy principle.

In the light of the foregoing discussion of the solitary wave, the statement that surges generally involve loss of energy must be further questioned. So long as the depth of the disturbance is more than twice as great as the depth of the undisturbed flow, it is evident that the wave front must eventually become one of the shock type. For depth ratios appreciably less than 2, however, such is not necessarily the case. Consider, for instance, a surge originally having the form indicated by the broken line in Fig. 221. In accordance with Eq. (261), the curved wave front would tend to advance more rapidly than the level portion just behind it, thus leaving a depression in the surface, followed by the development of another crest and depression, and so on. Such undulations, nevertheless, will travel as rapidly as the

original horizontal disturbance only if the crests lie above and the troughs below the original level of the disturbed fluid. If the undular profile is to have a permanent form, needless to say a definite relationship (as yet uninvestigated) must obtain between wave length and amplitude, for a given relative depth of the disturbance.

Undular surges of this nature are found in practice so long as the ratio y_2/y_1 is considerably less than 2, the amplitude of the undulations gradually decreasing with distance from the wave front. As the limit 2 is approached, a small surface roller begins to form just below the crest of the first undulation; and as the roller grows in size, the amplitudes of the successive undulations are diminished, attaining negligible magnitude when $y_2 = 2y_1$. But since the medium of energy dissipation—generation of eddies within the roller—does not exist in the purely undular profile, a question immediately arises as to the significance of Eq. (253) under such conditions. Two facts must be considered in seeking the answer: The energy loss defined by this relationship is quite small when $y_2/y_1 < 2$; and although the relationship was derived on the assumption of parallel motion a short distance either side of the wave front, the train of undulations necessarily gives rise to a pressure distribution departing sufficiently from the hydrostatic to introduce into the computations an error of at least the same order of magnitude.

Inasmuch as the celerity c of any wave is measured with respect to the undisturbed fluid, the wave velocity v_w relative to a point fixed in space will vary with the mean velocity V_1 of the undisturbed flow:

$$v_w = V_1 \pm c \quad (267)$$

Obviously, this expression is additive when the wave travels in the direction of the primary motion, and vice versa. While any state of uniform motion necessarily involves a rate of energy loss depending upon the velocity, depth, and boundary conditions of the channel, evidently both depth and mean velocity will be changed by the passage of a surge, thus establishing a different rate of energy loss in the disturbed flow. And as the wave front travels farther and farther from the original zone of disturbance, it follows that y_2 —and hence c —must gradually change in magnitude. Yet the form of the surface profile behind a surge

may be found by other methods (*cf.* Chapter XIII), so that means are at hand of determining the magnitude of c , and hence of v_w , at any point along the channel. As indicated by Fig. 222, the magnitude of $1/v_w$ may be plotted against distance along the channel. And since $t = \int \frac{dx}{v_w}$, graphical integration of the area under the curve will permit solution for the location of the traveling surge at any instant of time.

It should be evident, moreover, that a surge can advance against a state of uniform (or non-uniform) motion only so long as the celerity c is greater than the velocity of the oncoming flow,

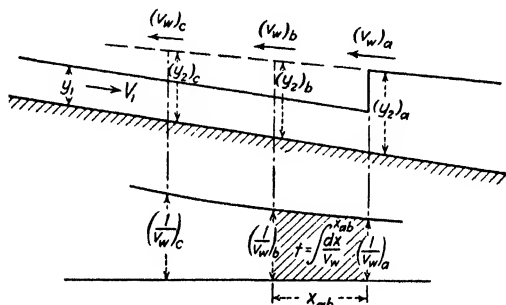


FIG. 222.—Determination of the progress of a surge with time.

and that once these two are equal in magnitude the surge will come to rest. Such a standing surge is merely a hydraulic jump, and methods have already been given whereby the location of the jump may be determined; by the method of Fig. 222 it is now possible to estimate the time required for the jump to approach a stable position. Needless to say, a surge may be formed regardless of whether the undisturbed flow is in the subcritical or the supercritical stage—but, as will be explained shortly, a standing surge is physically possible only if $y_1 < y_c$.

Certain inaccuracies in the foregoing treatment of the surge must still be noted. In developing Eq. (266) only pressure was considered to produce the essential change in fluid momentum. Boundary resistance was ignored, for that portion of the boundary included between the normal sections must be relatively short. And the longitudinal component of fluid weight was conveniently eliminated by considering a horizontal channel. Yet it is readily conceivable, notwithstanding the small slopes

ordinarily encountered in practice, that the slope may under some conditions be so pronounced that the weight of the fluid included between these sections will have a longitudinal component of considerable magnitude. Evidently, this will augment the wave celerity in the direction of downward slope, a surge thus traveling faster, with respect to the fluid, in one direction than in the other.

Despite the difficulty of analysis, one particular case in which such weight action is paramount has intrigued hydraulicians for more than half a century. Although supercritical flow has been treated in Chapter XIII by the usual methods of steady, gradually varied motion, it has been found in practice that such flow often takes place in a decidedly unsteady fashion, the water

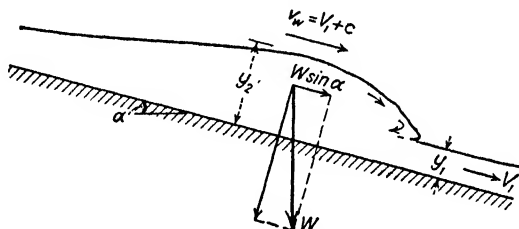


FIG. 223.—Profile of a roll wave.

proceeding down the channel in a procession of intermittent "slugs." So-called slug flow of this nature really consists of a series of wave fronts (sometimes referred to as roll waves) of the shock type, behind each of which the depth rapidly decreases to a minimum, as indicated in Fig. 223.

The reason for the original formation of these disturbances is still a moot question, although the problem is evidently one of instability of regime. Whatever irregularity in flow gives rise to the original superelevation of the surface, it is apparent that this wavelet will have a velocity v_w in the downstream direction in excess of the mean velocity V of the fluid, the celerity $c = v_w - V$ varying with the slope and the relative magnitude of the superelevation. A large wavelet will therefore travel more rapidly than a small one, with the result that the largest intermittent disturbances will gradually overtake and absorb those immediately ahead, and thereby increase repeatedly in amplitude and velocity of propagation. This process is readily observed in nature, often to such a degree that the channel bot-

tom is practically "dry" between successive surges. Although the minimum depth of flow resulting from this phenomenon is zero, the maximum depends largely upon the length of the channel—and unless the latter has been designed with ample freeboard, the crests of the surges will overflow the channel walls. It has been found that such intermittent motion will not occur if the channel bed is sufficiently irregular, which suggests a simple remedy to the problem; actual analysis of the phenomenon remains an inviting field for investigation.

86. The Hydraulic Jump as a Standing Surge. Certain important characteristics of the surge may best be studied in the pattern of steady two-dimensional motion on a horizontal bed obtained by superposing upon the flow a velocity equal and opposite to the velocity v_w of the surge. This pattern is evidently identical with that of the hydraulic jump, a case of steady motion that has attracted considerable attention among hydraulic engineers since the beginning of the last century. As the initial step in such a study, Eq. (266) may be written in the following pertinent form:¹

$$\frac{y_2}{y_1} = \frac{1}{2} \left(\sqrt{1 + 8 \frac{V_1^2}{gy_1}} - 1 \right)$$

Obviously, the depth of the standing surge is a function of a dimensionless ratio identical in form with the Froude number:

$$F^2 = \frac{V_1^2}{gy_1} = \frac{q^2}{gy_1^3} = \left(\frac{y_c}{y_1} \right)^3$$

whence

$$\frac{y_2}{y_1} = \frac{1}{2} (\sqrt{1 + 8F^2} - 1) \quad (268)$$

Needless to say, the same general conclusion would be reached through dimensional considerations, on the assumption that boundary resistance plays a negligible role. Although a similar Froude parameter could be written for Section 2, one need only note that the above choice is far more significant, in that it involves the depth of undisturbed flow and a velocity equal in magnitude to the celerity of the standing surge. That the functional relationship between y_2/y_1 and F which was derived analytically is in close accord with actual conditions may be

¹ BAKHMETEFF, "Hydraulics of Open Channels," p. 240.

seen from the proximity of plotted data obtained by Bakhmeteff and Matzke¹ to the analytical curve reproduced in Fig. 224. The slight discrepancies are attributable to the neglect of uneven velocity distribution (see page 54) and boundary drag. It will

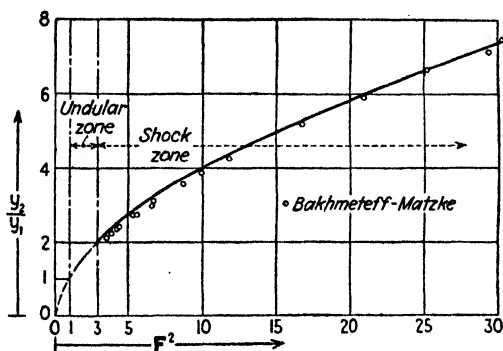


FIG. 224.—Depth ratio of the hydraulic jump as a function of the Froude number.

be noted from the plot that $F^2 = 3$ when $y_2/y_1 = 2$, conditions marking the boundary between jumps of the undular and shock types.

In like fashion it is possible to express other characteristics of the standing surge (height of jump, loss of head, and so on)

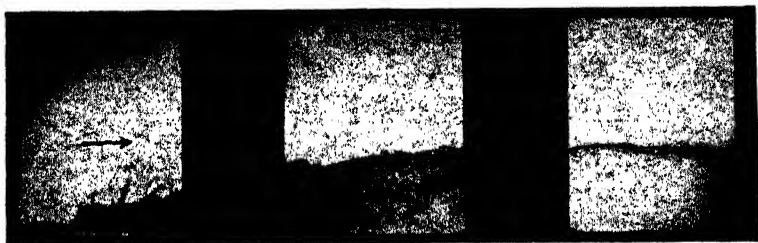


FIG. 225.—Profile of the hydraulic jump.

in their ratio to the undisturbed depth of flow y_1 , again as functions of the Froude parameter. This would indicate, in brief, the effect of variation in the numerator of $F = V_1/\sqrt{gy_1}$, the denominator thereby remaining constant. On the other hand, Bakhmeteff has shown that far more light is thrown upon the

¹ BAKHMETEFF, B. A., and MATZKE, A. E., The Hydraulic Jump in Terms of Dynamic Similarity, *Trans. A.S.C.E.*, vol. 101, 1936.

phenomenon by noting the variation in velocity and potential heads with F while the total head at Section 1 remains unchanged. In other words, the linear characteristics of the profile would then be referred to H_1 instead of to y_1 . Thus,

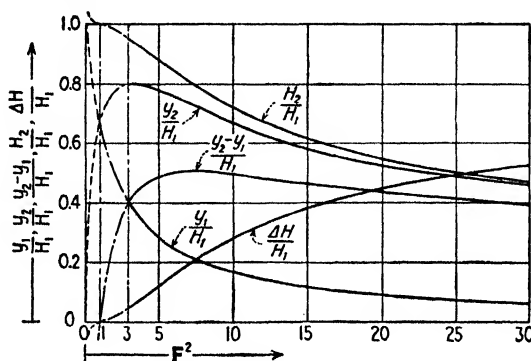


FIG. 226.—Vertical elements of the hydraulic jump.

in Fig. 226 are reproduced in dimensionless form the following analytic functions, which may easily be verified by the reader:

$$\frac{y_1}{H_1} = \frac{2}{2 + F^2} \quad (269)$$

$$\frac{y_2}{H_1} = \frac{1}{2 + F^2} (\sqrt{1 + 8F^2} - 1) \quad (270)$$

$$\frac{H_2}{H_1} = \frac{(\sqrt{1 + 8F^2} - 1)^3 + 4F^2}{(\sqrt{1 + 8F^2} - 1)^2 (2 + F^2)} \quad (271)$$

$$\frac{\Delta H}{H_1} = 1 - \frac{H_2}{H_1} \quad (272)$$

Three essential facts are to be noted from the accompanying illustration: (a) That portion of any curve lying to the left of the abscissa $F = 1$ is without physical significance; as may be seen from Fig. 224, a Froude number less than unity would correspond to a negative surge, whereas from the plot of $\Delta H/H_1$ it is evident that a negative surge would require a gain in energy as the fluid passes the wave front—a physical impossibility. (b) For a given total head of the approaching flow, the maximum value of y_1 occurs when $y_1 = y_2 = y_c$, whereas y_2 attains its maximum value at the upper limit of the undular regime. (c)

There is a maximum height of jump relative to the original energy-line elevation, occurring at $F^2 = 7.67$.

Aside from thus bringing attention to a proper dimensionless treatment of the vertical characteristics of the jump, the Bakhme-

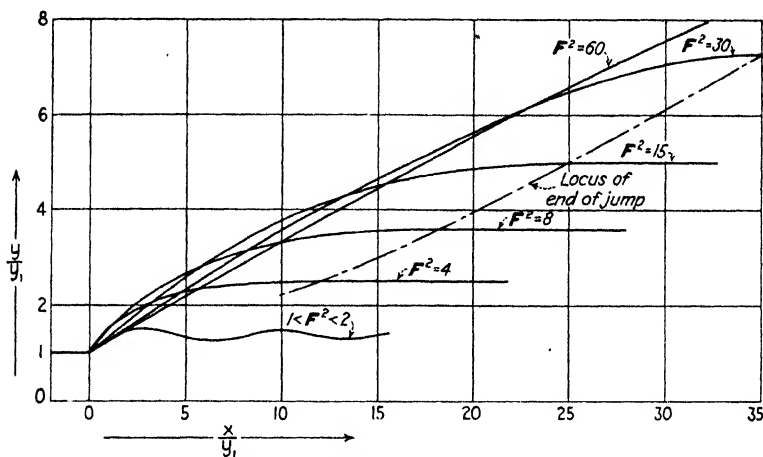


FIG. 227. Dimensionless profiles of the hydraulic jump.

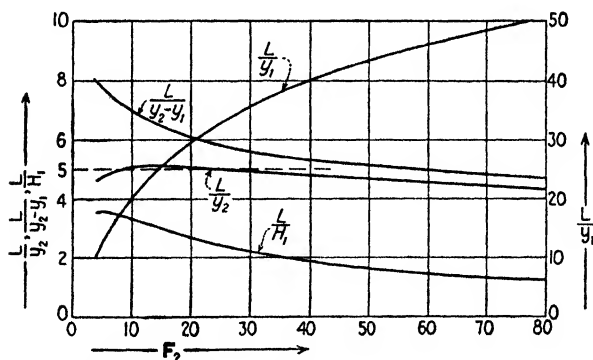


FIG. 228.—Relative length of the hydraulic jump.

teff-Matzke investigations gave particular heed to the longitudinal dimensions of the flow profile. Generalized results of their measurements may be seen from Fig. 227, in which all linear dimensions are based upon the depth of the undisturbed flow (note that the horizontal scale is reduced $2\frac{1}{2}$ times). The gradual change from the undular profile to a mean surface

slope that is practically linear is readily followed through the sequence of curves. Logically defining the limit of the jump as that section at which the flow again becomes essentially parallel, Bakhmeteff and Matzke determined the functional relationships between the relative length of jump and the Froude number reproduced in Fig. 228. The ratio of length L to y_2 is seen to remain nearly constant, with a mean value somewhat less than 5. As the limit $F^2 = 3$ ($y_2 = 2y_1$) is approached, however, the relative length of the transition becomes inde-

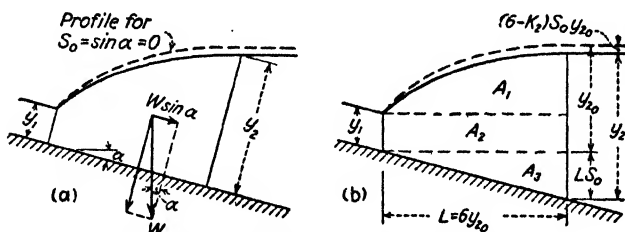


FIG. 229.—The hydraulic jump in a sloping channel.

terminate, for the development of undulations makes the region of parallel flow increasingly remote from the wave front.

In a more recent paper,¹ Bakhmeteff and Matzke extended their investigation of the jump to channels of appreciable slope. As may be seen from Fig. 229a (and as will be recalled from the discussion of the surge), the forces producing the change in momentum will then include the longitudinal component of the fluid weight between sections 1 and 2:

$$\rho V_1 y_1 (V_1 - V_2) = \gamma \frac{y_2^2 - y_1^2}{2} - W S_0 \quad (273)$$

Evaluation of the quantity $W = \gamma A_{1-2}$ evidently requires prior knowledge of the jump profile, which one might reasonably expect to vary with both the slope and the Froude number. However, measurements by Matzke of the actual profiles for slopes up to 0.07 substantiated earlier observations by Bakhmeteff that within this range the surface curve varies little from that of the jump in a horizontal channel. In no case was the length of the jump more than 20 per cent greater, while the

¹ BAKHMETEFF, B. A., and MATZKE, A. E., The Hydraulic Jump in Sloped Channels, *Trans. A.S.M.E., Hydraulics Division*, p. 111, February, 1938.

drop in tailwater elevation was always small in comparison with the drop in the channel floor, as indicated in Fig. 229a.

In view of the relatively small magnitude of the term $W S_0$, it was considered satisfactory, therefore, to use instead of the actual profiles those determined for the jump in a horizontal channel at corresponding Froude numbers. Since for slopes less than 0.1 it makes little difference whether y is measured in the vertical or normal to the channel bottom, the area of the profile was subdivided as shown in Fig. 229b, sections 1 and 2 being

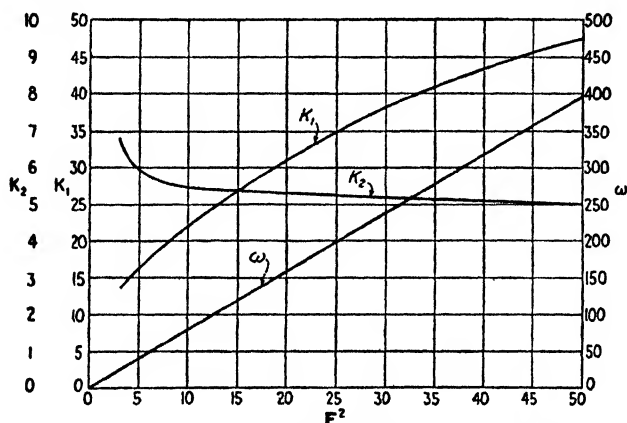


FIG. 230.—Characteristic parameters for hydraulic jumps in sloping channels.

vertical and a constant distance $6y_{2_0}$ apart. The elementary triangle and rectangle are simple functions of depth and slope, whereas from measured diagrams similar to those of Fig. 227 the portion A_1 was determined in the form $A_1 = \omega y_1^2$; the coefficient ω is a function of the Froude number alone and, as seen from Fig. 230, was found by Bakhmeteff and Matzke to vary linearly with F^2 .

Although a solution of Eq. (273) is possible once this function is introduced, its usefulness is limited by the fact that it is cubic in form. Nevertheless, a plot of y_2/y_1 as a function of S_0 and F , determined from this equation and checked experimentally, showed that this ratio varies linearly with S_0 for any value of F . In other words,

$$\frac{y_2}{y_1} = \frac{y_{2_0}}{y_1} + K_1 S_0 \quad (274)$$

the magnitude of K_1 depending only upon F , as shown in Fig. 230. This relationship was even further simplified to the form

$$\frac{y_2}{y_{2_0}} = 1 + K_2 S_0 \quad (275)$$

in which K_2 is again a function of F (see Fig. 230)—varying only slightly, in fact, from the value 5.

Although this semi-empirical expression will yield satisfactory results for slopes as great as $S_0 = 0.1$, Bakhmeteff and Matzke pointed out that the rate of divergence of the flow within a jump will not greatly exceed 20 per cent. If the channel slope is excessive, therefore, the presence of a surface roller will not necessarily indicate that the flow beneath is immediately decelerated. Indeed, under such conditions the high-velocity stream will simply plunge into the tailwater and continue in the rapid state a considerable distance beyond the toe of the roller—this phenomenon of submergence bearing little resemblance to the true hydraulic jump.

87. Wave Effects at Boundary Changes in the Vertical Plane. So far as the hydraulic engineer is concerned, the problem of wave propagation in confined flow is limited almost entirely to water hammer and allied phenomena. In other words, the celerity of an elastic wave is so much greater than normal velocities of flow that the rate at which disturbances travel through an enclosed fluid may be considered practically infinite. Flow with a free surface, on the contrary, has been found to offer no such convenient simplification. As a matter of fact, although non-uniform motion in open channels was treated in detail in Chapter XIII without direct reference to wave effects, the reader will long since have realized that the consistent use of the critical depth y_c as a flow parameter is in reality a tacit recognition of the dependence of that analysis upon wave criteria. From Eq. (212) it follows that when $y = y_c$, $V = V_c = \sqrt{gA/b}$; and since A/b is the mean depth of flow, V_c is equal in magnitude to the celerity c of the basic Lagrangian wave. It is evident, therefore, that the sole distinction between tranquil and rapid flow lies in the relation of the velocity to the celerity of an infinitesimal wave for the same mean depth of flow; the Froude parameter $F = V/\sqrt{gy_m}$ is less than unity in the former case, greater than unity in the latter.

From these considerations it will be seen that surface profiles in gradually varied flow are controlled at their downstream ends when $F < 1$, and at their upstream ends when $F > 1$, for the reason that disturbances can travel upstream so long as $c > V$, but only downstream when $V > c$. As a matter of fact, any surface profile may be considered that of a standing wave, although boundary resistance can no longer be ignored in determining its stable form; indeed, the latter influence is now of paramount importance. Such a conception will immediately become clear, for instance, if one visualize the formation of a non-uniform profile by the partial closure of a sluice gate in an originally uniform state of flow. A surge will form at once above the sluice and begin to travel upstream at a rate approximately in accordance with Eqs. (266) and (267). Boundary resistance necessarily leads to a gradual change in wave profile, the latter including not only the front of the wave but the entire portion of the flow involved in the disturbance. The height of the wave front must then diminish with distance from the source of disturbance, either approaching zero in the case of a disturbance of the M_1 class or remaining of the shock type for the wave profile S_1 . In a similar manner the negative disturbance traveling downstream from the sluice gate will have as its ultimate form a curve of the M_3 , S_2 , or S_3 type. A negative disturbance traveling upstream, on the other hand, will result in the M_2 profile.

It will be recalled by the reader that surface curves are classified generally according to whether S_0 is greater or less than zero, and whether y_0 is greater or less than y_c . Evidently, the relative magnitude of S_0 determines the direction of action of the longitudinal weight component of the wave. Moreover, if $y_0 > y_c$, $F = V/\sqrt{gy_m} < 1$; whereas when $y_0 < y_c$, $F > 1$. In a word, each surface profile of gradually varied motion represents the stable result of a positive or negative disturbance, the form of the standing wave depending upon the magnitude and nature of the disturbance and the magnitude of the Froude number for the undisturbed flow.

Similar considerations must apply to the case of rapidly varied flow, the sole distinction lying in the fact that resistance effects within the disturbance now give way to the inertial effects of curvilinear motion. The example used previously will suffice

to illustrate this conception. A change in vertical flow section, such as that caused by the sloping plate shown in Fig. 160, must necessarily disturb the otherwise uniform motion. For high values of the Froude number this disturbance will advance only sufficiently far upstream to establish equilibrium between the acting forces and the mass acceleration of the curvilinear motion; that is to say, although the surface curve is infinite in length, mathematically speaking (refer to the discussion of the solitary wave), the major portion of the disturbance is limited to the immediate vicinity of the boundary change. The celerity of every element of the wave is then exactly equal to the velocity of the oncoming flow. As the Froude number grows smaller, the reversal in curvature of the free surface will become more pronounced, until a limiting value of F is reached at which the celerity of the wave elements is greater than the mean velocity of the uniform motion. A surge will then form, and advance in the upstream direction until, as before, a state of equilibrium is reached in the region of gradually varied flow. Conditions at the vertical boundary change are thereby modified completely, the functional relationship between F and profile form then becoming discontinuous if based upon the constant depth of approach assumed in the illustration. It is to be noted that such discontinuity will not result if the ratio l/m exceeds a certain magnitude—the determination of which still invites experimental investigation. Under any circumstances, a study of profile form, and of the accompanying pressure and velocity distribution, must proceed as has been indicated in the foregoing pages, the gravity-wave parameter F playing thereby a very essential role.

88. Wave Effects at Boundary Changes in the Horizontal Plane. Variation in the longitudinal boundary profile of an open channel has a direct counterpart in horizontal variation of the channel walls—with the added feature that the resulting disturbance not only will be three-dimensional but also may be dissimilar along opposite walls. Equal convergence or divergence of the sides, for instance, or the presence of evenly spaced bridge piers, will produce a state of rapidly varied motion which, although definitely three-dimensional, is still symmetrical about a vertical plane through the channel axis. A change in direction of the channel axis, on the other hand, must necessarily result in

completely unsymmetrical surface contours. Even if the flow pattern is sensibly symmetrical in plan, since the problem is three-dimensional it can be treated at present in the light of two-dimensional motion only if the characteristic Froude parameter is well below unity. Similarly, channel curvature in the horizontal plane may be regarded as approximately symmetrical about a vertical axis of rotation only so long as the celerity of propagation of the wall disturbance is in excess of the mean velocity of flow.

A more rigorous treatment of three-dimensional motion at low values of F is so difficult that such cases have been ignored almost completely in the foregoing portion of this text. On the other hand, wall disturbances in flow at a velocity above the critical are far more susceptible to close analysis, owing to the nature of the resulting wave pattern. It is in this connection that the analogous characteristics of elastic and gravity waves are of particular importance, for methods originally used in the study of elastic effects are now proving of value in open-channel hydraulics.

If one assume that the curved boundary shown in Fig. 203 forms a portion of a vertical channel wall, it is reasonable to expect that when the Froude number of the undisturbed flow is greater than unity, the wall disturbance will take the form of a series of wavelets diverging from the boundary at the Mach angle β . As indicated in Fig. 231, the direction of a stream line will change only as it passes through the front of a wavelet, the character of the change being determined by the equations of continuity and momentum and by the geometry of the vector field. In other words, the reduction in fluid momentum on passing the wave front must be accompanied by an increase in depth, and vice versa. If forces other than pressure are ignored, this change in depth will be the same at all cross sections of a wavelet. It then follows that only the normal component of the velocity vector is involved in the momentum relationship, the tangential component thereby remaining unchanged (see Fig. 232).

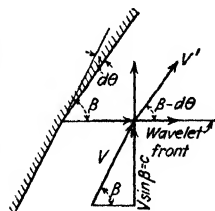


FIG. 231.—Change in momentum normal to wavelet resulting from boundary curvature.

Ippen and Knapp¹ were the first to analyze the problem of high-velocity flow at bends in this manner, in the effort to provide satisfactory principles for the design of bends in the flood relief channels of Los Angeles County. Assuming (a) hydrostatic distribution of pressure, (b) negligible effects of the longitudinal component of weight, and (c) constant specific energy of flow, they were able to integrate the resulting differential expression for depth as a function of the energy of flow and the angle of curvature of the boundary. The resulting equation, though somewhat involved, provided for the first time a means of determining the approximate superelevation of the water surface at the outside of the bend, as well as the drop in level along the inside wall.

As these writers pointed out, none of the foregoing assumptions is strictly fulfilled: the pressure distribution is sensibly hydrostatic only if the curvature is very gradual; the weight component on a slope of appreciable magnitude tends to modify the wave celerity; and the rate of energy loss decreases with increasing depth. A means was sought, therefore, of deriving a simpler expression yielding results in even closer accord with experimental measurements. It was found that the arbitrary assumption of a velocity vector of constant magnitude was actually in close agreement with measured results, and served in part to compensate for the slight discrepancies in the second and third assumptions. The corresponding vector diagram would then be that of Fig. 233, the momentum relationship still being applied only to the normal component of velocity. Integration of the resulting differential expression yielded the equation

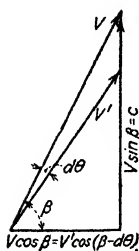


FIG. 232.—
Vector diagram
for Fig. 231.

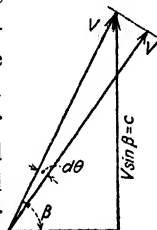


FIG. 233.—
Vector diagram
for constant V .

¹ IPPEN, A. T., and KNAPP, R. T., "A Study of High Velocity Flow in Curved Sections of Open Channels," Report prepared at the California Institute of Technology for the Los Angeles County Flood Control District, March 29, 1936. KÁRMÁN, TH. VON, Eine praktische Anwendung der Analogie zwischen Überschallströmung in Gasen und überkritischer Strömung in offenen Gerinnen. *Zeit. angew. Math. Mech.*, vol. 18, no. 1, p. 49, 1938.

$$\frac{y}{y_1} = \frac{V_1^2}{gy_1} \sin^2 \left(\beta_1 + \frac{\theta}{2} \right) = F^2 \sin^2 \left(\beta_1 + \frac{\theta}{2} \right) \quad (276)$$

in which the Mach angle β_1 of the wave front at the beginning of the curve is the following simple function of the Froude number for the undisturbed flow:

$$\beta_1 = \sin^{-1} \frac{\sqrt{gy_1}}{V_1} = \sin^{-1} \frac{1}{F}$$

These writers showed in addition that the negative wave proceeding across the channel from the inside of a bend would so counteract the tendency toward superelevation along the outer wall that no further rise would be encountered beyond the point of first reflection of the negative wave (except under unfavorable conditions of reflection and interference at sections farther downstream). The simple geometrical method by which Ippen and Knapp determined the location of this first section of maximum elevation is indicated in Fig. 234.

Since the series of negative wavelets produced at the convex side of a bend steadily diverge from one another, the front of the first wavelet remains free from interference on the part of its immediate neighbors (see Fig. 203). On the other hand, the series of positive wavelets generated at the concave side gradually converge; hence, unless the wave pattern at the outside of a channel bend is modified by interference from a negative wave generated at an adjacent inner wall, continued growth in wave amplitude must lead eventually to the formation of a wave front that is not only curved but of the shock type. Although the effect of shock-wave development is not felt immediately at the wall, it is evident that the extent of such influence is a relative matter, varying with the Froude number of the approaching flow and the rate of boundary curvature. From the standpoint of pressure action alone, therefore, the ultimate depth ratio at the end of a concave wall will be the same whether the wall

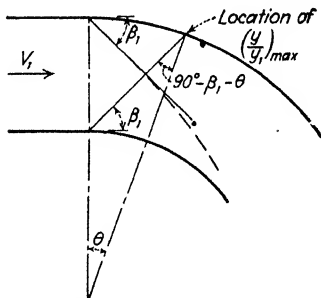


FIG. 234.—Point of first maximum surface elevation at outside of channel bend.

curves gradually or abruptly. Just as in the case of an elastic disturbance, the limiting case of a zero radius of curvature is thus of special interest.

As shown by the author and Dr. Merit P. White, in an unpublished study conducted early in 1937 for the Soil Conservation Service, the problem may be analyzed in the following manner: The vector relationship of the velocity pattern will be similar to that originally studied by Ippen and Knapp, the sole distinction being that the abrupt changes in velocity, depth, and energy will be of finite magnitude. Application of the momentum and continuity relationships between vertical sections parallel to and on either side of the wave front (see Figs. 235 and 236) will yield the following expression, indicating that the

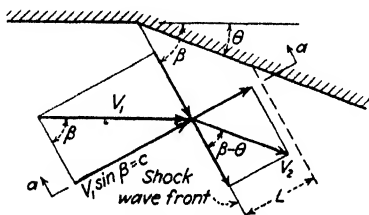


FIG. 235.—Vector relationship at the front of a shock wave resulting from an angle in a vertical boundary.

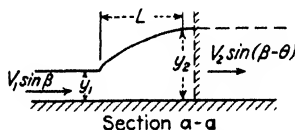


FIG. 236.—Normal section through wave front of Fig. 235.

depths and the normal components of velocity correspond exactly to the velocity-depth characteristics of the standing surge:

$$V_1 \sin \beta = c = \sqrt{\frac{g}{2} \frac{y_2}{y_1} (y_2 + y_1)}$$

The vector diagram, moreover, indicates that

$$V_1 \cos \beta = V_2 \cos (\beta - \theta)$$

while the equation of continuity provides the following relationship of depth, velocity, and angularity:

$$y_1 V_1 \sin \beta = y_2 V_2 \sin (\beta - \theta)$$

Solution of these three simultaneous equations results in the expression

$$\frac{y_2}{y_1} = \frac{1}{2} (\sqrt{1 + 8F^2 \sin^2 \beta} - 1) \quad (277)$$

which is strikingly similar to that for the standing surge, differing only with the Mach angle for the wave front; the latter, in turn, may be expressed in terms of the depth ratio and the boundary angle:

$$\tan \beta = \frac{c}{\sqrt{V_1^2 - c^2}} = \frac{\frac{y_2}{y_1} - 1 \pm \sqrt{\left(\frac{y_2}{y_1} - 1\right)^2 - 4 \frac{y_2}{y_1} \tan^2 \theta}}{2 \tan \theta} \quad (278)$$

Equations (277) and (278) are presented in plotted form in Fig. 237, showing in full lines the depth ratio y_2/y_1 as a function of the Froude number for a series of boundary angles, θ , and for the same Mach angles of the wave front, β , as broken lines.

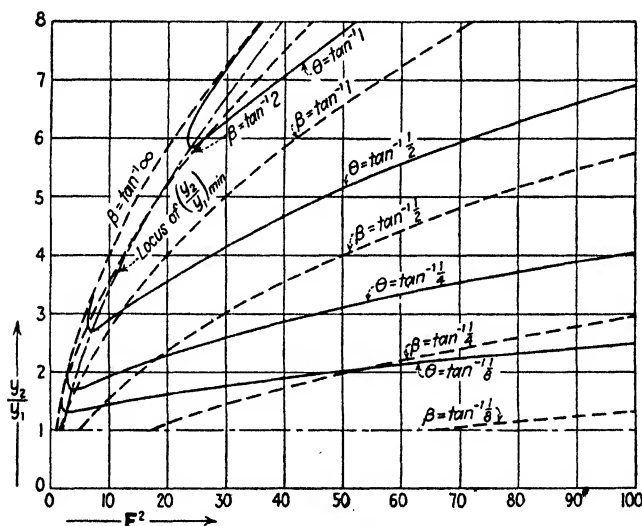


FIG. 237.—Relative depth as a function of the Froude number, for various angles of the boundary and of the wave front.

From this diagram it would seem that the assumed conditions are impossible below certain limiting values of F , since all curves are terminated at the broken line near the left of the plot for $\tan \beta = \infty$. This merely signifies that if the boundary angle is too great for a given Froude number, the disturbance will have a celerity greater than the velocity of the oncoming flow, the Mach angle will tend to exceed 90° , and the wave will advance

upstream from the deflecting boundary. Such conditions are shown schematically in Fig. 238.

Preliminary experimental study of this phenomenon indicates that the foregoing analysis is physically sound so far as the assumed conditions are actually fulfilled. The wave front a short distance from the boundary change displays all the characteristics of the standing surge (with an additional component of velocity parallel to the wave front), even to the extent of a surface roller at high values of y_2/y_1 and a hint of undulation when y_2/y_1 becomes less than 2. However, near the abrupt change in boundary angle,

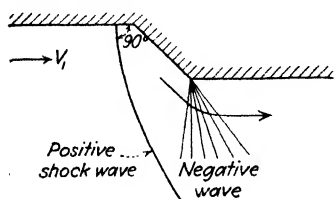


FIG. 238.—Displacement of wave front caused by large boundary angle.

since the profile shown in Fig. 236 has not yet fully developed, the necessarily rapid vertical acceleration produces a local increase in y_2/y_1 beyond that of the fully developed wave a short distance downstream. The effect shown in Fig. 238 may be produced with ease; needless to say, negative waves of the shock type are physically impossible, the surface falling away more or less abruptly, as indicated in the illustration, but without trace of induced turbulence.

APPENDIX

PHYSICAL PROPERTIES OF COMMON FLUIDS

As noted in the opening chapter of this volume, it is customary to relate the units of length, time, mass, and force according to the basic equation of mass acceleration. In any dimensional system, therefore, a unit force must accelerate a unit mass one unit length per unit time in one unit time. Any three of these units may then be arbitrarily established. Once established, however, corresponding units in all systems will bear a definite numerical relationship to one another, since they must describe the same characteristics of matter and motion.

In the metric system the primary standard of length is the International Prototype Meter, preserved in metal but reproducible in terms of the wave length of an arbitrary portion of the spectrum; the centimeter is $\frac{1}{100}$ of the standard meter. The primary standard of time is based upon the mean solar day, of which the second is $1/86,400$. The primary standard of mass is also preserved in metal, as the International Prototype Kilogram; the gram is $\frac{1}{1000}$ of the standard kilogram, and is almost exactly equal to the mass of a cubic centimeter of water under normal atmospheric pressure at 4°C . The unit of force, the dyne, is then defined as that force which will accelerate one gram one centimeter per second in one second.

Of the units adopted in America, only the second is the same as that in the metric system. The foot, slug, and pound are related as follows to the respective metric units:

$$1 \text{ foot} = 30.480 \text{ centimeters}$$

$$1 \text{ slug} = 14,594 \text{ grams}$$

$$1 \text{ pound} = 444,822 \text{ dynes}$$

$$1 \text{ centimeter} = 0.032808 \text{ foot}$$

$$1 \text{ gram} = 68,522 \times 10^{-9} \text{ slug}$$

$$1 \text{ dyne} = 22,481 \times 10^{-10} \text{ pound}$$

Too great emphasis cannot be placed upon the fact that the foregoing relationships are totally independent of terrestrial

gravitation. The latter factor becomes important in defining dimensions only when relating quantities that are used simultaneously as units of force and mass. Thus, the gram as a force unit is arbitrarily taken as that force which will accelerate one gram mass 980.665 centimeters per second per second; similarly, the pound mass will be accelerated 32.174 feet per second per second by one pound force. The gram force is then equivalent to 980.665 dynes, the slug is 32.174 pounds mass, and the pound force is 32.174 poundals. This "standard" magnitude of g corresponds roughly to that at sea level and 45° latitude, gravitational acceleration varying with latitude and elevation owing to the form and rotation of the earth:

$$g = 32.1721 - 0.08211 \cos 2\alpha - 0.000003h$$

The reader must be cautioned that the measurement of both force and mass by the familiar process of "weighing" may lead to slight inaccuracies, as a direct result of such variation in g .

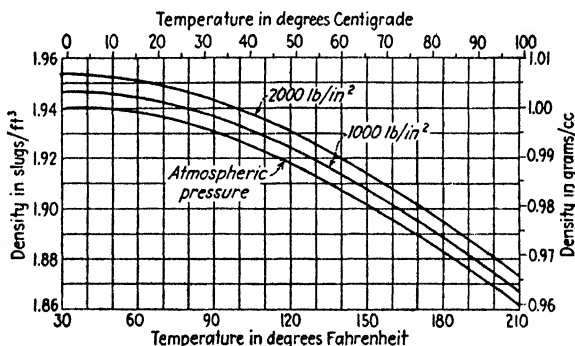


FIG. 239. Density ρ of pure water as a function of temperature and pressure intensity.

Balances of the spring type and of the beam type are used interchangeably, although, strictly speaking, the former measures relative force and the latter relative mass. If the balances are calibrated for standard gravitational conditions ($g_s = 32.174$ ft./sec.²), the spring balance will indicate an apparent variation in mass, and the beam balance an apparent variation in force, for other values of g , unless the proper corrections are made. Due care is therefore essential in precise determinations of flow characteristics and fluid properties.

The density ρ of any fluid is necessarily independent of g , but will change with temperature and pressure. In the case of liquids, which are relatively incompressible, ρ will depend primarily upon temperature, as shown for pure water in Fig. 239. The specific weight of a fluid, ordinarily presented in similar

TABLE V.—VALUES OF ρ AND γ FOR COMMON LIQUIDS

Liquid	Temperature °F.	Density ρ slugs/ft. ³	Specific weight γ lb./ft. ³
Alcohol.....	32	1.55	50.0
Gasoline.....	...	1.37	44
Glycerine.....	32	2.44	78.6
Kerosene.....	...	1.59	51
Mercury.....	32	26.38	848.7
	60	26.31	846.3
	100	26.20	843.0
Oil:			
Crude.....	...	1.71	55
Fuel.....	...	1.83	59
Lubricating.....	...	1.80	58
Water:			
Fresh.....	60	1.94	62.4
Sea.....	60	1.99	64.0

form, will depend as well upon the magnitude of g , since $\gamma = g\rho$. Needless to say, the density of a liquid—and, therefore, its specific weight—will also vary with the nature and concentration of dissolved salts; in such cases density determinations must be made through use of a calibrated hydrometer. On the other hand, extensive data for liquids of known chemical composition may be obtained from such standard references as the International Critical Tables and the Smithsonian Physical Tables. Typical values of ρ and γ for common liquids are given in Table V, the data for γ referring to the standard magnitude of g ; values for which no temperature is shown must be regarded as rough averages.

For all practical purposes, the change in density and specific weight of a gas with either temperature or pressure may be found from the ideal relationships

$$\frac{p}{\rho} = g, RT \quad \text{and} \quad \frac{p}{\gamma} = RT$$

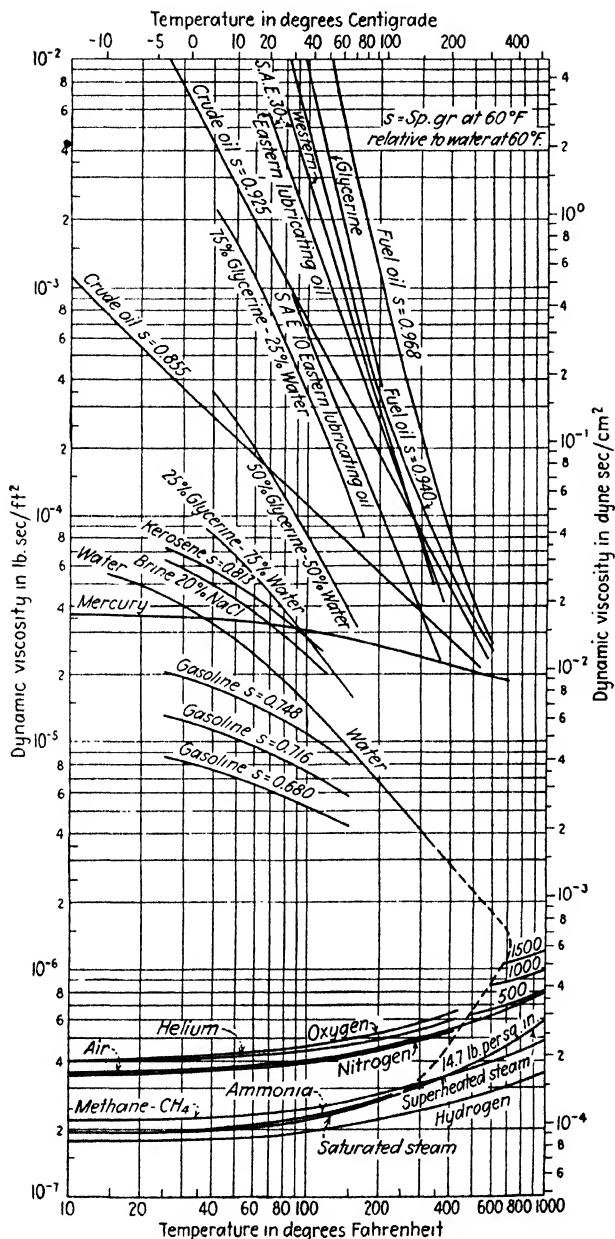
this value of γ referring specifically to g_s . The factor T represents absolute temperature—459.4 Fahrenheit degrees and 273 centigrade degrees below zero on the respective scales; likewise, p denotes absolute pressure intensity. R will be seen to have the dimension length/temperature, and will therefore depend in magnitude upon the dimensional system and the nature of the gas. Typical values of R based upon feet and degrees Fahrenheit will be found in Table VI. The accompanying values of ρ and γ are for a temperature of 32°F. and a pressure of 14.7 pounds per square inch.

TABLE VI.—VALUES OF R , ρ , γ , AND k FOR COMMON GASES

Gas	R	Density	Specific weight	k
	ft./°F.	ρ slugs/ft. ³	γ lb./ft. ³	
Acetylene.....	59.34	0.00237	0.0763	1.28
Air.....	53.34	0.00251	0.0807	1.40
Ammonia.....	90.50	0.00150	0.0481	1.31
Helium.....	386.0	0.000346	0.01114	1.66
Hydrogen.....	765.9	0.000174	0.00561	1.40
Methane.....	96.31	0.00139	0.0448	1.32
Oxygen.....	48.25	0.00277	0.0892	1.40
Nitrogen.....	54.99	0.00243	0.0781	1.40

Figures 240 and 241 show the variation of dynamic viscosity μ and kinematic viscosity ν with temperature for a number of common liquids and gases, after data presented in similar form by Daugherty.¹ As was mentioned in the opening chapter, the dynamic viscosity is generally independent of pressure intensity over a considerable range. On the other hand, the kinematic viscosity will vary with pressure in so far as the latter affects the density; the plots of ν correspond to normal atmospheric pressure. It is to be noted that a special unit is often used for dynamic viscosity in the metric system—the poise—corresponding to one dyne-second per square centimeter; similarly, the stoke is sometimes taken as the unit of kinematic viscosity, equal to one square centimeter per second; water, therefore, has dynamic and kinematic viscosities of approximately one centipoise and one centistoke, respectively.

¹ DAUGHERTY, "Hydraulics," pp. 7, 209.



A number of simple devices have been developed for the measurement of the kinematic viscosity of liquids, which yield results

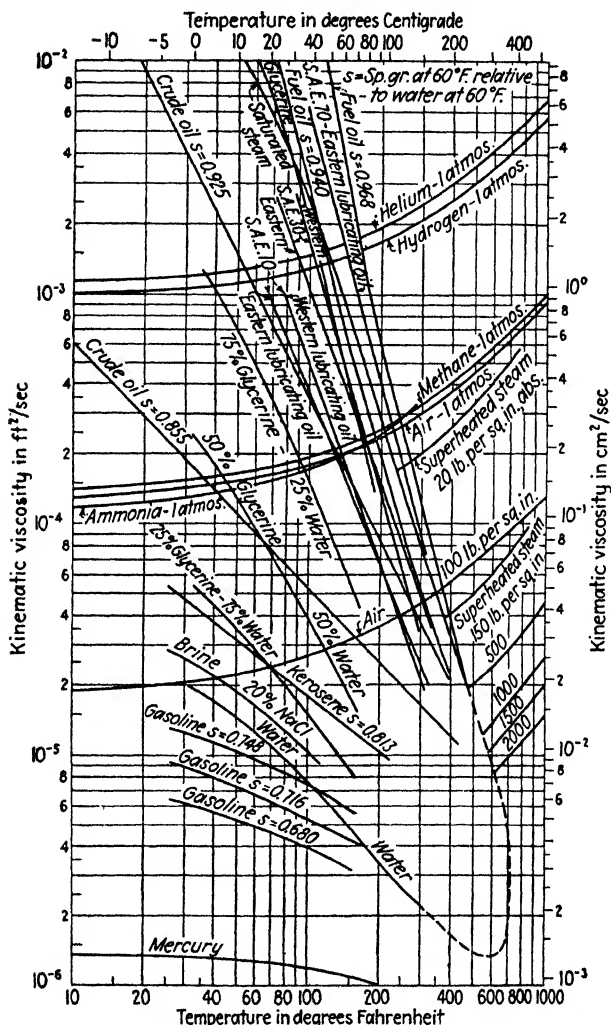


FIG. 241.—Kinematic viscosity ν of common fluids as a function of temperature.

of sufficient accuracy for general purposes. A viscometer of this nature generally consists of a container with a short capillary outlet in the bottom, through which the flow of a prescribed

quantity of fluid is timed. Owing to the relative shortness of the capillary tube, conversion of the measurements into basic viscosity units by analytical means is a difficult matter, and it has been found convenient to use the time of efflux as an indirect measure of ν . Such units, however, are peculiar to the type of viscometer used—and hence to the country in which that particular meter has been adopted; thus, America uses Saybolt seconds;

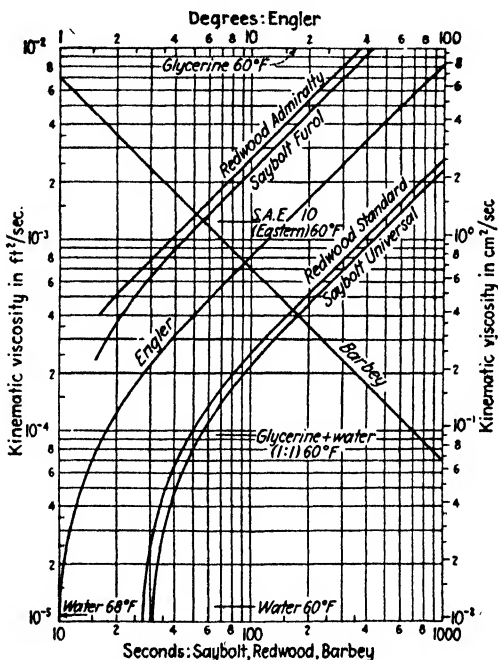


FIG. 242.—Viscometer characteristics.

England, Redwood seconds; France, Barbey seconds; and Germany, Engler degrees (the ratio of time of efflux to that required by water at 68°F.). The several units may be correlated empirically, with the results shown in Fig. 242. It is evident from the diagram that the Saybolt Furol and the Redwood Admiralty viscometers are designed for liquids of high viscosity.

Since molecular attraction is a secondary characteristic in fluid mechanics, a single plot of the surface tension of the water-air interface (Fig. 243) will suffice to indicate the variation in σ

with temperature. The surface tension of mercury in air is about 0.0352 and in water about 0.0269 pound per foot. The capillary rise (or depression) of a liquid in a tube of very small radius may be computed from the equation

$$h = \frac{2\sigma}{\gamma r} \cos \theta$$

in which θ represents the angle of contact between the liquid

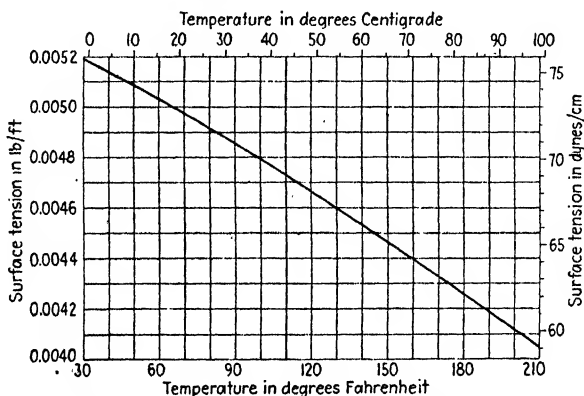


FIG. 243.—Surface tension σ of pure water in air.

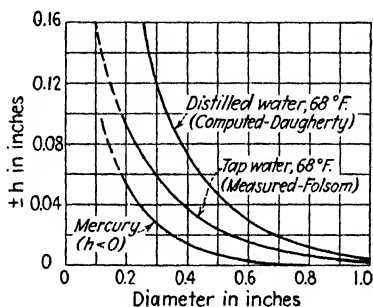


FIG. 244.—Capillary rise in glass tubes as a function of tube diameter.

surface and the boundary wall; this angle is practically zero between water and glass, if the surface is very clean. For larger diameters the analysis becomes more complex, the comparison between computed and measured values being shown, after Daugherty, in Fig. 244.

The elastic modulus of water is indicated as a function of temperature and pressure in Fig. 245; the plotted curves must be

regarded as approximate, particularly in the higher ranges. In comparison with a typical value for water of 300,000, glycerine has a modulus of about 630,000, mercury about 3,800,000, whereas that for oil will range in the mean from 180,000 to 270,000 pounds per square inch. So far as gases are concerned, it has already been shown that the elastic modulus under isothermal

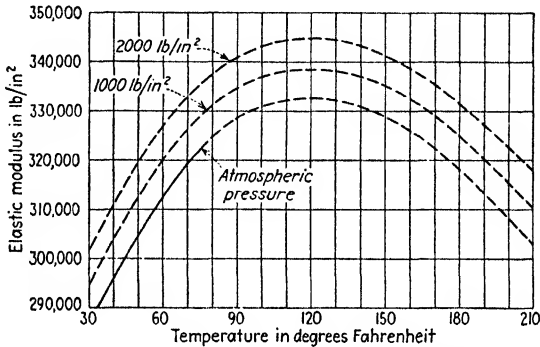


FIG. 245.—Elastic modulus e of water as a function of temperature and pressure intensity.

conditions is equal to the absolute pressure intensity, whereas for adiabatic variation it will depend as well upon the ratio of the specific heats for constant pressure and constant volume; that is,

$$e = kp$$

in which $k = c_p/c_v$. In Table VI will be found characteristic values of k for a number of common gases.

AUTHOR INDEX

A

Ackeret, J., 131
 Airy, G. B., 371-373
 Allen, H. S., 215
 Arnold, 215

B

Bakhmeteff, B. A., 164, 236, 298-300, 388, 389, 391-394
 Bazin, H., 277, 279, 309-311, 313
 Bernoulli, D., 48
 Betz, A., 122
 Blasius, H., 195, 197-199, 204, 246-248
 Boussinesq, J., 185, 186, 302, 377-379
 Bridgman, P. W., 2
 Buckingham, E., 14
 Burgers, J. M., 199

C

Camp, B. H., 348
 Carstanjen, M., 313
 Chang, Y. L., 335
 Chézy, De, 279
 Christiansen, J. E., 341

D

Darcy, H., 277
 Daugherty, R. L., 236, 263, 406, 410
 Dillman, O., 317, 318
 Du Boys, P., 334, 335
 Durand, W. F., 88, 121

E

Einstein, A. H., 332, 337
 Eisner, F., 221, 319

Ekman, V. W., 172
 Escande, L., 318
 Euler, L., 47

F

Fage, 227
 Favre, H., 337
 Faxén, H., 213
 Feodoroff, N. V., 164
 Flachsbart, 227
 Flamant, A., 377
 Folsom, 410
 Forchheimer, P., 236, 274, 377

G

Ganguillet, E., 279
 Gebers, 204
 Gibson, A. H., 368
 Gilbert, G. K., 333
 Goldstein, G., 214

H

Hagen, G. W., 163
 Hansen, N., 198, 199
 Hele-Shaw, H. J. S., 153
 Helmholtz, H. von, 122
 Hermann, R., 247, 248
 Hersey, M. D., 160
 Hinderks, A., 268
 Hofmann, A., 270
 Hohenemser, K., 122
 Hunsaker, J. C., 134
 Hurst, H. E., 340

I

Ippen, A. T., 398-400

J

Jacob, M., 262
 Jakuschoff, P., 339
 Jasmund, R., 274
 Jeffreys, H., 332
 Johansen, F. C., 227, 259, 260
 Joukowsky, N., 119

K

Kármán, Th. von, 178, 188-191, 202,
 204, 218, 238, 240, 242, 244, 248,
 249, 398
 Kaufmann, W., 158, 225
 Kempf, 204
 Kirchhoff, G., 122
 Knapp, R. T., 398-400
 Koch, A., 313, 316, 322
 Kretschmer, F., 262, 263
 Krey, H., 274
 Krober, G., 272
 Kröner, R., 265
 Krumbein, W. C., 348-350
 Kulka, H., 109
 Kutta, W. M., 117
 Kutter, R., 279

L

Ladenburg, R., 213
 Lamb, H., 65, 85, 122, 149, 183, 212,
 217, 371, 373, 374, 377, 380
 Lauck, A., 123, 309, 310
 Lees, C. H., 247, 248
 Leighly, J., 341
 Levi-Civita, T., 373, 381
 Liebster, H., 215
 Lunnon, 215

M

Maccoll, J. W., 367
 MacDougall, C. H., 337
 Manning, R., 279
 Matzke, A. E., 299, 389, 391-394
 Meyer-Peter, E., 337
 Mises, R. von, 19, 53, 122, 279, 309,
 310, 313

Mononobe, N., 297, 298
 Moody, L. F., 132

N

Neményi, P., 163
 Newton, I., 211
 Nikuradse, J., 237, 238, 241, 243-
 245, 248-252, 254, 264, 267, 276
 Nippert, H., 269

O

O'Brien, M. P., 335, 336
 Oseen, C. W., 214
 Otto, G. H., 343

P

Pajer, G., 314, 315
 Pannell, J. R., 247, 248
 Petersohn, E., 122
 Poiseuille, J. L. M., 163
 Poleni, G., 307
 Prandtl, L., 88, 122, 184, 186-192,
 194, 207, 212, 216, 225, 248, 267,
 268, 310

R

Rayleigh, Lord, 372, 373, 377, 379-
 381
 Rehbock, Th., 309-311
 Reid, L., 317, 318
 Reynolds, O., 130, 171, 172, 179, 183,
 185
 Rindlaub, B. D., 335
 Rouse, H., 59, 215, 236, 317, 324,
 342, 400
 Russell, J. Scott, 381, 382

S

Saph, A. V., 246
 Schach, W., 122
 Schardin, H., 368
 Schiller, L., 215, 247, 248
 Schlichting, H., 253-255
 Schmiedel, H., 215

Schoder, E. W., 246, 312

Schoklitsch, A., 337

Sorenson, A. E., 132

Spannhake, W., 120

Stanton, T. E., 236, 247, 248

Stevens, J. C., 298

Stokes, G. G., 212

T

Taylor, G. I., 155, 189, 367

Thoma, D., 39

Thomsen, G. C., 160

Tietjens, O., 88, 122, 216, 225

Tolman, C. F., 163

Turner, K. B., 312

W

Wadell, H., 345

Wattendorf, F. L., 178

Weinstein, A., 381

Weisbach, J., 308, 309

White, M. P., 400

Wieselsberger, C., 204, 215, 227,

Witte, R., 257, 260

SUBJECT INDEX

A

Absolute pressure, 12, 127, 129, 405
 Absolute roughness, 234, 251-255,
 262, 280, 281
 Absolute viscosity, 8
 Acceleration, convective, 44
 equations of, 44-47, 149, 179
 gravitational, 28, 404
 local, 44
 total (substantial), 44
 Acoustic velocity, 28, 365
 Adhesion, 9, 10
 Adiabatic variation, 11, 128, 367
 Adverse slope, 292-294
 Air, properties of, 406-408
 Airfoil, 119, 223-225
 Ammonia, properties of, 406-408
 Anemometer, hot-wire, 178
 Angle of attack, 224
 Angular deformation, 67-70

B

Backwater curve, 293, 295, 298
 Bazin roughness coefficient, 279, 280
 Bazin weir coefficient, 309-311
 Bed load, 331-339
 Bends, in closed conduits, 268-271
 in open channels, 397-400
 Bernoulli theorem, 48
 Bore, 383
 Boundary conditions, definition of,
 12, 37
 Boundary layer, in bed-load move-
 ment, 336
 laminar, 195-200
 in pipes, 232-234, 249-251
 thickness of, 198
 turbulent, 200-204
 Broad-crested weir, 320-323

C

Capillary effect on weir discharge,
 305, 306, 310
 Capillary rise in tubes, 410, 411
 Capillary waves, 373-376
 Cartesian coordinate system, 42
 Cauchy integral theorem, 121-124
 Cauchy number, 17, 23, 357
 Cauchy-Riemann equations, 101
 Cavitation, 129-134
 Celerity, capillary wave, 374, 375
 definition of, 355
 elastic wave, 364-368
 gravity wave, 368-373
 Centripetal acceleration, 45
 Chézy coefficient, 279, 289, 296
 Circulation, definition of, 72, 73
 Classical hydrodynamics, 2, 13, 19,
 31
 Cohesion, 9
 Complex numbers, definition of, 96
 operations with, 97-98
 Components, of, acceleration, 43, 44
 of force vector, 59-64
 of velocity vector, 43
 of vortex vector, 70, 71, 74
 Compressibility, 10
 Conformal mapping, significance of,
 98-102
 Continuity equation, 52, 69, 70, 95
 Contraction coefficient, 256-262,
 308, 310, 313-315, 325
 Convective acceleration, definition
 of, 44
 Converging flow, 172, 263, 287
 Correlation, 177, 178
 Critical depth, 283-288, 291-294,
 300, 319-326, 333, 394, 395
 Critical-depth meters, 319-326

- Critical flow, Cauchy criterion, 356, 357
 Froude criterion, 283
 Reynolds criterion, 172
 Critical slope, 292-294
 Critical tractive force, 335-337
 Cumulative grading curves, 346-349
 Curl, definition of, 70
 Cylinder, flow around, 110-112, 216-222
 rotating, 222
 Cylindrical coordinate system, 42, 87, 160
- D**
- Deformation, 7, 8, 67-70, 79, 143-146
 Deformation drag, 209
 Density, of common fluids, 409
 definition of, 6
 variation in, 126-129
 of water, 404
 Deviation, standard, 348, 349
 Diameter, sediment, 336, 338, 344, 349
 Differential equation, of stream line, 66
 of vortex line, 74
 Dimensional analysis, 2, 13, 18-24
 Dimensional homogeneity, 13
 Dimensional units, 3-5, 403, 404
 Dimensionless parameters, 17
 Dimensions, table of, 11
 theory of, 2-5
 Discharge coefficient, 257-262, 308-316, 318, 321
 Discharge diagram, 284-287
 Discontinuity, 136
 Disk ratio, 228, 229
 Disks, drag of, 215, 228, 229
 Dissipation of energy, 146-148, 183, 184, 208, 235, 265, 266, 283-285
 Diverging flow, 173, 263-266, 287
 Doublet, three-dimensional, 88
 two-dimensional, 110
 Drag, of airfoils, 223-225
 of cylinders, 216-223
 of disks, 215, 228, 229
 of flat plates, 225-227
 fundamental concepts of, 209-212
 of spheres, 212-216
 Drag coefficient, 228
 Drop-down curve, 293, 296
 Du Boys bed-load equation, 334-335
 Dynamic pressure, 48
 Dynamic viscosity, 8, 11, 405-407
- E**
- Eddy viscosity, 185-188
 Elastic modulus, of common fluids, 411
 definition of, 10-12
 Elastic waves, 363-368
 Electrical analogy, 121-124
 Empiricism, 1, 2, 31
 Energy criteria, 126
 Energy-discharge diagram, 285, 287
 Energy equations, 47-49
 Energy line, 49, 50
 Establishment of flow, 232, 233, 395, 396
 Euler, equations of, 47, 66, 70, 71
 method of, 35
- F**
- Filament, stream, 36, 37
 vortex, 74, 75
 Flow characteristics, 12, 13
 Flow net, 54-59
 Flow patterns, steady vs. unsteady, 37-42
 Fluctuation, velocity of, 176, 177
 Fluid mechanics, 1, 2, 13, 30, 31
 Fluid motion, characteristics of, 12, 13
 Fluid particle, definition of, 35
 Fluid properties, 5-12, 405-411
 Force, 3-6, 403, 404
 Force field, 60-63
 Force potential, 59-63
 Force properties, definition of, 6-12
 Forced vortex, 78

Forces acting on a fluid element, 45,
46, 141-146

Form drag, 209, 210, 234

Free surface, influence of, 49, 57, 123

Free vortex, 77

Froude number, 17, 23, 28, 29, 303-
305, 357, 376, 388-402

G

Gasoline properties of, 405, 407, 408

Geodetic head, 49

Geometric mean diameter, 344

Glycerine, properties of, 405, 407,
408

Gradient, energy, 165, 289

potential force 59-64

velocity, 84-85

pressure, 46, 59-64

velocity, 44, 65

weight, 46, 59-64

Grading characteristics of sediment,
338, 344-350

Gradually varied flow, 288-301

Gravitational acceleration, 28, 404

Gravitational attraction, 1

Gravity waves, deep-water, 371-373
solitary, 377-382

surges, 382-388

Grid, 220

Group velocity, 375

Guide vanes, 272

H

Half body, three-dimensional, 89

Head, 49

Heat transfer, 189

Hole-Shaw apparatus, 153, 154

Helium, properties of, 406-408

Hodograph, 122, 314

Hydraulic jump, 299-301, 388-394

Hydraulic radius, 278

Hydrodynamics, classical, 2, 13, 19,
31

Hydrogen, properties of, 406-408

Hydromechanics, fundamentals of,
35-137

Hydrostatic pressure, 48

I

Imaginary number, definition of, 96

Immersed bodies, resistance of, 209-
229

Inertia, 6

Instability, 155, 170-173

Interference of waves, 358

Irrotational motion, characteristics
of, 84, 85

definition of, 71, 72

Isothermal variation, 11

Isovel, 267, 268

J

Joukowski profile, construction of,
120

Joukowski transformation, 118

Jump, hydraulic, 299-301, 388-394

K

Kinematic viscosity, 11, 28, 406-411

Kinetic energy, 48

of turbulence, 182-184

Kutta transformation, 118, 119

Kutter formula, 279

L

Lagrange, method of, 35, 65

Lagrangian wave, 369, 371

Laminar flow, through circular tube,
160-163

definition of, 150, 169

between parallel boundaries, 150-
156

through pervious material, 163-
168

Laminar sublayer, 201

Laplace, equation of, 85, 94

Length, 3-6, 403

of hydraulic jump, 391-393

Lift, 223-225

coefficient of, for airfoils, 224-225
for rotating cylinders, 222

Line integral, 72, 73

Linear deformation, 67-69

Local acceleration, definition of, 44
Lubrication, 156-160

M

Mach angle, 356, 399, 401
Magnus effect, 114
Manning formula, 279-280
Mass, 3-6, 403-404
Mass attraction, 6, 7
Maximum discharge, 284-288
Mean, 344
Mean diameter, geometric, 348, 349
Mechanical analysis of sediment, 344-349
Median, 344
Mercator projection, 102
Mercury, properties of, 405, 407, 408, 410, 411
Methane, properties of, 406-408
Metric system, 403, 404
Mild slope, 292-294
Minimum energy, 283-288
Mixing length, definition of, 188, 189
Models, 24-30
Modulus, of elasticity, of common fluids, 411
 definition of, 10-12
Molecular attraction, 9
Molecular friction, 8
Momentum equation, 52-54
Momentum transport, 180, 181, 188

N

Nappe profile, 63, 64, 122-124, 304, 305, 311, 312, 317
Natural coordinate system, 42, 43
Navier-Stokes equations, 148, 149
Newtonian equation of acceleration, 12
Nitrogen, properties of, 406-408
Non-uniform flow, definition of, 36
Normal depth, 291-299

O

Oil, properties of, 405, 407, 408, 411
Open channels, flow in, 273-326
Orifice discharge, 18-20, 256-261

Overfall, 59-62, 287, 323, 324
Oxygen, properties of, 406-408

P

Path line, 36, 41, 42
Percolation, 163-168
Permeability, coefficient of, 164, 165
Phi-notation, 348-350
Pi-theorem, 13-18
Pipe resistance, 245-251
Pipes, velocity distribution in, 236-245
Pitting, 131
Plate, flow around, 115-117
Poise, 408
Porosity, 344
Potential energy, 48
Potential flow, 83-123, 153, 154, 165-168
Potential head, 49
Pressure distribution, around a cylinder, 221
 in a steep channel, 281
Pressure gradient, 46
Pressure head, 49
Pressure intensity, 13, 141
Pressure line, 49, 50
Probability function, 345-350
Propagation of waves, 353-355

R

Radius, hydraulic, 278
Rankine combined vortex, 76, 79, 80
Rankine-Hugoniot equation, 367
Rapid flow, 284
Rapidly varied flow, 301-307
Rational analysis, 1, 2
Real number, definition of, 96
Reflection of waves, 360, 361
Rehbock weir equation, 309-311
Relative roughness, 234, 235, 240, 241, 243-255, 261, 278-281
Relative velocity, 39
Resistance, boundary layer, 192-2
 circular pipes, 245-271
 immersed bodies, 209-229
 open channels, 276-280
Reynolds apparatus, 171, 172

Reynolds equations, 179
 Reynolds number, 17, 150, 170, 192,
 199-204, 208-220, 224, 228-230,
 232-255, 258-265, 270, 271, 275,
 276, 278, 279, 302, 303, 305,
 306, 338, 339, 354
 Ripples, sand, 332, 333
 waves, 374, 375
 Roll waves, 387, 388
 Rotation, 67-70
 of flow pattern, 102, 103, 115-117
 Rotational motion, definition of, 71
 Rotoscope, 39
 Roughness, 234, 235, 243, 249-255,
 261, 262, 278-280
 coefficients of 280

S

Scale ratios, 25-30
 table of, 26
 Secondary flow, 266-272
 Section changes in closed conduits,
 asymmetrical, 266-272
 symmetrical, 255-266
 Sediment, characteristics of, 164,
 165, 335, 336, 338, 343-350
 distribution of, 330, 340-343
 suspension of, 339-343
 transportation of, 327-343
 Separation, 134-136, 205-208, 264,
 265, 317-319
 Shape, sediment, 344
 Shear, 7, 8, 141
 Shock waves, development of, 361-
 363
 elastic, 366, 367
 gravity, 370, 371, 382-402
 Silt transport, 188
 Similarity hypothesis, 189, 190
 Latitude, 24-30
 angular line, point, 86
 sluice, three-dimensional, 87
 two-dimensional, 105, 106
 frequency curves, 346-348
 Smoothness, 348
 Slope, channel, 276, 290, 292
 energy-line, 276, 289-292
 free surface, 276, 292

Sluice gate, 58, 286, 313, 316
 Sound wave, 367
 Source, three-dimensional, 87
 two-dimensional, 105, 106
 Specific energy, definition of, 282
 Specific-energy diagram, 283, 284
 Specific gravity, definition of, 6
 Specific heat, 11, 189, 411
 Specific weight, of common fluids,
 405, 406
 definition of, 405
 Sphere, flow around, 91, 212-216
 Spillway design, 316-319
 Spiral flow, 266-269
 Stagnation pressure, 58, 91
 Stagnation point, 58, 62, 63, 90, 91,
 111, 112, 117, 134
 Standard deviation, 348, 349
 Standard gravitational acceleration,
 404
 Steady flow, definition of, 36
 Steep slope, 292-294
 Stoke, 408
 Stokes' law, 213
 Streak line, definition of, 42
 Steam filament, definition of, 36, 37
 Stream function, definition of, 93
 Stream line, definition of, 35, 36
 differential equation of, 66
 Streamlining, effect of, 229
 Submergence, of sluice, 315
 of weir, 312, 313
 Substantial acceleration, definition
 of, 44
 Superelevation at a bend, 397-400
 Surface drag, 209
 Surface profiles, 290-294, 296, 395,
 396
 Surface tension, definition of, 9
 of water, 410, 411
 Surge, 382-388
 Suspended load, 339-343
 Sustaining slope, 292-294

T

Thomson's law, 80, 81
 Time, 3-6, 403

Total acceleration, definition of, 44
 Total energy, 48
 Total head, 49
 Tractive force, 334-337
 Tranquil flow, 284
 Translation, of the coordinate system, 39
 of a fluid element, 67-69
 Trochoidal wave, 372
 True critical depth, 322-325
 Turbulence, 169-191
 development of, 170-175
 kinetic energy of, 182-184
 similarity hypothesis, 189, 190
 Turbulent boundary layer, 200-204
 Tyler standard sieve series, 345, 348

U

Undular jump, 389, 390
 Undular surge, 384
 Uniform flow, definition of, 36
 Universal resistance equations, 248-252
 Universal turbulence constant, 190
 Universal velocity equations, 238-245
 Unsteady flow, definition of, 36

V

Vanes, guide, 272
 Vapor pressure, 129, 132, 133
 Vector, force, 59, 63
 velocity, 35, 36
 vorticity (rotation), 70, 71
 Velocity, of fall, 340, 344
 Velocity coefficient, 256-261, 314, 315
 Velocity distribution, circular pipes, 236-245
 converging flow, 263
 diverging flow, 263
 laminar flow, 152, 155, 162, 174
 open channels, 274-277
 sediment-laden flow, 328-330
 turbulent flow, 174
 Velocity fields, 37-42, 60-62
 graphical combination of, 41

Velocity head, 49
 Velocity-head correction factor, energy, 51, 52
 momentum, 54
 Velocity potential, definition of, 83
 in viscous flow, 149, 153, 165
 Velocity vector, 35, 36
 Venturi flume, 321
 Venturi meter, 263
 Venturi throat, 130-133, 264, 265
 Viscometer characteristics, 409, 410
 Viscosity, dynamic, definition of, 8, 144
 kinematic, definition of, 28
 Voids ratio, 344
 Vortex, combined, 79
 forced, 78
 potential free, 77
 Vortex filament, 74, 75
 Vortex motion, 80, 81
 Vortex trails, 217, 218, 220
 Vorticity, 72-76
 Vorticity transport, 189

W

Wake, turbulent, 208
 Water, properties of, 404-411
 Wave celerity, 355
 Wave front, 355, 362-364, 398-407
 Wave group, 359
 Wave interference, 358
 Wave reflection, 360, 361
 Waves, capillary, 373-376
 deep-water, 371-373
 elastic, 363-368
 gravity, 368-373, 377-401
 roll, 387, 388
 shock, 361-363, 366, 367, 370, 373-382-402
 solitary, 377-382
 Weber number, 17, 23, 357, 376
 Weight, 7
 Weir discharge, 20, 21, 63, 64, 300-313
 Wentworth sieve series, 345, 348
 Wetted perimeter, 278
 Wind pressure, 229-231

